

**DEVELOPMENT AND CHARACTERIZATION OF  
PHOTOCROSSLINKABLE HYALURONIC ACID HYDROGELS FOR CARTILAGE  
REGENERATION**

Cindy Chung

A DISSERTATION

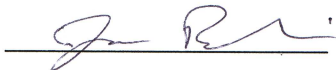
in

Bioengineering

Presented to the Faculties of the University of Pennsylvania  
in Partial Fulfillment of the Requirements for the Degree of Doctor of Philosophy

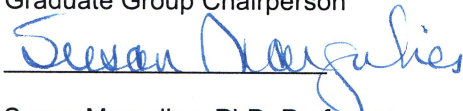
2009

Supervisor of Dissertation

A handwritten signature in black ink, appearing to read "Jason Burdick", written over a horizontal line.

Jason A. Burdick, PhD, Assistant Professor

Graduate Group Chairperson

A handwritten signature in blue ink, appearing to read "Susan Margulies", written over a horizontal line.

Susan Margulies, PhD, Professor

Dissertation Committee

G. Russell Huffman, MD, MPH, Assistant Professor

Robert L. Mauck, PhD, Assistant Professor

Casim A. Sarkar, PhD, Assistant Professor

## ACKNOWLEDGEMENTS

First and foremost I'd like to thank my parents for giving me the boundless opportunity to pursue a future in science and engineering. Without their hardships and sacrifices, I would not be here and I would not be who I am today. I'd also like to thank my friends who have made Philadelphia my home for the past few years, sharing with me the up and downs of research as well as adventures outside of the academic world. The life experiences and connections that I have made here will stay with me for a lifetime.

I'd like to acknowledge the members of the Burdick lab both past and present, with special thanks to Darren and Jamie, with whom I've had countless conversations with throughout my research. The lab has been a very dynamic place, changing from year to year, with people and ideas constantly coming in and going out. I watched it grow from one bench of borrowed lab space to a small enterprise of research and knowledge on the fourth floor of Skirkanich Hall, and it has been a pleasure to be a part of it. I am especially grateful to Dr. Steve Nicoll who provided a home for me in his lab for my first year and then allowed me the continued use of his equipment for much of my work, as well as his lab members who taught me all I know about histology.

I would also like to thank my thesis committee: Dr. Rob Mauck for all of our collaborations and our talks that would always made me feel more up-beat and excited about research, Dr. Russ Huffman for repairing my torn labrum and providing a clinical perspective to my work, and Dr. Casim Sarkar for taking on the duties of chairing my thesis committee. Of course, I am especially grateful for my advisor Dr. Jason Burdick, who has guided and pushed me throughout my research, making me a better researcher, writer (despite my complaints), and speaker. I could not have imagined everything working out as well as it had. Additionally, I am grateful for my funding sources: National Science Foundation, National Institute of Health, and NRSA T32 Musculoskeletal Training Grant.

Lastly, I'd like to give special thanks to Daquiri, my cat, who has slept by my side through the many endless nights spent on papers, progress reports, presentation making, and the writing of this dissertation. She has provided much comfort and entertainment.

## **ABSTRACT**

# **DEVELOPMENT AND CHARACTERIZATION OF PHOTOCROSSLINKABLE HYALURONIC ACID HYDROGELS FOR CARTILAGE REGENERATION**

Cindy Chung

Advisor: Jason A. Burdick, Ph.D.

Damage to cartilage from general wear, disease, or injury can lead to joint pain and tissue degeneration. With its limited ability for self-repair, cartilage has become a target for tissue engineering (TE). As current treatments have yet to provide long-term functional cartilage repair, this dissertation introduces the development and use of photopolymerizable hyaluronic acid (HA) based hydrogels for TE to optimize cellular interactions and neocartilage formation. By altering hydrogel design parameters (e.g., molecular weight and macromer concentration), a wide range of hydrogel properties were obtained. These hydrogels all preserved the rounded morphology of chondrocytes, but cell viability and neocartilage formation were dependent on hydrogel design, where increased crosslinking resulted in cell death and increased macromer molecular weight yielded inhomogeneities in cell and ECM distribution within the hydrogel. These variables also influenced the formed neocartilage properties.

The ability of HA hydrogels to promote neocartilage formation was also dependent on cell source and culture. The expansion of chondrocytes in 2D *in vitro* affected neocartilage formation in HA hydrogels after the second passage, as construct properties further decreased with continued passage. Chondrocytes from different tissue sources also behaved variably in the

hydrogels; auricular chondrocytes excelled in static culture and subcutaneous culture over articular chondrocytes, while articular chondrocytes were stimulated in a mechanically loaded environment.

As the use of chondrocytes for cartilage TE is limited clinically, we turned to mesenchymal stem cells (MSCs). *In vitro* culture of MSC-laden HA hydrogels demonstrated that these HA hydrogels not only supported, but enhanced chondrogenesis when compared to relatively inert hydrogels, potentially due to receptor interactions with HA. However, in these hydrogels, ECM was localized to pericellular regions. To accelerate the diffusion and distribution of ECM proteins, hydrolytically degradable HA macromers were synthesized to create a dynamic environment. When degradation complemented ECM deposition, ECM distribution and ultimately the functional maturation of the construct were improved.

While this dissertation focused on material development to improve cartilage regeneration, growth factor delivery optimization and successful implementation of these hydrogels in cartilage defect models remain, towards our goal of a successful long-term repair solution to cartilage damage.



# TABLE OF CONTENTS

## CHAPTER 1 -

<i>Introduction</i> .....	1
1.1 Cartilage.....	1
1.2 The Cartilage Problem: Clinical Aspects.....	1
1.3 Developing a Cartilage Solution: Cartilage Tissue Engineering .....	3
<i>References:</i> .....	6

## CHAPTER 2 -

<i>Research Overview</i> .....	8
2.1 Specific Aims & Hypotheses .....	8
2.2 Research Summary .....	9

## CHAPTER 3 -

<i>Engineering Cartilage Tissue: A Review</i> .....	12
3.1 Introduction .....	12
3.2 Cell Source.....	13
3.2.1 Chondrocytes .....	14
3.2.2 Fibroblasts .....	20
3.2.3 Stem Cells .....	21
3.3 Scaffolds .....	25
3.3.1 Hydrogels .....	28
3.3.2 Sponges .....	32
3.3.3 Meshes .....	34
3.4 Stimulating Factors .....	36
3.4.1 Growth Factors and Additives .....	36
3.4.2 Gene Therapy .....	38

3.4.3 Hydrostatic Pressure .....	39
3.4.4 Dynamic Compression .....	40
3.4.5 Bioreactors .....	41
3.5 Conclusions.....	42
References:.....	43

## SECTION I.

### ENZYMATICALLY DEGRADABLE HYALURONIC ACID HYDROGELS

#### CHAPTER 4 -

<i>Synthesis and Characterization of Methacrylated Hyaluronic Acid Hydrogels.....</i>	<b>73</b>
4.1 Introduction .....	73
4.2 Materials & Methodology .....	74
4.2.1 Macromer Synthesis and Polymerization.....	74
4.2.2 Hydrogel Characterization.....	76
4.2.3 Cell Viability.....	78
4.2.4 Statistical Analysis.....	78
4.3 Results & Discussion .....	79
4.3.1 Network Synthesis.....	79
4.3.2 Network Swelling, Mechanics, and Degradation.....	80
4.3.3 Cell Encapsulation and Viability.....	84
4.4 Conclusions.....	85
References:.....	86

#### CHAPTER 5 -

##### *Optimization of Methacrylated HA Hydrogel Properties for Neocartilage*

##### *Formation by Auricular Chondrocytes.....*

5.1 Introduction .....	88
------------------------	----

5.2 Materials & Methodology .....	90
5.2.1 Macromer Synthesis and Polymerization.....	90
5.2.2 Chondrocyte Isolation and Photoencapsulation.....	90
5.2.3 Implantation in Nude Mice.....	91
5.2.4 Biochemical Analysis.....	91
5.2.5 Histological Analysis.....	92
5.2.6 Statistical Analysis.....	93
5.3 Results & Discussion .....	93
5.3.1 Macroscopic Appearance.....	94
5.3.2 Biochemical Analysis.....	94
5.3.3 Histological Analysis.....	98
5.4 Conclusions.....	100
References:.....	101

## SECTION II.

### EXPLORATION OF CELL SOURCE AND CELL BEHAVIOR

#### CHAPTER 6 -

##### *Effects of Chondrocyte Expansion on Neocartilage Formation*

<i>in Hyaluronic Acid Hydrogels .....</i>	<b>104</b>
6.1 Introduction .....	104
6.2 Materials & Methodology .....	105
6.2.1 Macromer Synthesis and Polymerization.....	105
6.2.2 Chondrocyte Isolation, Expansion, and Photoencapsulation.....	106
6.2.3 Implantation in Nude Mice.....	107
6.2.4 Mechanical Testing .....	107
6.2.5 Biochemical Analysis.....	108

6.2.6 Histological Analysis.....	109
6.2.7 Statistical Analysis.....	110
6.3 Results & Discussion .....	110
6.3.1 Mechanical Behavior.....	110
6.3.2 Biochemical Analysis.....	112
6.3.3 Immunohistochemical Analysis .....	115
6.4 Conclusions.....	117
References:.....	118

## CHAPTER 7 -

### *Auricular and Articular Cartilage:*

<i>How do chondrocytes differ in Hyaluronic Acid Hydrogels?.....</i>	<b>121</b>
7.1 Introduction .....	121
7.2 Materials & Methodology .....	123
7.2.1 Macromer Synthesis and Polymerization.....	123
7.2.2 Chondrocyte Isolation and Photoencapsulation.....	123
7.2.3 In Vivo and In Vitro Culture Methods .....	123
7.2.4 Mechanical Stimulation .....	124
7.2.5 Mechanical Testing .....	125
7.2.6 Biochemical Analysis.....	126
7.2.7 Viability .....	126
7.2.8 Gene Expression Analysis .....	126
7.2.9 Histological Analysis.....	127
7.2.10 Statistical Analysis.....	128
7.3. Results & Discussion .....	128
7.3.1 In Vivo Culture.....	128
7.3.2 In Vitro Culture .....	134

7.3.3 Mechanical Stimulation .....	137
7.4 Conclusions .....	139
References: .....	140

## CHAPTER 8 -

<i>Mesenchymal Stem Cell Chondrogenesis in Hyaluronic Acid Hydrogels</i> .....	<b>144</b>
8.1 Introduction .....	144
8.2 Materials & Methodology .....	145
8.2.1 CD44 Staining and Flow Cytometry .....	145
8.2.2 Macromer Syntheses .....	145
8.2.3 Mechanical Characterization .....	146
8.2.4 MSC Photoencapsulation and Culture .....	147
8.2.5 Viability .....	147
8.2.6 Gene Expression Analysis .....	148
8.2.7 Microarray Assay .....	149
8.2.8 Histological Analysis .....	149
8.2.9 Statistical Analysis .....	149
8.3 Results & Discussion .....	150
8.3.1 MSC interactions with HA .....	150
8.3.2 MSC Chondrogenesis .....	151
8.3.3 Comparison between HA and PEG hydrogels .....	157
8.4 Conclusions .....	164
References: .....	165

## SECTION III.

### DYNAMIC HYALURONIC ACID HYDROGELS

#### CHAPTER 9 -

<i>Synthesis of Hydrolytically Degradable Hyaluronic Acid Hydrogels.....</i>	<b>169</b>
9.1 Introduction .....	169
9.2 Materials & Methodology .....	170
9.2.1 Methacrylated HA (MeHA) Macromer Synthesis .....	170
9.2.2 Methacrylated Lactic Acid HA (MeLAHA) Macromer Synthesis .....	170
9.2.3 Methacrylated Caprolactone HA (MeCLHA) Macromer Synthesis .....	172
9.2.4 Hydroxyethyl Methacrylated HA (Hema-HA) Macromer Synthesis.....	174
9.2.5 Hydrogel Formation and Acellular Characterization .....	174
9.2.6 Short-Term Cell Viability and Matrix Elaboration In Vitro.....	175
9.3 Results & Discussion .....	176
9.3.1 Synthesis of MeLAHA Macromer.....	176
9.3.2 Synthesis of MeCLHA and Hema-HA Macromers .....	181
9.3.3 Characterization of Hydrolytically Degradable HA Hydrogels.....	183
9.3.4 Cell Viability and Matrix Elaboration.....	185
9.4 Conclusions.....	185
References:.....	187

#### CHAPTER 10 -

<i>Influence of Temporal Degradation on</i>	
<i>Matrix Deposition in Hyaluronic Acid Hydrogels .....</i>	<b>191</b>
10.1 Introduction .....	191
10.2 Materials & Methodology .....	192
10.2.1 Macromer Syntheses .....	192

10.2.2 Acellular Characterization .....	193
10.2.3 MSC Photoencapsulation and Culture .....	193
10.2.4 Cellular Characterization .....	194
10.2.5 Statistical Analysis.....	196
10.3 Results & Discussion .....	196
10.3.1 Acellular Characterization .....	196
10.3.2 Cellular Characterization.....	198
10.3.3 Gene Expression Analysis .....	200
10.3.4 Long-Term In Vitro Culture.....	202
10.3.5 Mechanical Properties.....	204
10.3.6 DNA and Biochemical Content.....	206
10.3.7 Immunohistochemical Analysis.....	208
10.3.8 Importance of Degradation Rate .....	209
10.3.9 Importance of a Dynamic Hydrogel.....	209
10.4 Conclusions.....	212
References:.....	213

## **CHAPTER 11 -**

<i>Conclusions, Limitations, and Future Directions .....</i>	<b>217</b>
11.1 Conclusions.....	217
11.2 Limitations .....	221
11.3 Future Directions.....	223
11.3.1 TGF- $\beta$ 3 Delivery.....	223
11.3.2 In Vivo Defect Model.....	227
References:.....	229

## LIST OF TABLES

<b>Table 3.1</b> Cell sources used in the regeneration of cartilage tissues.....	14
<b>Table 3.2</b> Types of biomaterials used in cartilage tissue engineering.....	27
<b>Table 4.1</b> MeHA hydrogel compositions.....	79
<b>Table 4.2</b> MeHA hydrogel mesh size.....	80
<b>Table 7.1</b> Porcine primer & probe sequences for real-time PCR .....	127
<b>Table 8.1</b> Human quantitative PCR primers and probes.....	148
<b>Table 10.1</b> MeHA:MeCLHA hydrogel compositions .....	194
<b>Table 10.2</b> Volumetric swelling ratios of MeHA:MeCLHA hydrogels .....	198



## LIST OF FIGURES

<b>Figure 3.1</b> Schematic of cartilage tissue engineering approaches .....	13
<b>Figure 3.2</b> Scaffold architectures used in engineered cartilage tissues.....	26
<b>Figure 4.1</b> Synthetic scheme and <sup>1</sup> H NMR of MeHA .....	75
<b>Figure 4.2</b> Schematic of free radical polymerization of MeHA.....	76
<b>Figure 4.3</b> Volumetric swelling ratios of MeHA hydrogels.....	80
<b>Figure 4.4</b> Mechanical properties of MeHA hydrogels .....	81
<b>Figure 4.5</b> Degradation of MeHA hydrogels by exogenous hyaluronidase.....	82
<b>Figure 4.6</b> Viability of 3T3-fibroblasts in MeHA hydrogels .....	84
<b>Figure 5.1</b> Schematic of photoencapsulation and subsequent analysis .....	91
<b>Figure 5.2</b> Macroscopic appearances of explanted MeHA constructs cultured <i>in vivo</i> .....	94
<b>Figure 5.3</b> Water content of MeHA constructs after <i>in vivo</i> culture.....	95
<b>Figure 5.4</b> DNA content of MeHA constructs after <i>in vivo</i> culture.....	96
<b>Figure 5.5</b> Glycosaminoglycan content of MeHA constructs after <i>in vivo</i> culture .....	97
<b>Figure 5.6</b> Collagen content of MeHA constructs after <i>in vivo</i> culture .....	98
<b>Figure 5.7</b> Histological stains for ECM in MeHA constructs after <i>in vivo</i> culture .....	99
<b>Figure 6.1</b> Schematic of chondrocyte expansion, encapsulation, and subsequent analysis.....	106
<b>Figure 6.2</b> Uniaxial confined compression testing setup.....	108
<b>Figure 6.3</b> Macroscopic image of explanted MeHA constructs with passaged chondrocytes ....	110
<b>Figure 6.4</b> Mechanical properties of MeHA constructs compared to native cartilage.....	111
<b>Figure 6.5</b> Water content of MeHA constructs compared to native cartilage.....	112
<b>Figure 6.6</b> DNA content of MeHA constructs compared to native cartilage.....	113
<b>Figure 6.7</b> Biochemical content of MeHA constructs compared to native cartilage.....	114
<b>Figure 6.8</b> Elastin content of MeHA constructs compared to native cartilage .....	115
<b>Figure 6.9</b> Histological stains for ECM in MeHA constructs with passaged chondrocytes.....	116
<b>Figure 7.1</b> Schematic of chondrocyte isolation, encapsulation, and analysis.....	125
<b>Figure 7.2</b> Mechanical properties of explanted AU and AR constructs .....	129

<b>Figure 7.3</b> Water content of explanted AU and AR constructs .....	130
<b>Figure 7.4</b> DNA and biochemical content of explanted AU and AR constructs .....	131
<b>Figure 7.5</b> Histological stains for ECM in explanted AU and AR constructs.....	133
<b>Figure 7.6</b> Viability of AU and AR constructs <i>in vitro</i> .....	134
<b>Figure 7.7</b> Gene expression of AU and AR constructs cultured <i>in vitro</i> .....	136
<b>Figure 7.8</b> Histological stains for ECM in AU and AR constructs cultured <i>in vitro</i> .....	137
<b>Figure 7.9</b> Gene expression of dynamically loaded AU and AR constructs <i>in vitro</i> .....	138
<b>Figure 8.1</b> CD44 expression by MSCs.....	151
<b>Figure 8.2</b> Gene expression of MSC-laden MeHA constructs <i>in vitro</i> .....	152
<b>Figure 8.3</b> Hyaluronidase gene expression of MSC-laden MeHA constructs <i>in vitro</i> .....	153
<b>Figure 8.4</b> Histological stains for ECM in MSC-laden constructs cultured <i>in vitro</i> .....	154
<b>Figure 8.5</b> Gene expression of MSC-laden MeHA constructs <i>in vivo</i> .....	155
<b>Figure 8.6</b> Histological stains for ECM in MSC-laden constructs cultured <i>in vivo</i> .....	156
<b>Figure 8.7</b> Comparison of MSC viability and elastic moduli of MeHA and PEG hydrogels .....	157
<b>Figure 8.8</b> Gene expression of MeHA constructs normalized to PEG constructs ( <i>in vitro</i> ) .....	158
<b>Figure 8.9</b> Histological stains for ECM in MSC-laden MeHA and PEG constructs ( <i>in vitro</i> ).....	158
<b>Figure 8.10</b> Gene expression of MeHA constructs normalized to PEG constructs ( <i>in vivo</i> ).....	159
<b>Figure 8.11</b> PCA plot of HA and PEG constructs cultured <i>in vitro</i> .....	160
<b>Figure 8.12</b> Heat map comparison of MSC-laden HA and PEG constructs ( <i>in vitro</i> ) .....	163
<b>Figure 9.1</b> Reaction schematic for the synthesis of MeLAHA.....	172
<b>Figure 9.2</b> Reaction schematic for the synthesis of MeCLHA macromer .....	173
<b>Figure 9.3</b> Reaction schematic for the synthesis of Hema-HA macromer .....	174
<b>Figure 9.4</b> <sup>1</sup> H NMR spectrum of MeLA-OH, MeLA-COOH, and MeLA-NHS .....	177
<b>Figure 9.5</b> <sup>1</sup> H NMR spectrum of the sodium and TBA salt of hyaluronic acid .....	179
<b>Figure 9.6</b> <sup>1</sup> H NMR spectrum of MeLAHA macromer .....	179
<b>Figure 9.7</b> DOSY spectrum .....	180
<b>Figure 9.8</b> <sup>1</sup> H NMR of MeCLHA and Hema-HA .....	182

<b>Figure 9.9</b> Degradation times and profiles of MeLAHA, Hema-HA, and MeCLHA .....	184
<b>Figure 9.10</b> Degradation of MeHA:MeCLHA copolymer hydrogels .....	184
<b>Figure 9.11</b> Viability and histological staining for CS for MeHA:MeLAHA hydrogels .....	185
<b>Figure 10.1</b> Elastic moduli of MeHA:MeCLHA copolymer hydrogels.....	197
<b>Figure 10.2</b> Live/Dead stains of MeHA:MeCLHA constructs .....	199
<b>Figure 10.3</b> Metabolic activity of MeHA:MeCLHA constructs .....	199
<b>Figure 10.4</b> Gene expression of MeHA:MeCLHA constructs.....	201
<b>Figure 10.5</b> Appearance, dimension, and weight of MeHA:MeCLHA constructs .....	203
<b>Figure 10.6</b> Mechanical properties of MeHA:MeCLHA constructs .....	205
<b>Figure 10.7</b> DNA and biochemical content of MeHA:MeCLHA constructs .....	207
<b>Figure 10.8</b> Histological stains for ECM in MeHA:MeCLHA constructs .....	208

# CHAPTER 1

## *Introduction*

### **1.1 Cartilage**

Cartilage is a specialized connective tissue that is found lining the articulating surfaces of joints and in the ear, nose, larynx, rib, and intervertebral disc. It can be classified into three types: elastic, hyaline, and fibrocartilage, where each type is specifically adapted for its given function, from defining facial structures to distributing mechanical loads and providing frictionless gliding surfaces in articulating joints. Cartilage is composed of sparsely distributed chondrocytes, found in lacunae, embedded within a dense extracellular matrix (ECM) that is composed primarily of type II collagen and proteoglycan aggregates. Collagen (5-30% by wet weight) provides tensile strength, while the highly negatively charged proteoglycan aggregates (2-10% by wet weight) retain water to resist compressive forces [1,2]. The composition, architecture, and remodeling of cartilage are adapted to function over a lifetime of repetitive use. However, when injury and wear does occur, self-repair is limited. Due to the predominantly avascular, aneural, and alymphatic nature of cartilage, healing is usually slow and unsatisfactory, as regenerated tissue is biochemically and mechanically inferior to healthy cartilage.

### **1.2 The Cartilage Problem: Clinical Aspects**

Currently, injured hyaline cartilage is the culprit behind knee pain experienced by millions of people young and old. Resulting from acute trauma, general wear, aging, or disease, cartilage lesions cause intermittent or chronic pain and can be accompanied by swelling, joint locking, the weakening of surrounding muscles, and/or reduced range of motion. An estimated 41,000 surgical procedures are performed annually in the United States to repair cartilaginous defects[3], where treatment outcomes depend on the size, depth, location, and pathology of the injured cartilage. With an aging population and a growing problem of obesity, joint pain is on a steady

increase, where both increases in age and obesity are correlated with a higher prevalence of osteoarthritis (OA) [4]. Already, 9% of the United States population aged 30 and older suffer from OA of the hip or knee, (totaling over 21 million people), costing an estimated \$28.6 billion dollars[5,6], and more than 250,000 knee and hip replacements are performed each year for end-stage disease joint failure [7]. In addition, with a more active adult population, cartilage damage resulting from sports injuries can also result in premature cartilage degeneration.

Current treatments attempt to provide symptomatic relief, allowing patients to return to high physical activity and delay the option of replacement surgery. These treatments include: 1) lavage and debridement, 2) microfracture, 3) periosteal and perichondral grafting, 4) autologous chondrocyte implantation (ACI), and 5) osteochondral autografts and allografts. Lavage and debridement involves the removal of any unstable cartilage flaps to relieve pain and decreases synovitis and concentrations of intra-articular inflammatory mediators [8,9]. Microfracture involves penetration of the subchondral bone to allow mesenchymal elements from the bone marrow to colonize the wound bed and promote the growth of fibrocartilage, which is mechanically inferior to hyaline cartilage, within defect site [10,11]. Periosteal and perichondral grafts can be placed in large defects, and it is thought that the milieu of cells present in these grafts can give rise to hyaline-like cartilage. Since 1987, ACI has garnered much excitement and has been used to treat full-thickness chondral defects in 12,000+ patients worldwide [12]. This approach involves harvesting small biopsies of cartilage from the patient in a minimally invasive manner, isolating chondrocytes from the donor tissue, and expanding the cells *in vitro*. These cells are then delivered to the cartilage defect site under a periosteum flap to produce new cartilage tissue. Unfortunately, this tissue is often not superior to microfracture results in the long term [13], despite the procedure being more costly and invasive. More recently, Genzyme has patented a treatment called matrix-induced autologous chondrocyte implantation (MACI). Here, harvested chondrocytes are grown on a collagen 1 membrane prior to implantation. MACI addresses problems associated with the use of periosteum in ACI by replacing it with an inert porcine collagen membrane that is pre-cultured with chondrocytes to prevent the leakage of

cells[14]. Lastly, Osteochondral autografts are taken from non-weight bearing healthy cartilage and inserted at the site of the load-bearing defect, while allografts involve the transplantation of cadaveric grafts. All of these treatments have shown variable success and are often limited by cell and tissue availability, donor site morbidity, graft rejection, fear of disease transmission, insufficient integration, or fibrocartilage repair [15]. Thus, their long-term use in clinical applications remains inadequate.

As current treatment methods have yet to provide long-term functional cartilage repair, researchers have turned to tissue engineering (TE) for a cartilage repair solution. Here, the goal is to use cells, scaffolds, and signaling factors, alone or in combination, to engineer a tissue that is structurally and functionally equivalent to healthy, native cartilage at the site of a defect.

### **1.3 Developing a Cartilage Solution: Cartilage Tissue Engineering**

In cartilage TE, cells (typically chondrocytes) are combined with a biocompatible scaffold to provide a suitable three-dimensional (3D) environment for cartilage tissue regeneration. These 3D environments more closely mimic the natural environment of chondrocytes, favoring phenotype preservation and ECM elaboration. Ideally the scaffold should: 1) have directed and controlled degradation, 2) promote cell viability, differentiation (in the case of stem cells), and ECM production, 3) allow for the diffusion of nutrients and waste products, 4) adhere and integrate with the surrounding native cartilage, 5) span and assume the size of the defect, and 6) provide mechanical integrity in the case of an articular cartilage defect.

To date, a wide range of materials (natural and synthetic) and scaffold architectures (e.g., hydrogels, porous sponges, fibrous meshes) have been explored for cartilage TE applications (see Chapter 3). Natural materials can often interact with cells via cell surface receptors to regulate or direct cell function, while synthetic materials are often more controllable and predictable with specified chemical and physical properties to dictate mechanical and degradation

characteristics. These materials can then be fabricated into a variety of scaffolds (e.g., hydrogels, sponges, and meshes).

Hydrogels are water swollen networks that support the encapsulation of cells and bioactive agents. As injectable scaffolds, they easily fill defects of any size and shape, and can be implanted in a minimally invasive manner. Physically crosslinked hydrogels are held together by molecular entanglements and/or secondary forces like ionic or hydrogen bonding or hydrophobic interactions, while chemically crosslinked hydrogels are covalently bonded. Here, molecular weight, macromer concentration, method of crosslinking, and crosslinking density can dictate the physical and chemical properties of the hydrogel.

For porous sponges, scaffold properties depend on pore size, porosity, and interconnectivity. Porosity dictates surface area [16] for cell adhesion, while pore size and interconnectivity affect cell infiltration and migration, matrix deposition and distribution [17], and nutrient and waste exchange. Methods used to manufacture these scaffolds include: porogen leaching, freeze-drying, and gas foaming. These manufacturing methods affect scaffold architecture, which in turn affects tissue formation. Porous scaffolds can also be filled with hydrogels for the delivery of growth factors or other bioactive agents [18].

Fibrous meshes are networks of woven and non-woven fibers, where variations in void volume, fiber diameter, and fiber directionality affect cell behavior. Three-dimensional fiber deposition is a technique used to form scaffolds with regulated patterns [19], and electrospinning is a technique used to produce micro- and nano-scale fibers that mimic collagen fibrils in cartilage ECM [20]. Fibers are generated as the surface charge of the polymer droplet overcomes its surface tension in an applied electric field, causing an instability that creates jets of polymer that can then be collected as solvent evaporates. Electrospun scaffolds have high surface areas to volume ratios and fully interconnected pores, and are capable of being aligned for heterogeneous scaffold properties. Scaffolds of all types have been incorporated with chondrocytes and stem cells to produce cartilaginous tissue, and an indepth review of current cartilage TE approaches can be found in Chapter 3. However, advances in new materials,

understanding of cells, and the development of more complex culture environments provide an opportunity for further TE approaches that may optimize healing and regeneration of cartilage.

*With these limitations in current cartilage repair techniques and the advancement of the field of TE, this thesis will introduce the development and use of engineered hydrogels, based on hyaluronic acid, for optimization of neocartilage formation by both chondrocytes and stem cells. This work presents an investigation of engineering tools and principles towards the advancement of cartilage TE.*



**References:**

- [1] Muir H. The chemistry of the ground substance of a joint cartilage. In: Sokoloff L, editor. The Joints and Synovial Fluid. New York: Academic Press, 1980. p. 27-94.
- [2] Williamson AK, Chen AC, Sah RL. Compressive properties and function-composition relationships of developing bovine articular cartilage. J Orthop Res 2001;19(6):1113-21.
- [3] Borg J. Cartilage injuries of the knee - causes, diagnosis and treatment review. [cited 2009 February 16]; Available from: <http://www.sportsinjurybulletin.com/archive/cartilage-injuries.html>
- [4] Das SK, Farooqi A. Osteoarthritis. Best Pract Res Clin Rheumatol 2008;22(4):657-75.
- [5] Felson DT, Zhang Y. An update on the epidemiology of knee and hip osteoarthritis with a view to prevention. Arthritis Rheum 1998;41(8):1343-55.
- [6] Osteoarthritis. Arthritis Foundation, 2007.
- [7] Elisseeff J. Injectable cartilage tissue engineering. Expert Opinion on Biological Therapy 2004;4(12):1849-59.
- [8] Clarke HD, Scott WN. The role of debridement: through small portals. J Arthroplasty 2003;18(3 Suppl 1):10-3.
- [9] Jackson RW, Dieterichs C. The results of arthroscopic lavage and debridement of osteoarthritic knees based on the severity of degeneration: a 4- to 6-year symptomatic follow-up. Arthroscopy 2003;19(1):13-20.
- [10] Bae DK, Yoon KH, Song SJ. Cartilage healing after microfracture in osteoarthritic knees. Arthroscopy 2006;22(4):367-74.
- [11] Minas T, Nehrer S. Current concepts in the treatment of articular cartilage defects. Orthopedics 1997;20(6):525-38.
- [12] Marlovits S, Zeller P, Singer P, Resinger C, Vecsei V. Cartilage repair: generations of autologous chondrocyte transplantation. Eur J Radiol 2006;57(1):24-31.

- [13] Knutsen G, Engebretsen L, Ludvigsen TC, Drogset JO, Grontvedt T, Solheim E, et al. Autologous chondrocyte implantation compared with microfracture in the knee. A randomized trial. *J Bone Joint Surg Am* 2004;86-A(3):455-64.
- [14] Keen J. MACI: Matrix Induced Autologous Chondrocyte Implantation, Patient Information. Australia: Genzyme Australasia Pty Ltd, 2006.
- [15] Jakobsen RB, Engebretsen L, Slauterbeck JR. An analysis of the quality of cartilage repair studies. *J Bone Joint Surg Am* 2005;87(10):2232-9.
- [16] Sontjens SHM, Nettles DL, Carnahan MA, Setton LA, Grinstaff MW. Biodendrimer-based hydrogel scaffolds for cartilage tissue repair. *Biomacromolecules* 2006;7(1):310-6.
- [17] Bhardwaj T, Pilliar RM, Grynpas MD, Kandel RA. Effect of material geometry on cartilagenous tissue formation in vitro. *Journal of Biomedical Materials Research* 2001;57(2):190-9.
- [18] Hile DD, Amirpour ML, Akgerman A, Pishko MV. Active growth factor delivery from poly(D,L-lactide-co-glycolide) foams prepared in supercritical CO<sub>2</sub>. *J Control Release* 2000;66(2-3):177-85.
- [19] Woodfield TB, Malda J, de Wijn J, Peters F, Riesle J, van Blitterswijk CA. Design of porous scaffolds for cartilage tissue engineering using a three-dimensional fiber-deposition technique. *Biomaterials* 2004;25(18):4149-61.
- [20] Li WJ, Danielson KG, Alexander PG, Tuan RS. Biological response of chondrocytes cultured in three-dimensional nanofibrous poly(epsilon-caprolactone) scaffolds. *Journal of Biomedical Materials Research Part A* 2003;67A(4):1105-14.

## CHAPTER 2

### *Research Overview*

#### **2.1 Specific Aims & Hypotheses**

Although research in cartilage TE has led to significant advances, the properties and structure of native cartilage have not been entirely mimicked by any engineered replacement. Thus, novel scaffolds that optimize the amount, the quality, and the organizational structure of engineered cartilage remain to be developed. This dissertation describes work towards this general aim with the development, characterization, and assessment of engineered photocrosslinked hyaluronic acid (HA)-based hydrogels with encapsulated cells for cartilage regeneration.

*Hypothesis:* We hypothesized that engineering a cell-laden HA scaffold, capable of providing cellular cues and a temporal microenvironment, would lead to optimal neocartilage formation and cartilage repair. Specifically, (1) variations in molecular weight, macromer concentration, and degree of modification can lead to HA-based hydrogels with tunable properties, (2) encapsulated cells (chondrocytes and mesenchymal stem cells, MSCs) will form neocartilage tissue in HA hydrogels based on the hydrogel structure, (3) stem cells will receive specific cues towards differentiation based on HA chemistry, and (4) the introduction of a hydrolytically degradable component will assist in matrix production and elaboration.

To test these hypotheses, the following specific aims were proposed:

**Specific Aim 1: Synthesize and characterize photocrosslinked methacrylated hyaluronic acid (HA) hydrogels.** Hydrogels of varying HA molecular weights and macromer concentrations are explored and characterized for swelling, mechanics, degradation, and cytocompatibility. The effects of hydrogel properties on neocartilage formation by encapsulated chondrocytes are also examined.

**Specific Aim 2: Investigate cellular response and neocartilage formation of encapsulated chondrocyte and mesenchymal stem cells in photocrosslinked HA hydrogels.** Using an optimized hydrogel composition, chondrocyte expansion, source, and response to mechanical stimulation are explored. MSC chondrogenesis in HA hydrogels is also investigated and compared to inert non-bioactive hydrogels. Gene expression, immunohistochemistry, biochemical assays, and mechanical testing were performed to assess cellular response, matrix elaboration, and tissue formation.

**Specific Aim 3: Develop hydrolytically degradable HA macromers to enhance ECM deposition and distribution.** Novel hydrolytically degradable HA-based macromers are synthesized and incorporated into the hydrogel system to tailor degradation to enhance ECM distribution. Networks are formed through copolymerization of these macromers with enzymatically degradable macromers to develop a wide range of temporal formulations.

## **2.2 Research Summary**

The motivation for developing cartilage tissue engineering (TE) scaffolds has already been set in Chapter 1. Cartilage has a limited ability for self repair, and the need for a cartilage solution is evident and growing. Following an extensive review on cartilage TE approaches in Chapter 3, the remainder of this dissertation, on the development and assessment of photocrosslinkable HA hydrogels for cartilage regeneration, is organized into three sections: 1) enzymatically degradable HA hydrogels, 2) exploration of cell source and cell behavior, and 3) dynamic HA hydrogels.

Chapter 4 will explore the synthesis and characterization of enzymatically degradable methacrylated HA (MeHA) hydrogels. The versatility of this photocrosslinkable system is investigated by simply altering molecular weight and macromer concentration to vary volumetric swelling, mechanical properties, and degradation time of the hydrogel. The effects of variations

in these hydrogel parameters on chondrocytes and neocartilage formation are then described in Chapter 5. Chondrocytes are directly encapsulated in the MeHA hydrogels and biochemical and histological outcomes are assessed after culture in a subcutaneous model in mice.

The choice of cell source is discussed in chapters 6, 7, and 8. Chondrocytes maintain and remodel surrounding cartilage tissue and are the natural choice for cellular cartilage scaffolds. However, these cells comprise only 10% of native cartilage by weight, and would require *in vitro* expansion for clinical use. Unfortunately, chondrocytes have been shown to dedifferentiate when expanded *in vitro*, and the effects of expansion on chondrocyte phenotype and neocartilage quality are investigated in chapter 6. Additionally, chondrocytes can be harvested from a variety of cartilage sources in the body including: ears, ribs, nose, and knees. The cartilage in each of these sources serves different functions; and thus, differences in chondrocyte sources and how these cells respond in MeHA hydrogels are explored in chapter 7, where the influence of mechanical loading on these specific cell types is also investigated.

Despite the vast work in the literature on chondrocytes in TE scaffolds, the use of chondrocytes for clinical applications are still limited by low cell yields, dedifferentiation, and donor site morbidity. Thus, MSCs have emerged as an alternative cell source. These multipotent progenitor cells have the ability to be expanded *in vitro* for several passages without loss of phenotype and can be photoencapsulated in the HA hydrogels. Given the appropriate cues, MSCs can differentiate toward a chondrogenic pathway, which is discussed in chapter 8, and produce type II collagen and sulfated-glycosaminoglycans. Importantly, the control over MSC chondrogenesis by hydrogel chemistry is also investigated by comparing HA hydrogels to inert hydrogel systems.

However, the use of enzymatically degradable hydrogels is limited, as extracellular matrix (ECM) proteins accumulate primarily in pericellular regions within MSC-laden MeHA hydrogels and do not distribute throughout the hydrogel, leading to inferior properties. Therefore, to enhance ECM distribution, hydrolytically degradable HA macromers were synthesized with a range of hydrolytically labile groups. The detailed synthetic schemes of these degradable

macromers with a range of degradation parameters is described in chapter 9. Copolymerization of both enzymatically and hydrolytically degrading HA macromers then provided a tunable platform to investigate the effects of temporal degradation on chondrogenesis and ECM deposition. The benefits of these dynamic hydrogels over static hydrogels are discussed in chapter 10.

Lastly, in chapter 11, overall conclusions and future directions are discussed. This includes limitations of the work presented, as well as a description of pilot studies towards the inclusion of peptides in the hydrogels to alter and control growth factor delivery and presentation to encapsulated cells.

## CHAPTER 3

### *Engineering Cartilage Tissue: A Review*

(Adapted from: **C Chung** and JA Burdick, "Engineering Cartilage Tissue," *Adv Drug Deliv Rev*, 2008, 60(2): 243-62)

#### **3.1 Introduction**

Tissue engineering is an evolving field that has the potential to provide permanent solutions to tissue damage and tissue loss to millions of people each year [1]. The basic approach to tissue engineering involves the use of cells, scaffolds, and signaling factors, alone or in combination. Engineering cartilage is no exception to this approach. Due to its limited ability to self repair, cartilage is an ideal candidate for tissue engineering. As research in the field of cartilage tissue engineering advances, new techniques, cell sources, and biomaterials are being explored to overcome the limitations of current treatments, mentioned in Chapter 1, which include: limited cell and tissue availability, donor site morbidity, graft rejection, fear of disease transmission, insufficient integration, or fibrocartilage repair. To date, the properties and structure of native cartilage have not been entirely mimicked by any engineered replacement. This chapter provides an overview of the emerging trends in cartilage tissue engineering, looking at cell source, scaffolds, and stimulating factors. The wide range of approaches investigated for cartilage tissue engineering is summarized in Figure 3.1. Briefly, cells (e.g., chondrocytes, fibroblasts, stem cells) are isolated from the body and expanded *in vitro* with the addition of growth factors, scaffolds, or bioreactors to sufficient numbers without loss of phenotype. These cells are then combined with a scaffold (with or without growth factors) for polymerization *in situ*, direct implantation, or subcultured with mechanical stimulation, soluble factors, or in bioreactors prior to implantation. Once implanted, the TE construct would ideally degrade over time as new tissue is deposited and integrated with the surrounding native cartilage, generating a suitable repair for the cartilage defect.

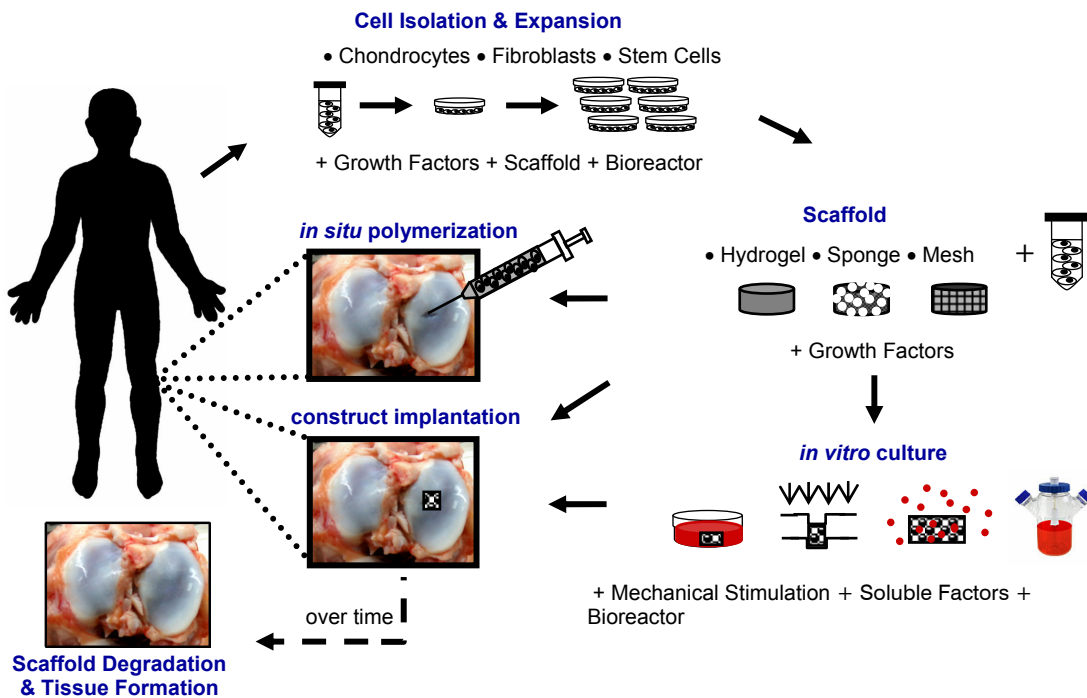


**Figure 3.1** General schematic of approaches used in cartilage tissue engineering, ranging from injectable systems to *in vitro* culture prior to implantation, and numerous biomaterials and culturing methodologies.

### 3.2 Cell Source

The optimal cell source for cartilage tissue engineering is still being identified. Chondrocytes, fibroblasts, stem cells, and genetically modified cells have all been explored for their potential as a viable cell source for cartilage repair (Table 3.1). Chondrocytes are the most obvious choice since they are found in native cartilage and have been extensively studied to assess their role in producing, maintaining, and remodeling the cartilage ECM. Also, fibroblasts are easily obtained in high numbers and can be directed toward a chondrogenic phenotype [2]. Recent work has focused more on stem cells, which have multi-lineage potential and can be isolated from a plethora of tissues. These progenitor cells can be expanded through several



passages without loss of differentiation potential. Additionally, all of these cells can be modified genetically to induce or enhance chondrogenesis. The goal is to find an ideal cell source that can be easily isolated, is capable of expansion, and can be cultured to express and synthesize cartilage-specific molecules (e.g., type II collagen and aggrecan).

**Table 3.1** Cell sources used in the regeneration of cartilage tissues.

<b><i>Cell Source</i></b>	<b><i>Example References</i></b>
Chondrocytes	
Articular	[3-9]
Auricular	[10-14]
Costal	[12,15-17]
Nasoseptal	[18-22]
Fibroblasts	[2,23-25]
Stem Cells	
Bone-marrow derived	[26-31]
Adipose-derived	[32-37]
Muscle-derived	[38-40]
Synovium-derived	[41-43]
Periosteum-derived	[44-46]
Embryonic	[47-51]

### **3.2.1 Chondrocytes**

Differentiated chondrocytes are characterized by a rounded morphology and the production of ECM molecules such as type II collagen and sulfated glycosaminoglycans (GAGs). Chondrocytes maintain and remodel cartilage matrix tissue by a careful balance of catabolic and anabolic processes involving matrix metalloproteinases (MMPs) and tissue inhibitors of metalloproteinases (TIMPs). Preserving these characteristics is crucial for chondrocytes to be used as a cell source for cartilage repair. A variety of key issues involving the use of chondrocytes as a cell source for clinical application will be covered in this section.

#### ***Chondrocyte Expansion***

As mentioned above, one of the major challenges for cartilage tissue engineering is obtaining sufficient cell numbers to fill a clinically relevant defect. Chondrocytes are limited in

number, comprising only 5 to 10% of cartilage tissue, and thus, need to be expanded prior to use. Unfortunately, monolayer expansion causes dedifferentiation of chondrocytes, which is characterized by decreased proteoglycan synthesis and type II collagen expression and increased type I collagen expression. Changes in the expression of collagens [52,53], integrins [54], growth factors [55], and matrix modulators [56] and the activation of signaling proteins like src homology collagen (SHC) and extracellular signal-regulated kinase 1/2 (Erk1/2) [57] accompany dedifferentiation and are used as early markers or signs of irreversibly dedifferentiated cells. Darling *et al*, showed changes in articular chondrocyte gene expression (type I and type II collagen, aggrecan, and superficial zone protein) as early as the first passage, even when encapsulated in alginate beads [58]. Furthermore, the use of passaged cells can have dramatic effects on engineered cartilage tissue [10].

A variety of substrates [59-61] and growth factors (GFs) like fibroblast growth factor-2 (FGF-2) [62] have been used to prevent or slow chondrocyte dedifferentiation in monolayer cultures. For instance, the gene expression of chondrocytes was similar when grown on aggrecan-coated polystyrene to cells redifferentiated in 3D agarose gels [61]. However, substrates coated with fibronectin and type I/II collagen were unable to prevent the loss of phenotype [60,61]; though type II collagen-expanded human articular chondrocytes are able to regain their phenotype when cultured in pellets in chondrogenic medium and expressed higher mRNA for type II collagen and greater GAG production over tissue culture polystyrene-expanded chondrocytes [59].

Three dimensional cultures, such as agarose [63], alginate beads [64], and fibrin glue [65] may preserve the chondrocyte phenotype (i.e., increased aggrecan production and type II collagen expression). However, some complications may be encountered during cell recovery [65]. Thermoreversible hydrogels, like poly(N-isopropylacrylamide-co-acrylic acid) (PNiPAAm-co-Aac), have also been used to expand chondrocytes without loss of phenotype, and the thermoreversible nature of the gels allows for easy cell recovery [66]. Once expanded, differentiated chondrocytes can be released and seeded onto other scaffolds. Also, Malda *et al*

showed that nasal and articular chondrocytes could be expanded without dedifferentiation on macroporous gelatin CultiSher and Cytodex-1 microcarriers, respectively, with doubling times comparable to standard T-flask expansion [67,68].

In addition, a variety of methods have been employed to redifferentiate chondrocytes including the use of 3D scaffolds, bioreactors (e.g., rotating wall reactors) [69], reduced oxygen tension [70], and with GFs like transforming growth factor- $\beta$  (TGF- $\beta$ ), FGF, and insulin-like growth factor (IGF) [71]. In addition, co-culture with up to 20% of primary cells has up-regulated expression of aggrecan, type II collagen, and transcription factor Sox 9, while down-regulating type I collagen [72]. Finally, redifferentiation can be affected by surface chemistry. Woodfield *et al* showed that a substrate with low adhesion supported a chondrocytic phenotype, where cells exhibited a round morphology and minimal expression of the  $\alpha 5 \beta 1$  fibronectin integrin [73].

### *Zonal Organization*

Articular cartilage is an anisotropic tissue composed of a superficial, middle, and deep zone. Each distinct zone varies in structure and function, responds to different stimuli, and secretes different proteins [58]. Chondrocytes isolated from each zone have unique growth rates [74], gene expression [75,76], and levels of biosynthesis [5,77]. For instance, chondrocytes isolated from the superficial layer exhibit increased superficial zonal protein (SZP) expression, while chondrocytes from middle and deep zones exhibit increased type II collagen expression [75,76]. An increase in GAG and collagen is observed with increased depth, providing the deep zone with superior mechanical properties compared to the superficial zone [5,77]. Typically, articular cartilage engineering studies use homogenous cell mixtures from immature animals, which yield chondrocytes that produce large amounts of ECM, but lack zonal organization. Recently, more attention has been focused on the differences among these zones, and methods of recreating zonal organization in engineered constructs are being explored, including multilayer hydrogels and porous gradient scaffolds.

Bilayer poly(ethylene oxide) diacrylate (PEODA) [78] and multilayer poly(ethylene glycol) diacrylate (PEGDA) [79] hydrogels have been engineered to support the growth of isolated articular chondrocyte subpopulations. Using sequential photopolymerization of multiple layers, cell populations can be distributed in layers throughout a 3D construct. These multilayered constructs exhibited similar cell and ECM distribution patterns to that of native cartilage [79] and the bilayer constructs expressed greater shear and compressive strengths than homogenous cell-seeded constructs [78]. In addition, the influence of anisotropic pore architecture on zonal organization has also been investigated. Porous poly(ethylene glycol)-terephthalate–poly(butylene terephthalate) (PEGT/PBT) copolymer scaffolds with either homogenous pores or pore-size gradients were developed using a 3D fiber deposition technique. *In vitro* cultures yielded inhomogenous cell distributions and zonal distributions of GAGs and type II collagen similar to that of native cartilage [80]. The regeneration of zonal organization of engineered cartilage may be important towards the development of functional tissue.

#### *Chondrocyte Sources*

Many studies have focused on the use of articular chondrocytes as a viable cell source for cartilage repair. However, the harvesting of joint cartilage is a highly invasive procedure accompanied by the potential for donor site morbidity and loss of function. In addition, low cell yields, low mitotic rates, and low bioactivity can further limit the use of articular chondrocytes in a clinical setting. With these limitations in mind, other potential autologous chondrocyte sources in the body including auricular, nasoseptal and costal cartilage are being investigated. Known differences among these chondrocyte sources in terms of function, structure, and composition make each unique in elaborating an ECM with discrete biochemical, physical and biomechanical properties; and thus, the eventual choice of chondrocyte depends on the desired application.

Auricular cartilage is an elastic cartilage found in the ear and epiglottis. In a study by van Osch *et al*, human auricular chondrocytes were investigated for their potential use in cartilage repair [14]. Compared to articular cartilage, auricular chondrocyte isolation resulted in cell yields

2-fold higher and cell proliferation rates 4 times faster, while retaining chondrogenic potential when cultured in alginate beads. With *in vivo* culture, constructs exhibited proteoglycan-rich matrices with positive type II collagen staining and faint elastin staining. In addition, auricular chondrocyte samples produced neocartilage with greater biochemical and histological similarity to that of native cartilage than articular counterparts when implanted *in vivo* [13].

Nasoseptal cartilage is a hyaline cartilage that has received attention for applications in craniofacial and plastic surgeries. Adult nasal chondrocytes are capable of generating a matrix with high collagen II/I ratio and GAG accumulation [18]. In addition, nasal chondrocytes proliferate 4 times faster than articular chondrocytes in monolayer [18], and can be seeded at very low seeding densities with an 838-fold expansion in one passage without dedifferentiation [81]. Also, nasal chondrocytes have been successfully cultured as macroaggregates [82], on collagen microcarriers [83], and in a number of scaffold systems including alginate [64], PEGT/PBT block copolymer [19], methylcellulose [22], and HYAFF(R)11 [84], a hyaluronic acid (HA) derivative. These cells show good viability and produce an ECM-rich tissue with high expression of type II collagen under appropriate culture conditions [19,22,82-84]. Additional studies show that nasal chondrocytes respond to growth factors like TGF- $\beta$ 1, FGF-2, bone morphogenic protein-2 (BMP-2), and IGF-1 [20,21] in serum-free culture with enhanced proliferation and/or matrix deposition.

In a chondrocyte source comparison study, bovine nasal, articular, costal, and auricular chondrocytes were grown on poly(L-lactide- $\epsilon$ -caprolactone) scaffolds for 4 weeks [15]. Growth rates and gene expression varied with cell type, where the highest expression of type II collagen and aggrecan was found for costal chondrocytes, followed by nasoseptal, articular, and auricular chondrocytes. The construct size also varied, with auricular cell constructs having the largest diameter and costal constructs the greatest thickness. Another study looked at the effect of GFs on auricular, nasal, and costal chondrocytes and showed that all cell types exhibited increased proliferation, GAG/DNA content, and up-regulation of type II collagen expression after GF supplementation. However, redifferentiation was only achieved in auricular and nasal

chondrocyte cell pellets [16]. Furthermore, Johnson *et al* demonstrated that articular, auricular, and costal chondrocytes were all able to form new cartilaginous matrix when cultured in fibrin glue-cartilage composites *in vivo* [12].

#### *Aged, Osteoarthritic, Cryogenically-Preserved Chondrocytes*

As mentioned previously, efforts in cartilage regeneration have focused primarily on chondrocytes isolated from immature animals. These neonatal and young chondrocytes have faster growth rates, the capacity for rapid *in vitro* expansion, and greater chondrogenic potential (increased Sox 9 and type II collagen expression) over chondrocytes from older donors [76]. Although these traits are advantageous for expanding chondrocytes and producing ECM-rich neocartilage, the use of immature cartilage in a clinical setting for older patients may not be possible. Thus, the proliferative and chondrogenic potential of adult, osteoarthritic, and even cryogenically preserved chondrocytes are also explored as alternative cell sources.

In agarose gels, older chondrocytes exhibit decreased cell yields [85], lower proliferation rates [76,85-87], diminished chondrogenic potential [76,87] and decreased tensile stiffness [88] when compared to fetal and young chondrocytes. However, these limitations can be countered with the addition of GFs like TGF- $\beta$ 1 [85], TGF- $\beta$ 2 [87], FGF-2 [85], platelet-derived growth factor (PDGF) [85], and/or IGF-1 [87]. Also, culture in serum-free media resulted in increased proliferation rates, a greater ratio of type II to type I collagen, and decreased expression of MMP-3, which is commonly associated with matrix degradation [86]. When articular chondrocytes from young and old sheep were encapsulated in fibrin glue and cultured subcutaneously in nude mice for 7 and 12 weeks, constructs from old and young donors exhibited similar patterns of ECM deposition, with increasing DNA, GAG, and hydroxyproline content over culture time [8]. Other culture environments like the rotating wall vessel (RWV) with controlled oxygen tension were used to show that aged articular chondrocytes were capable of aggregating and forming solid tissue with positive staining for type II collagen after 12 weeks [89]. Research still needs to be

performed to optimize culture techniques for these aged cells and to define their limitations and potential use in a clinical setting.

Osteoarthritic (OA) chondrocytes have also been investigated for their potential in cartilage repair. Both *in vitro* and *in vivo* culture of OA cells on HYAFF®11 yielded positive staining for type II collagen and sulfated proteoglycans and negative staining for type I collagen [90]. Furthermore, OA articular chondrocytes can be transduced with Sox 9 via adenoviral and retroviral vectors to stimulate type II collagen expression and deposition in both monolayer and alginate bead cultures [6]. Finally, cryogenically preserved cells may provide an alternative source for cartilage regeneration. Septal chondrocytes frozen for 3 years showed evidence of hyaline growth on knitted polygalactin 910 woven mesh scaffolds after 6 weeks of culture in a slowly turning lateral vessel [91].

### **3.2.2 Fibroblasts**

Skin presents a minimally invasive, relatively abundant source of fibroblasts for tissue engineering. Although the direct transplantation of fibroblasts on PLA meshes in a cartilage defect leads to fibrous tissue production [92], fibroblasts can be redirected towards a chondrocytic phenotype when cultured under the appropriate conditions. Human dermal fibroblasts pretreated with IGF-1 and cultured on aggrecan form dense aggregates that stain positive for GAGs and type II collagen [24]. In addition, dermal fibroblasts cultured in the presence of demineralized bone [93], or grown as high density micromass cultures in the presence of lactic acid [2] express cartilage specific matrix proteins like aggrecan and type II collagen. Also, fibroblasts expressing active TGF- $\beta$ 1 were injected into cartilage defects and showed evidence of newly formed hyaline cartilage after 6 weeks [25]. Recently, Deng *et al* isolated a subpopulation of skin-derived cells called dermis-isolated, aggrecan-sensitive (DIAS) cells [23]. These cells up-regulate aggrecan, cartilage oligomeric matrix protein (COMP), and type II collagen over unpurified dermis cells.

Furthermore, 3D self-assembled constructs developed from DIAS cells show evidence of rich cartilage-specific ECM.

### **3.2.3 Stem Cells**

Recently, stem cells have generated significant interest in cartilage tissue engineering as an alternative to autologous chondrocytes. Stem cells are multipotent cells that can be differentiated down multiple cell lineages given the appropriate cues. In 1998, bone-marrow derived stem cells were found to undergo chondrogenesis when cultured in cell aggregates in the presence of TGF- $\beta$ 1[94]. More recently, adipose tissue has been identified as a source of stem cells that can be isolated under local anesthesia with minimal discomfort [37]. Other sources of stem cells investigated for cartilage repair include muscle [38,40], synovium [41-43], and periosteum [44].

#### ***Bone Marrow-derived Stem Cells***

Bone marrow-derived stem cells (BMSCs) undergo chondrogenesis in a variety of culture conditions, which typically involves induction with TGF- $\beta$  and a 3D culture environment (e.g., cell pellets and micromasses). For *in vitro* culture, the addition of TGF- $\beta$  has generally stimulated enhanced chondrogenesis, regardless of culture method or scaffold; however, the degree of chondrogenesis is scaffold dependent [95]. For example, Coleman *et al* showed increased sulfated GAG production by BMSCs in alginate over agarose gels [95]. To date, numerous scaffolds have been used in conjunction with TGF- $\beta$  and chondrogenic media supplementation towards the chondrogenesis of BMSCs including: agarose [95,96], alginate [95], poly(ethylene glycol) (PEG) [29], poly(glycolic acid) (PGA) [97], silk [98,99], poly(DL-lactic-co-glycolic acid)-collagen (PLGA-collagen) meshes [100], gelatin/chondroitin/HA tri-copolymer [101], and electrospun polycaprolactone (PCL) [27]. Evidence of chondrogenesis was characterized by enhanced type II collagen and aggrecan expression and accumulation. In addition to TGF- $\beta$ , the



cycling of growth factors (BMP-6 and IGF-1) during *in vitro* culture also affects chondrogenesis [102]. In addition, cultures of BMSCs with components of the joint cavity, like synovial fluid or synovial cells, induce chondrogenesis *in vitro* [26].

For *in vivo* delivery, a controlled method of TGF- $\beta$  introduction is usually employed to induce chondrogenesis. Alginate beads loaded with TGF- $\beta$ 1 exhibited sustained release for 35 days in PBS at 37°C and induced chondrogenesis [103]. Others have loaded TGF- $\beta$ 1 in gelatin microspheres, which enhanced MSC repair in a full-thickness defect over *in vitro* differentiated cells [104]. Using a gene therapy approach, human MSCs lipofected with TGF- $\beta$ 2 showed an up-regulation of type II collagen and aggrecan expression and enhanced matrix synthesis for up to 4 weeks [105]. In addition, differentiation *in vivo* without GF release has also been investigated. In these cases, BMSCs rely on the scaffold and the natural *in vivo* environment for differentiation cues. Various scaffolds without incorporated GF release have been investigated including: HA [106], PGA [107], and beta-tricalcium phosphate ceramic [105] scaffolds. One study showed that cryopreserved human BMSCs were capable of producing cartilaginous tissue when subcultured on PGA scaffolds *in vitro*, followed by implantation in nude mice for 10 weeks [97]. Furthermore, osteoarthritic BMSCs maintained their differentiation potential during monolayer expansion in the presence of FGF-2 [108]. Additionally, the co-culture of BMSCs and chondrocytes increased cell proliferation and cartilaginous ECM deposition with positive expression for type II collagen [109,110]. This may be attributed to GF secretion and cell-cell interactions [109] or a chondrogenic microenvironment provided by the chondrocytes to promote the *in vivo* chondrogenesis of MSCs [110].

However, a limitation of BMSCs is the mechanical integrity of the matrix they produce [28]. In a long-term agarose culture, chondrogenesis was observed in the MSC-laden gels, but the amount of matrix produced and mechanical properties were inferior to that produced by chondrocytes from the same donor [28]. The GAG content and the equilibrium modulus of MSC-laden gels plateaued with time, suggesting diminished chondrogenic capacity rather than delayed differentiation.

### *Adipose-derived Stem Cells*

A fibroblast-like population of stem cells can be isolated from adipose tissue and cultured *in vitro* for an extended period with stable expansion and low levels of senescence [37]. These cells are mesenchymal in origin, as determined by immunofluorescence and flow cytometry, and are capable of differentiating into chondrocytes in the presence of TGF- $\beta$ , ascorbate, and dexamethasone in combination with a 3D culture environment [37,111]. Differentiation has been achieved in high density micromass cultures [35,112], and in alginate [32,34,36], agarose [32], and collagen-based scaffolds [32,113]. During *in vitro* culture, chondro-induced ADSCs produced cartilage-specific matrix proteins and exhibited an increase in equilibrium compressive and shear moduli with accumulation of sulfated-GAGs [32]. In monolayer culture, these cells exhibited prehypertrophic alteration in late stages after induction [36]. Masuoka *et al* showed hyaline cartilage repair in full-thickness defects in rabbits using ADSCs and an atelopeptide type I collagen honeycomb-shaped scaffold [113]. In addition, a novel elastin-like polypeptide (ELP) has been shown to promote chondrogenic differentiation of ADSCs without media supplements [33]. After 2 weeks of culture, similar accumulations of sulfated GAGs and type II collagen were observed in constructs cultured in chondrogenic and standard media.

The use of GFs, like FGF-2 and BMP-6, also affects the chondrogenesis of ADSCs. FGF-2 increases cell proliferation and enhances chondrogenesis by inducing N-Cadherin, FGF-R2, and Sox 9 in micromass culture [112]. BMP-6 alone also upregulates the expression of aggrecan (205-fold) and type II collagen (38-fold) in alginate culture [114]. Despite their ability to undergo chondrogenesis, comparative studies suggest that ADSCs have lower chondrogenic potential than stem cells isolated from other sources such as bone marrow [30,42,115,116]. A lower accumulation of cartilage-specific matrix proteins [42,115,116] and lower type II collagen gene expression [30,115] over other cell types suggests that more research needs to be done to optimize the chondrogenic potential of ADSCs.

### *Other Adult Stem Cells*

Besides bone marrow and adipose tissue, muscle, synovium, and periosteum are other sources of adult stem cells being explored for applications in cartilage repair. Nawata *et al* generated cartilaginous tissue with muscle-derived stem cells (MDSCs) using type I collagen scaffolds with the addition of BMP-2 and diffusion chambers [40]. These constructs were then implanted into full thickness rat defects, and resembled mature cartilage after 5 weeks. MDSC-seeded type I collagen gels performed similarly to chondrocyte-seeded constructs in full thickness defects [38].

Stem cells isolated from synovium have been cultured in micromasses [41], and in alginate [41] and collagen gels [43] to produce cartilaginous tissue. In alginate culture, BMP-2 stimulates a dose-dependent expression of Sox 9, type II collagen, and aggrecan in these encapsulated cells that was comparable to articular chondrocytes [41]. However, this was not true for TGF- $\beta$  isoforms, suggesting that the effects of GFs may differ depending on stem cell source. In a comparative study of mesenchymal stem cells (MSCs) isolated from 5 different tissue sources, synovium-derived stem cells were shown to have the greatest chondrogenic potential [42]. In fracture healing and callus distraction, periosteum-derived stem cells (PDSCs) differentiated into chondrocytes during endochondral ossification. Although the factors regulating this process are still unclear, GFs assist periosteum-derived stem cell chondrogenesis. In an *in vitro* agarose culture, the addition of IGF-1 improved PDSC chondrogenesis in a dose-dependent manner and was improved with the addition of TGF- $\beta$ 1 [44].

### *Embryonic Stem Cells*

Embryonic stem cells (ESCs) are obtained from the inner cell mass of blastocyst stage embryos. These cells are capable of many doublings and have the ability to differentiate into all somatic cell types. Although ESCs are appealing as a cell source for their vast proliferation capabilities, difficulties in ESC selection and purity, as well as antigenicity and ethical issues, may hinder their clinical use. For chondrogenesis, ESCs must pass through an aggregation stage of

embryonic bodies (EBs) before differentiation. Mouse embryonic bodies encapsulated in PEG hydrogels showed chondrogenesis with upregulation of cartilage specific markers, while stimulation with TGF- $\beta$ 1 resulted in basophilic ECM deposition characteristic of neocartilage [47,48]. In addition, mouse ESCs undergo chondrogenesis with the addition of BMP-2 and BMP-4, exhibiting increased Alcian blue and type II collagen staining [49]. However, different mouse embryonic stem cells lines exhibit varying degrees of spontaneous chondrogenic differentiation [117]. A study with human ESCs demonstrated that human ESC-derived EBs were capable of complete chondrogenesis from chondrogenic induction to hypertrophic maturation [50]. EB cells dissociated and plated as high-density micromasses, as well as the addition of BMP-2, accelerated and enhanced chondrogenesis with the formation of a cartilage-rich ECM composed of collagen and proteoglycans. Furthermore, co-culture of human ESCs with primary chondrocytes was shown to induce chondrogenesis, where the co-cultured cells expressed Sox 9 and type II collagen, whereas cultures of human ESCs alone did not [51]. Overall cartilage tissue engineering research with ESCs is still relatively new and as we learn more about ESCs, new strategies for purification and differentiation will be identified to fully access their potential as a viable cell source for cartilage engineering.

*In the work presented in this dissertation, all studies utilized either primary swine chondrocytes (both auricular and articular) or primary human bone-marrow derived stem cells.*

### **3.3 Scaffolds**

Numerous scaffolding materials have been used for cell delivery in cartilage regeneration. The primary focus has been on polymeric materials, in forms of hydrogels, sponges, and fibrous meshes (Figure 3.2).

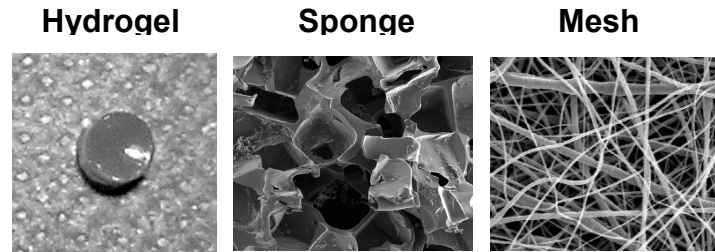


**Figure 3.2** Examples of different scaffold architectures used in the engineering of cartilage tissues.

Scaffolds provide a 3D environment that is desirable for the production of cartilaginous tissue. Ideally the scaffold should: 1) have directed and controlled degradation, 2) promote cell viability, differentiation, and ECM production, 3) allow for the diffusion of nutrients and waste products, 4) adhere and integrate with the surrounding native cartilage, 5) span and assume the size of the defect, and 6) provide mechanical integrity depending on the defect location. Scaffold degradation can occur hydrolytically or enzymatically, and by controlling degradation temporally and spatially, scaffolds can enhance and direct new tissue growth. For example, scaffolds with degradable and non-degradable units show improved ECM distribution compared to completely non-degradable scaffolds [118]. However, a balance must be found since slow degradation may impede new cartilaginous ECM production, while fast degradation may compromise structural support and shape retention. For instance, Solchaga *et al* showed that scaffolds with slower degradation rates yielded cartilage of greater thickness in an osteochondral defect model, but cracks and fissures were evident on the cartilage surface [119].

In designing a scaffold, cell seeding density and seeding method should be carefully considered since the appropriate numbers of cells must be used to ensure adequate cell-cell interactions. Many approaches attempt to mimic the natural condensation of cells during embryonic cartilage development by seeding in aggregates or at high densities. Higher initial seeding densities tend to facilitate greater ECM synthesis and deposition, presumably due to cell-cell interactions [96,120,121]. The method of seeding, statically or dynamically, can dictate cell

distribution and infiltration into the scaffold. In sponge and mesh scaffolds, dynamic seeding can improve cellular distribution [120], whereas hydrogels typically support uniform cell distributions if cells are adequately suspended during gelation.

To date, a wide range of natural and synthetic materials have been investigated as scaffolding for cartilage repair. Natural polymers that have been explored as bioactive scaffolds for cartilage engineering include: alginate, agarose, fibrin, HA, collagen, gelatin, chitosan, chondroitin sulfate, and cellulose (Table 3.2).

**Table 3.2** Types of biomaterials used in cartilage tissue engineering.

<i><b>Biomaterial</b></i>	<i><b>Example References</b></i>
<b>Natural Polymers</b>	
agarose	[7,28,63,122,123]
alginate	[41,103,124-126]
cellulose	[22,127]
collagen	[128-132]
chitosan	[133-137]
chondroitin sulfate	[104,138,139]
fibrin glue	[140-143]
gelatin	[137,144-146]
hyaluronic acid	[11,84,147-150]
silk fibroin	[98,99,151-153]
<b>Synthetic Polymers</b>	
poly( $\alpha$ -hydroxy esters)	[154-160]
poly(ethylene glycol/oxide)	[29,48,79,118,161-163]
poly(NiPAAm)	[66,164-166]
poly(propylene fumarate)	[167-169]
poly(urethane)	[141,170-172]
poly(vinyl alcohol)	[173-175]
<b>Self-assembling Peptides</b>	[176-179]

Natural polymers can often interact with cells via cell surface receptors and regulate or direct cell function. However, due to this interaction, these polymers may also stimulate an immune system response; thus, antigenicity and disease transfer are of concern when using these biomaterials. In addition, natural polymers may be inferior mechanically and subject to variable enzymatic host degradation. On the other hand, synthetic polymers are more controllable and predictable, where chemical and physical properties of a polymer can be modified to alter mechanical and degradation characteristics. Synthetic polymers currently

explored for cartilage repair include: poly( $\alpha$ -hydroxy esters), PEG, poly(NiPAAm), poly(propylene fumarates), and polyurethanes (Table 3.2). However, unless specifically incorporated, synthetic polymers do not benefit from direct cell-scaffold interactions, which can play a role in adhesion, cell signaling, directed degradation, and matrix remodeling. In addition, degradation byproducts may be toxic or elicit an inflammatory response. Finally, scaffold architecture also plays a major role in dictating cellular behavior. Scaffolds can be categorized into hydrogels, sponges, and fibrous meshes (Figure 3.2). The following sections outline the advantages and disadvantages to each scaffold structure and introduce materials that have been investigated for cartilage tissue engineering.

### **3.3.1 Hydrogels**

Hydrogels are water swollen networks, suitable for the delivery of cells and bioactive agents. Hydrogels may be used as injectable scaffolds since they easily fill defects of any size and shape and may be implanted in a minimally invasive manner. Hydrogels support the transport of nutrients and waste, and can homogeneously suspend cells in a 3D environment, where encapsulated cells typically retain a rounded morphology that may induce a chondrocytic phenotype. Hydrogels are also capable of transducing mechanical loads to exert controlled forces on encapsulated cells, similar to physiological conditions. Though their mechanical properties can be altered by crosslinking density (which may compromise cell viability) limited mechanics may be the major drawback to using hydrogels [4].

Hydrogels are crosslinked either physically or chemically. Physically crosslinked gels are held together by molecular entanglements and/or secondary forces like ionic or hydrogen bonding or hydrophobic interactions, while chemically crosslinked gels are covalently bonded. Molecular weight, macromer concentration, method of crosslinking, crosslinking density, and mesh size dictate the physical and chemical properties of the hydrogel including: swelling ratio, mechanics, cell viability, and degradation rate. Photopolymerization is one approach to chemically crosslink

hydrogels using ultraviolet or visible light, and provides uniform cell seeding with both spatial and temporal control over polymerization [180]. Careful screening of photoinitiating conditions has been performed to optimize cell viability within these crosslinked networks [181].

PEG is a relatively inert polymer and supports chondrogenesis when crosslinked into hydrogels [4]. Further modifications to PEG, including the addition of hydrolyzable units and bioactive peptides have improved cartilage tissue growth [118]. For instance, degradable lactic acid units have been added to PEG hydrogels to increase cell proliferation and ECM deposition [4,118,182,183]. Recently, Lee and colleagues covalently incorporated a collagen mimetic peptide (CMP) into PEG hydrogels [163]. CMP is known to associate with type I collagen and other ECM fibers, forming physical crosslinks that can then be manipulated by cells. This study showed that PEG hydrogels conjugated with CMP limited the diffusion of exogenous type I collagen and increased ECM production by encapsulated chondrocytes. PEG has also been combined with methacrylated poly(glycerol succinic acid) dendrimers [184].

Another polymer used for cartilage tissue regeneration is HA, a linear polysaccharide found natively in cartilage. It functions as a core molecule for the binding of keratin sulfate and chondroitin sulfate in forming aggrecan in cartilage and degrades primarily by hyaluronidases found throughout the body. HA plays a role in cellular processes like cell proliferation, morphogenesis, inflammation, and wound repair [185], and may function as a bioactive scaffold, where cell surface receptors for HA (CD44, CD54, and CD168) allow for cell/scaffold interactions. For photopolymerization, HA can be modified with methacrylate groups [150,186], and by varying the molecular weight and concentration of the modified HA, a wide range of properties can be obtained [147]. Increases in macromer concentrations significantly increased the network compressive modulus and degradation time while decreasing the swelling ratio and cell viability [147]. These variations in scaffold properties also affected neocartilage formation by auricular chondrocytes *in vivo* [11]. In a recent *in vivo* rabbit defect model, Liu *et al* investigated the quality of repair using HA-gelatin hydrogels seeded with MSCs. Defects with MSCs alone exhibited hyaline-like cartilage on the peripheral defect area and fibrous repair in the middle, whereas



defects filled with a scaffold and MSCs resulted in elastic, firm, translucent cartilage with zonal architecture and good integration with the surrounding cartilage [187]. Chondroitin sulfate, another major constituent of cartilage, can also be photopolymerized with similar modifications to produce hydrogels that exhibit viscoelastic behavior [139]. These chondroitin sulfate based hydrogels support viable chondrocytes and can be degraded in the presence of chondroitinase ABC. Furthermore, chondroitin sulfate can be copolymerized with PEG to increase the hydrogel pore size and provide bioactive cues for encapsulated cells [139].

Fibrin glue is a natural polymer formed from the polymerization of fibrinogen with thrombin, and it elicits good biocompatibility as a wound adhesive and can facilitate cell-matrix interaction via integrin binding [188]. It is attractive as a natural scaffold because it can be made from autologous blood. However, one drawback is that gels tend to shrink *in vivo*. Recently, a long-term stable fibrin gel has been developed that is transparent and stable for 3 weeks [140]. This gel exhibits a broad linear viscoelastic region, withstands loads of 0.0001 to 10kPa, and supports chondrocyte proliferation and cartilaginous ECM production while retaining its size and shape. Studies in nude mice have shown the suitability of using fibrin glue as a biomaterial, where degradation and polymerization time can be controlled by fibrinogen and thrombin concentrations, respectively [142]. Fibrin glue has also been combined with other polymers like polyurethane and improved cell seeding viability and distribution, and increased the expression of aggrecan and type II collagen [141].

Type I and type II collagen scaffolds have inherent biological cues that allow chondrocytes to interact and remodel the hydrogel. A type I collagen gel seeded with autologous chondrocytes has been used to treat full thickness defects in rabbits with newly regenerated cartilaginous tissue formation seen after 6 months and tissue organization after 12 months [129]. Gelatin, which is derived from collagen, is also biocompatible and can be modified to crosslink with visible light and support chondrocytes, though some potential diffusion limitations may exist [145]. Also, gelatin/alginate gels promoted chondrocyte proliferation, a rounded morphology, and

expression of hyaline matrix molecules with increased spatial deposition of proteoglycans and constant expression of type II collagen [189].

Alginate is a polyanionic polymer found in brown algae, and can be crosslinked with bivalent cations to form stable ionically crosslinked gels. Alginate beads and hydrogels have been used to expand chondrocytes and induce stem cell differentiation [32,34,36]. Recently, investigators have modified alginate gels with synthetic adhesion peptides [190] or combined alginate with other materials to make hybrid scaffolds [189,191,192]. RGD-functionalized alginate has been shown to affect articular chondrocyte attachment and morphology and chondrogenesis [124,190]. Also with increasing crosslinking density and substrate stiffness, chondrocytes grown on alginate gels exhibited a more flattened morphology with stress fibers observed via phalloidin staining [124]. Despite its advantages for studying *in vitro* chondrogenesis, limitations to alginate gels include low mechanical properties and slow degradation rate.

Agarose is a linear polysaccharide derived from Asian seaweeds that solidifies when cooled, and has been widely used to study chondrocyte response to deformational loading since it is able to transmit applied mechanical forces to cells during compression [7]. Chitosan is a biosynthetic polysaccharide derivative of chitin that is found in the exoskeletons of arthropods that is a liquid at room temperature and gels at physiological temperatures. It is a semi-crystalline polymer that is biocompatible, degraded *in vivo* by lysozymes, and can interact with GFs and adhesion proteins. In addition, a number of methods have been used to ionically or covalently crosslink chitosan or chitosan derivatives, to improve mechanical properties [136,193]. Chitosan and chitosan hybrid hydrogels support normal chondrocyte phenotypes in 2D [136,193] and 3D cultures [194]. Some synthetic copolymers have also been investigated as thermoreversible hydrogels, with gelation occurring above their lower critical solution temperature (LCST). These include p(NiPAAm-co-AAC) and poly(propylene fumarate-co-ethylene glycol) (p(PF-co-EG)), which are capable of retaining chondrocyte phenotype and viability [164,167]. Within these gels, cells remained responsive to co-encapsulated soluble factors like HA and TGF- $\beta$ 3, which can lead to increased expression and synthesis of cartilage-specific ECM proteoglycans [165].

Self-assembling peptides constitute another class of biomaterials that can be made into hydrogels, and form by amino acid sequences of alternating ionic hydrophobic and uncharged hydrophilic side groups. These self-assembling peptide hydrogels form stable  $\beta$ -sheets of interwoven nanofibers when exposed to an electrolyte solution and are capable of rapidly encapsulating chondrocytes at physiological electrolyte concentrations and pH levels. RAD-, ELK-, and EAK-based peptides form strong  $\beta$ -sheet secondary structures in aqueous solutions [176]. For example, Zhang and coworkers have produced a stable self-assembling EAK16 membrane that does not dissolve by the addition of heat, acidic or alkaline solutions, or proteolytic enzymes [179]. This stability may be due to complementary ionic bonds between glutamic and lysine side chains. Kisiday *et al* showed that articular chondrocytes maintain their phenotype and produce cartilage-like ECM after 4 weeks when encapsulated in self-assembling peptide KLD-12 hydrogels *in vitro* [177] and respond to dynamic compression loading, with an increase in proteoglycan synthesis and mechanical properties over free-swelling controls [178]. In addition, synthetic self-assembling peptides can be modified to incorporate biologically active motifs that promote cell-matrix interactions [176].

### **3.3.2 Sponges**

Sponges are porous scaffolds whose properties are dependent on pore size, porosity, and interconnectivity. Porosity dictates surface area [184] for cell adhesion, while pore size and interconnectivity affect cell infiltration and migration, matrix deposition and distribution [195], and nutrient and waste exchange. To date, several methods have been employed to manufacture sponges, including: porogen leaching, freeze-drying, and gas foaming. These manufacturing methods affect scaffold architecture, which in turn affects tissue formation, and can be used to encapsulate GFs [196]. To date, numerous materials have been used to fabricate sponge scaffolds, including poly( $\alpha$ -hydroxy esters) [197,198], alginate [126], polyglactin/polydioxanone [199], chitosan [134,135,137], silk fibroin [98,99,151,153], HA [104,119], collagen [200] and

gelatin [104,137,144]. A novel biodegradable elastomer scaffold from poly(1,8 octanediol citrate) (POC) has been fabricated by salt-leaching and supported the growth of chondrocytes *in vitro* [201]. This POC scaffold is capable of complete recovery from compressive deformation, and may provide good structural support in the mechanically loaded knee environment. In addition, resorbable polyglactin/polydioxanone scaffolds have been used in full thickness equine defects and showed good cartilage repair with integration into surrounding tissue [199].

Chitosan can also be formed into sponges via freeze-drying and lyophilization [135]. In a study by Kuo *et al*, chitosan and chitin hybridized scaffolds in various compositions were investigated as potential scaffolds [134]. An increase from 20 to 50 wt % of chitin resulted in smaller pore diameters, increased surface area, a higher Young's modulus, and lower extensibility, which resulted in increased cell numbers and ECM production in 28 days. Chitosan has also been hybridized with gelatin, which serves as a substrate for cell adhesion [137]. This chitosan/gelatin scaffold was used for elastic cartilage repair and neocartilage exhibited type II collagen, elastic fibers, and GAG production, with total GAG content ~90% of that found in native auricular cartilage [137].

Silk fibroin is composed of a filament core protein called fibroin with a glue-like coat of sericin proteins. Sponges can be formed from silk fibroin by a solvent casting/salt leaching method that supports both chondrocytes [152] and stem cells [99]. Compared to fast degrading collagen scaffolds, silk scaffolds supported greater proliferation and chondrogenesis of MSCs [98,151]. Collagen and collagen hybrid sponges have also been formed that support chondrocyte growth and phenotype retention [200]. The use of collagen microsponges in the porous openings of PLGA fibers [202] and sponges [198] has yielded new hybrid scaffolds with improved properties. Furthermore, type II collagen-GAG scaffolds with varying crosslinking densities can mediate cell behavior. In a study by Vickers *et al*, chondrocytes seeded on type II collagen-GAG scaffolds with low crosslinking densities experienced cell-mediated contraction, an increase in cell number, enhanced chondrogenesis, and increased degradation rates [200].

### 3.3.3 Meshes

Meshes are networks of woven and non-woven fibers, where variations in void volume and fiber diameter and directionality can dictate cell behavior. Non-woven meshes have high void volumes and surface areas that are well suited for tissue regeneration, whereas woven meshes exhibit greater strengths and can be made in a wide range of porosities. In general, these prefabricated forms can be cultured *in vitro* with cells to create mechanically stable scaffolds and then implanted *in vivo* for complete repair. A drawback to prefabricated scaffolds is a difficulty in filling irregularly shaped-defects, where incomplete contact with surrounding cartilage may hinder complete integration. 3D fiber deposition is one technique used to form scaffolds with regulated patterns [203]. Moroni *et al* were able to produce a scaffold with biomechanical properties comparable to bovine articular cartilage using 3D fiber deposition of poly(ethylene oxide) terephthalate/poly(butylene) terephthalate (PEOT/PBT) [204]. This group also adapted the method to develop a shell-core fiber architecture [205].

Recently, electrospinning has generated much interest to produce biomaterials with nano-scale polymer fibers that mimic collagen fibrils in cartilage ECM [156]. Fibers are generated as the surface charge of the polymer droplet overcomes its surface tension in an applied electric field, causing an instability that creates jets of polymer that can then be collected as solvent evaporates. Advantages to using electrospun scaffolds include high surface areas to volume ratios and fully interconnected pores, and the ability to create aligned fibers. By collecting the nanofibers on a rotating mandrel, aligned fibrous scaffolds can be fabricated, and can mimic the anisotropic morphology of some tissues. These nanofibrous scaffolds support chondrocytes and stem cells [27,156].

The most commonly used meshes are made of poly( $\alpha$ -hydroxy esters). These meshes have been used since the early 1990's for cartilage regeneration and include poly(lactic acid) (PLA), PGA, and their copolymers (PLGA). PGA is the most hydrophilic of this group and degrades into a natural metabolite that is completely resorbed through metabolic pathways. On the other hand, PLA, with an additional methyl group, is more hydrophobic, resulting in slower

degradation. Copolymers of PLA and PGA can be optimized for mechanical and degradation properties. Shin *et al* showed that changes in copolymer composition resulted in differential degradation, where PLGA at a 50:50 composition degraded faster than 75:25 due to the higher PGA content [158]. Furthermore, polyester scaffolds can be modified with biological agents like type II collagen [155] and HA [206]. Immobilization of type II collagen on PLLA/PLGA scaffolds increased chondrocyte proliferation and GAG deposition while decreasing inflammatory responses by preventing host tissue infiltration and capsule formation [155]. Immobilization of HA to the surface of PLGA scaffolds enhanced chondrocyte attachment and substantially increased GAG and collagen synthesis [206]. Furthermore, MSCs seeded on PLGA scaffolds resulted in smooth, shiny white hyaline-like tissue after 12 weeks of *in vivo* culture in a rabbit defect [160]. PCL is another member of the poly( $\alpha$ -hydroxy ester) family with slower degradation kinetics. Recently, PCL has been electrospun to form nanofibrous scaffolds capable of supporting proliferating chondrocytes that produce proteoglycan-rich matrices [156]. Furthermore, these scaffolds can also support chondrogenesis of MSCs comparable to cell pellet controls [27].

Several natural materials have also been processed as fibrous scaffolds, including cellulose [127] and HA derivatives [84,149,207,208]. Non-woven cellulose II fabrics coated with calcium phosphate supported better cell adhesion than unmodified fabrics, where calcium leaching from the scaffold has the potential to mimic the cartilage microenvironment in the vicinity of subchondral bone [127]. Non-woven HA esters (HYAFF® derivatives) are semisynthetic, resorbable meshes that support cell adhesion, proliferation, and production of cartilage-specific ECM *in vitro* [84,207,208] and *in vivo* [119,149]. In a pilot study by Radice *et al*, HYAFF®11 elicited no inflammatory response and completely degraded within 4 months of implantation [149]. In a clinical setting, Hyalograft® C (a graft composed of autologous chondrocytes grown on a HYAFF®11 scaffold) has been used to treat a number of human articular cartilage defects [148,209,210]. Hyalograft® C repaired cartilage showed significant improvements over pre-

operation assessments with cartilage regeneration even in joints with progressed osteoarthritis [210].

*In the work presented in this dissertation, all studies utilized photopolymerizable methacrylated hyaluronic acid hydrogels engineered for controlled degradation (enzymatic versus hydrolytic) as cell carriers. Photopolymerizable poly(ethylene glycol) hydrogels were routinely used as control materials.*

### **3.4 Stimulating Factors**

As the third component of the tissue engineering triad, stimulating factors have been employed to induce, accelerate, and/or enhance cartilage formation. For instance, GFs and other additives may be added to culture media *in vitro* or incorporated into scaffolds for *in vivo* delivery to control cellular differentiation and tissue formation. In addition, gene therapy has emerged as another method of local delivery, where cells can be engineered to over-express bioactive molecules. An additional approach is the introduction of mechanical signals through loading regimes such as hydrostatic or dynamic pressure or through the use of bioreactors. Since many types of cartilage depend on mechanical forces to maintain healthy function, this approach has been used to alter cellular differentiation and tissue production.

#### **3.4.1 Growth Factors and Additives**

A number of growth factors like TGF- $\beta$  [211-213], FGF [130,214,215], BMP [216-218] and IGF [168,219,220], along with other soluble factors like HA [126,144,221], chondroitin sulfate [128,130], and insulin [222], have been explored for their effects on cartilage tissue engineering. These factors have been investigated independently and synergistically, with outcomes dependent on cell type and culture conditions. Members of the TGF- $\beta$  family have been shown to play a major role in cartilage development. They are commonly used to induce chondrogenesis

in embryonic [47] and adult MSCs [212,223], to increase cartilage ECM synthesis [133], and to enhance proliferation of chondrocytes [211,224]. Several studies have shown that TGF- $\beta$  isoforms differ in their effects on various cell types, where TGF- $\beta$ 1 is responsible for initial cell-cell interactions between condensing progenitor cells [213], TGF- $\beta$ 2 mediates hypertrophic differentiation, and TGF- $\beta$ 3 has stronger effects on MSC differentiation [225,226]. Another growth factor, IGF-1, acts in an anabolic manner to increase the production of proteoglycans and type II collagen [44,227].

FGF-2 is a mitogen involved in wound healing that has been used to preserve the chondrogenic potential of monolayer expanded chondrocytes [228,229] and to increase cell proliferation [214,229,230], which in turn can result in greater ECM deposition [215] and accelerated repair [130]. BMPs impact both chondrogenesis and osteogenesis, and are attractive for *in vivo* osteochondral defect studies as they can assist osteochondral integration at the implant site. These morphogens regulate chondrocyte differentiation states and ECM composition. Specifically, BMP-2 and -7 have been shown to increase matrix production in chondrocytes and progenitor cells. BMP-2 increases TIMP-1 [231], Sox 9 [41], type II collagen [41,216], and aggrecan [41] expression levels, while BMP-7 stimulates the production of proteoglycan-rich ECM and suppresses fibroblast infiltration into the scaffold [217]. BMP-7 transfection into periosteal-derived MSCs resulted in complete or near complete bone and cartilage regeneration in an osteochondral rabbit defect model with a PGA scaffold after 8 weeks [218]. Furthermore, BMP-2 and -7 act synergistically, resulting in even better matrix production [216].

Methods to incorporate GFs and other soluble factors directly into scaffolds have been developed to improve cartilage formation. For delivery *in vivo*, these additives can be loaded in the scaffold itself and/or in microspheres or microparticles, which are then incorporated into the scaffold. Release profiles of these additives are dictated by degradation and diffusion properties. For *in vivo* applications, TGF- $\beta$  has been incorporated into hydrogels composed of oligo(poly(ethylene glycol) fumarate) (OPF) [168,232], PEOA [233], and fibrin [234], and/or



loaded into microspheres or microparticles, made of PLGA [235], gelatin [104,168], and chitosan [133,236]. Thus, growth factor release can be controlled by crosslinking density and/or variations in the size of the microparticles. In general, the burst release of the GF is decreased when loaded microspheres are encapsulated within a scaffold [168,235]. Many *in vitro* studies have shown additive benefits of using TGF- $\beta$  and IGF-1 in combination [123]. However, Holland and colleagues showed that these *in vitro* results may not be as effective in an *in vivo* environment. In an osteochondral repair in rabbits, microparticle delivery of IGF-1 in OPF gels with articular chondrocytes showed significantly better repair overall over controls without IGF-1, yet this enhancement was not observed when delivered in combination with TGF- $\beta$ 1 [237].

In addition, others have incorporated soluble HA to improve tissue quality. Scaffolds supplemented with soluble HA have improved cell proliferation [144], increased expression of cartilage-specific matrix proteins [221], and increased matrix synthesis [119,126,144,238]. Furthermore, for photopolymerization applications, HA increases the viscosity of the precursor solution, allowing for better retention of the solution at the injection site [233]. The addition of chondroitin sulfate has been shown to promote cell ingrowth and tissue formation [128], while chondroitinase ABC treatment has been shown to induce maturational growth and enhanced tensile integrity of cartilage explants [239].

### **3.4.2 Gene Therapy**

Many biological agents have a short half life, which limits their *in vivo* efficacy. Gene therapy is an alternative approach to encapsulating bioactive molecules in scaffolds. *Ex vivo* gene therapy has drawn much interest as a method to transiently over-express and release proteins from cell-seeded scaffolds to provide local delivery [240]. Both viral (e.g. retroviruses and adenoviruses) and non-viral agents (polymers and liposomes) can be used to transfect cells. Viral vectors typically have higher transfection efficiencies but carry greater safety concerns, whereas non-viral vectors exhibit lower transfection efficiencies and carry fewer safety concerns.

FuGene 6 is a non-viral vector that has been successfully used to transfect articular chondrocytes at an efficiency of 35% with the transgene IGF-1 [219]. Encapsulation of these transfected cells in alginate spheres resulted in IGF-1 expression for up to 6 weeks. Transfection of BMSCs has also been accomplished within the scaffold, where porous chitosan/collagen scaffolds were created by freeze drying with TGF- $\beta$ 1 plasmids [241]. Transfected scaffolds increased proliferation rates and the expression of type II collagen and aggrecan. Success has also been shown with PGA sponges, where periosteal-derived stem cells were transduced *ex vivo* with BMP-7, and showed improved healing of full thickness cartilage defects after only 6 weeks [242]. With gene therapy for cartilage regeneration in its infancy, much remains to be investigated, including endless combinations of modified cells and scaffolds.

### **3.4.3 Hydrostatic Pressure**

In the joint cavity, cartilage exists in an environment of reduced oxygen and intermittent hydrostatic pressure. Thus, mimicking these conditions may provide a means to improve chondrogenesis *in vitro*. Low oxygen tension (5%) has stimulated the proliferation and type II collagen expression [243], as well as increased cartilage-specific biosynthesis [70,244], of chondrocytes. Hydrostatic pressure applied within physiological levels has been beneficial [244-247]; however, the effects of loading are highly dependent on the loading regimen [243] and require much optimization. Chondrocytes loaded at 10MPa and 1Hz for 4hours/day, 5 days/week, for up to 8 weeks showed an increase in collagen production and prevention of GAG loss over static controls [247]. The benefits of hydrostatic loading were also noted in chondro-induced MSCs, where 0.1MPa of loading increased Sox 9 and aggrecan expression and 10MPa of loading generated a maximum response for type II collagen, while matrix condensation was observed with increasing hydrostatic pressure [245]. Hansen and colleagues reported that chondrocytes loaded at 0.2MPa and 0.1Hz for 30/2 or 2/30 minutes of on/off loading showed

inhibited proliferation and increased collagen secretion or increased proliferation and lowered collagen expression, respectively [244].

#### **3.4.4 Dynamic Compression**

There is significant evidence that dynamic compressive loading has a stimulatory effect on cartilage, chondrocytes, and stem cells. Chondrocytes exhibit compressibility and behavioral changes with compressive load as a function of strain. Numerous loading regimes ranging from a single application [248,249] to continuous loading [7,132,250,251] have been investigated as a means to accelerate and improve tissue formation. In each case, loading regimes must be optimized for cell type, seeding density, and scaffold. Recently Ng and colleagues attempted to engineer a stratified cartilage construct with layered 2% and 3% agarose with dynamic loading over 28 days. However, increased bulk mechanical and biochemical properties were only seen in the 2% gel [252]. In addition, chondrocytes encapsulated in fibrin glue were not affected by dynamic loading, even though loading has been shown to positively stimulate chondrocytes in agarose [253].

Studies have shown catabolic and anabolic effects of compressive loading, hinting at a structural remodeling effect of the newly synthesized matrix through loading [248]. A single application of a uniaxial compressive load (1kPa, 1Hz, 30min) increased collagen and proteoglycan synthesis and improved mechanical properties [249]. This single application of load transiently increased MMP-3 and MMP-13 expression, and produced a catabolic change 2 hours post-stimulation characterized by the release of proteoglycans and collagen into the culture media. This was followed by an anabolic change with an increase in type II collagen and aggrecan expression 12 hours post-stimulation, indicating that cyclic loading has a remodeling effect involving the mitogen-activated protein kinase (MAPK) pathway.

Furthermore, the addition of growth factors with loading appears to have a synergistic effect. Mauck *et al* showed that stimulatory responses could be increased with the addition of

TGF- $\beta$ 1 and IGF, including increased proteoglycan and collagen contents and equilibrium aggregate modulus of chondrocytes cultured in agarose gels [123]. Furthermore, Chowdhury and colleagues showed that TGF- $\beta$ 3 modulates cellular responses during dynamic loading via an integrin mediated mechanotransduction, where the addition of the peptide GRGDSP, a competitive ligand for  $\alpha$ 5 $\beta$ 1 integrin binding, was able to reverse the compression-induced stimulation [254]. However, one problem encountered with dynamic loading is the loss of newly synthesized matrix proteins to the culture media [132].

### **3.4.5 Bioreactors**

Bioreactors have been employed to accelerate and improve the growth of engineered cartilage *in vitro*. They serve to enhance nutrient transport and provide a hydrodynamic environment that imposes a fluid-induced shear stress to promote the synthesis of cartilage-specific matrix proteins. Dynamic cell seeding of porous scaffolds, typically done in spinner flasks, has led to faster adhesion and better cell distributions [120]. Though the effects are scaffold dependent, chondrocyte-laden scaffolds grown in perfusion culture increased cell proliferation and biochemical content compared to static culture [255,256]. For long-term *in vitro* culture, low shear stresses stimulate ECM synthesis and deposition, yielding greater tissue formation, while high shear stresses suppress GAG deposition. In general, higher seeding densities have enhanced GAG content, potentially due to cell-cell interactions [69,120], while scaffolds seeded at low cell densities fail to elicit a response in bioreactor culture [257]. Bioreactors currently being investigated for cartilage tissue engineering include: a parallel-plate bioreactor [258], rotating wall bioreactor [69], and a concentric cylinder bioreactor [259]. Recently, a newly developed wavy-wall bioreactor (WWB) has been shown to increase chondrocyte proliferation and ECM deposition on PGA scaffolds over the common spinner flask culture [260]. Compared to a spinner flask, the novel bioreactor reduces fluid shear stresses and

increases axial mixing. The addition of growth factors, like IGF-1, can also be used in combination with bioreactors to further enhance matrix accumulation [227].

*In the work presented in this dissertation, constructs were either cultured statically in vitro or implanted subcutaneously in nude mice. One study utilized dynamic compression of formed constructs. For experiments investigating mesenchymal stem cells, constructs were cultured in the presence of transforming growth factor –  $\beta$ 3 as an induction molecule.*

### **3.5 Conclusions**

Cell source, scaffolds, and signaling factors make up the tissue engineering triad. One of the biggest challenges for cartilage tissue engineering is cell source. Current work on alternatives to chondrocytes is expanding, and the potential and limitations of fibroblasts and stem cells are being explored. Novel biomaterials are being continuously developed and are leading to unique interactions with cells through controlled biomaterial chemistry, structure, and the addition of biological molecules. Also, the incorporation of stimulatory factors such as bioactive molecules, gene therapy, mechanical loading, and bioreactors are leading to enhanced cartilage production. Ultimately, clinical translation and feasibility needs to be considered with all of these approaches if a successful tissue engineered cartilage product is to make it through the regulatory process and into patients.

**References:**

- [1] Langer RS, Vacanti JP. Tissue engineering: The challenges ahead. *Sci Am* 1999;280(4):86-9.
- [2] Nicoll SB, Wedrychowska A, Smith NR, Bhatnagar RS. Modulation of proteoglycan and collagen profiles in human dermal fibroblasts by high density micromass culture and treatment with lactic acid suggests change to a chondrogenic phenotype. *Connect Tissue Res* 2001;42(1):59-69.
- [3] Brittberg M, Lindahl A, Nilsson A, Ohlsson C, Isaksson O, Peterson L. Treatment of deep cartilage defects in the knee with autologous chondrocyte transplantation. *N Engl J Med* 1994;331(14):889-95.
- [4] Bryant SJ, Anseth KS. Hydrogel properties influence ECM production by chondrocytes photoencapsulated in poly(ethylene glycol) hydrogels. *Journal of Biomedical Materials Research* 2002;59(1):63-72.
- [5] Klein TJ, Schumacher BL, Schmidt TA, Li KW, Voegtline MS, Masuda K, et al. Tissue engineering of stratified articular cartilage from chondrocyte subpopulations. *Osteoarthritis and Cartilage* 2003;11(8):595-602.
- [6] Li Y, Tew SR, Russell AM, Gonzalez KR, Hardingham TE, Hawkins RE. Transduction of passaged human articular chondrocytes with adenoviral, retroviral, and lentiviral vectors and the effects of enhanced expression of SOX9. *Tissue Engineering* 2004;10(3-4):575-84.
- [7] Mauck RL, Soltz MA, Wang CCB, Wong DD, Chao PHG, Valhmu WB, et al. Functional tissue engineering of articular cartilage through dynamic loading of chondrocyte-seeded agarose gels. *Journal of Biomechanical Engineering-Transactions of the Asme* 2000;122(3):252-60.
- [8] Mesa JM, Zaporozhan V, Weinand C, Johnson TS, Bonassar L, Randolph MA, et al. Tissue engineering cartilage with aged articular chondrocytes in vivo. *Plastic and Reconstructive Surgery* 2006;118(1):41-9.

- [9] Vunjak-Novakovic G, Martin I, Obradovic B, Treppo S, Grodzinsky AJ, Langer R, et al. Bioreactor cultivation conditions modulate the composition and mechanical properties of tissue-engineered cartilage. *J Orthop Res* 1999;17(1):130-8.
- [10] Chung C, Mesa J, Miller GJ, Randolph MA, Gill TJ, Burdick JA. Effects of auricular chondrocyte expansion on neocartilage formation in photocrosslinked hyaluronic acid networks. *Tissue Engineering* 2006;12(9):2665-73.
- [11] Chung C, Mesa J, Randolph MA, Yaremchuk M, Burdick JA. Influence of gel properties on neocartilage formation by auricular chondrocytes photoencapsulated in hyaluronic acid networks. *J Biomed Mater Res A* 2006;77(3):518-25.
- [12] Johnson TS, Xu JW, Zaporozhan VV, Mesa JM, Weinand C, Randolph MA, et al. Integrative repair of cartilage with articular and nonarticular chondrocytes. *Tissue Eng* 2004;10(9-10):1308-15.
- [13] Panossian A, Ashiku S, Kirchhoff CH, Randolph MA, Yaremchuk MJ. Effects of cell concentration and growth period on articular and ear chondrocyte transplants for tissue engineering. *Plastic and Reconstructive Surgery* 2001;108(2):392-402.
- [14] van Osch GJVM, Mandl EW, Jahr H, Koevoet W, Nolst-Trenite G, Verhaar JA. Considerations on the use of ear chondrocytes as donor chondrocytes for cartilage tissue engineering. *Biorheology* 2004;41(3-4):411-21.
- [15] Isogai N, Kusuhara H, Ikada Y, Ohtani H, Jacquet R, Hillyer J, et al. Comparison of different chondrocytes for use in tissue engineering of cartilage model structures. *Tissue Engineering* 2006;12(4):691-703.
- [16] Tay AG, Farhadi J, Suetterlin R, Pierer G, Heberer M, Martin I. Cell yield, proliferation, and postexpansion differentiation capacity of human ear, nasal, and rib chondrocytes. *Tissue Engineering* 2004;10(5-6):762-70.
- [17] Kato Y, Gospodarowicz D. Sulfated Proteoglycan Synthesis by Confluent Cultures of Rabbit Costal Chondrocytes Grown in the Presence of Fibroblast Growth-Factor. *Journal of Cell Biology* 1985;100(2):477-85.

- [18] Kafienah W, Jakob M, Demarteau O, Frazer A, Barker MD, Martin I, et al. Three-dimensional tissue engineering of hyaline cartilage: Comparison of adult nasal and articular chondrocytes. *Tissue Engineering* 2002;8(5):817-26.
- [19] Miot S, Woodfield T, Daniels AU, Suetterlin R, Peterschmitt I, Heberer M, et al. Effects of scaffold composition and architecture on human nasal chondrocyte redifferentiation and cartilaginous matrix deposition. *Biomaterials* 2005;26(15):2479-89.
- [20] Richmon JD, Sage AB, Shelton E, Schumacher BL, Sah RL, Watson D. Effect of growth factors on cell proliferation, matrix deposition, and morphology of human nasal septal chondrocytes cultured in monolayer. *Laryngoscope* 2005;115(9):1553-60.
- [21] van Osch GJVM, Marijnissen WJCM, van der Veen SW, Verwoerd-Verhoef HL. The potency of culture-expanded nasal septum chondrocytes for tissue engineering of cartilage. *American Journal of Rhinology* 2001;15(3):187-92.
- [22] Vinatier C, Magne D, Moreau A, Gauthier O, Malard O, Vignes-Colombeix C, et al. Engineering cartilage with human nasal chondrocytes and a silanized hydroxypropyl methylcellulose hydrogel. *Journal of Biomedical Materials Research Part A* 2007;80A(1):66-74.
- [23] Deng Y, Hu JC, Athanasiou KA. Isolation and chondroinduction of a dermis-isolated, aggrecan-sensitive subpopulation with high chondrogenic potential. *Arthritis and Rheumatism* 2007;56(1):168-76.
- [24] French MM, Rose S, Canseco J, Athanasiou KA. Chondrogenic differentiation of adult dermal fibroblasts. *Annals of Biomedical Engineering* 2004;32(1):50-6.
- [25] Lee KH, Song SU, Hwang TS, Yi Y, Oh IS, Lee JY, et al. Regeneration of hyaline cartilage by cell-mediated gene therapy using transforming growth factor beta 1-producing fibroblasts. *Hum Gene Ther* 2001;12(14):1805-13.
- [26] Chen JW, Wang CY, Lu SH, Wu JZ, Guo XM, Duan CM, et al. In vivo chondrogenesis of adult bone-marrow-derived autologous mesenchymal stem cells. *Cell and Tissue Research* 2005;319(3):429-38.



- [27] Li WJ, Tuli R, Okafor C, Derfoul A, Danielson KG, Hall DJ, et al. A three-dimensional nanofibrous scaffold for cartilage tissue engineering using human mesenchymal stem cells. *Biomaterials* 2005;26(6):599-609.
- [28] Mauck RL, Yuan X, Tuan RS. Chondrogenic differentiation and functional maturation of bovine mesenchymal stem cells in long-term agarose culture. *Osteoarthritis and Cartilage* 2006;14(2):179-89.
- [29] Williams CG, Kim TK, Taboas A, Malik A, Manson P, Elisseeff J. In vitro chondrogenesis of bone marrow-derived mesenchymal stem cells in a photopolymerizing hydrogel. *Tissue Engineering* 2003;9(4):679-88.
- [30] Winter A, Breit S, Parsch D, Benz K, Steck E, Hauner H, et al. Cartilage-like gene expression in differentiated human stem cell spheroids: a comparison of bone marrow-derived and adipose tissue-derived stromal cells. *Arthritis Rheum* 2003;48(2):418-29.
- [31] Yoo JU, Barthel TS, Nishimura K, Solchaga L, Caplan AI, Goldberg VM, et al. The chondrogenic potential of human bone-marrow-derived mesenchymal progenitor cells. *J Bone Joint Surg Am* 1998;80(12):1745-57.
- [32] Awad HA, Wickham MQ, Leddy HA, Gimple JM, Guilak F. Chondrogenic differentiation of adipose-derived adult stem cells in agarose, alginate, and gelatin scaffolds. *Biomaterials* 2004;25(16):3211-22.
- [33] Betre H, Ong SR, Guilak F, Chilkoti A, Fermor B, Setton LA. Chondrocytic differentiation of human adipose-derived adult stem cells in elastin-like polypeptide. *Biomaterials* 2006;27(1):91-9.
- [34] Erickson GR, Gimple JM, Franklin DM, Rice HE, Awad H, Guilak F. Chondrogenic potential of adipose tissue-derived stromal cells in vitro and in vivo. *Biochemical and Biophysical Research Communications* 2002;290(2):763-9.
- [35] Huang JI, Zuk PA, Jones NF, Zhu M, Lorenz HP, Hedrick MH, et al. Chondrogenic potential of multipotential cells from human adipose tissue. *Plastic and Reconstructive Surgery* 2004;113(2):585-94.

- [36] Lin YF, Luo E, Chen XZ, Liu L, Qiao J, Yan ZB, et al. Molecular and cellular characterization during chondrogenic differentiation of adipose tissue-derived stromal cells in vitro and cartilage formation in vivo. *Journal of Cellular and Molecular Medicine* 2005;9(4):929-39.
- [37] Zuk PA, Zhu M, Mizuno H, Huang J, Futrell JW, Katz AJ, et al. Multilineage cells from human adipose tissue: implications for cell-based therapies. *Tissue Eng* 2001;7(2):211-28.
- [38] Adachi N, Sato K, Usas A, Fu FH, Ochi M, Han CW, et al. Muscle derived, cell based ex vivo gene therapy for treatment of full thickness articular cartilage defects. *Journal of Rheumatology* 2002;29(9):1920-30.
- [39] Kuroda R, Usas A, Kubo S, Corsi K, Peng HR, Rose T, et al. Cartilage repair using bone morphogenetic protein 4 and muscle-derived stem cells. *Arthritis and Rheumatism* 2006;54(2):433-42.
- [40] Nawata M, Wakitani S, Nakaya H, Tanigami A, Seki T, Nakamura Y, et al. Use of bone morphogenetic protein 2 and diffusion chambers to engineer cartilage tissue for the repair of defects in articular cartilage. *Arthritis and Rheumatism* 2005;52(1):155-63.
- [41] Park Y, Sugimoto M, Watrin A, Chiquet M, Hunziker EB. BMP-2 induces the expression of chondrocyte-specific genes in bovine synovium-derived progenitor cells cultured in three-dimensional alginate hydrogel. *Osteoarthritis and Cartilage* 2005;13(6):527-36.
- [42] Sakaguchi Y, Sekiya I, Yagishita K, Muneta T. Comparison of human stem cells derived from various mesenchymal tissues: superiority of synovium as a cell source. *Arthritis Rheum* 2005;52(8):2521-9.
- [43] Yokoyama A, Sekiya I, Miyazaki K, Ichinose S, Hata Y, Muneta T. In vitro cartilage formation of composites of synovium-derived mesenchymal stem cells with collagen gel. *Cell and Tissue Research* 2005;322(2):289-98.
- [44] Fukumoto T, Sperling JW, Sanyal A, Fitzsimmons JS, Reinholz GG, Conover CA, et al. Combined effects of insulin-like growth factor-1 and transforming growth factor-beta1 on periosteal mesenchymal cells during chondrogenesis in vitro. *Osteoarthritis Cartilage* 2003;11(1):55-64.

- [45] Nakata K, Nakahara H, Kimura T, Kojima A, Iwasaki M, Caplan AI, et al. Collagen Gene-Expression during Chondrogenesis from Chick Periosteum-Derived Cells. *Febs Lett* 1992;299(3):278-82.
- [46] Park J, Gelse K, Frank S, von der Mark K, Aigner T, Schneider H. Transgene-activated mesenchymal cells for articular cartilage repair: a comparison of primary bone marrow-, perichondrium/periosteum- and fat-derived cells. *J Gene Med* 2006;8(1):112-25.
- [47] Hwang NS, Kim MS, Sampattavanich S, Baek JH, Zhang ZJ, Elisseeff J. Effects of three-dimensional culture and growth factors on the chondrogenic differentiation of murine embryonic stem cells. *Stem Cells* 2006;24(2):284-91.
- [48] Hwang NS, Varghese S, Zhang Z, Elisseeff J. Chondrogenic differentiation of human embryonic stem cell-derived cells in arginine-glycine-aspartate modified hydrogels. *Tissue Engineering* 2006;12(9):2695-706.
- [49] Kramer J, Hegert C, Guan K, Wobus AM, Muller PK, Rohwedel J. Embryonic stem cell-derived chondrogenic differentiation in vitro: activation by BMP-2 and BMP-4. *Mech Dev* 2000;92(2):193-205.
- [50] Toh WS, Yang Z, Liu H, Heng BC, Lee EH, Cao T. Effects of culture conditions and bone morphogenetic protein 2 on extent of chondrogenesis from human embryonic stem cells. *Stem Cells* 2007;25(4):950-60.
- [51] Vats A, Bielby RC, Tolley N, Dickinson SC, Boccaccini AR, Hollander AP, et al. Chondrogenic differentiation of human embryonic stem cells: the effect of the micro-environment. *Tissue Eng* 2006;12(6):1687-97.
- [52] Goessler UR, Bugert P, Bieback K, Baisch A, Sadick H, Verse T, et al. Expression of collagen and fiber-associated proteins in human septal cartilage during in vitro dedifferentiation. *International Journal of Molecular Medicine* 2004;14(6):1015-22.
- [53] Goessler UR, Bugert P, Bieback K, Sadick H, Baisch A, Hormann K, et al. In vitro analysis of differential expression of collagens, integrins, and growth factors in cultured human chondrocytes. *Otolaryngology-Head and Neck Surgery* 2006;134(3):510-5.

- [54] Goessler UR, Bieback K, Bugert P, Heller T, Sadick H, Hormann K, et al. In vitro analysis of integrin expression during chondrogenic differentiation of mesenchymal stem cells and chondrocytes upon dedifferentiation in cell culture. *International Journal of Molecular Medicine* 2006;17(2):301-7.
- [55] Goessler UR, Bugert P, Bieback K, Deml M, Sadick H, Hormann K, et al. In-vitro analysis of the expression of TGF beta-superfamily-members during chondrogenic differentiation of mesenchymal stem cells and chondrocytes during dedifferentiation in cell culture. *Cellular & Molecular Biology Letters* 2005;10(2):345-62.
- [56] Goessler UR, Bieback K, Bugert P, Naim R, Schafer C, Sadick H, et al. Human chondrocytes differentially express matrix modulators during in vitro expansion for tissue engineering. *International Journal of Molecular Medicine* 2005;16(4):509-15.
- [57] Schulze-Tanzil G, Mobasheri A, de Souza P, John T, Shakibaei M. Loss of chondrogenic potential in dedifferentiated chondrocytes correlates with deficient Shc-Erk interaction and apoptosis. *Osteoarthritis and Cartilage* 2004;12(6):448-58.
- [58] Darling EM, Athanasiou KA. Rapid phenotypic changes in passaged articular chondrocyte subpopulations. *Journal of Orthopaedic Research* 2005;23(2):425-32.
- [59] Barbero A, Grogan SP, Mainil-Varlet P, Martin I. Expansion on specific substrates regulates the phenotype and differentiation capacity of human articular chondrocytes. *Journal of Cellular Biochemistry* 2006;98(5):1140-9.
- [60] Brodtkin KR, Garcia AJ, Levenston ME. Chondrocyte phenotypes on different extracellular matrix monolayers. *Biomaterials* 2004;25(28):5929-38.
- [61] Darling EM, Athanasiou KA. Retaining zonal chondrocyte phenotype by means of novel growth environments. *Tissue Engineering* 2005;11(3-4):395-403.
- [62] Martin I, Vunjak-Novakovic G, Yang J, Langer R, Freed LE. Mammalian chondrocytes expanded in the presence of fibroblast growth factor 2 maintain the ability to differentiate and regenerate three-dimensional cartilaginous tissue. *Experimental Cell Research* 1999;253(2):681-8.

- [63] Buschmann MD, Gluzband YA, Grodzinsky AJ, Kimura JH, Hunziker EB. Chondrocytes in agarose culture synthesize a mechanically functional extracellular matrix. *J Orthop Res* 1992;10(6):745-58.
- [64] Homicz MR, Chia SH, Schumacher BL, Masuda K, Thonar EJ, Sah RL, et al. Human septal chondrocyte redifferentiation in alginate, polyglycolic acid scaffold, and monolayer culture. *Laryngoscope* 2003;113(1):25-32.
- [65] Lin Z, Willers C, Xu JA, Zheng MH. The chondrocyte: Biology and clinical application. *Tissue Engineering* 2006;12(7):1971-84.
- [66] An YH, Webb D, Gutowska A, Mironov VA, Friedman RJ. Regaining chondrocyte phenotype in thermosensitive gel culture. *Anat Rec* 2001;263(4):336-41.
- [67] Malda J, Kreijveld E, Temenoff JS, van Blitterswijk CA, Riesle J. Expansion of human nasal chondrocytes on macroporous microcarriers enhances redifferentiation. *Biomaterials* 2003;24(28):5153-61.
- [68] Malda J, Van Blitterswijk CA, Grojec M, Martens DE, Tramper J, Riesle J. Expansion of bovine chondrocytes on microcarriers enhances redifferentiation. *Tissue Engineering* 2003;9(5):939-48.
- [69] Freed LE, Hollander AP, Martin I, Barry JR, Langer R, Vunjak-Novakovic G. Chondrogenesis in a cell-polymer-bioreactor system. *Experimental Cell Research* 1998;240(1):58-65.
- [70] Kurz B, Domm C, Jin MS, Sellckau R, Schunke M. Tissue engineering of articular cartilage under the influence of collagen I/III membranes and low oxygen tension. *Tissue Engineering* 2004;10(7-8):1277-86.
- [71] Mandl EW, van der Veen SW, Verhaar JAN, van Osch GJVM. Serum-free medium supplemented with high-concentration FGF2 for cell expansion culture of human ear chondrocytes promotes redifferentiation capacity. *Tissue Engineering* 2002;8(4):573-80.
- [72] Gan L, Kandel RA. In vitro cartilage tissue formation by co-culture of primary and passaged chondrocytes. *Tissue Engineering* 2007;13(4):831-42.

- [73] Woodfield TBF, Miot S, Martin I, van Blitterswijk CA, Riesle J. The regulation of expanded human nasal chondrocyte re-differentiation capacity by substrate composition and gas plasma surface modification. *Biomaterials* 2006;27(7):1043-53.
- [74] Kim HT, Zaffagnini S, Mizuno S, Abelow S, Safran MR. A peek into the possible future of management of articular cartilage injuries: Gene therapy and scaffolds for cartilage repair. *Journal of Orthopaedic & Sports Physical Therapy* 2006;36(10):765-73.
- [75] Darling EM, Hu JCY, Athanasiou KA. Zonal and topographical differences in articular cartilage gene expression. *Journal of Orthopaedic Research* 2004;22(6):1182-7.
- [76] Hidaka C, Cheng C, Alexandre D, Bhargava M, Torzilli PA. Maturation differences in superficial and deep zone articular chondrocytes. *Cell and Tissue Research* 2006;323(1):127-35.
- [77] Klein TJ, Chaudhry M, Bae WC, Sah RL. Depth-dependent biomechanical and biochemical properties of fetal, newborn, and tissue-engineered articular cartilage. *Journal of Biomechanics* 2007;40(1):182-90.
- [78] Sharma B, Williams CG, Kim TK, Sun DN, Malik A, Khan M, et al. Designing zonal organization into tissue-engineered cartilage. *Tissue Engineering* 2007;13(2):405-14.
- [79] Kim TK, Sharma B, Williams CG, Ruffner MA, Malik A, McFarland EG, et al. Experimental model for cartilage tissue engineering to regenerate the zonal organization of articular cartilage. *Osteoarthritis and Cartilage* 2003;11(9):653-64.
- [80] Woodfield TBF, Van Blitterswijk CA, De Wijn J, Sims TJ, Hollander AP, Riesle J. Polymer scaffolds fabricated with pore-size gradients as a model for studying the zonal organization within tissue-engineered cartilage constructs. *Tissue Engineering* 2005;11(9-10):1297-311.
- [81] Hicks DL, Sage AB, Schumacher BL, Sah RL, Watson D. Growth and phenotype of low-density nasal septal chondrocyte monolayers. *Otolaryngology-Head and Neck Surgery* 2005;133(3):417-22.

- [82] Naumann A, Dennis JE, Aigner J, Coticchia J, Arnold J, Berghaus A, et al. Tissue engineering of autologous cartilage grafts in three-dimensional in vitro macroaggregate culture system. *Tissue Engineering* 2004;10(11-12):1695-706.
- [83] Shikani AH, Fink DJ, Sohrabi A, Phan P, Polotsky A, Hungerford DS, et al. Propagation of human nasal chondrocytes in microcarrier spinner culture. *American Journal of Rhinology* 2004;18(2):105-12.
- [84] Aigner J, Tegeler J, Hutzler P, Campoccia D, Pavesio A, Hammer C, et al. Cartilage tissue engineering with novel nonwoven structured biomaterial based on hyaluronic acid benzyl ester. *Journal of Biomedical Materials Research* 1998;42(2):172-81.
- [85] Barbero A, Grogan S, Schafer D, Heberer M, Mainil-Varlet P, Martin I. Age related changes in human articular chondrocyte yield, proliferation and post-expansion chondrogenic capacity. *Osteoarthritis and Cartilage* 2004;12(6):476-84.
- [86] Giannoni P, Pagano A, Maggi E, Arbico R, Randazzo N, Grandizio M, et al. Autologous chondrocyte implantation (ACI) for aged patients: development of the proper cell expansion conditions for possible therapeutic applications. *Osteoarthritis and Cartilage* 2005;13(7):589-600.
- [87] Terada S, Fuchs JR, Yoshimoto H, Fauza DO, Vacanti JP. In vitro cartilage regeneration from proliferated adult elastic chondrocytes. *Annals of Plastic Surgery* 2005;55(2):196-201.
- [88] Tran-Khanh N, Hoemann CD, McKee MD, Henderson JE, Buschmann MD. Aged bovine chondrocytes display a diminished capacity to produce a collagen-rich, mechanically functional cartilage extracellular matrix. *Journal of Orthopaedic Research* 2005;23(6):1354-62.
- [89] Marlovits S, Tichy B, Truppe M, Gruber D, Schlegel W. Collagen expression in tissue engineered cartilage of aged human articular chondrocytes in a rotating bioreactor. *International Journal of Artificial Organs* 2003;26(4):319-30.

- [90] Wenger R, Hans MG, Welter JF, Solchaga LA, Sheu YR, Malesud CJ. Hydrostatic pressure increases apoptosis in cartilage-constructs produced from human osteoarthritic chondrocytes. *Frontiers in Bioscience* 2006;11:1690-5.
- [91] Gorti GK, Lo J, Falsafi S, Kosek J, Quan SY, Khuu DT, et al. Cartilage tissue engineering using cryogenic chondrocytes. *Archives of Otolaryngology-Head & Neck Surgery* 2003;129(8):889-93.
- [92] Yan H, Yu C. Repair of full-thickness cartilage defects with cells of different origin in a rabbit model. *Arthroscopy* 2007;23(2):178-87.
- [93] Yates KE, Forbes RL, Glowacki J. New chondrocyte genes discovered by representational difference analysis of chondroinduced human fibroblasts. *Cells Tissues Organs* 2004;176(1-3):41-53.
- [94] Johnstone B, Hering TM, Caplan AI, Goldberg VM, Yoo JU. In vitro chondrogenesis of bone marrow-derived mesenchymal progenitor cells. *Exp Cell Res* 1998;238(1):265-72.
- [95] Coleman RM, Case ND, Guldberg RE. Hydrogel effects on bone marrow stromal cell response to chondrogenic growth factors. *Biomaterials* 2007;28(12):2077-86.
- [96] Huang CYC, Reuben PM, D'Ippolito G, Schiller PC, Cheung HS. Chondrogenesis of human bone marrow-derived mesenchymal stem cells in agarose culture. *Anatomical Record Part a-Discoveries in Molecular Cellular and Evolutionary Biology* 2004;278A(1):428-36.
- [97] Pang YG, Cui PC, Chen WX, Gao PF, Zhang HZ. Quantitative study of tissue-engineered cartilage with human bone marrow mesenchymal stem cells. *Archives of Facial Plastic Surgery* 2005;7(1):7-11.
- [98] Meinel L, Hofmann S, Karageorgiou V, Zichner L, Langer R, Kaplan D, et al. Engineering cartilage-like tissue using human mesenchymal stem cells and silk protein scaffolds. *Biotechnology and Bioengineering* 2004;88(3):379-91.
- [99] Wang YZ, Kim UJ, Blasioli DJ, Kim HJ, Kaplan DL. In vitro cartilage tissue engineering with 3D porous aqueous-derived silk scaffolds and mesenchymal stem cells. *Biomaterials* 2005;26(34):7082-94.



- [100] Chen GP, Liu DC, Tadokoro M, Hirochika R, Ohgushi H, Tanaka J, et al. Chondrogenic differentiation of human mesenchymal stem cells cultured in a cobweb-like biodegradable scaffold. *Biochemical and Biophysical Research Communications* 2004;322(1):50-5.
- [101] Fan HB, Hu YY, Zhang CL, Li XS, Lv R, Qin L, et al. Cartilage regeneration using mesenchymal stem cells and a PLGA-gelatin/chondroitin/hyaluronate hybrid scaffold. *Biomaterials* 2006;27(26):4573-80.
- [102] Indrawattana N, Chen GP, Tadokoro M, Shann LH, Ohgushi H, Tateishi T, et al. Growth factor combination for chondrogenic induction from human mesenchymal stem cell. *Biochemical and Biophysical Research Communications* 2004;320(3):914-9.
- [103] Park KS, Jin CM, Kim SH, Rhee JM, Khang G, Han CW, et al. Chondrogenic differentiation of bone marrow stromal cells in transforming growth factor-beta(1) loaded alginate bead. *Macromolecular Research* 2005;13(4):285-92.
- [104] Fan HB, Hu YY, Qin L, Li XS, Wu H, Lv R. Porous gelatin-chondroitin-hyaluronate tri-copolymer scaffold containing microspheres loaded with TGF-beta 1 induces differentiation of mesenchymal stem cells in vivo for enhancing cartilage repair. *Journal of Biomedical Materials Research Part A* 2006;77A(4):785-94.
- [105] Guo XM, Wang CY, Zhang YF, Xia RY, Hu M, Duan CM, et al. Repair of large articular cartilage defects with implants of autologous mesenchymal stem cells seeded into beta-tricalcium phosphate in a sheep model. *Tissue Engineering* 2004;10(11-12):1818-29.
- [106] Kayakabe M, Tsutsumi S, Watanabe H, Kato Y, Takagishi K. Transplantation of autologous rabbit BM-derived mesenchymal stromal cells embedded in hyaluronic acid gel sponge into osteochondral defects of the knee. *Cytherapy* 2006;8(4):343-53.
- [107] Tatebe M, Nakamura R, Kagami H, Okada K, Ueda M. Differentiation of transplanted mesenchymal stem cells in a large osteochondral defect in rabbit. *Cytherapy* 2005;7(6):520-30.
- [108] Akaogi H, Akimoto T, Miyaki S, Ushida T, Ochiai N, Tateishi T, et al. Basic fibroblast growth factor supports in vitro chondrogenesis of bone marrow-derived mesenchymal stem cells

- from patients with osteoarthritis. *Materials Science & Engineering C-Biomimetic and Supramolecular Systems* 2004;24(3):403-6.
- [109] Tsuchiya K, Chen GP, Ushida T, Matsuno T, Tateishi T. The effect of coculture of chondrocytes with mesenchymal stem cells on their cartilaginous phenotype in vitro. *Materials Science & Engineering C-Biomimetic and Supramolecular Systems* 2004;24(3):391-6.
- [110] Zhou GD, Liu W, Cui L, Cao YL. In vivo chondrogenesis of BMSCs at non-chondrogenesis site by co-transplantation of BMSCs and chondrocytes with pluronic as biomaterial. *Asbm6: Advanced Biomaterials Vi* 2005;288-289:3-6.
- [111] Zuk PA, Zhu M, Ashjian P, De Ugarte DA, Huang JI, Mizuno H, et al. Human adipose tissue is a source of multipotent stem cells. *Mol Biol Cell* 2002;13(12):4279-95.
- [112] Chiou M, Xu Y, Longaker MT. Mitogenic and chondrogenic effects of fibroblast growth factor-2 in adipose-derived mesenchymal cells. *Biochemical and Biophysical Research Communications* 2006;343(2):644-52.
- [113] Masuoka K, Asazuma T, Hattori H, Yoshihara Y, Sato M, Matsumura K, et al. Tissue engineering of articular cartilage with autologous cultured adipose tissue-derived stromal cells using atelocollagen honeycomb-shaped scaffold with a membrane sealing in rabbits. *Journal of Biomedical Materials Research Part B-Applied Biomaterials* 2006;79B(1):25-34.
- [114] Estes BT, Wu AW, Guilak F. Potent induction of chondrocytic differentiation of human adipose-derived adult stem cells by bone morphogenetic protein 6. *Arthritis Rheum* 2006;54(4):1222-32.
- [115] Huang JI, Kazmi N, Durbhakula MM, Hering TM, Yoo JU, Johnstone B. Chondrogenic potential of progenitor cells derived from human bone marrow and adipose tissue: a patient-matched comparison. *J Orthop Res* 2005;23(6):1383-9.

- [116] Im GI, Shin YW, Lee KB. Do adipose tissue-derived mesenchymal stem cells have the same osteogenic and chondrogenic potential as bone marrow-derived cells? *Osteoarthritis Cartilage* 2005;13(10):845-53.
- [117] Kramer J, Hegert C, Hargus G, Rohwedel J. Mouse ES cell lines show a variable degree of chondrogenic differentiation in vitro. *Cell Biol Int* 2005;29(2):139-46.
- [118] Bryant SJ, Anseth KS. Controlling the spatial distribution of ECM components in degradable PEG hydrogels for tissue engineering cartilage. *Journal of Biomedical Materials Research Part A* 2003;64A(1):70-9.
- [119] Solchaga LA, Temenoff JS, Gao JZ, Mikos AG, Caplan AI, Goldberg VM. Repair of osteochondral defects with hyaluronan- and polyester-based scaffolds. *Osteoarthritis and Cartilage* 2005;13(4):297-309.
- [120] Freed LE, Marquis JC, Vunjaknovakovic G, Emmanuel J, Langer R. Composition of Cell-Polymer Cartilage Implants. *Biotechnology and Bioengineering* 1994;43(7):605-14.
- [121] Iwasa J, Ochi M, Uchio Y, Katsube K, Adachi N, Kawasaki K. Effects of cell density on proliferation and matrix synthesis of chondrocytes embedded in atelocollagen gel. *Artificial Organs* 2003;27(3):249-55.
- [122] Buschmann MD, Gluzband YA, Grodzinsky AJ, Hunziker EB. Mechanical compression modulates matrix biosynthesis in chondrocyte/agarose culture. *J Cell Sci* 1995;108 ( Pt 4):1497-508.
- [123] Mauck RL, Nicoll SB, Seyhan SL, Ateshian GA, Hung CT. Synergistic action of growth factors and dynamic loading for articular cartilage tissue engineering. *Tissue Engineering* 2003;9(4):597-611.
- [124] Genes NG, Rowley JA, Mooney DJ, Bonassar LJ. Effect of substrate mechanics on chondrocyte adhesion to modified alginate surfaces. *Arch Biochem Biophys* 2004;422(2):161-7.

- [125] Hauselmann HJ, Fernandes RJ, Mok SS, Schmid TM, Block JA, Aydelotte MB, et al. Phenotypic stability of bovine articular chondrocytes after long-term culture in alginate beads. *J Cell Sci* 1994;107 ( Pt 1):17-27.
- [126] Miralles G, Baudoin R, Dumas D, Baptiste D, Hubert P, Stoltz JF, et al. Sodium alginate sponges with or without sodium hyaluronate: In vitro engineering of cartilage. *Journal of Biomedical Materials Research* 2001;57(2):268-78.
- [127] Muller FA, Muller L, Hofmann I, Greil P, Wenzel MM, Staudenmaier R. Cellulose-based scaffold materials for cartilage tissue engineering. *Biomaterials* 2006;27(21):3955-63.
- [128] Buma P, Pieper JS, van Tienen T, van Susante JLC, van der Kraan PM, Veerkamp JH, et al. Cross-linked type I and type II collagenous matrices for the repair of full-thickness articular cartilage defects - A study in rabbits. *Biomaterials* 2003;24(19):3255-63.
- [129] De Franceschi L, Grigolo B, Roseti L, Facchini A, Fini M, Giavaresi G, et al. Transplantation of chondrocytes seeded on collagen-based scaffold in cartilage defects in rabbits. *Journal of Biomedical Materials Research Part A* 2005;75A(3):612-22.
- [130] Fujisato T, Sajiki T, Liu Q, Ikada Y. Effect of basic fibroblast growth factor on cartilage regeneration in chondrocyte-seeded collagen sponge scaffold. *Biomaterials* 1996;17(2):155-62.
- [131] Lee CR, Breinan HA, Nehrer S, Spector M. Articular cartilage chondrocytes in type I and type II collagen-GAG matrices exhibit contractile behavior in vitro. *Tissue Engineering* 2000;6(5):555-65.
- [132] Lee CR, Grodzinsky AJ, Spector A. Biosynthetic response of passaged chondrocytes in a type II collagen scaffold to mechanical compression. *Journal of Biomedical Materials Research Part A* 2003;64A(3):560-9.
- [133] Kim SE, Park JH, Cho YW, Chung H, Jeong SY, Lee EB, et al. Porous chitosan scaffold containing microspheres loaded with transforming growth factor-beta 1: Implications for cartilage tissue engineering. *Journal of Controlled Release* 2003;91(3):365-74.

- [134] Kuo YC, Lin CY. Effect of genipin-crosslinked chitin-chitosan scaffolds with hydroxyapatite modifications on the cultivation of bovine knee chondrocytes. *Biotechnology and Bioengineering* 2006;95(1):132-44.
- [135] Nettles DL, Elder SH, Gilbert JA. Potential use of chitosan as a cell scaffold material for cartilage tissue engineering. *Tissue Engineering* 2002;8(6):1009-16.
- [136] Sechriest VF, Miao YJ, Niyibizi C, Westerhausen-Larson A, Matthew HW, Evans CH, et al. GAG-augmented polysaccharide hydrogel: A novel biocompatible and biodegradable material to support chondrogenesis. *Journal of Biomedical Materials Research* 1999;49(4):534-41.
- [137] Xia WY, Liu W, Cui L, Liu YC, Zhong W, Liu DL, et al. Tissue engineering of cartilage with the use of chitosan-gelatin complex scaffolds. *Journal of Biomedical Materials Research Part B-Applied Biomaterials* 2004;71B(2):373-80.
- [138] Chang CH, Liu HC, Lin CC, Chou CH, Lin FH. Gelatin-chondroitin-hyaluronan tri-copolymer scaffold for cartilage tissue engineering. *Biomaterials* 2003;24(26):4853-8.
- [139] Li Q, Williams CG, Sun DD, Wang J, Leong K, Elisseff JH. Photocrosslinkable polysaccharides based on chondroitin sulfate. *J Biomed Mater Res A* 2004;68(1):28-33.
- [140] Eyrich D, Brandl F, Appel B, Wiese H, Maier G, Wenzel M, et al. Long-term stable fibrin gels for cartilage engineering. *Biomaterials* 2007;28(1):55-65.
- [141] Lee CR, Grad S, Gorna K, Gogolewski S, Goessl A, Alini M. Fibrin-polyurethane composites for articular cartilage tissue engineering: A preliminary analysis. *Tissue Engineering* 2005;11(9-10):1562-73.
- [142] Silverman RP, Passaretti D, Huang W, Randolph MA, Yaremchuk MJ. Injectable tissue-engineered cartilage using a fibrin glue polymer. *Plast Reconstr Surg* 1999;103(7):1809-18.
- [143] Ting V, Sims CD, Brecht LE, McCarthy JG, Kasabian AK, Connelly PR, et al. In vitro prefabrication of human cartilage shapes using fibrin glue and human chondrocytes. *Ann Plast Surg* 1998;40(4):413-20; discussion 20-1.

- [144] Goodstone NJ, Cartwright A, Ashton B. Effects of high molecular weight hyaluronan on chondrocytes cultured within a resorbable gelatin sponge. *Tissue Engineering* 2004;10(3-4):621-31.
- [145] Hoshikawa A, Nakayama Y, Matsuda T, Oda H, Nakamura K, Mabuchi K. Encapsulation of chondrocytes in photopolymerizable styrenated gelatin for cartilage tissue engineering. *Tissue Engineering* 2006;12(8):2333-41.
- [146] Ibusuki S, Fujii Y, Iwamoto Y, Matsuda T. Tissue-engineered cartilage using an injectable and in situ gelable thermoresponsive gelatin: fabrication and in vitro performance. *Tissue Eng* 2003;9(2):371-84.
- [147] Burdick JA, Chung C, Jia XQ, Randolph MA, Langer R. Controlled degradation and mechanical behavior of photopolymerized hyaluronic acid networks. *Biomacromolecules* 2005;6(1):386-91.
- [148] Marcacci M, Berruto M, Brocchetta D, Delcogliano A, Ghinelli D, Gobbi A, et al. Articular cartilage engineering with Hyalograft (R) C - 3-year clinical results. *Clinical Orthopaedics and Related Research* 2005;(435):96-105.
- [149] Radice M, Brun P, Cortivo R, Scapinelli R, Battaliard C, Abatangelo G. Hyaluronan-based biopolymers as delivery vehicles for bone-marrow-derived mesenchymal progenitors. *Journal of Biomedical Materials Research* 2000;50(2):101-9.
- [150] Smeds KA, Pfister-Serres A, Miki D, Dastgheib K, Inoue M, Hatchell DL, et al. Photocrosslinkable polysaccharides for in situ hydrogel formation. *J Biomed Mater Res* 2001;54(1):115-21.
- [151] Hofmann S, Knecht S, Langer R, Kaplan DL, Vunjak-Novakovic G, Merkle HP, et al. Cartilage-like tissue engineering using silk scaffolds and mesenchymal stem cells. *Tissue Engineering* 2006;12(10):2729-38.
- [152] Wang YZ, Blasioli DJ, Kim HJ, Kim HS, Kaplan DL. Cartilage tissue engineering with silk scaffolds and human articular chondrocytes. *Biomaterials* 2006;27(25):4434-42.

- [153] Wang YZ, Kim HJ, Vunjak-Novakovic G, Kaplan DL. Stem cell-based tissue engineering with silk biomaterials. *Biomaterials* 2006;27(36):6064-82.
- [154] Freed LE, Marquis JC, Nohria A, Emmanuel J, Mikos AG, Langer R. Neocartilage formation in vitro and in vivo using cells cultured on synthetic biodegradable polymers. *J Biomed Mater Res* 1993;27(1):11-23.
- [155] Hsu SH, Chang SH, Yen HJ, Whu SW, Tsai CL, Chen DC. Evaluation of biodegradable polyesters modified by type II collagen and Arg-Gly-Asp as tissue engineering scaffolding materials for cartilage regeneration. *Artificial Organs* 2006;30(1):42-55.
- [156] Li WJ, Danielson KG, Alexander PG, Tuan RS. Biological response of chondrocytes cultured in three-dimensional nanofibrous poly(epsilon-caprolactone) scaffolds. *Journal of Biomedical Materials Research Part A* 2003;67A(4):1105-14.
- [157] Li WJ, Laurencin CT, Caterson EJ, Tuan RS, Ko FK. Electrospun nanofibrous structure: a novel scaffold for tissue engineering. *J Biomed Mater Res* 2002;60(4):613-21.
- [158] Shin HJ, Lee CH, Cho IH, Kim YJ, Lee YJ, Kim IA, et al. Electrospun PLGA nanofiber scaffolds for articular cartilage reconstruction: mechanical stability, degradation and cellular responses under mechanical stimulation in vitro. *Journal of Biomaterials Science-Polymer Edition* 2006;17(1-2):103-19.
- [159] Sittering M, Reitzel D, Dauner M, Hierlemann H, Hammer C, Kastenbauer E, et al. Resorbable polyesters in cartilage engineering: Affinity and biocompatibility of polymer fiber structures to chondrocytes. *Journal of Biomedical Materials Research* 1996;33(2):57-63.
- [160] Uematsu K, Hattori K, Ishimoto Y, Yamauchi J, Habata T, Takakura Y, et al. Cartilage regeneration using mesenchymal stem cells and a three-dimensional poly-lactic-glycolic acid (PLGA) scaffold. *Biomaterials* 2005;26(20):4273-9.
- [161] Bryant SJ, Bender RJ, Durand KL, Anseth KS. Encapsulating Chondrocytes in degrading PEG hydrogels with high modulus: Engineering gel structural changes to facilitate cartilaginous tissue production. *Biotechnology and Bioengineering* 2004;86(7):747-55.

- [162] Elisseeff J, McIntosh W, Anseth K, Riley S, Ragan P, Langer R. Photoencapsulation of chondrocytes in poly(ethylene oxide)-based semi-interpenetrating networks. *Journal of Biomedical Materials Research* 2000;51(2):164-71.
- [163] Lee HJ, Lee JS, Chansakul T, Yu C, Elisseeff JH, Yu SM. Collagen mimetic peptide-conjugated photopolymerizable PEG hydrogel. *Biomaterials* 2006;27(30):5268-76.
- [164] Au A, Ha J, Polotsky A, Krzyminski K, Gutowska A, Hungerford DS, et al. Thermally reversible polymer gel for chondrocyte culture. *Journal of Biomedical Materials Research Part A* 2003;67A(4):1310-9.
- [165] Na K, Kim S, Woo DG, Sun BK, Yang HN, Chung HM, et al. Synergistic effect of TGF beta-3 on chondrogenic differentiation of rabbit chondrocytes in thermo-reversible hydrogel constructs blended with hyaluronic acid by in vivo test. *Journal of Biotechnology* 2007;128(2):412-22.
- [166] Song E, Kim SY, Chun T, Byun HJ, Lee YM. Collagen scaffolds derived from a marine source and their biocompatibility. *Biomaterials* 2006;27(15):2951-61.
- [167] Fisher JP, Jo S, Mikos AG, Reddi AH. Thermoreversible hydrogel scaffolds for articular cartilage engineering. *Journal of Biomedical Materials Research Part A* 2004;71A(2):268-74.
- [168] Holland TA, Tabata Y, Mikos AG. Dual growth factor delivery from degradable oligo(poly(ethylene glycol) fumarate) hydrogel scaffolds for cartilage tissue engineering. *Journal of Controlled Release* 2005;101(1-3):111-25.
- [169] Liao E, Yaszemski M, Krebsbach P, Hollister S. Tissue-engineered cartilage constructs using composite hyaluronic acid/collagen I hydrogels and designed poly(propylene fumarate) scaffolds. *Tissue Engineering* 2007;13(3):537-50.
- [170] Chia SL, Gorna K, Gogolewski S, Alini M. Biodegradable elastomeric polyurethane membranes as chondrocyte carriers for cartilage repair. *Tissue Eng* 2006;12(7):1945-53.



- [171] Grad S, Kupcsik L, Gorna K, Gogolewski S, Alini M. The use of biodegradable polyurethane scaffolds for cartilage tissue engineering: potential and limitations. *Biomaterials* 2003;24(28):5163-71.
- [172] Liu Y, Webb K, Kirker KR, Bernshaw NJ, Tresco PA, Gray SD, et al. Composite articular cartilage engineered on a chondrocyte-seeded aliphatic polyurethane sponge. *Tissue Eng* 2004;10(7-8):1084-92.
- [173] Bray JC, Merrill EW. Poly(vinyl alcohol) hydrogels for synthetic articular cartilage material. *J Biomed Mater Res* 1973;7(5):431-43.
- [174] Bryant SJ, Davis-Arehart KA, Luo N, Shoemaker RK, Arthur JA, Anseth KS. Synthesis and characterization of photopolymerized multifunctional hydrogels: Water-soluble poly(vinyl alcohol) and chondroitin sulfate macromers for chondrocyte encapsulation. *Macromolecules* 2004;37(18):6726-33.
- [175] Martens PJ, Bryant SJ, Anseth KS. Tailoring the degradation of hydrogels formed from multivinyl poly(ethylene glycol) and poly(vinyl alcohol) macromers for cartilage tissue engineering. *Biomacromolecules* 2003;4(2):283-92.
- [176] Holmes TC. Novel peptide-based biomaterial scaffolds for tissue engineering. *Trends Biotechnol* 2002;20(1):16-21.
- [177] Kisiday J, Jin M, Kurz B, Hung H, Semino C, Zhang S, et al. Self-assembling peptide hydrogel fosters chondrocyte extracellular matrix production and cell division: implications for cartilage tissue repair. *Proc Natl Acad Sci U S A* 2002;99(15):9996-10001.
- [178] Kisiday JD, Jin MS, DiMicco MA, Kurz B, Grodzinsky AJ. Effects of dynamic compressive loading on chondrocyte biosynthesis in self-assembling peptide scaffolds. *Journal of Biomechanics* 2004;37(5):595-604.
- [179] Zhang S, Holmes T, Lockshin C, Rich A. Spontaneous assembly of a self-complementary oligopeptide to form a stable macroscopic membrane. *Proc Natl Acad Sci U S A* 1993;90(8):3334-8.

- [180] Bryant SJ, Anseth KS. The effects of scaffold thickness on tissue engineered cartilage in photocrosslinked poly(ethylene oxide) hydrogels. *Biomaterials* 2001;22(6):619-26.
- [181] Bryant SJ, Nuttelman CR, Anseth KS. Cytocompatibility of UV and visible light photoinitiating systems on cultured NIH/3T3 fibroblasts in vitro. *J Biomater Sci Polym Ed* 2000;11(5):439-57.
- [182] Bryant SJ, Durand KL, Anseth KS. Manipulations in hydrogel chemistry control photoencapsulated chondrocyte behavior and their extracellular matrix production. *Journal of Biomedical Materials Research Part A* 2003;67A(4):1430-6.
- [183] Rice MA, Anseth KS. Encapsulating chondrocytes in copolymer gels: Bimodal degradation kinetics influence cell phenotype and extracellular matrix development. *Journal of Biomedical Materials Research Part A* 2004;70A(4):560-8.
- [184] Sontjens SHM, Nettles DL, Carnahan MA, Setton LA, Grinstaff MW. Biodendrimer-based hydrogel scaffolds for cartilage tissue repair. *Biomacromolecules* 2006;7(1):310-6.
- [185] Chen WY, Abatangelo G. Functions of hyaluronan in wound repair. *Wound Repair Regen* 1999;7(2):79-89.
- [186] Nettles DL, Vail TP, Morgan MT, Grinstaff MW, Setton LA. Photocrosslinkable hyaluronan as a scaffold for articular cartilage repair. *Ann Biomed Eng* 2004;32(3):391-7.
- [187] Liu YC, Shu XZ, Prestwich GD. Osteochondral defect repair with autologous bone marrow-derived mesenchymal stem cells in an injectable, in situ, cross-linked synthetic extracellular matrix. *Tissue Engineering* 2006;12(12):3405-16.
- [188] Mosesson MW. Fibrinogen and fibrin structure and functions. *J Thromb Haemost* 2005;3(8):1894-904.
- [189] Schagemann JC, Mrosek EH, Landers R, Kurz H, Erggelet C. Morphology and function of ovine articular cartilage chondrocytes in 3-D hydrogel culture. *Cells Tissues Organs* 2006;182(2):89-97.
- [190] Connelly JT, Garcia AJ, Levenston ME. Inhibition of in vitro chondrogenesis in RGD-modified three-dimensional alginate gels. *Biomaterials* 2007;28(6):1071-83.

- [191] Iwasaki N, Yamane ST, Majima T, Kasahara Y, Minami A, Harada K, et al. Feasibility of polysaccharide hybrid materials for scaffolds in cartilage tissue engineering: Evaluation of chondrocyte adhesion to polyion complex fibers prepared from alginate and chitosan. *Biomacromolecules* 2004;5(3):828-33.
- [192] Wayne JS, McDowell CL, Shields KJ, Tuan RS. In vivo response of polylactic acid-alginate scaffolds and bone marrow-derived cells for cartilage tissue engineering. *Tissue Engineering* 2005;11(5-6):953-63.
- [193] Subramanian A, Lin HY. Crosslinked chitosan: Its physical properties and the effects of matrix stiffness on chondrocyte cell morphology and proliferation. *Journal of Biomedical Materials Research Part A* 2005;75A(3):742-53.
- [194] Chen JP, Cheng TH. Thermo-responsive chitosan-graft-poly(N-isopropylacrylamide) injectable hydrogel for cultivation of chondrocytes and meniscus cells. *Macromolecular Bioscience* 2006;6(12):1026-39.
- [195] Bhardwaj T, Pilliar RM, Gryn timer MD, Kandel RA. Effect of material geometry on cartilaginous tissue formation in vitro. *Journal of Biomedical Materials Research* 2001;57(2):190-9.
- [196] Hile DD, Amirpour ML, Akgerman A, Pishko MV. Active growth factor delivery from poly(D,L-lactide-co-glycolide) foams prepared in supercritical CO<sub>2</sub>. *J Control Release* 2000;66(2-3):177-85.
- [197] Sato T, Chen GP, Ushida T, Ishii T, Ochiai N, Tateishi T, et al. Evaluation of PLLA-collagen hybrid sponge as a scaffold for cartilage tissue engineering. *Materials Science & Engineering C-Biomimetic and Supramolecular Systems* 2004;24(3):365-72.
- [198] Chen GP, Sato T, Ushida T, Ochiai N, Tateishi T. Tissue engineering of cartilage using a hybrid scaffold of synthetic polymer and collagen. *Tissue Engineering* 2004;10(3-4):323-30.

- [199] Barnewitz D, Endres M, Kruger I, Becker A, Zimmermann M, Wilke I, et al. Treatment of articular cartilage defects in horses with polymer-based cartilage tissue engineering grafts. *Biomaterials* 2006;27(14):2882-9.
- [200] Vickers SM, Squitieri LS, Spector M. Effects of cross-linking type II collagen-GAG scaffolds on chondrogenesis in vitro: Dynamic pore reduction promotes cartilage formation. *Tissue Engineering* 2006;12(5):1345-55.
- [201] Kang Y, Yang J, Khan S, Anissian L, Ameer GA. A new biodegradable polyester elastomer for cartilage tissue engineering. *Journal of Biomedical Materials Research Part A* 2006;77A(2):331-9.
- [202] Chen GP, Sato T, Ushida T, Hirochika R, Shirasaki Y, Ochiai N, et al. The use of a novel PLGA fiber/collagen composite web as a scaffold for engineering of articular cartilage tissue with adjustable thickness. *Journal of Biomedical Materials Research Part A* 2003;67A(4):1170-80.
- [203] Woodfield TB, Malda J, de Wijn J, Peters F, Riesle J, van Blitterswijk CA. Design of porous scaffolds for cartilage tissue engineering using a three-dimensional fiber-deposition technique. *Biomaterials* 2004;25(18):4149-61.
- [204] Moroni L, de Wijn JR, van Blitterswijk CA. 3D fiber-deposited scaffolds for tissue engineering: influence of pores geometry and architecture on dynamic mechanical properties. *Biomaterials* 2006;27(7):974-85.
- [205] Moroni L, Hendriks JAA, Schotel R, De Wijn JR, Van Blitterswijk CA. Design of biphasic polymeric 3-dimensional fiber deposited scaffolds for cartilage tissue engineering applications. *Tissue Engineering* 2007;13(2):361-71.
- [206] Yoo HS, Lee EA, Yoon JJ, Park TG. Hyaluronic acid modified biodegradable scaffolds for cartilage tissue engineering. *Biomaterials* 2005;26(14):1925-33.
- [207] Girotto D, Urbani S, Brun P, Renier D, Barbucci R, Abatangelo G. Tissue-specific gene expression in chondrocytes grown on three-dimensional hyaluronic acid scaffolds. *Biomaterials* 2003;24(19):3265-75.

- [208] Grigolo B, Lisignoli G, Piacentini A, Fiorini M, Gobbi P, Mazzotti G, et al. Evidence for redifferentiation of human chondrocytes grown on a hyaluronan-based biomaterial (HYAFF (R) 11): molecular, immunohistochemical and ultrastructural analysis. *Biomaterials* 2002;23(4):1187-95.
- [209] Gobbi A, Kon E, Berruto M, Francisco R, Filardo G, Marcacci M. Patellofemoral full-thickness chondral defects treated with hyalograft-C - A clinical, arthroscopic, and histologic review. *American Journal of Sports Medicine* 2006;34(11):1763-73.
- [210] Hollander AP, Dickinson SC, Sims TJ, Brun P, Cortivo R, Kon E, et al. Maturation of tissue engineered cartilage implanted in injured and osteoarthritic human knees. *Tissue Engineering* 2006;12(7):1787-98.
- [211] Rosier RN, O'Keefe RJ, Crabb ID, Puzas JE. Transforming growth factor beta: an autocrine regulator of chondrocytes. *Connect Tissue Res* 1989;20(1-4):295-301.
- [212] Seyedin SM, Rosen DM, Segarini PR. Modulation of chondroblast phenotype by transforming growth factor-beta. *Pathol Immunopathol Res* 1988;7(1-2):38-42.
- [213] Tuli R, Tuli S, Nandi S, Huang X, Manner PA, Hozack WJ, et al. Transforming growth factor-beta-mediated chondrogenesis of human mesenchymal progenitor cells involves N-cadherin and mitogen-activated protein kinase and Wnt signaling cross-talk. *J Biol Chem* 2003;278(42):41227-36.
- [214] Stevens MM, Marini RP, Martin I, Langer R, Shastri VP. FGF-2 enhances TGF-beta 1-induced periosteal chondrogenesis. *Journal of Orthopaedic Research* 2004;22(5):1114-9.
- [215] Veilleux N, Spector M. Effects of FGF-2 and IGF-1 on adult canine articular chondrocytes in type II collagen-glycosaminoglycan scaffolds in vitro. *Osteoarthritis and Cartilage* 2005;13(4):278-86.
- [216] Hicks DL, Sage AB, Shelton E, Schumacher BL, Sah RL, Watson D. Effect of bone morphogenetic proteins 2 and 7 on septal chondrocytes in alginate. *Otolaryngology-Head and Neck Surgery* 2007;136(3):373-9.

- [217] Kaps C, Bramlage C, Smolian H, Haisch A, Ungethum U, Burmester GR, et al. Bone morphogenetic proteins promote cartilage differentiation and protect engineered artificial cartilage from fibroblast invasion and destruction. *Arthritis and Rheumatism* 2002;46(1):149-62.
- [218] Mason JM, Breitbart AS, Barcia M, Porti D, Pergolizzi RG, Grande DA. Cartilage and bone regeneration using gene-enhanced tissue engineering. *Clinical Orthopaedics and Related Research* 2000;(379):S171-S8.
- [219] Madry H, Kaul G, Cucchiaroni M, Stein U, Zurakowski D, Remberger K, et al. Enhanced repair of articular cartilage defects in vivo by transplanted chondrocytes overexpressing insulin-like growth factor I (IGF-I). *Gene Ther* 2005;12(15):1171-9.
- [220] Mcquillan DJ, Handley CJ, Campbell MA, Bolis S, Milway VE, Herington AC. Stimulation of Proteoglycan Biosynthesis by Serum and Insulin-Like Growth Factor-I in Cultured Bovine Articular-Cartilage. *Biochem J* 1986;240(2):423-30.
- [221] Allemann M, Mizuno S, Eid K, Yates KE, Zaleske D, Glowacki J. Effects of hyaluronan on engineered articular cartilage extracellular matrix gene expression in 3-dimensional collagen scaffolds. *Journal of Biomedical Materials Research* 2001;55(1):13-9.
- [222] Kellner K, Schulz MB, Gopferich A, Blunk T. Insulin in tissue engineering of cartilage: A potential model system for growth factor application. *Journal of Drug Targeting* 2001;9(6):439-48.
- [223] Iwasaki M, Nakata K, Nakahara H, Nakase T, Kimura T, Kimata K, et al. Transforming growth factor-beta 1 stimulates chondrogenesis and inhibits osteogenesis in high density culture of periosteum-derived cells. *Endocrinology* 1993;132(4):1603-8.
- [224] Vivien D, Galera P, Lebrun E, Loyau G, Pujol JP. Differential effects of transforming growth factor-beta and epidermal growth factor on the cell cycle of cultured rabbit articular chondrocytes. *J Cell Physiol* 1990;143(3):534-45.

- [225] Gooch KJ, Kwon JH, Blunk T, Langer R, Freed LE, Vunjak-Novakovic G. Effects of mixing intensity on tissue-engineered cartilage. *Biotechnology and Bioengineering* 2001;72(4):402-7.
- [226] Roberts AB, Kondaiah P, Rosa F, Watanabe S, Good P, Danielpour D, et al. Mesoderm induction in *Xenopus laevis* distinguishes between the various TGF-beta isoforms. *Growth Factors* 1990;3(4):277-86.
- [227] Gooch KJ, Blunk T, Courter DL, Sieminski AL, Bursac PM, Vunjak-Novakovic G, et al. IGF-I and mechanical environment interact to modulate engineered cartilage development. *Biochemical and Biophysical Research Communications* 2001;286(5):909-15.
- [228] Martin I, Suetterlin R, Baschong W, Heberer M, Vunjak-Novakovic G, Freed LE. Enhanced cartilage tissue engineering by sequential exposure of chondrocytes to FGF-2 during 2D expansion and BMP-2 during 3D cultivation. *Journal of Cellular Biochemistry* 2001;83(1):121-8.
- [229] Miot S, de Freitas PS, Wirz D, Daniels AU, Sims TJ, Hollander AP, et al. Cartilage tissue engineering by expanded goat articular chondrocytes. *Journal of Orthopaedic Research* 2006;24(5):1078-85.
- [230] Schmal H, Mehlhorn AT, Zwingmann J, Muller CA, Stark GB, Sudkamp NP. Stimulation of chondrocytes in vitro by gene transfer with plasmids coding for epidermal growth factor (hEGF) and basic fibroblast growth factor (bFGF). *Cytotherapy* 2005;7(3):292-300.
- [231] Frenkel SR, Saadeh PB, Mehrara BJ, Chin GS, Steinbrech DS, Brent B, et al. Transforming growth factor beta superfamily members: Role in cartilage modeling. *Plastic and Reconstructive Surgery* 2000;105(3):980-90.
- [232] Park H, Temenoff JS, Holland TA, Tabata Y, Mikos AG. Delivery of TGF-beta 1 and chondrocytes via injectable, biodegradable hydrogels for cartilage tissue engineering applications. *Biomaterials* 2005;26(34):7095-103.

- [233] Sharma B, Williams CG, Khan M, Manson P, Elisseeff JH. In vivo chondrogenesis of mesenchymal stem cells in a photopolymerized hydrogel. *Plastic and Reconstructive Surgery* 2007;119(1):112-20.
- [234] Huang Q, Hutmacher DW, Lee EH. In vivo mesenchymal cell recruitment by a scaffold loaded with transforming growth factor beta 1 and the potential for in situ chondrogenesis. *Tissue Engineering* 2002;8(3):469-82.
- [235] DeFail AJ, Chu CR, Izzo N, Marra KG. Controlled release of bioactive TGF-beta(1) from microspheres embedded within biodegradable hydrogels. *Biomaterials* 2006;27(8):1579-85.
- [236] Lee JE, Kim SE, Kwon IC, Ahn HJ, Cho H, Lee SH, et al. Effects of a chitosan scaffold containing TGF-beta 1 encapsulated chitosan microspheres on in vitro chondrocyte culture. *Artificial Organs* 2004;28(9):829-39.
- [237] Holland TA, Bodde EWH, Cuijpers VMJI, Baggett LS, Tabata Y, Mikos AG, et al. Degradable hydrogel scaffolds for in vivo delivery of single and dual growth factors in cartilage repair. *Osteoarthritis and Cartilage* 2007;15(2):187-97.
- [238] Yamane S, Iwasaki N, Majima T, Funakoshi T, Masuko T, Harada K, et al. Feasibility of chitosan-based hyaluronic acid hybrid biomaterial for a novel scaffold in cartilage tissue engineering. *Biomaterials* 2005;26(6):611-9.
- [239] Asanbaeva A, Masuda K, Thonar EJMA, Klisch SM, Sah RL. Mechanisms of cartilage growth - Modulation of balance between proteoglycan and collagen in vitro using chondroitinase ABC. *Arthritis and Rheumatism* 2007;56(1):188-98.
- [240] Saraf A, Mikos AG. Gene delivery strategies for cartilage tissue engineering. *Advanced Drug Delivery Reviews* 2006;58(4):592-603.
- [241] Tong JC, Yao SL. Novel scaffold containing transforming growth factor-beta 1 DNA for cartilage tissue engineering. *Journal of Bioactive and Compatible Polymers* 2007;22(2):232-44.



- [242] Grande DA, Mason J, Light E, Dines D. Stem cells as platforms for delivery of genes to enhance cartilage repair. *Journal of Bone and Joint Surgery-American Volume* 2003;85A:111-6.
- [243] Hansen U, Schunke M, Domm C, Ioannidis N, Hassenpflug J, Gehrke T, et al. Combination of reduced oxygen tension and intermittent hydrostatic pressure: a useful tool in articular cartilage tissue engineering. *Journal of Biomechanics* 2001;34(7):941-9.
- [244] Scherer K, Schunke M, Sellckau R, Hassenpflug J, Kurz B. The influence of oxygen and hydrostatic pressure on articular chondrocytes and adherent bone marrow cells in vitro. *Biorheology* 2004;41(3-4):323-33.
- [245] Miyanishi K, Trindade MCD, Lindsey DP, Beaupre GS, Carter DR, Goodman SB, et al. Dose- and time-dependent effects of cyclic hydrostatic pressure on transforming growth factor-beta 3-induced chondrogenesis by adult human mesenchymal stem cells in vitro. *Tissue Engineering* 2006;12(8):2253-62.
- [246] Miyanishi K, Trindade MCD, Lindsey DP, Beaupre GS, Carter DR, Goodman SB, et al. Effects of hydrostatic pressure and transforming growth factor-beta 3 on adult human mesenchymal stem cell chondrogenesis in vitro. *Tissue Engineering* 2006;12(6):1419-28.
- [247] Hu JC, Athanasiou KA. The effects of intermittent hydrostatic pressure on self-assembled articular cartilage constructs. *Tissue Engineering* 2006;12(5):1337-44.
- [248] De Croos JNA, Dhaliwal SS, Gryn timer MD, Pilliar RM, Kandel RA. Cyclic compressive mechanical stimulation induces sequential catabolic and anabolic gene changes in chondrocytes resulting in increased extracellular matrix accumulation. *Matrix Biology* 2006;25(6):323-31.
- [249] Waldman SD, Couto DC, Gryn timer MD, Pilliar RM, Kandel RA. A single application of cyclic loading can accelerate matrix deposition and enhance the properties of tissue-engineered cartilage. *Osteoarthritis and Cartilage* 2006;14(4):323-30.

- [250] Davisson T, Kunig S, Chen A, Sah R, Ratcliffe A. Static and dynamic compression modulate matrix metabolism in tissue engineered cartilage. *Journal of Orthopaedic Research* 2002;20(4):842-8.
- [251] Angele P, Schumann D, Angele M, Kinner B, Englert C, Hente R, et al. Cyclic, mechanical compression enhances chondrogenesis of mesenchymal progenitor cells in tissue engineering scaffolds. *Biorheology* 2004;41(3-4):335-46.
- [252] Ng KW, Mauck RL, Statman LY, Lin EY, Ateshian GA, Hung CT. Dynamic deformational loading results in selective application of mechanical stimulation in a layered, tissue-engineered cartilage construct. *Biorheology* 2006;43(3-4):497-507.
- [253] Hunter CJ, Mouw JK, Levenston ME. Dynamic compression of chondrocyte-seeded fibrin gels: effects on matrix accumulation and mechanical stiffness. *Osteoarthritis and Cartilage* 2004;12(2):117-30.
- [254] Chowdhury TT, Salter DM, Bader DL, Lee DA. Integrin-mediated mechanotransduction processes in TGF beta-stimulated monolayer-expanded chondrocytes. *Biochemical and Biophysical Research Communications* 2004;318(4):873-81.
- [255] Pazzano D, Mercier KA, Moran JM, Fong SS, DiBiasio DD, Rulfs JX, et al. Comparison of chondrogenesis in static and perfused bioreactor culture. *Biotechnology Progress* 2000;16(5):893-6.
- [256] Xu X, Urban JPG, Tirlapur U, Wu MH, Cui Z, Cui ZF. Influence of perfusion on metabolism and matrix production by bovine articular chondrocytes in hydrogel scaffolds. *Biotechnology and Bioengineering* 2006;93(6):1103-11.
- [257] Hu JC, Athanasiou KA. Low-density cultures of bovine chondrocytes: effects of scaffold material and culture system. *Biomaterials* 2005;26(14):2001-12.
- [258] Gemmiti CV, Guldberg RE. Fluid flow increases type II collagen deposition and tensile mechanical properties in bioreactor-grown tissue-engineered cartilage. *Tissue Engineering* 2006;12(3):469-79.

- [259] Saini S, Wick TM. Concentric cylinder bioreactor for production of tissue engineered cartilage: Effect of seeding density and hydrodynamic loading on construct development. *Biotechnology Progress* 2003;19(2):510-21.
- [260] Bueno EM, Bilgen B, Barabino GA. Wavy-walled bioreactor supports increased cell proliferation and matrix deposition in engineered cartilage constructs. *Tissue Engineering* 2005;11(11-12):1699-709.

## CHAPTER 4

### *Synthesis and Characterization of Methacrylated Hyaluronic Acid Hydrogels*

(Adapted from: JA Burdick, **C Chung**, X Jia, MA Randolph, R Langer, "Controlled degradation and mechanical behavior of photopolymerized hyaluronic acid networks," *Biomacromolecules*, 2005, 6(1): 386-91)

#### **4.1 Introduction**

The choice of hyaluronic acid (HA) as the base material for this tissue engineering (TE) scaffold is inspired by cartilage itself. Found natively in cartilage, hyaluronic acid is a linear polysaccharide of alternating D-glucuronic acid and  $\beta$ -N-acetyl-D-glucosamine that functions as a core molecule for the binding of keratin sulfate and chondroitin sulfate in forming aggrecan and degrades primarily by hyaluronidases found within the body or through oxidative mechanisms to yield oligosaccharides and glucuronic acid. This natural polymer plays a role in cellular processes like cell proliferation, morphogenesis, inflammation, and wound repair [1], and can function as a bioactive scaffold, where cell surface receptors for HA (CD44, CD54, and CD168) allow for cell/scaffold interactions. For TE, it can be readily modified through its carboxyl [2,3] and hydroxyl groups [4-6] and polymerized to form 3D scaffolds in the form of hydrogels [7-9], sponges [10], and meshes [11]. The HA scaffolds are biocompatible and can serve as delivery vehicles for cells.

Photopolymerization is one approach to chemically crosslink hydrogels using ultraviolet or visible light, and provides uniform cell seeding with both spatial and temporal control over polymerization [12]. Since hydrogels are water-swollen networks, they are typically suitable for the delivery of cells and bioactive agents, and can be used as injectable scaffolds, filling cartilage defects of any size and shape in a minimally invasive manner. These scaffolds support the transport of nutrients and waste, and can homogeneously suspend cells in a 3D environment, where encapsulated cells typically retain a rounded morphology. Elisseeff and coworkers [13]

were the first to report the use of photopolymerization to suspend chondrocytes in hydrogels for cartilage regeneration. These efforts have focused primarily on photopolymerizable hydrogels based on poly(ethylene glycol) (PEG). Careful screening of photoinitiating conditions has been performed to optimize cell viability within these crosslinked networks [14]. Through this screening, one specific initiating system that uses a water soluble initiator, 2-methyl-1-[4-(hydroxyethoxy)phenyl]-2-methyl-1-propanone (I2959) at 0.05wt%, was found to be cytocompatible, supporting a high viability of photoencapsulated chondrocytes. Later, Bryant and Anseth showed that photocrosslinked scaffolds, spanning the thickness of native cartilage found *in vivo*, could be fabricated while maintaining spatial uniformity of glycosaminoglycans, and that the hydrogel properties (e.g. crosslinking density) influence both the mechanical properties of the hydrogel and the production of collagen by encapsulated chondrocytes [12]. In addition, Setton and coworkers[4] illustrated the ability to encapsulate articular chondrocytes in one photopolymerizable HA network *in vivo*.

The objective of this study is to combine the benefits of a photocrosslinkable network with the desirable properties of HA for future application in cartilage tissue engineering. In this chapter, the effects of HA molecular weight, the degree of methacrylation and macromer concentration on the physical properties (e.g., swelling, mechanics, and degradation) of the resulting hydrogels are systematically investigated. In addition, photoencapsulated cell viability was investigated as a preliminary test for the potential use of photopolymerizable HA networks as cell carriers for cartilage regeneration.

## **4.2 Materials & Methodology**

### **4.2.1 Macromer Synthesis and Polymerization**

Methacrylated HA (MeHA) was synthesized as previously described [6]. Briefly, methacrylic anhydride (Sigma, ~20-fold excess) was added to a solution of 1 wt% HA (Lifecore, MW = 50kDa, 350kDa, 1100kDa) in deionized water, adjusted to a pH of 8 with 5 N NaOH

(Aldrich), and reacted on ice for 24 hours (Figure 4.1A). The macromer solution was purified via dialysis (MW cutoff 5-8kDa) against deionized water for a minimum of 48 hours with repeated changes of water. The final product was obtained by lyophilization and stored at -20°C in powder form prior to use.  $^1\text{H}$  NMR (Bruker Advance 360 MHz, Bruker) was used to determine the final functionality and purity of the macromer (Figure 4.1B). Percent modification (Table 4.1) was determined by the integration and comparison of methacrylate peaks to HA backbone peaks (Figure 4.1).

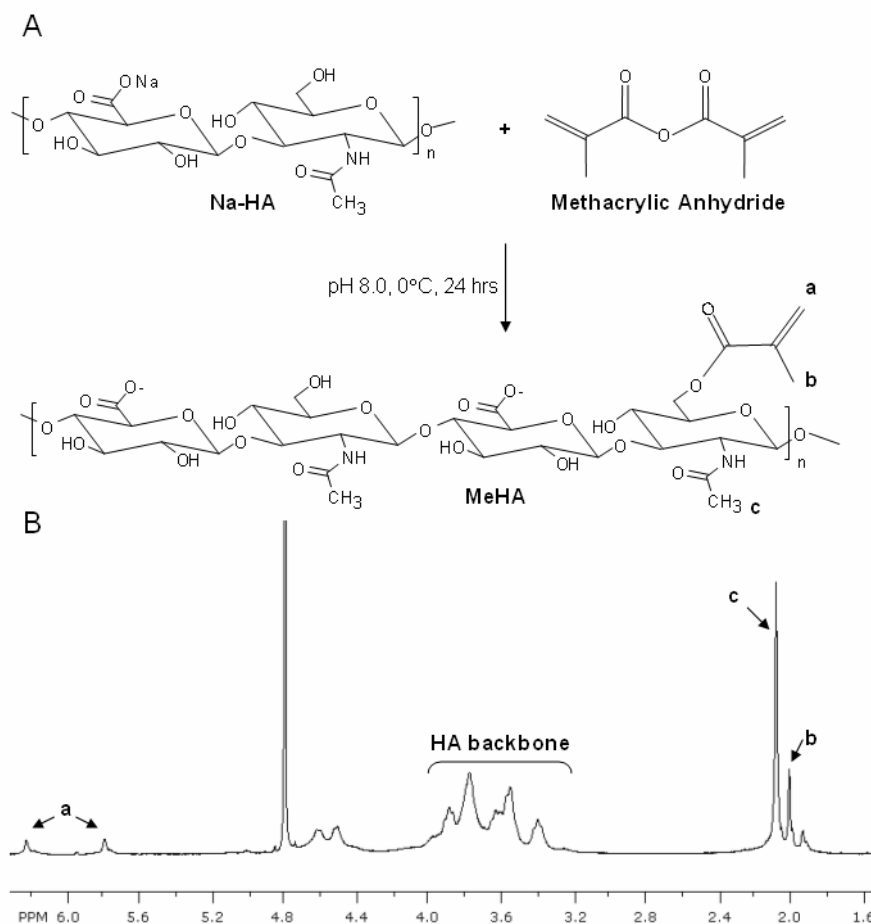


**Figure 4.1** (A) Synthetic Scheme of MeHA. (B)  $^1\text{H}$  NMR of MeHA macromer in  $\text{D}_2\text{O}$ . The HA backbone consists of 10 protons, while **a**, **b**, and **c** represent protons associated with methacrylate alkene (2 protons), the methyl group on the methacrylate (3 protons), and the methyl group on HA (3 protons).

Hydrogels were fabricated by dissolving the MeHA macromers at various concentrations (2, 5, 10, 20 wt%) in phosphate buffered saline (PBS) containing 0.05 wt% I2959 (Ciba). Macromer solutions were pipetted between glass slides with a 1 mm spacer and polymerized with the addition of  $\sim 4 \text{ mW/cm}^2$  ultraviolet light for 10 minutes using a long-wave ultraviolet lamp (Model 100AP, Blak-Ray). A general schematic of the free radical polymerization of MeHA to form crosslinked hydrogel networks is illustrated in Figure 4.2.

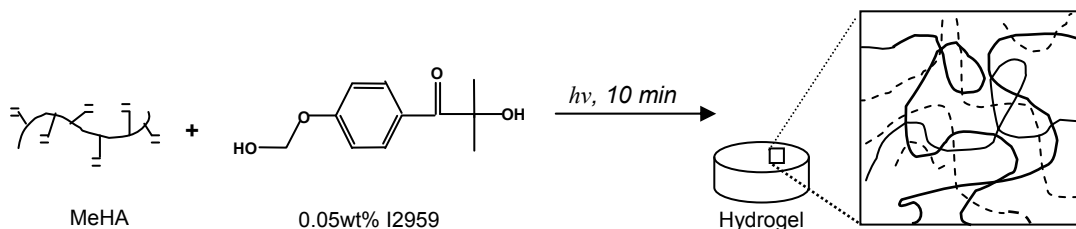


**Figure 4.2** A general schematic of the free radical polymerization of MeHA to form crosslinked hydrogel networks. This process involves the formation of radicals from the exposure of the initiator to light, which propagate through the vinyl groups of the MeHA to form kinetic chains (shown as dashed lines). These networks eventually degrade by enzymatic cleavage of the HA backbone.

#### 4.2.2 Hydrogel Characterization

After polymerization, hydrogels were swollen in PBS for 48 hours to equilibrium, weighed (wet weight), and dried (dry weight) to determine volumetric swelling ratio ( $Q_V$ ) ( $n=3$ ).  $Q_V$  is determined by:

$$\text{Eq. 4.1} \quad Q_M = (\text{wet weight} / \text{dry weight})$$

$$\text{Eq. 4.2} \quad Q_V = 1 + (\rho_P / \rho_S) \times (Q_M - 1),$$

where  $\rho_P$  is the density of the dry polymer ( $1.23 \text{ g/cm}^3$ ) and  $\rho_S$  is the density of the solvent ( $1 \text{ g/cm}^3$ )<sup>16</sup>.

The average molecular weight between crosslinks ( $M_c$ ) can then be calculated using the Flory-Rehner equation:

$$\text{Eq. 4.3} \quad Q_v^{5/3} \cong (v M_c)/V_1 \times (0.5 - X) \quad [15,16],$$

where  $v$  is the specific volume of polymer (for HA in water at 37°C:  $v = 0.547 \text{ cm}^3/\text{g}$ ) [17],  $M_c$  is the average molecular weight between crosslinks,  $V_1$  is the molar volume of the solvent (for  $\text{H}_2\text{O}$ :  $V_1 = 18 \text{ mol}/\text{cm}^3$ ), and  $X$  is the Flory polymer-solvent interaction parameter. Assuming HA is comparable to dextran and differences between soluble, unmodified HA and crosslinked HA is negligible,  $X = 0.473$ [18]. In addition, effective crosslinking density and theoretical mesh size can be estimated using:

$$\text{Eq. 4.4} \quad \nu_c = \text{effective crosslinking density} = \rho_P / M_c$$

$$\text{Eq. 4.5} \quad \xi = \text{mesh size (nm)} = 0.1748 (M_c)^{1/2} Q_v^{1/3} \quad [18,19].$$

Samples ( $n=5$ ) for mechanical testing ( $\sim 2 \text{ mm}$  height,  $\sim 7 \text{ mm}$  diameter) were compressed at a strain rate of 10% initial thickness/min until 60% of the initial thickness or failure on an Instron 5542 mechanical tester using a parallel plate apparatus. The compressive modulus was determined as the slope of the stress versus strain curve at low strains ( $<20\%$ ).

For degradation studies, polymer disks (1 mm thickness, 9 mm diameter) were punched from hydrogel slabs using stainless steel bores. Samples ( $n = 3$ ) were degraded in solutions of either 10 or 100 U hyaluronidase (Sigma)/ml PBS (replaced every 48 hours throughout the study and stored frozen until analysis) at 37°C on an orbital shaker. The amount of uronic acid (a degradation component of HA) released during degradation was measured using a previously established carbazole reaction technique[20]. Briefly, 100 $\mu\text{l}$  of the degradation solution was added to a concentrated sulfuric acid/sodium tetraborate decahydrate (Sigma) solution and heated to 100°C for 10 minutes. After adding 100 $\mu\text{l}$  of 0.125% carbazole (Sigma) in absolute ethanol and heating to 100°C for 15 minutes, the solution absorbance at 530 nm was measured. The amount of uronic acid was determined using solutions of known concentrations of the 50 kDa



HA as a standard. Degradation products were also analyzed with  $^1\text{H}$  NMR to determine if any unreacted or partially reacted monomer was present.

#### *4.2.3 Cell Viability*

For cell encapsulation, lyophilized macromer was sterilized using a germicidal lamp in a laminar flow hood for 30 minutes prior to dissolving in a sterile solution of PBS containing 0.05 wt% I2959 for polymerization. This technique was used for sterilization because higher concentrations of MeHA solution were too viscous to filter sterilize. As an initial assessment of viability, 3T3-fibroblasts (ATCC, p=5) were suspended in 50 $\mu\text{l}$  of the sterile macromer solution at a concentration of  $40 \times 10^6$  cells/ml and polymerized with the addition of  $\sim 4 \text{ mW/cm}^2$  ultraviolet light for 10 minutes using a long-wave ultraviolet lamp. Viability of photoencapsulated fibroblasts was assessed immediately after encapsulation and after 1 week of in vitro culture (DMEM, 10% fetal bovine serum, Invitrogen) using a commercially available MTT viability assay (ATCC). Briefly, 100 $\mu\text{l}$  of MTT reagent (tetrazolium salt solution) was added to each well and incubator at 37°C for 4 hours. The purple formazan produced by active mitochondria was solubilized by construct homogenization in 1 ml of the detergent solution and orbital shaking for 2 hours. The absorbance was then read at 570nm (Molecular Devices SpectraMax 384).

#### *4.2.4 Statistical Analysis*

Statistical analysis was performed using a Student's t-test (only to compare two individual samples) with a minimum confidence level of 0.05 for statistical significance. All values are reported as the mean and standard error of the mean.

## 4.3 Results & Discussion

### 4.3.1 Network Synthesis

HA networks were fabricated from MeHA precursors with varying molecular weights and methacrylations and with different MeHA concentrations to determine the range of properties possible for these potentially useful biomaterials. As illustrated in Figure 4.2, the MeHA macromers undergo a free radical polymerization with the addition of light and an initiator to form a crosslinked hydrogel that consists of HA and kinetic chains of poly(methacrylic acid). The various MeHA solutions investigated in this work are summarized in Table 4.1.

**Table 4.1** Hydrogel Compositions

Macromer MW (kDa)	% Methacrylation*	Macromer wt%
1100	6	2
350	7	2
		5
50	12	2
		5
		10
		20

\*Determined by  $^1\text{H}$  NMR

Although the MeHA macromers were synthesized using the same techniques and with the same concentrations of HA and methacrylic anhydride, a slightly higher methacrylation was obtained with the 50 kDa HA. This is potentially explained due to decreased viscosity during this reaction compared to the 350 and 1100 kDa HA, increasing the mobility of various species during the reaction. The macromer concentrations investigated were chosen as the highest concentrations of MeHA that could still be pipetted into molds or for suspending cells. For instance, this was only possible up to 2 wt% of the 1100 kDa MeHA macromer, but was possible for a 10-fold higher amount of the 50 kDa macromer, allowing for a wider range of network properties.

#### 4.3.2 Network Swelling, Mechanics, and Degradation

The equilibrium volumetric swelling ratio of the various HA networks are shown in Figure 4.3. As expected, a decrease in  $Q_V$  is seen with an increase in the concentration of macromer in the precursor solutions. For example,  $Q_V$  is ~41 for networks fabricated from 2 wt% of the 50 kDa macromer, but decreases to ~8 when the macromer concentration is increased 10-fold to 20 wt%. The same trend is seen for the 350 kDa macromer. For each of the molecular weights, there is a statistically significant ( $p > 0.05$ ) decrease in  $Q_V$  with an increase in macromer concentration, but there were no statistical differences between the different MeHA molecular weights when the same concentration of macromer was used for network formation. Using Flory-Rehner calculations[15], the network mesh size and the crosslinking density, which are important when explaining mechanics and degradation, are directly correlated to  $Q_V$  (Table 4.2).

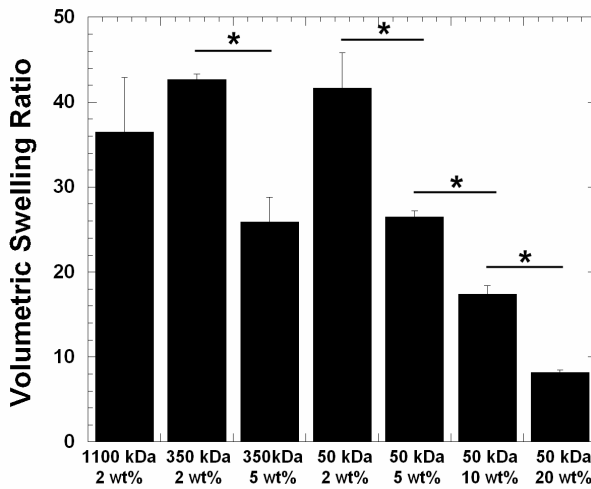


**Table 4.2** Mesh Size

Macromer MW (kDa)	Macromer wt%	Mesh Size (nm)
1100	2	400 ± 60
350	2	486 ± 6
	5	270 ± 26
50	2	470 ± 40
	5	279 ± 6
	10	171 ± 8
	20	71 ± 2

**Figure 4.3**  $Q_V$  for various photocrosslinked HA networks. Statistical difference ( $p < 0.05$ ) between groups is denoted by \*.

The general slope of the stress-strain data is linear at low strains (<20%) and then increases with an increase in strain. Overall, the modulus (i.e., slope of stress versus strain curve at low strain) correlates well with the network crosslinking density (i.e., swelling). As the

macromer concentration increases for each of the MeHA molecular weights, a statistically significant increase in the modulus is seen. For instance, networks fabricated from 2 wt% of the 50 kDa macromer had a modulus of only ~12 kPa, but increased substantially to ~100 kPa when the macromer concentration was increased to 20 wt%. These follow trends with the network mesh size with a decrease in the mesh size corresponding to an increase in the compressive modulus.

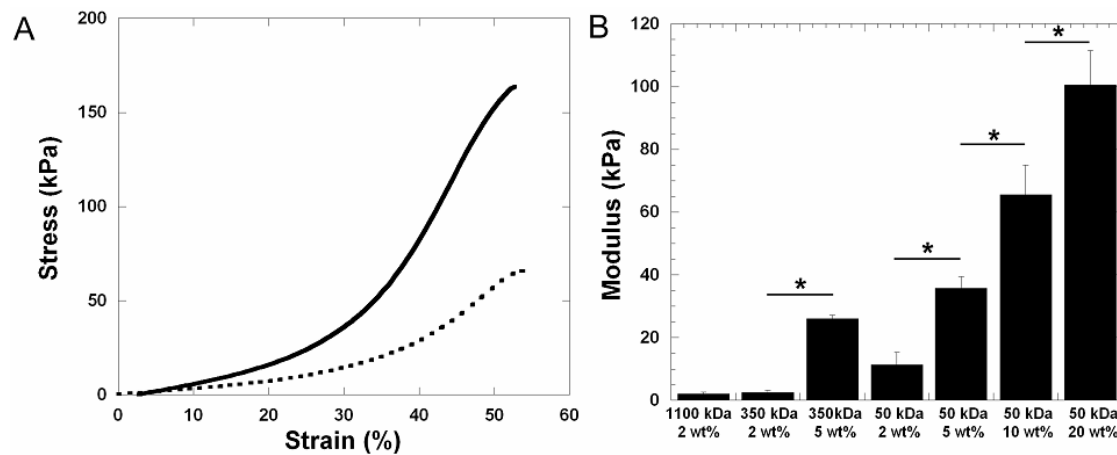


**Figure 4.4** (A) Representative stress versus strain plots of hydrogels fabricated from 10 (solid) and 5 (dotted) wt% macromers (50 kDa MeHA). (B) Compressive modulus for various HA networks at equilibrium swelling. Statistical difference ( $p < 0.05$ ) between groups is denoted by \*.

The hyaluronidase degradation of HA results in the cleavage of internal beta-N-acetyl-D-glucosaminidic linkages, which yields fragments with N-acetyl-glucosamine at the reducing terminus and glucuronic acid at the non-reducing end. In the body, these hyaluronidases are located in lysosomes and are most active at low pH levels. Because predicting the quantity or concentration of hyaluronidase that is active in specific locations in the body is not feasible, the chosen enzyme concentrations (100 U hyaluronidase/ ml of PBS) served merely to illustrate the trend of HA network degradation in relation to changes in molecular weight and macromer concentration overall time (Figure 4.5).

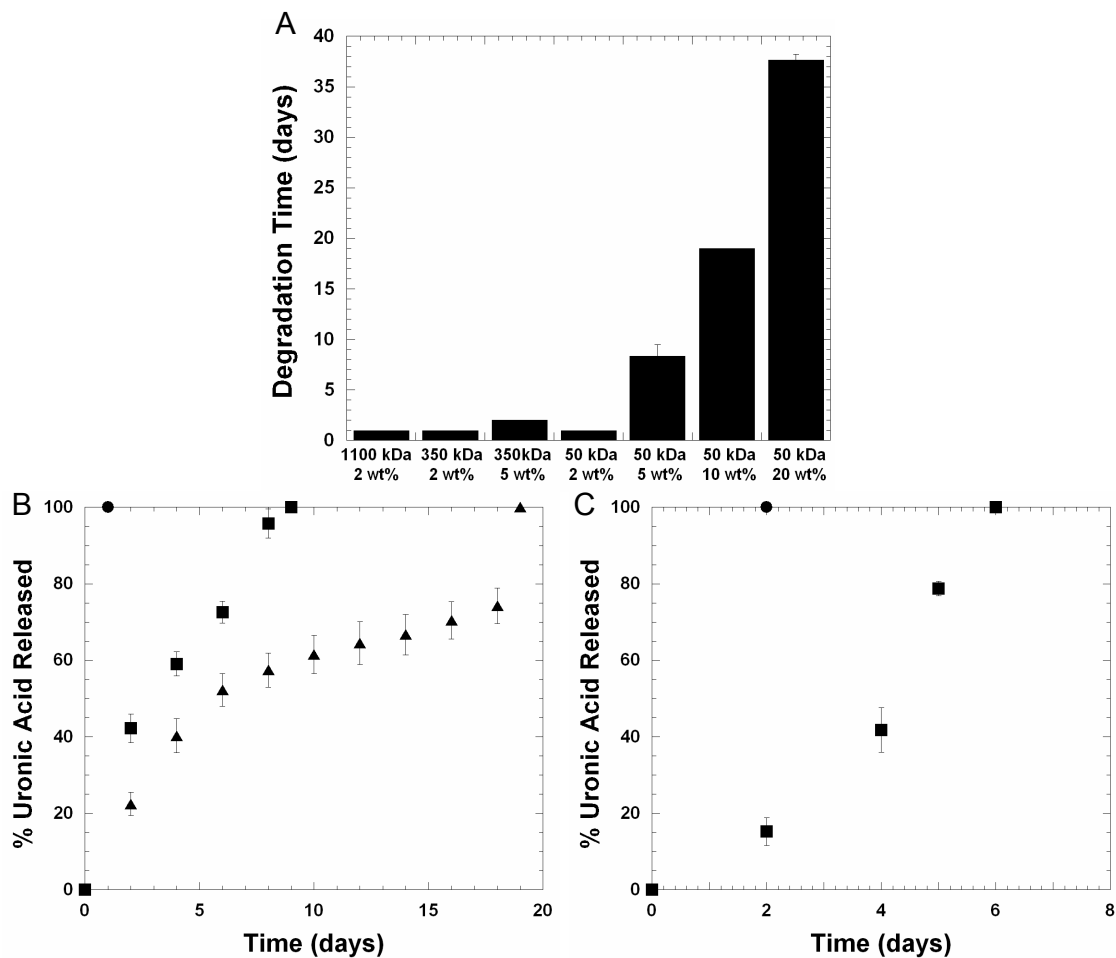


**Figure 4.5** (A) Time for complete degradation of HA hydrogels in 100 U hyaluronidase/ml of PBS, where the hyaluronidase was replenished every other day throughout degradation. (B) Cumulative percentage of uronic acid detected for HA hydrogels formed from 2 (●), 5 (■), and 10 (▲) wt% of the 50 kDa MeHA and degraded in 100 U hyaluronidase/ml. (C) Cumulative percentage of uronic acid detected for HA hydrogels formed from 5 wt% 350 kDa MeHA and degraded in both 100 (●) and 10 (■) U hyaluronidase/ml.

In general, the swollen networks decreased in size throughout the degradation and exposure to the hyaluronidase. This behavior was previously seen for other crosslinked

hyaluronic acid hydrogels [21]. This is potentially due to both an increase in erosion at the surface of the gels due to diffusion restrictions of the enzyme into the interior of the gel (particularly with networks with higher crosslinking densities) and an attraction of the positive amine groups produced during degradation and the negatively charged carboxylic acid groups of the HA. Again, there was good correlation between degradation time and the hydrogel crosslinking density. An increase in macromer concentration extended the time for complete degradation in a dose-dependant fashion. Also, no measurable double bonds were found during NMR analysis of the degradation products, indicating that the radical polymerization reaches near 100% conversion with the initiation conditions used (i.e., 10 minutes, 10 mW/ cm<sup>2</sup>, 0.05wt% I2959). It should be noted that the degradation products are not simply HA fragments, but HA fragments attached to kinetic chains from the radical polymerization of the methacrylate groups, which could influence any potential biological activity and metabolic catabolism of the degradation products.

The amount of uronic acid (a component of HA) in the degradation solutions is shown in Figure 4.5 (B and C) and plotted as the overall percentage of uronic acid detected with degradation time. For networks formed with the 50 kDa MeHA macromer, an increase in the macromer concentration (i.e., crosslinking density) extended the time for complete uronic acid release. For the 5 wt% HA network, ~40% of uronic acid is detected within two days of degradation and then a near linear release of uronic acid is observed until complete degradation. For the 10 wt% HA network, ~50% of the uronic acid is detected in the first 5 days of degradation, yet degradation extends to almost 20 days. A burst is observed at the end of degradation, due to the rapid solubilization of kinetic chains and HA when the network becomes loosely crosslinked. The rapid uronic acid release at short degradation periods could be due to the release of HA with low methacrylation, as a distribution of methacrylations is expected throughout the MeHA macromers. As seen in Figure 4.5C, the overall time and rate of hydrogel degradation is faster with a higher enzyme concentration (100 versus 10 U/ml).

#### 4.3.3 Cell Encapsulation and Viability

3T3-fibroblasts were encapsulated in the various networks and their viability was determined both immediately after encapsulation and after 1 week of in vitro culture. These results are shown in Figure 4.6.

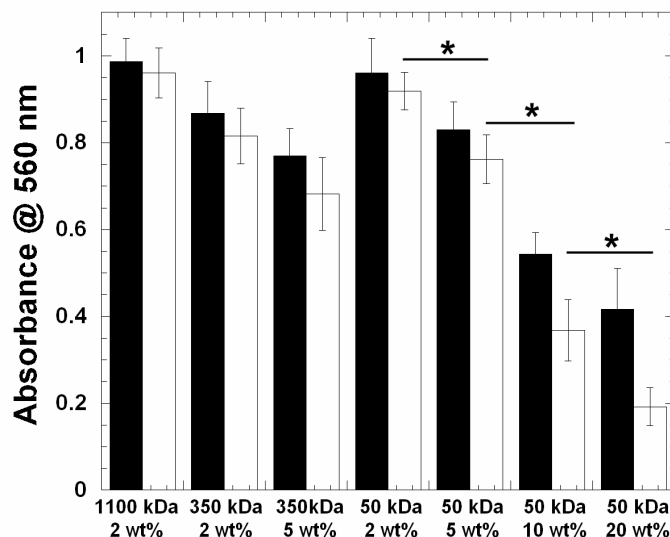


**Figure 4.6** Viability of photoencapsulated 3T3-fibroblasts in the HA hydrogels. Absorbance (indicative of encapsulated cell mitochondrial activity and viability) for the various HA networks after 1 day (black) and 1 week (white) of in vitro culture. The MTT solution was diluted 4-fold for all samples to obtain absorbance values in the linear range. The absorbance is statistically different (denoted by \* between two bars) between the different macromer concentrations for the 50 kDa MeHA at the 1 week time point.

Immediately after polymerization, a range of fibroblast viability is noted, with a decrease in viability as the macromer concentration increased. This could potentially be attributed to an increase in the radical concentration during encapsulation due to an increase in the reactive group concentration (i.e., methacrylates) in the precursor solutions with higher macromer concentrations. The reduction in MeHA molecular weight did not seem to affect the viability of the encapsulated cells. After 1 week of culture, a further decrease in viability is seen with many of

the macromer solutions, especially with the more highly crosslinked ones. For the 50 kDa macromer, a statistically significant decrease in viability is found with each increase in macromer concentration. The high crosslinking density can decrease the ability of nutrients and wastes to be exchanged between the encapsulated cells and surrounding culture media and lead to compromised cell viability. In general, the highest and sustained viability was observed in both the 1100 kDa and 50 kDa macromers at 2 wt%. Overall, these results indicate that although the higher macromer concentrations led to desirable mechanical properties, their application as cell carriers is limited due to low viability of photoencapsulated cells.

#### **4.4 Conclusions**

This work presents a systematic study of the ability to fabricate photopolymerizable HA networks with a wide range of properties. Specifically, alterations in the HA molecular weight allowed high macromer concentrations to be incorporated in the precursor solution, leading to networks with high crosslinking densities. Although networks with a compressive modulus over 100 kPa were formed, the viability of fibroblasts in these networks was compromised potentially due to restrictions in nutrient transport through the network and a high radical concentration during polymerization. However, in the less crosslinked networks, viability was sustained. The variability in macromer molecular weight at concentrations that promoted cell viability will allow for a wide variety of precursor solution viscosities, which will be important for clinical and non-invasive implantation of these gels.



**References:**

- [1] Chen WY, Abatangelo G. Functions of hyaluronan in wound repair. *Wound Repair Regen* 1999;7(2):79-89.
- [2] Grigolo B, Roseti L, Fiorini M, Fini M, Giavaresi G, Aldini NN, et al. Transplantation of chondrocytes seeded on a hyaluronan derivative (hyaff-11) into cartilage defects in rabbits. *Biomaterials* 2001;22(17):2417-24.
- [3] Marcacci M, Berruto M, Brocchetta D, Delcogliano A, Ghinelli D, Gobbi A, et al. Articular cartilage engineering with Hyalograft C: 3-year clinical results. *Clin Orthop Relat Res* 2005;(435):96-105.
- [4] Nettles DL, Vail TP, Morgan MT, Grinstaff MW, Setton LA. Photocrosslinkable hyaluronan as a scaffold for articular cartilage repair. *Ann Biomed Eng* 2004;32(3):391-7.
- [5] Ramamurthi A, Vesely I. Ultraviolet light-induced modification of crosslinked hyaluronan gels. *J Biomed Mater Res A* 2003;66(2):317-29.
- [6] Smeds KA, Pfister-Serres A, Miki D, Dastgheib K, Inoue M, Hatchell DL, et al. Photocrosslinkable polysaccharides for in situ hydrogel formation. *J Biomed Mater Res* 2001;54(1):115-21.
- [7] Liu YC, Shu XZ, Prestwich GD. Osteochondral defect repair with autologous bone marrow-derived mesenchymal stem cells in an injectable, in situ, cross-linked synthetic extracellular matrix. *Tissue Engineering* 2006;12(12):3405-16.
- [8] Park YD, Tirelli N, Hubbell JA. Photopolymerized hyaluronic acid-based hydrogels and interpenetrating networks. *Biomaterials* 2003;24(6):893-900.
- [9] Shu XZ, Liu Y, Luo Y, Roberts MC, Prestwich GD. Disulfide cross-linked hyaluronan hydrogels. *Biomacromolecules* 2002;3(6):1304-11.
- [10] Solchaga LA, Dennis JE, Goldberg VM, Caplan AI. Hyaluronic acid-based polymers as cell carriers for tissue-engineered repair of bone and cartilage. *Journal of Orthopaedic Research* 1999;17(2):205-13.

- [11] Brun P, Abatangelo G, Radice M, Zacchi V, Guidolin D, Gordini DD, et al. Chondrocyte aggregation and reorganization into three-dimensional scaffolds. *Journal of Biomedical Materials Research* 1999;46(3):337-46.
- [12] Bryant SJ, Anseth KS. The effects of scaffold thickness on tissue engineered cartilage in photocrosslinked poly(ethylene oxide) hydrogels. *Biomaterials* 2001;22(6):619-26.
- [13] Elisseeff J, Anseth K, Sims D, McIntosh W, Randolph M, Yaremchuk M, et al. Transdermal photopolymerization of poly(ethylene oxide)-based injectable hydrogels for tissue-engineered cartilage. *Plastic and Reconstructive Surgery* 1999;104(4):1014-22.
- [14] Bryant SJ, Nuttelman CR, Anseth KS. Cytocompatibility of UV and visible light photoinitiating systems on cultured NIH/3T3 fibroblasts in vitro. *J Biomater Sci Polym Ed* 2000;11(5):439-57.
- [15] Flory P. *Principles of Polymer Chemistry*. Ithaca, NY: Cornell University Press, 1953.
- [16] Leach JB, Bivens KA, Collins CN, Schmidt CE. Development of photocrosslinkable hyaluronic acid-polyethylene glycol-peptide composite hydrogels for soft tissue engineering. *J Biomed Mater Res A* 2004;70(1):74-82.
- [17] Gomez-Alejandre S, de la Blanca ES, de Usera CA, Rey-Stolle MF, Hernandez-Fuentes I. Partial specific volume of hyaluronic acid in different media and conditions. *Int J Biol Macromol* 2000;27(4):287-90.
- [18] Cleland RL, Wang JL. Ionic polysaccharides. 3. Dilute solution properties of hyaluronic acid fractions. *Biopolymers* 1970;9(7):799-810.
- [19] Baier Leach J, Bivens KA, Patrick CW, Jr., Schmidt CE. Photocrosslinked hyaluronic acid hydrogels: natural, biodegradable tissue engineering scaffolds. *Biotechnol Bioeng* 2003;82(5):578-89.
- [20] Bitter T, Muir HM. A Modified Uronic Acid Carbazole Reaction. *Analytical Biochemistry* 1962;4:330-4.
- [21] Prestwich GD, Marecak DM, Marecak JF, Vercruysse KP, Zieball MR. *J Controlled Release* 1998;53:93-103.

## CHAPTER 5

### *Optimization of Methacrylated HA Hydrogel Properties for Neocartilage*

#### *Formation by Auricular Chondrocytes*

(Adapted from: **C Chung**, J Mesa, MA Randolph, M Yaremchuk, JA Burdick, "Influence of Gel Properties on Neocartilage Formation by Auricular Chondrocytes Photoencapsulated in Hyaluronic Acid Networks," J Biomed Mater Res A, 2006, 77(3): 518-25)

#### **5.1 Introduction**

Cells have the ability to sense their environment, where physical and chemical cues can dictate cell morphology, viability, and metabolism. Chondrocytes are no exception as they have been shown to differentially respond to scaffolds of varying chemistry [1-3], architecture [4], and stiffness [5], as well as to external mechanical stimulation [6-9]. The addition of bioactive molecules (e.g., chondroitin sulfate, hyaluronic acid) to the relatively inert synthetic scaffolds resulted in up-regulation of cartilage specific genes and glycosaminoglycan (GAG) and collagen matrix production [2,3], demonstrating that scaffold chemistry can regulate cell function. Furthermore, the addition of bioactive molecules also alters chondrocyte response to mechanical stimulation. In a study by Appelman *et al*, various proteins were conjugated within PEG hydrogels and exhibited differential chondrocyte responses when mechanically stimulated [10].

Extensive work with poly(ethylene glycol) (PEG) hydrogels has shown that increased crosslinking density can compromise cell viability and limit cell proliferation [4]. Restricted diffusion of nutrients and waste may contribute to a decrease in viability, while physical restrictions of encapsulated chondrocytes may inhibit cell proliferation. Similarly, increased crosslinking density can also limit the diffusion of extracellular matrix (ECM) proteins resulting in pericellular accumulation. When mechanically loaded, increased crosslinking density in the

hydrogel can yield greater cell deformations, which can lead to changes in mechanically transduced signaling pathways [6].

Tied hand in hand with crosslinking density in many hydrogel systems are volumetric swelling ratio and mechanical properties. Lower crosslinking densities yield higher swelling ratios that can improve the diffusion of newly synthesized glycosaminoglycans (GAGs). Surprisingly, in a study by Bryant and Anseth, PEG hydrogels with moduli of 360 kPa showed increased type II collagen synthesis compared to hydrogels with moduli of 960 and 30 kPa. This study also demonstrated that the addition of degradable components was able to increase type II collagen synthesis and distribution of GAGs within the hydrogel [11]. Thus, in optimizing cartilage tissue engineering (TE) scaffolds, the critical balance of hydrogel swelling, mechanics, and degradation must be found.

In the previous chapter, we showed that by altering hyaluronic acid (HA) macromer concentration and molecular weight, the properties of the hydrogel can be varied. As properties of a scaffold can affect cell morphology, viability, proteoglycan biosynthesis, and ECM distribution, this chapter investigates how these same changes in the network structure and properties influence the ability of photoencapsulated chondrocytes to produce cartilaginous tissue *in vivo*. To accomplish this, auricular chondrocytes were harvested from swine, photoencapsulated in the various HA hydrogels, and implanted subcutaneously in nude mice. Biochemical assays and histological analysis were then used to compare cartilage production between the various hydrogels.

## **5.2 Materials & Methodology**

### *5.2.1 Macromer Synthesis and Polymerization*

Methacrylated hyaluronic acid (MeHA) was synthesized as described in Chapter 4 (section 4.2). For cell encapsulation, MeHA of varying molecular weights (50 kDa, 350 kDa, 1100 kDa) was sterilized with exposure to the germicidal lamp in a laminar flow hood for 30 minutes and dissolved in a sterile solution of PBS containing 0.05 wt% I2959 (Ciba).

### *5.2.2 Chondrocyte Isolation and Photoencapsulation*

Swine aged 3 to 6 months were euthanized using an overdose of Pentobarbital (100 mg/kg IV) and auricular cartilage tissue was harvested in a sterile fashion from the ears of the swine. The harvested cartilage was cut into  $\sim 1\text{mm}^3$  pieces, washed in PBS, and digested for 18 hours at 37°C in a sterile 0.1% collagenase (Worthington) solution in Ham's F-12 medium. After digestion, the solution was passed through a 100  $\mu\text{m}$  filter to remove undigested cartilage and centrifuged to obtain a chondrocyte pellet. The chondrocytes were washed twice with PBS, counted using a hemacytometer, and determined viable using the trypan blue exclusion dye test prior to encapsulation. Chondrocytes ( $40 \times 10^6$  cells/ml) were photoencapsulated in the various hydrogel networks by suspension in a solution of 2, 5, 10, and 20 wt% macromer (MeHA) containing 0.05 wt% I2959. Solutions were pipetted into sterile molds (50  $\mu\text{l}$  volume) and polymerized with  $\sim 4 \text{ mW/cm}^2$  ultraviolet light for 10 minutes using a long-wave ultraviolet lamp (Model 100AP, Blak-Ray). These conditions were previously determined to be cytocompatible for the photoencapsulation of chondrocytes[12]. A general schematic of the chondrocyte photoencapsulation process and subsequent analysis is depicted in Figure 5.1. Auricular and articular cartilage were harvested from the same source and used as controls for biochemical analysis.

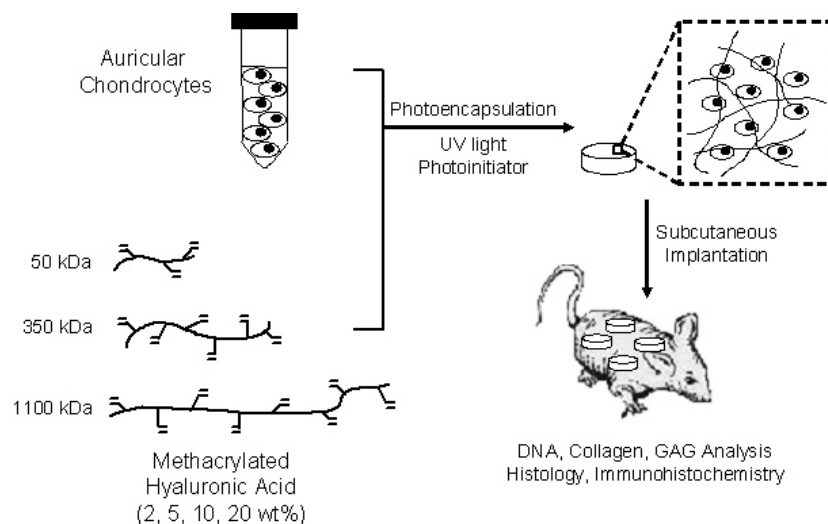


**Figure 5.1** General schematic of the photoencapsulation process and subsequent analysis.

### 5.2.3 Implantation in Nude Mice

Nude mice were anesthetized with ketamine (80 mg/kg) and xylazine (12 mg/kg). A 2 cm midline incision was made on the back of each mouse and 4 subcutaneous pockets were made using blunt dissection. A chondrocyte/hydrogel construct was placed in each of these pockets and the wound was closed with sterile stainless steel skin clips. After 6 and 12 weeks, mice were euthanized and constructs were harvested for analysis. NIH guidelines for the care and use of laboratory animals (NIH Publication #85-23 Rev. 1985) were observed.

### 5.2.4 Biochemical Analysis

For biochemical analysis ( $n = 4$ ), constructs were weighed initially (wet weight), lyophilized and weighed again (dry weight). Samples were digested in a papain solution (125  $\mu\text{g/ml}$  papain type III, 10 mM l-cysteine, 100 mM phosphate, and 10 mM EDTA at pH 6.3) for 15 hours at 60°C. Total DNA content was determined using a PicoGreen dsDNA Assay[13] with chondrocyte number determined using a conversion factor of 7.7 pg of DNA per chondrocyte [14]. Briefly, 10  $\mu\text{l}$  of sample were combined with 90  $\mu\text{l}$  of 1xTris-HCl, EDTA buffer (pH 7.5) and 100  $\mu\text{l}$  of

picogreen solution, mixed, and incubated with 3 minutes. Fluorescence was read using a microplate reader (ex: 480nm, em: 520nm). Total GAG content was determined using the dimethylmethylen blue (DMMB) dye method [15] with chondroitin sulfate as a standard. Briefly, 5 $\mu$ l of each sample was combined with 200 $\mu$ l of DMMB dye (8mg 1,9 dimethylmethlene blue, 2.5ml ethanol, 1g sodium formate, and 1ml formic acid in 500ml of DI water), and absorbance was read in a 96-well microplate reader at a wavelength of 525nm to determine GAG content. Total collagen content was determined using the hydroxyproline assay [16], with a collagen to hydroxyproline ratio of 7.25 [17,18]. Samples were hydrolyzed in 6N HCl for 16 hours overnight at 110°C. HCl was evaporated with nitrogen and the hydrolyzate was reconstituted with DI water. Sample was then combined with chloramine-T solution (1.41g chloramines-T, 10ml DI water, 10ml n-propanol, 80ml OHP buffer (25g citric acid·H<sub>2</sub>O, 12ml acetic acid, 60g sodium acetate·3H<sub>2</sub>O, 12g sodium hydroxide, 600ml DI water, 150ml n-propanol, pH 6.0)), and incubated at room temperature for 20 minutes. This was then followed by the addition of p-DAB solution (15g p-dimethyl-amino-benzaldehyde, 60ml n-propanol, 26ml percloric acid) and incubation at 60°C for 15 minutes. Absorbance was read in a microplate reader at a wavelength of 550nm for hydroxyproline content. Values reported for GAG and collagen contents were normalized to construct wet weight.

#### *5.2.5 Histological Analysis*

For histological analysis, constructs were fixed in 10% formalin for 24 hours, embedded in paraffin, and processed using standard histological procedures. The histological sections (7  $\mu$ m thick) were stained with hematoxylin and eosin to observe the morphology and distribution of encapsulated chondrocytes and Safranin O to visualize glycosaminoglycans (GAG). Type I and type II collagen distributions were detected using a Vectastain Universal Elite ABC Kit (Vector Laboratories) and a DAB Substrate Kit for Peroxidase (Vector Laboratories). Sections were predigested in 0.5 mg/ml hyaluronidase for 30 min at 37°C and incubated in 0.5 N acetic acid for

4 hours at 4°C prior to overnight incubation with primary antibodies at dilutions of 1:200 and 1:3 for type I (mouse monoclonal anti-collagen type 1, Sigma) and type II collagen antibodies (mouse monoclonal anti-collagen type II, Developmental Studies Hybridoma Bank), respectively.

#### *5.2.6 Statistical Analysis*

Anova with Tukey's post-hoc test was used to determine significant difference among groups, with  $p < 0.05$ . All values are reported as the mean  $\pm$  the standard deviation.

### **5.3 Results & Discussion**

Photocrosslinkable hyaluronic acid hydrogels were investigated in this study as carriers for auricular chondrocytes for cartilage regeneration. In the fabrication of these hydrogels, several factors including the molecular weight of the HA, the acrylation percentage, and the concentration of the HA in the prepolymer solution can influence the properties of the resulting construct. The previous chapter investigated the fabrication of these networks and illustrated the wide range of hydrogel properties that can be obtained. Auricular chondrocytes were used in this study to investigate the influence of hydrogel properties on neocartilage formation, which has direct implications for plastic surgery applications and also a consideration for articular cartilage regeneration. Auricular cartilage is easily harvested with little donor-site morbidity and auricular chondrocytes can be obtained at yields twice as high as articular chondrocytes[19]. Proliferating approximately four times faster than articular chondrocytes in monolayer culture, auricular chondrocytes have also been shown to express high levels of type II collagen and glycosaminoglycans when implanted in vivo in 3-dimensional scaffolds[19].



### 5.3.1 Macroscopic Appearance

After 12 weeks, the macroscopic appearance (Figure 5.2) of the constructs varied dramatically depending on the prepolymer solution (e.g., macromer molecular weight and concentration) used for encapsulation.

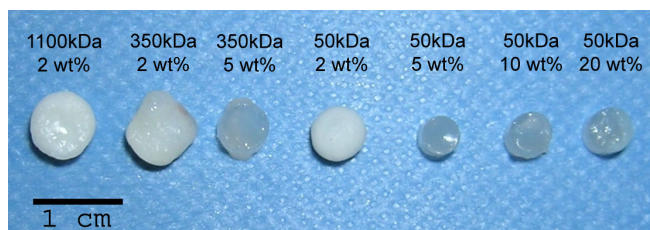


**Figure 5.2** Explanted HA constructs 12 weeks after subcutaneous implantation in nude mice.

Specifically, constructs fabricated from 2wt% of the macromers were noticeably more opaque, exhibiting a white, shiny appearance, compared to those fabricated with higher macromer concentrations, which remained relatively translucent. Restrictions in nutrient transport through the construct and high radical concentration during polymerization potentially compromised cell viability, growth, and ECM production in these higher wt% hydrogels. In addition, the 2wt% 350 and 1100 kDa hydrogels exhibited a noticeable increase in size after the 12 weeks of subcutaneous culture in nude mice, which may be due to a lower degree of methacrylation modification, whereas the 2 wt% 50 kDa hydrogel more closely maintained initial construct dimensions (i.e., 5 mm diameter).

### 5.3.2 Biochemical Analysis

The water content of the explanted constructs was determined from wet and dry weights (Figure 5.3). In general, constructs exhibited a decrease in water content from 6 weeks to 12 weeks, where a significant decrease was noted for the 2wt% 1100, 350, and 50 kDa constructs. The observed decrease in water content is likely due to increased tissue formation (e.g., cell proliferation and extracellular matrix deposition) within the construct. Of the 12 week explants,

the 2 wt% 50 kDa construct ( $81 \pm 2.7\%$  water) was most comparable to auricular ( $74 \pm 2.4\%$  water) and articular ( $79 \pm 5.1\%$  water) cartilage, and no statistically significant differences were found between the values.

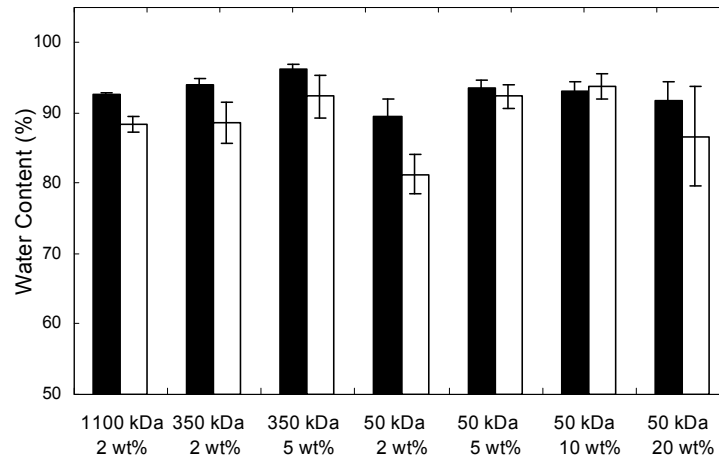


**Figure 5.3** Water content of HA constructs after 6 (black) and 12 (white) weeks of subcutaneous culture in nude mice (n=4). Significant decrease ( $p < 0.05$ ) in water content for the 50 kDa, 2wt% constructs from 6 to 12 weeks. All groups were significantly different from native auricular and articular cartilage at 12 weeks with the exception of the 50 kDa, 2wt% group.

The total DNA content was determined for all harvested constructs and converted into numbers of chondrocytes per sample (Figure 5.4). The 2wt% constructs exhibited an increase in chondrocyte number from 6 to 12 weeks, indicating cellular proliferation with culture time. Constructs with macromer concentrations greater than 2 wt% showed little cell growth, potentially due to compromised cell viability during encapsulation or higher crosslinking densities that can limit 3-dimensional cell proliferation. The 2wt% constructs appeared to support the greatest number of chondrocytes regardless of molecular weight, where the 2 wt% 50 kDa constructs had the greatest number of chondrocytes at ~600,000 cells per sample after 12 weeks. Values were also normalized to sample wet weight for comparison to control auricular and articular cartilage (not shown). The 2 wt% 50 kDa constructs exhibited the greatest amount of DNA per wet

weight, which was approximately 80 and 87% of that found for native auricular and articular cartilage, respectively. No significant differences were detected for the 2 wt% 1100 kDa and 2 wt% 50 kDa hydrogels when compared to auricular and articular cartilage for the normalized DNA values. Hydrogels (2 wt% 50 kDa) without encapsulated cells served as a control and exhibited minimal fluorescence, comprising less than 3.5% of any sample.

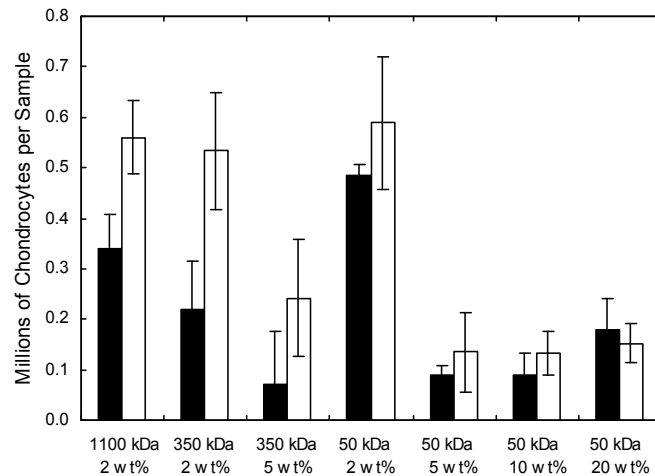


**Figure 5.4** Number of chondrocytes per sample for HA constructs after 6 (black) and 12 (white) weeks of subcutaneous culture in nude mice (n=4). For the 12 week explants, the 2 wt% constructs showed a statistical difference ( $p < 0.05$ ) from constructs with higher macromer concentrations.

GAG content was measured in the explanted constructs and is reported as the quantity of chondroitin sulfate normalized to sample wet weight (Figure 5.5). The GAG content in constructs increased from 6 to 12 weeks, where the 2 wt% 1100 and 50 kDa constructs showed the greatest amount of GAGs ( $0.049 \pm 0.007$  and  $0.049 \pm 0.005$   $\mu\text{g GAGs}/\mu\text{g wet weight}$ , respectively) after 12 weeks of culture. This value is approximately 80% and 53% of the GAG content found in native auricular and articular cartilage, respectively. There was no significant difference between GAG production by chondrocytes encapsulated in the 2 wt% networks formed from both the 1100 and 50 kDa macromers compared to native auricular cartilage. Virtually no

measurable GAGs were found in the hydrogels fabricated from the higher macromer concentrations (5 to 20wt%). HA hydrogel controls showed little GAG detection and were similar to control hydrogels formed from a non-polysaccharide PEG hydrogel [20].

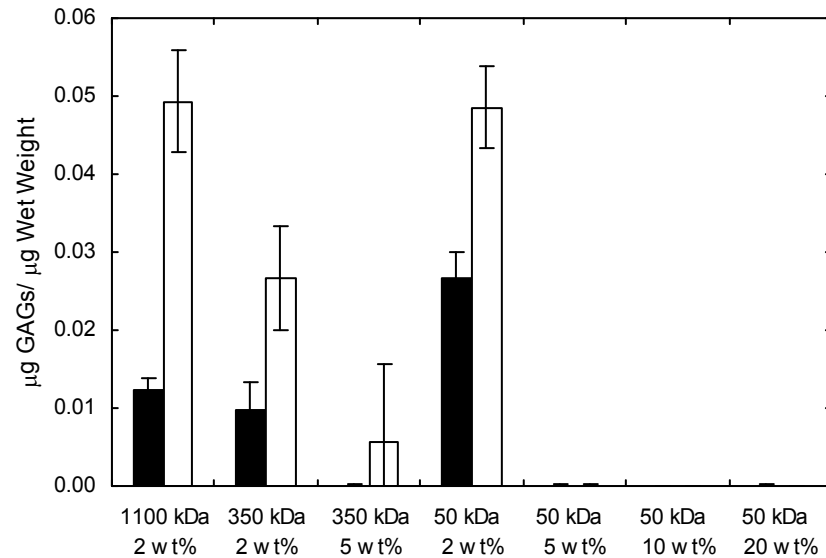


**Figure 5.5** Glycosaminoglycan content of HA constructs normalized to construct wet weight after 6 (black) and 12 (white) weeks of subcutaneous culture in nude mice (n=4). The 2 wt% constructs are statistically different ( $p < 0.05$ ) from those with higher macromer concentration after both 6 and 12 weeks.

As a final quantification of biochemical content, the amount of collagen in the explanted constructs was determined by the hydroxyproline content and is normalized to sample wet weight (Figure 5.6). Similar to the GAG content, the majority of the constructs exhibited an increase in collagen content from 6 to 12 weeks. The 2 wt% 50 kDa construct is statistically different ( $p < 0.05$ ) from all of the samples after 6 weeks and showed the greatest amount collagen content ( $0.0658 \pm 0.0161$  μg collagen/μg wet weight) after 12 weeks. This value represents ~65% and ~74% of the total collagen that was found in control samples of auricular and articular cartilage,

respectively. Again, only small amounts of collagen were detected in the hydrogels fabricated from the higher macromer concentrations (5 to 20 wt%).

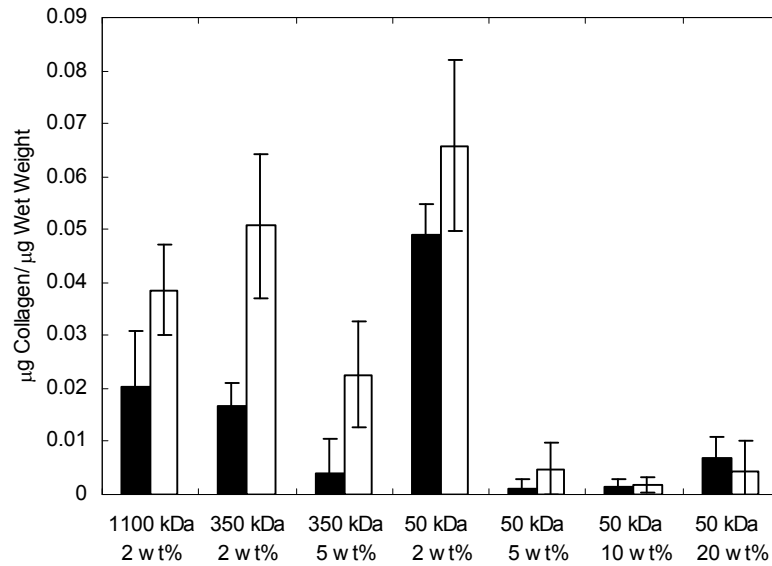


**Figure 5.6** Total collagen content of HA constructs normalized to construct wet weight after 6 (black) and 12 (white) weeks of subcutaneous culture in nude mice (n=4). The 2 wt% constructs are statistically different ( $p<0.05$ ) from those with higher macromer concentration after 12 weeks.

### 5.3.3 Histological Analysis

Representative stains for GAG, type I collagen, and type II collagen are shown in Figure 5.7 for several constructs harvested 12 weeks after implantation. Specifically, the histology is shown for the two compositions that looked the most promising both macroscopically and biochemically (i.e., 2 wt% of 1100 and 50 kDa macromers) and, for contrast, a sample that showed little production of extracellular matrix (10 wt% 50 kDa macromer). Unfortunately, the hydrogels exhibit background staining for HA when using the Safranin O stain, but the images still capture the large production of GAGs after 12 weeks *in vivo* and illustrate the morphology and distribution of the cells.

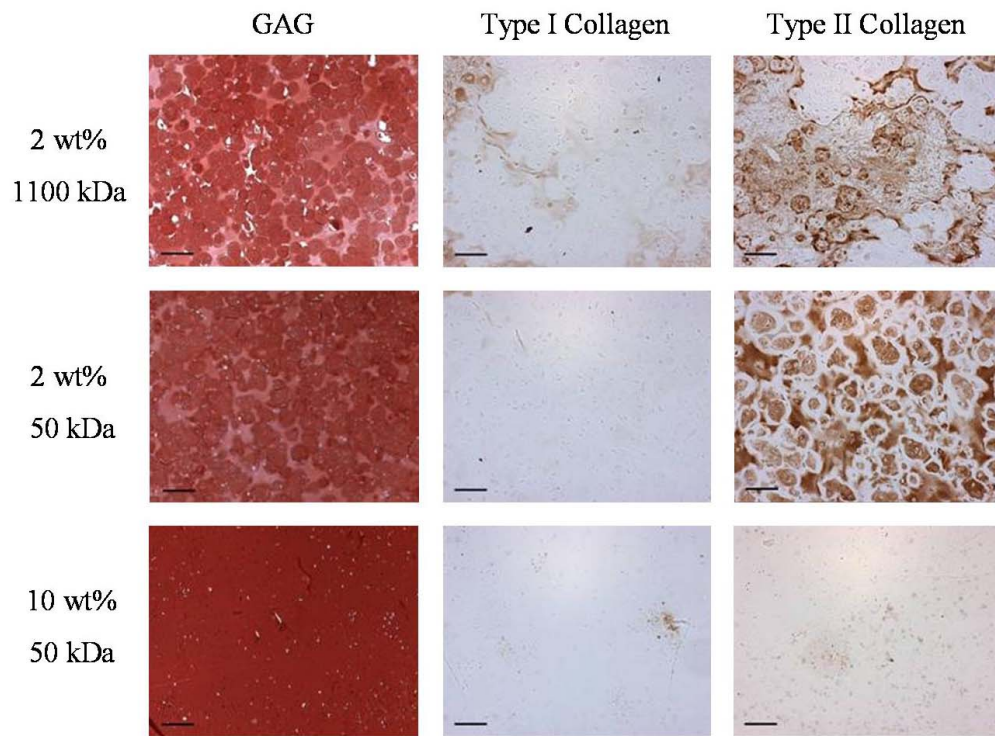


**Figure 5.7** Representative histological sections of 2 wt% 1100 kDa, 2 wt% 50 kDa, and 10 wt% 50 kDa constructs stained for glycosaminoglycans, type I collagen, and type II collagen after 12 weeks of subcutaneous culture in nude mice. Scale bar = 100  $\mu$ m.

In constructs fabricated with a 2 wt% macromer solution, chondrocytes are evenly distributed and appear viable throughout the gels. In contrast, morphology indicative of cell death is evident in constructs fabricated with higher macromer concentrations (5 to 20 wt%) as illustrated by the 10 wt% 50 kDa construct. GAG staining is found abundantly throughout the histological sections, including the pericellular regions surrounding the cells in the 2 wt% hydrogels. The representative stains for type I and type II collagen support results observed in the biochemical analysis, where more intense staining is observed in the 2 wt% 1100 and 50 kDa constructs in contrast to the other samples. Though light staining for type I collagen is observed sporadically throughout the 1100 kDa sample, type II collagen appears more abundant. The lack

of type II collagen staining in certain regions of the 2 wt% 1100 kDa construct is potentially due to cell clustering, as the highly viscous precursor solution may have prevented an even cell distribution. For the 2 wt% 50 kDa sample, viscosity did not play a hindering role, and an even distribution of type II collagen is found throughout the constructs, while no staining for type I collagen is present. Again, no staining is observed in the 5 to 20 wt% 50kDa samples for either type I or type II collagen, illustrating the lack of ECM production in these constructs.

## **5.4 Conclusions**

Overall, this chapter illustrates the importance of HA hydrogel structure for both the quality and distribution of tissue produced by encapsulated cells. After screening several factors, the results indicate that hydrogels formed from 2 wt% of the 50 kDa macromer supported the greatest amount of biochemical components and the best distribution of extracellular matrix components. The enhanced neocartilage production in the 2 wt% hydrogels may be due to: (i) a lower radical concentration during the polymerization of the 2 wt% hydrogels than for higher macromer concentrations, which may increase cell viability, (ii) an increase in nutrient and waste transport with a more loosely crosslinked hydrogel, and (iii) more rapid hydrogel degradation with a larger hydrogel mesh size, which may increase the distribution of extracellular matrix components. Additionally, the low viscosity of the 2 wt% solution makes it more amenable not only in the distribution of encapsulated chondrocytes, but also clinical application of these gel solutions through arthroscopic techniques.

**References:**

- [1] Erickson IE, Huang AH, Chung C, Li RT, Burdick JA, Mauck RL. Differential maturation and structure-function relationships in mesenchymal stem cell- and chondrocyte-seeded hydrogels. *Tissue Eng Part A* 2009;15(5):1041-52.
- [2] Varghese S, Hwang NS, Canver AC, Theprungsirikul P, Lin DW, Elisseeff J. Chondroitin sulfate based niches for chondrogenic differentiation of mesenchymal stem cells. *Matrix Biol* 2008;27(1):12-21.
- [3] Yoo HS, Lee EA, Yoon JJ, Park TG. Hyaluronic acid modified biodegradable scaffolds for cartilage tissue engineering. *Biomaterials* 2005;26(14):1925-33.
- [4] Bryant SJ, Chowdhury TT, Lee DA, Bader DL, Anseth KS. Crosslinking density influences chondrocyte metabolism in dynamically loaded photocrosslinked poly(ethylene glycol) hydrogels. *Ann Biomed Eng* 2004;32(3):407-17.
- [5] Genes NG, Rowley JA, Mooney DJ, Bonassar LJ. Effect of substrate mechanics on chondrocyte adhesion to modified alginate surfaces. *Arch Biochem Biophys* 2004;422(2):161-7.
- [6] Bryant SJ, Anseth KS, Lee DA, Bader DL. Crosslinking density influences the morphology of chondrocytes photoencapsulated in PEG hydrogels during the application of compressive strain. *J Orthop Res* 2004;22(5):1143-9.
- [7] Buschmann MD, Gluzband YA, Grodzinsky AJ, Hunziker EB. Mechanical compression modulates matrix biosynthesis in chondrocyte/agarose culture. *J Cell Sci* 1995;108 ( Pt 4):1497-508.
- [8] De Croos JN, Dhaliwal SS, Grynblas MD, Pilliar RM, Kandel RA. Cyclic compressive mechanical stimulation induces sequential catabolic and anabolic gene changes in chondrocytes resulting in increased extracellular matrix accumulation. *Matrix Biol* 2006;25(6):323-31.



- [9] Smith RL, Lin J, Trindade MC, Shida J, Kajiyama G, Vu T, et al. Time-dependent effects of intermittent hydrostatic pressure on articular chondrocyte type II collagen and aggrecan mRNA expression. *J Rehabil Res Dev* 2000;37(2):153-61.
- [10] Appelman TP, Mizrahi J, Elisseeff JH, Seliktar D. The differential effect of scaffold composition and architecture on chondrocyte response to mechanical stimulation. *Biomaterials* 2009;30(4):518-25.
- [11] Bryant SJ, Anseth KS. Hydrogel properties influence ECM production by chondrocytes photoencapsulated in poly(ethylene glycol) hydrogels. *J Biomed Mater Res* 2002;59(1):63-72.
- [12] Bryant SJ, Nuttelman CR, Anseth KS. Cytocompatibility of UV and visible light photoinitiating systems on cultured NIH/3T3 fibroblasts in vitro. *J Biomater Sci Polym Ed* 2000;11(5):439-57.
- [13] Singer VL, Jones LJ, Yue ST, Haugland RP. Characterization of PicoGreen reagent and development of a fluorescence-based solution assay for double-stranded DNA quantitation. *Anal Biochem* 1997;249(2):228-38.
- [14] Kim YJ, Sah RL, Doong JY, Grodzinsky AJ. Fluorometric assay of DNA in cartilage explants using Hoechst 33258. *Anal Biochem* 1988;174(1):168-76.
- [15] Farndale RW, Sayers CA, Barrett AJ. A direct spectrophotometric microassay for sulfated glycosaminoglycans in cartilage cultures. *Connect Tissue Res* 1982;9(4):247-8.
- [16] Stegemann H, Stalder K. Determination of hydroxyproline. *Clin Chim Acta* 1967;18(2):267-73.
- [17] Herbage D, Bouillet J, Bernengo JC. Biochemical and physiochemical characterization of pepsin-solubilized type-II collagen from bovine articular cartilage. *Biochem J* 1977;161(2):303-12.
- [18] Williamson AK, Chen AC, Sah RL. Compressive properties and function-composition relationships of developing bovine articular cartilage. *J Orthop Res* 2001;19(6):1113-21.

- [19] Van Osch GJ, Mandl EW, Jahr H, Koevoet W, Nolst-Trenite G, Verhaar JA. Considerations on the use of ear chondrocytes as donor chondrocytes for cartilage tissue engineering. *Biorheology* 2004;41(3-4):411-21.
- [20] Burdick JA, Chung C, Jia X, Randolph MA, Langer R. Controlled degradation and mechanical behavior of photopolymerized hyaluronic acid networks. *Biomacromolecules* 2005;6(1):386-91.

## CHAPTER 6

### *Effects of Chondrocyte Expansion on Neocartilage Formation*

#### *in Hyaluronic Acid Hydrogels*

(Adapted from: **C Chung**, J Mesa, GJ Miller, MA Randolph, Gill TJ, JA Burdick, "Effects of Auricular Chondrocyte Expansion on Neocartilage Formation in Photocrosslinked Hyaluronic Acid Networks," Tissue Eng, 2006, 12(9): 2665-73)

#### **6.1 Introduction**

Chondrocytes, native inhabitants of cartilage tissue, are the natural selection as a TE scaffold cell source. However, comprising only 10% of cartilage tissue by wet weight, these harvested cells need to be expanded *in vitro* to provide the quantity of cells acceptable for adequate repair using a TE scaffold. Unfortunately, for rapid expansion in monolayer culture, chondrocytes isolated from both articular and auricular cartilage have been shown to dedifferentiate, losing their chondrogenic phenotype [1,2]. Originally rounded in shape, chondrocytes flatten and take on a more fibroblastic phenotype with *in vitro* expansion [2,3]. Additionally, when chondrocytes are removed from their extracellular matrix (ECM) environment, a decrease in type II collagen and an increase in type I collagen are seen [4], leading to a mechanically inferior fibrocartilage tissue. Although dedifferentiation seems inevitable in monolayer culture, some studies have shown slower dedifferentiation, stabilization of the differentiated phenotype, or even redifferentiation (i.e., return to a chondrocytic phenotype after dedifferentiation) when chondrocytes are cultured under conditions such as in liquid suspension[5], agarose [1], alginate [6], or methacrylated HA hydrogels [7].

In chapter 5, we showed retention of the chondrogenic phenotype by auricular chondrocytes when photoencapsulated in 2 wt%, 50 kDa hyaluronic acid (HA) hydrogels, which exhibited continued glycosaminoglycan and type II collagen production [8]. Auricular cartilage proves to be a promising cell source for cartilage regeneration for applications in plastic surgery

and potentially for articular surface repair. Auricular chondrocytes are easily harvested with little donor-site morbidity and can be obtained at yields twice as high as articular chondrocytes [9] and proliferate approximately four times faster than articular chondrocytes when grown in monolayer culture[10]. Additionally, when implanted *in vivo* on three-dimensional scaffolds, primary auricular chondrocytes have been shown to express high levels of type II collagen and glycosaminoglycans [9]. Furthermore, auricular chondrocytes have been successfully encapsulated in a variety of materials such as poly(glycolic acid ) [11,12], alginate [13], chitosan[14], and Pluronic F127 [15], and have been shown to produce extracellular matrix and form neocartilage. In a study by Xu *et al* [16] auricular chondrocytes encapsulated in fibrin polymer exhibited the highest equilibrium modulus compared to those encapsulated with articular and costal chondrocytes.

The overall objective of this study was to examine the effects of *in vitro* expansion of auricular chondrocytes on neocartilage formation in a previously optimized HA hydrogel. This work also allows more insight into the potential use of auricular chondrocytes as a cell source for cartilage regeneration. To accomplish this, initially isolated (p = 0) and expanded (p = 1 and p = 2) swine auricular chondrocytes were photoencapsulated in a HA hydrogel, implanted subcutaneously in nude mice for 12 weeks, and explanted for mechanical, biochemical, and immunohistochemical analysis with comparisons to controls of the HA gel alone and native cartilage tissue.

## **6.2 Materials & Methodology**

### **6.2.1 Macromer Synthesis and Polymerization**

Methacrylated hyaluronic acid (MeHA) was synthesized as described in Chapter 4 (section 4.2). 50 kDa MeHA was sterilized with exposure to the germicidal lamp in a laminar flow hood for 30 minutes and dissolved in a sterile solution of PBS containing 0.05 wt% I2959 (Ciba) for cell encapsulation. A general schematic of the experimental layout is illustrated in Figure 6.1.

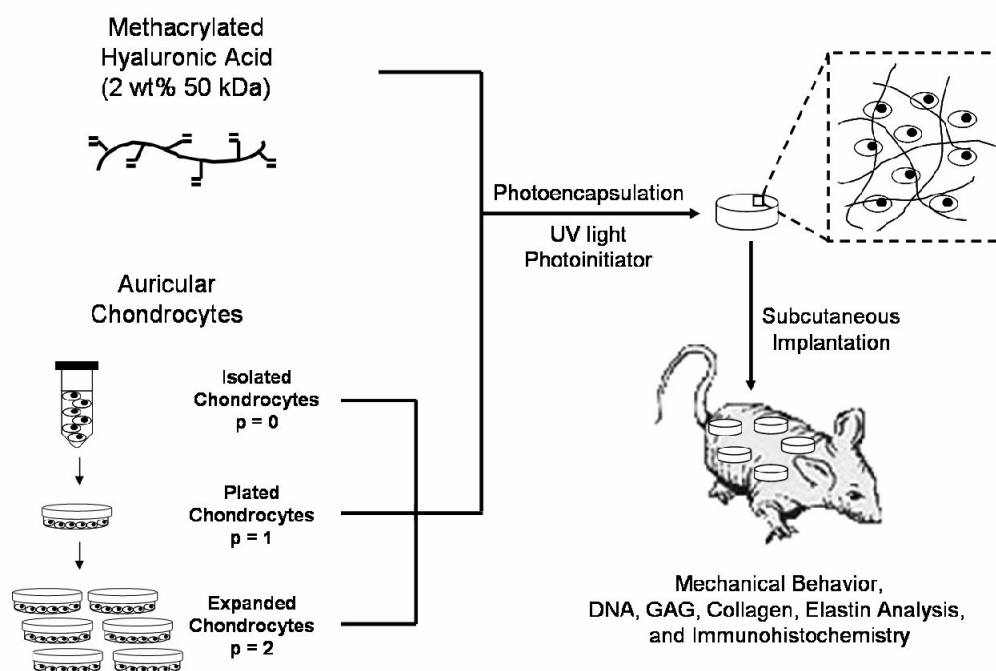


**Figure 6.1** General schematic of chondrocyte expansion, photoencapsulation, and subsequent analysis.

### 6.2.2 Chondrocyte Isolation, Expansion, and Photoencapsulation

As described in Chapter 5 (section 5.2), cartilage tissue was harvested in a sterile fashion from the ears (auricular) of 3 to 6 months old swine that were euthanized with an overdose of Pentobarbital (100 mg/kg IV). Briefly, the harvested auricular cartilage was cut into  $\sim 1\text{mm}^3$  pieces, washed in PBS, and digested overnight at  $37^\circ\text{C}$  in Ham's F-12 medium containing 0.1% collagenase (Worthington). Digested tissue was passed through a  $100\ \mu\text{m}$  filter and centrifuged to obtain a chondrocyte pellet. Chondrocytes were washed with PBS, counted using a hemacytometer, and determined viable using the trypan blue exclusion dye test prior to encapsulation and plating. Chondrocytes ( $40 \times 10^6$  cells/ml) were photoencapsulated in hydrogel networks by suspension in a 2 wt% MeHA solution containing 0.05 wt% I2959. The solution was

pipetted into sterile molds (50  $\mu$ l volume) and polymerized with  $\sim 4$  mW/cm<sup>2</sup> ultraviolet light for 10 minutes using a long-wave ultraviolet lamp (Model 100AP, Blak-Ray). Remaining chondrocytes were plated in T-150 flasks at a seeding density of  $1 \times 10^6$  cells/150 cm<sup>2</sup> ( $\sim 6700$  chondrocytes/cm<sup>2</sup>) for expansion in Ham's F-12 culture medium containing 10% FBS, 1% penicillin-streptomycin, and 1% non-essential amino acids. After reaching  $\sim 90\%$  confluency, chondrocytes were trypsinized and photoencapsulated as stated above ( $p=1$ ) or replated at  $1 \times 10^6$  cells/150 cm<sup>2</sup>, trypsinized, and photoencapsulated after reaching  $\sim 90\%$  confluency again ( $p=2$ ). Constructs were placed in culture media and implanted within 2 hours of gelation.

### 6.2.3 Implantation in Nude Mice

Nude mice were anesthetized with ketamine (80 mg/kg) and xylazine (12 mg/kg). A 2 cm midline incision was made on the dorsum of each mouse and 5 subcutaneous pockets were made using blunt dissection. One chondrocyte/hydrogel construct was placed in each of these pockets and the wound was closed with sterile stainless steel skin clips. After 12 weeks, mice were euthanized and constructs were harvested for analysis. NIH guidelines for the care and use of laboratory animals (NIH Publication #85-23 Rev. 1985) were observed.

### 6.2.4 Mechanical Testing

Samples ( $n=5$ ) were cored with a 3/16 inch diameter punch and weighed (wet weight). Cored samples were mechanically tested in confined compression in a PBS bath (Figure 6.2). For complete confinement, samples were initially loaded in creep to a tare load of 5 grams until reaching equilibrium (defined as less than 10  $\mu$ m of change in 10 min) before undergoing stress relaxation. Stress relaxation was carried out by applying a ramped displacement to 10% strain, and then the sample was allowed to relax to equilibrium (defined as less than 0.5 g of change in 10 min). The equilibrium confined compression modulus ( $E_Y$ ) for each sample was calculated by:  $\sigma = E_Y \epsilon$ , where  $\sigma = F$  (force, N) /  $A$  (loaded area, m<sup>2</sup>).

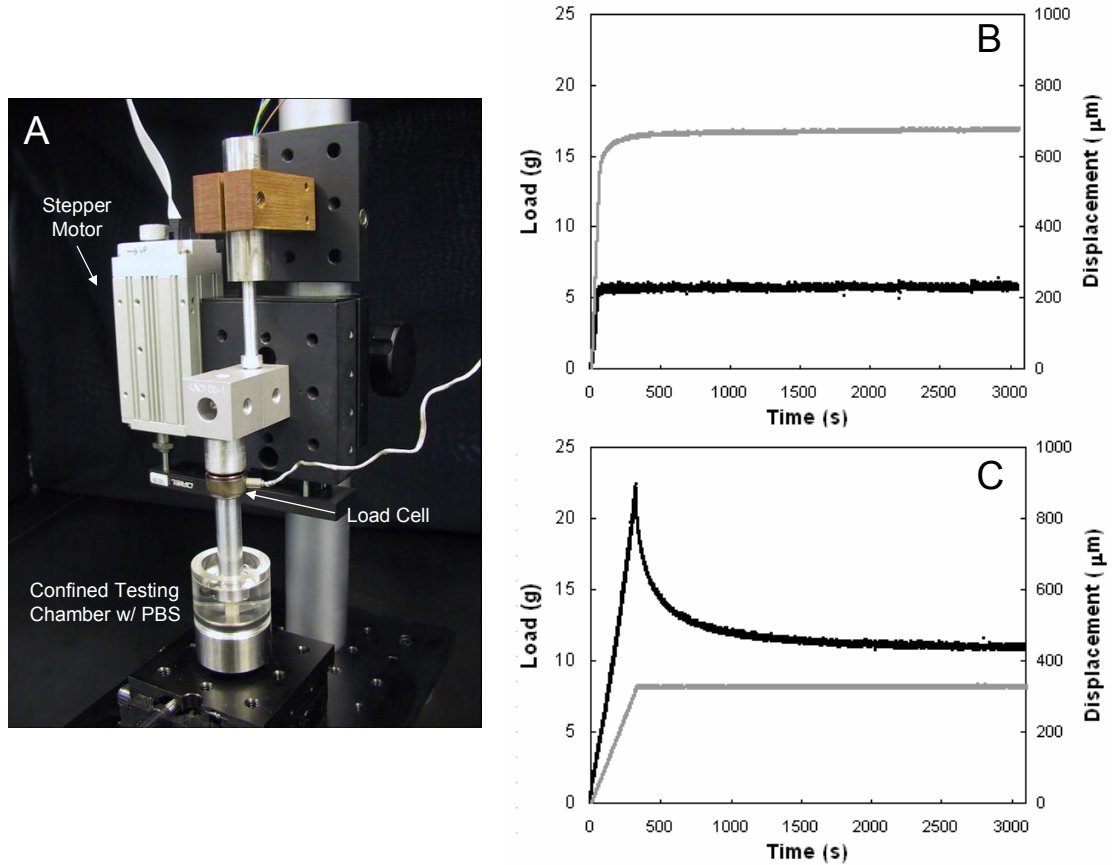


**Figure 6.2** (A) Custom-made mechanical tester used for confined compression testing [17,18]. The tester consisted of a computer-controlled stepper motor, a linear variable differential transformer to measure displacement, and a 250g or 1000g load cell to measure load. Labview software (National Instruments) was used for stepper motor control and data acquisition. Representative plots of creep (B) and stress relaxation (C), where load (black) and displacement (gray) are plotted over time.

#### 6.2.5 Biochemical Analysis

For biochemical analysis ( $n = 5$ ), mechanically tested samples were lyophilized, weighed (dry weight), and digested in a proteinase K solution (200 μg/ml proteinase K (Roche), 100 mM

ammonium acetate, pH 7.0) overnight at 60°C. Proteinase K was then inactivated at 100°C for 5 min. Total DNA, GAG, and collagen contents were determined using the PicoGreen dsDNA Assay[19], the dimethylmethylene blue dye method[20] with chondroitin sulfate as a standard, and the hydroxyproline assay[21] using a collagen to hydroxyproline ratio of 7.25[22,23], respectively (as described in section 5.2). Values reported for DNA, GAG, and collagen content were normalized to the sample wet weight. Elastin content was measured using the Fastin Elastin Assay (Accurate Chemical & Scientific Corp)[24] with an  $\alpha$ -elastin solution as a standard. Briefly, 100  $\mu$ l of the sample digest solution was combined with 200  $\mu$ l of 90% ammonium sulfate and 1 ml of Fastin dye reagent to form the elastin-dye complex. Contents were reacted for 1 hr and centrifuged to pellet the complex. The pellet was solubilized with the Fastin dissociation reagent and the absorbance was measured at a wavelength of 513 nm. The proteinase K digestion solution was used as a negative control for the hydroxyproline and elastin assays.

#### *6.2.6 Histological Analysis*

For histological analysis, constructs were fixed in 10% formalin for 24 hours, embedded in paraffin, and processed using standard histological procedures. The histological sections (7  $\mu$ m thick) were stained for chondroitin sulfate and collagen distributions using the Vectastain ABC kit (Vector Labs) and the DAB Substrate kit for peroxidase (Vector Labs). Sections were predigested in 0.5 mg/ml hyaluronidase for 30 min at 37°C and incubated in 0.5 N acetic acid for 4 hours at 4°C to swell prior to overnight incubation with primary antibodies at dilutions of 1:100, 1:200, and 1:3 for chondroitin sulfate (mouse monoclonal anti-chondroitin sulfate, Sigma), and type I (mouse monoclonal anti-collagen type 1, Sigma) and type II collagen antibodies (mouse monoclonal anti-collagen type II, Developmental Studies Hybridoma Bank), respectively. Non-immune controls underwent the same procedure without primary antibody incubation.



### 6.2.7 Statistical Analysis

Anova with Tukey's post-hoc test was used to determine significant difference among groups, with  $p < 0.05$ . All values are reported as the mean  $\pm$  the standard deviation.

## 6.3 Results & Discussion

One of the major obstacles for cartilage tissue engineering is finding a cell source and adequate cell numbers for delivery to a defect. Auricular chondrocytes, chosen for their ease of harvest, high yield, and rapid proliferation[9], were photoencapsulated in 2wt%, 50 kDa MeHA hydrogels (optimized in the previous chapter) to determine the effects of chondrocyte expansion ( $p = 0, 1$  and  $2$ ) on neocartilage formation. Constructs were explanted, mechanically tested, analyzed, and compared to controls of the HA gel alone and native auricular and articular cartilage. Macroscopically, the explants were white and opaque and resembled native cartilage tissue. The  $p = 0$  and  $p = 1$  constructs are noticeably larger (0.5 cm diameter when implanted) and more opaque, potentially indicating more ECM production and neocartilage formation, compared to the  $p = 2$  constructs (Figure 6.3) that appeared slightly translucent.

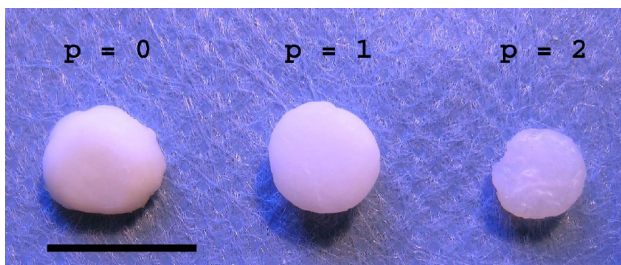


**Figure 6.3** Explanted HA constructs 12 weeks after subcutaneous implantation. Scale bar = 1cm.

### 6.3.1 Mechanical Behavior

Samples were tested in confined compression in a PBS bath to simulate a cartilage defect environment using a protocol similar to those that have been previously used to determine equilibrium moduli of hydrogel systems[25] and native cartilage[26]. In Figure 6.4, the

p = 0 and p = 1 engineered constructs ( $51.2 \pm 8.0$  kPa and  $72.5 \pm 35.2$  kPa, respectively) exhibited a significant increase in compressive equilibrium moduli from the HA hydrogel ( $12.3 \pm 1.3$  kPa), indicative of ECM deposition. However, no significant difference was detected for the p = 2 constructs ( $26.8 \pm 14.9$  kPa) and the HA hydrogel, suggesting limitations due to cell expansion. Though the moduli of the engineered constructs were all significantly lower than the articular cartilage ( $259.2 \pm 20.0$  kPa), they were all either higher than or not statistically different than that of native auricular cartilage ( $35.1 \pm 12.2$  kPa). Although the equilibrium moduli reported here for native cartilage is lower than the aggregate moduli reported in other literature[27], these differences in literature can be attributed to the specific conditions of the testing system (e.g. percent total strain) or testing method (e.g. indentation), and relative comparisons between the HA hydrogel constructs and native cartilage can still be made. It is important to note that the equilibrium moduli we obtained for articular cartilage is comparable to that determined by Strauss *et al*[26], using a similar protocol.

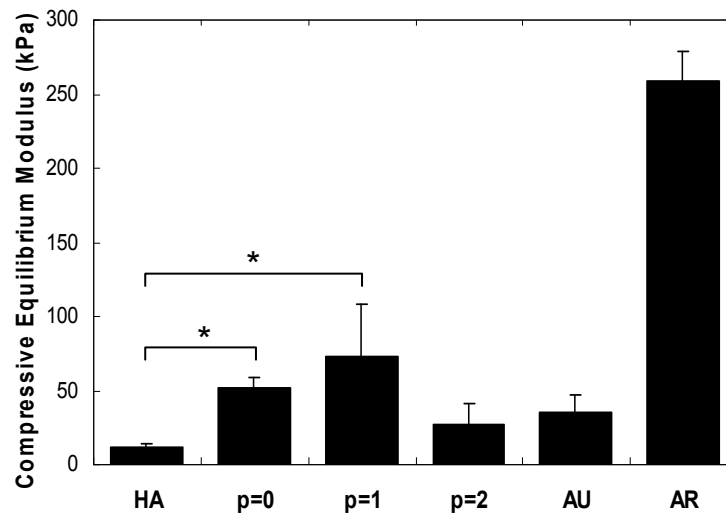


**Figure 6.4** Compressive equilibrium modulus of constructs after 12 weeks of subcutaneous implantation in nude mice compared to controls of the HA gel alone and native auricular (AU) and articular (AR) cartilage. Significant difference ( $p < 0.05$ ) is denoted by \*. Native articular cartilage is significantly greater than all groups.

### 6.3.2 Biochemical Analysis

The water content of the tissue engineered constructs and control samples were determined from wet and dry weights (Figure 6.5). In general, constructs exhibited an increase in water content with passage number. All constructs exhibited a significantly lower water content, due to the deposition of ECM proteins, when compared to the HA gel ( $97.0 \pm 0.3\%$  water), while having a significantly higher water content when compared to native auricular ( $66.5 \pm 2.7\%$  water) and articular ( $72.7 \pm 4.0\%$  water) cartilage. The  $p = 0$  constructs ( $83.1 \pm 1.3\%$  water) were most comparable to native articular cartilage.

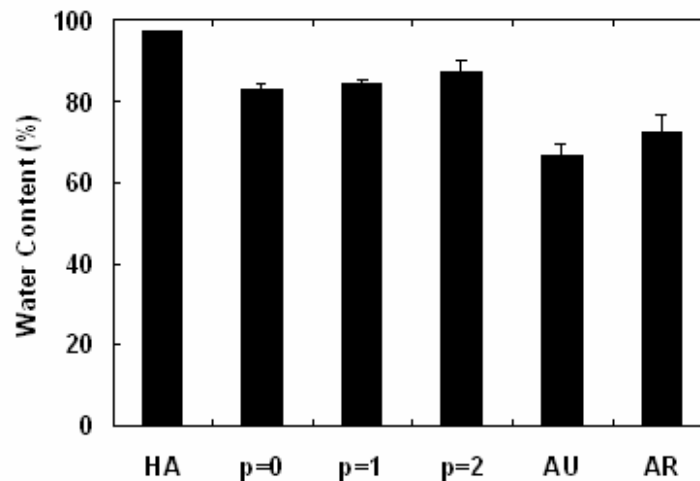


**Figure 6.5** Water content of constructs after 12 weeks of subcutaneous implantation in nude mice compared to controls of the HA gel alone and auricular and articular cartilage. The water content of all constructs ( $p=0$ ,  $p=1$ ,  $p=2$ ) was significantly less than that of HA gel alone and significantly greater than that of native auricular and articular cartilage ( $p < 0.05$ ).

Total DNA content was determined using the dsPicoGreen assay and normalized to sample wet weight in Figure 6.6. Minimal background fluorescence was detected for the HA gel and was determined to be insignificant when normalized to wet weight. In general, no significant differences were detected among sample groups, with DNA content ranging from  $\sim 0.3$  to  $0.5$  pg

DNA/  $\mu\text{g}$  wet weight. However, the  $p = 1$  constructs exhibited the lowest amount of DNA/wet weight among the engineered constructs.

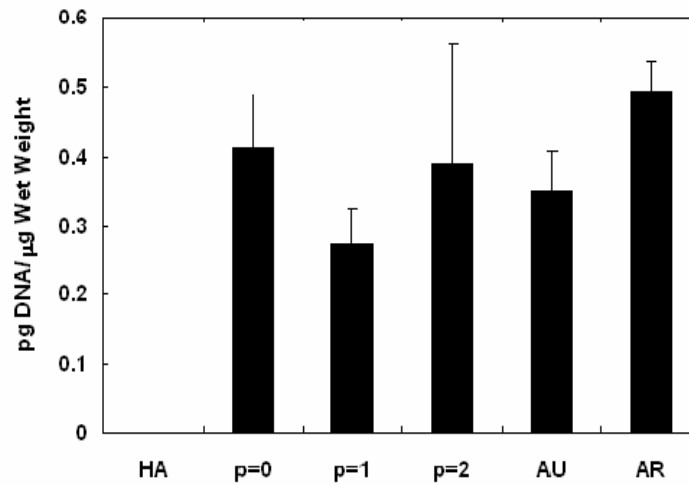


**Figure 6.6** DNA content normalized to wet weight for constructs after 12 weeks of subcutaneous implantation compared to controls of the HA gel alone and native auricular and articular cartilage. There were no statistically significant differences between groups.

In Figure 6.7A, GAG content is reported as the quantity of chondroitin sulfate normalized to sample wet weight. In general, constructs exhibited a decrease in GAG content with passage number, where  $p = 0$  and  $p = 1$  constructs ( $0.049 \pm 0.009$  and  $0.046 \pm 0.004$   $\mu\text{g CS/} \mu\text{g}$  wet weight, respectively) are significantly greater than the  $p = 2$  constructs ( $0.029 \pm 0.005$   $\mu\text{g CS/} \mu\text{g}$  wet weight). All engineered constructs exhibited a significantly higher GAG content than the control HA gels, indicating neocartilage formation, while the significant decrease from  $p = 1$  to  $p = 2$  potentially indicates the dedifferentiation of the encapsulated chondrocytes during expansion. When compared to native cartilage, the  $p = 0$  and  $p = 1$  constructs are ~75-80% and ~53-57% of the GAG content measured for auricular and articular cartilage, respectively. Articular cartilage was significantly greater than all engineered constructs, but there was no significant difference

detected in GAG content between auricular cartilage and the p = 0 constructs. Non-significant GAG content was detected for the HA gels.

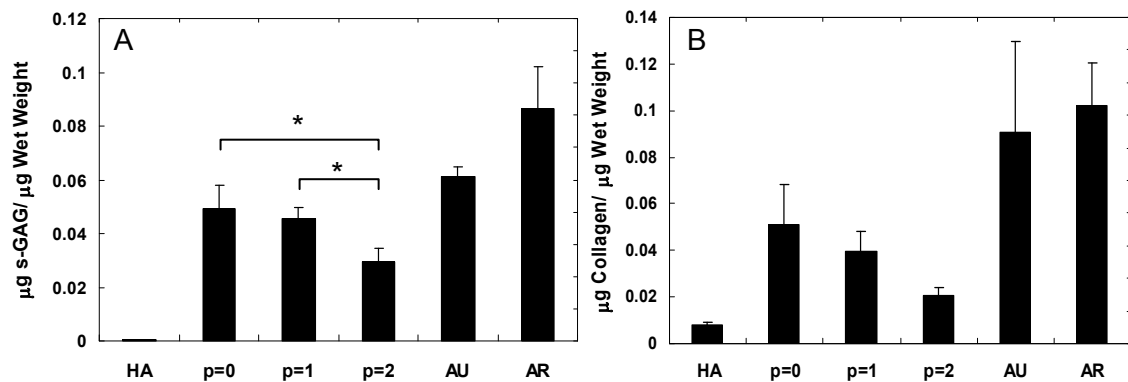


**Figure 6.7** Sulfated GAG (A) and collagen (B) content of samples normalized to construct wet weight after 12 weeks of subcutaneous implantation compared to controls of the HA gel alone and native auricular and articular cartilage. Significant difference ( $p < 0.05$ ) among constructs is denoted by \*. Sulfated GAG and collagen contents for native articular cartilage are significantly greater ( $p < 0.05$ ) than all constructs.

Total collagen content, normalized to wet weight and reported in Figure 6.7B, exhibited similar trends to those observed for GAG content, with a general decrease in collagen observed with passage number. The collagen content of the p = 0 constructs ( $0.051 \pm 0.017$  μg collagen/μg wet weight) was most comparable to native cartilage (i.e., ~57% and ~50% of measured collagen content for auricular and articular cartilage, respectively). Again, the control HA gels showed minimal levels with this assay.

As a final measure of construct biochemical levels, elastin was quantified to determine if the implanted auricular chondrocytes still produced elastin after isolation and expansion (Figure 6.8). In general, the trend of elastin content with passage was similar to that of the GAG content and similar to findings by van Osch *et al*, where phenotypic changes and decreases in elastin were observed as auricular chondrocytes are expanded 2-dimensionally *in vitro*[9]. Elastin content decreased with passage number, with a significant decrease from p = 1 to p = 2.

However, no significant difference for  $p = 0$  ( $2.7 \pm 0.4$  pg elastin/  $\mu$ g wet weight) or  $p = 1$  constructs ( $2.5 \pm 0.5$  pg elastin/  $\mu$ g wet weight) was observed when compared to auricular cartilage ( $2.9 \pm 0.5$  pg elastin/  $\mu$ g wet weight), indicating a retention of the auricular chondrocyte phenotype. Lower levels of elastin were detected in articular cartilage and  $p = 2$  constructs ( $0.3 \pm 0.4$  and  $1.1 \pm 0.7$  pg elastin/  $\mu$ g wet weight, respectively), which were significantly lower than elastin found in the  $p = 0$  and  $p = 1$  constructs and auricular cartilage. No elastin was detected in the HA gels.

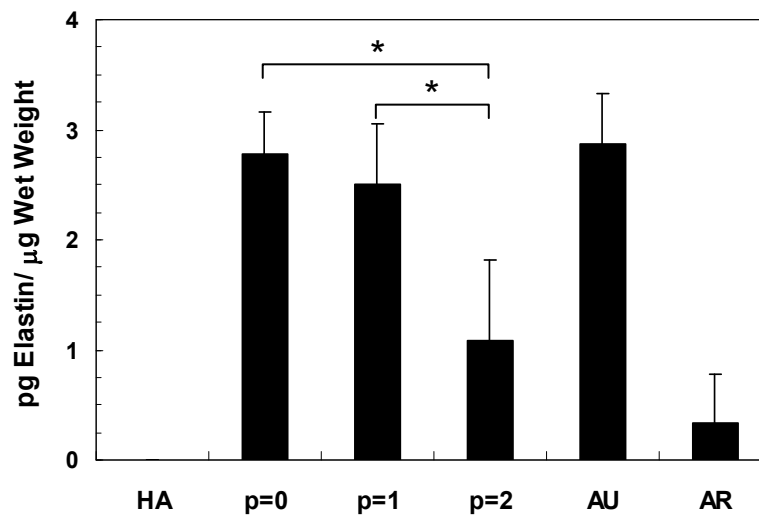


**Figure 6.8** Elastin content of constructs normalized to construct wet weight after 12 weeks of subcutaneous implantation compared to controls of the HA gel alone and native auricular and articular cartilage. Significant difference ( $p < 0.05$ ) among constructs is denoted by \*. Elastin content for native articular cartilage is significantly lower than that of  $p=0$  and  $p=1$  groups.

### 6.3.3 Immunohistochemical Analysis

Representative stains for chondroitin sulfate, type I collagen, and type II collagen are shown in Figure 6.9 with non-immune controls for comparison.

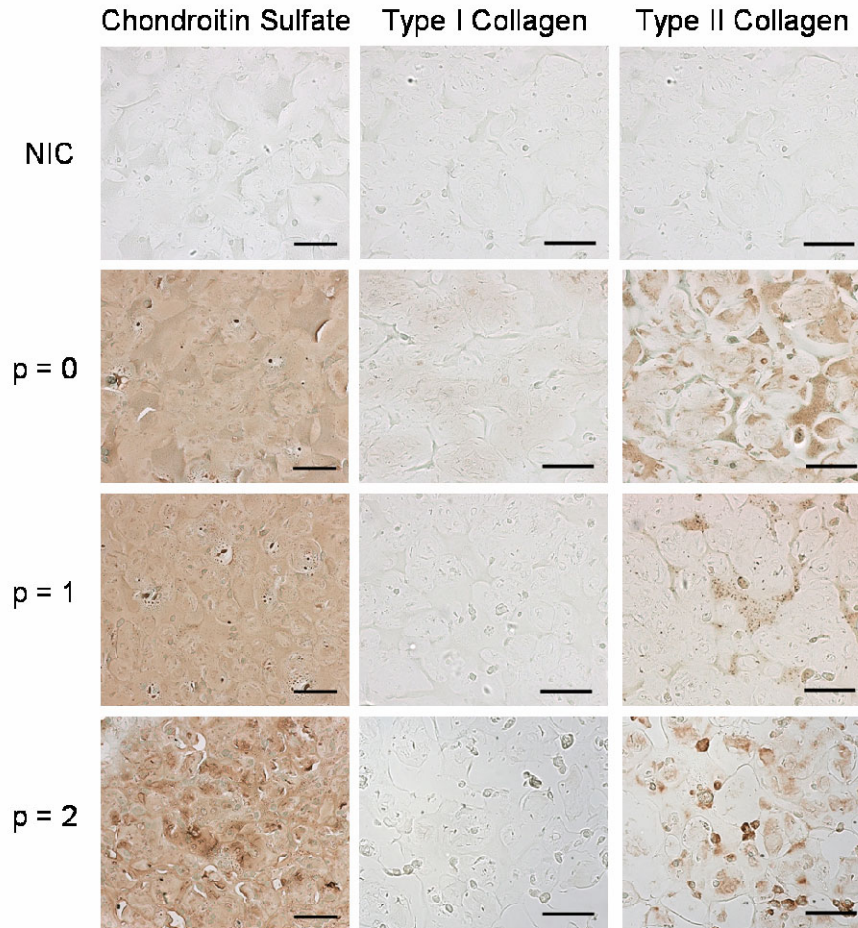


**Figure 6.9** Histological sections of constructs stained for chondroitin sulfate and type I and type II collagen compared to non-immune controls (NIC), with no primary antibody, after 12 weeks of subcutaneous implantation in nude mice. Scale bar = 100um.

In general, histological sections illustrate the morphology and distribution of the auricular chondrocytes and the distribution of extracellular components. Chondroitin sulfate is evenly distributed throughout all constructs with similar intensity. Though little to no type I collagen staining was detected, type II collagen staining was detected in all constructs, where it was most intense and most widely distributed for the p = 0 constructs. Differences in chondroitin sulfate and type II collagen distribution can result from a difference in molecule size, where smaller chondroitin sulfate molecules can fill voids of the hydrogel with greater ease. The histological

observations of ECM deposition and distribution are consistent with the results from the biochemical analysis. The non-immune controls exhibited no background staining of the constructs.

#### **6.4 Conclusions**

This study showed that  $p = 0$  and  $p = 1$  auricular chondrocytes retain a more chondrogenic phenotype when photoencapsulated in a HA hydrogel for 12 weeks while possible changes in phenotype may occur after  $p = 1$  and may compromise neocartilage formation *in vivo*. Although constructs were all mechanically inferior to articular cartilage, the  $p = 0$  and  $p = 1$  constructs showed comparable if not greater compressive moduli than auricular cartilage and show an increase in modulus over the HA gel. Even though biochemical content generally decreased with passage, significant decreases were only found after  $p = 1$ . Histologically, all constructs exhibited aggrecan and type II collagen staining, characteristic of native cartilage. These results show that  $p = 0$  and  $p = 1$  auricular chondrocytes produce cartilaginous tissue in a 2 wt%, 50 kDa hyaluronic acid hydrogel that is comparable to auricular cartilage, but are lower than values for articular cartilage. However, it is possible that mechanical stimuli or the introduction of growth factors could lend to the production of more hyaline-like cartilage (i.e., articular cartilage).



**References:**

- [1] Benya PD, Shaffer JD. Dedifferentiated chondrocytes reexpress the differentiated collagen phenotype when cultured in agarose gels. *Cell* 1982;30(1):215-24.
- [2] von der Mark K, Gauss V, von der Mark H, Muller P. Relationship between cell shape and type of collagen synthesised as chondrocytes lose their cartilage phenotype in culture. *Nature* 1977;267(5611):531-2.
- [3] Takigawa M, Shirai E, Fukuo K, Tajima K, Mori Y, Suzuki F. Chondrocytes dedifferentiated by serial monolayer culture form cartilage nodules in nude mice. *Bone Miner* 1987;2(6):449-62.
- [4] Mayne R, Vail MS, Mayne PM, Miller EJ. Changes in type of collagen synthesized as clones of chick chondrocytes grow and eventually lose division capacity. *Proc Natl Acad Sci U S A* 1976;73(5):1674-8.
- [5] Villar-Suarez V, Calles-Venal I, Bravo IG, Fernandez-Alvarez JG, Fernandez-Caso M, Villar-Lacilla JM. Differential Behavior Between Isolated and Aggregated Rabbit Auricular Chondrocytes on Plastic Surfaces. *J Biomed Biotechnol* 2004;2004(2):86-92.
- [6] Chia SH, Homicz MR, Schumacher BL, Thonar EJ, Masuda K, Sah RL, et al. Characterization of human nasal septal chondrocytes cultured in alginate. *J Am Coll Surg* 2005;200(5):691-704.
- [7] Nettles DL, Vail TP, Morgan MT, Grinstaff MW, Setton LA. Photocrosslinkable hyaluronan as a scaffold for articular cartilage repair. *Ann Biomed Eng* 2004;32(3):391-7.
- [8] Chung C, Mesa J, Randolph MA, Yaremchuk M, Burdick JA. Influence of Gel Properties on Neocartilage Formation by Auricular Chondrocytes Photoencapsulated in Hyaluronic Acid Networks. *J Biomed Mater Res In Review*.
- [9] Van Osch GJ, Mandl EW, Jahr H, Koevoet W, Nolst-Trenite G, Verhaar JA. Considerations on the use of ear chondrocytes as donor chondrocytes for cartilage tissue engineering. *Biorheology* 2004;41(3-4):411-21.

- [10] Kafienah W, Jakob M, Demarteau O, Frazer A, Barker MD, Martin I, et al. Three-dimensional tissue engineering of hyaline cartilage: comparison of adult nasal and articular chondrocytes. *Tissue Eng* 2002;8(5):817-26.
- [11] Rotter N, Ung F, Roy AK, Vacanti M, Eavey RD, Vacanti CA, et al. Role for interleukin 1alpha in the inhibition of chondrogenesis in autologous implants using polyglycolic acid-polylactic acid scaffolds. *Tissue Eng* 2005;11(1-2):192-200.
- [12] Cao Y, Rodriguez A, Vacanti M, Ibarra C, Arevalo C, Vacanti CA. Comparative study of the use of poly(glycolic acid), calcium alginate and pluronics in the engineering of autologous porcine cartilage. *J Biomater Sci Polym Ed* 1998;9(5):475-87.
- [13] Chang SC, Tobias G, Roy AK, Vacanti CA, Bonassar LJ. Tissue engineering of autologous cartilage for craniofacial reconstruction by injection molding. *Plast Reconstr Surg* 2003;112(3):793-9; discussion 800-1.
- [14] Xia W, Liu W, Cui L, Liu Y, Zhong W, Liu D, et al. Tissue engineering of cartilage with the use of chitosan-gelatin complex scaffolds. *J Biomed Mater Res B Appl Biomater* 2004;71(2):373-80.
- [15] Kamil SH, Kojima K, Vacanti MP, Bonassar LJ, Vacanti CA, Eavey RD. In vitro tissue engineering to generate a human-sized auricle and nasal tip. *Laryngoscope* 2003;113(1):90-4.
- [16] Xu JW, Zaporozhan V, Peretti GM, Roses RE, Morse KB, Roy AK, et al. Injectable tissue-engineered cartilage with different chondrocyte sources. *Plast Reconstr Surg* 2004;113(5):1361-71.
- [17] Mauck RL, Wang CCB, Oswald ES, Ateshian GA, Hung CT. The role of cell seeding density and nutrient supply for articular cartilage tissue engineering with deformational loading. *Osteoarthritis and Cartilage* 2003;11(12):879-90.
- [18] Soltz MA, Ateshian GA. Experimental verification and theoretical prediction of cartilage interstitial fluid pressurization at an impermeable contact interface in confined compression. *Journal of Biomechanics* 1998;31(10):927-34.

- [19] Singer VL, Jones LJ, Yue ST, Haugland RP. Characterization of PicoGreen reagent and development of a fluorescence-based solution assay for double-stranded DNA quantitation. *Anal Biochem* 1997;249(2):228-38.
- [20] Farndale RW, Sayers CA, Barrett AJ. A direct spectrophotometric microassay for sulfated glycosaminoglycans in cartilage cultures. *Connect Tissue Res* 1982;9(4):247-8.
- [21] Stegemann H, Stalder K. Determination of hydroxyproline. *Clin Chim Acta* 1967;18(2):267-73.
- [22] Herbage D, Bouillet J, Bernengo JC. Biochemical and physiochemical characterization of pepsin-solubilized type-II collagen from bovine articular cartilage. *Biochem J* 1977;161(2):303-12.
- [23] Williamson AK, Chen AC, Sah RL. Compressive properties and function-composition relationships of developing bovine articular cartilage. *J Orthop Res* 2001;19(6):1113-21.
- [24] Brown AN, Kim BS, Alsberg E, Mooney DJ. Combining chondrocytes and smooth muscle cells to engineer hybrid soft tissue constructs. *Tissue Eng* 2000;6(4):297-305.
- [25] Mauck RL, Soltz MA, Wang CC, Wong DD, Chao PH, Valhmu WB, et al. Functional tissue engineering of articular cartilage through dynamic loading of chondrocyte-seeded agarose gels. *J Biomech Eng* 2000;122(3):252-60.
- [26] Strauss EJ, Goodrich LR, Chen CT, Hidaka C, Nixon AJ. Biochemical and biomechanical properties of lesion and adjacent articular cartilage after chondral defect repair in an equine model. *Am J Sports Med* 2005;33(11):1647-53.
- [27] Mow VC, Gibbs MC, Lai WM, Zhu WB, Athanasiou KA. Biphasic indentation of articular cartilage--II. A numerical algorithm and an experimental study. *J Biomech* 1989;22(8-9):853-61.

# CHAPTER 7

## *Auricular and Articular Cartilage:*

### *How do chondrocytes differ in Hyaluronic Acid Hydrogels?*

Adapted from: **C Chung**, IE Erickson, RL Mauck, JA Burdick, "Differential Behavior of Auricular and Articular Chondrocytes in Hyaluronic Acid Hydrogels," Tissue Eng Part A, 2008, 14(7): 1121-31.)

#### **7.1 Introduction**

As mentioned in chapter 6, the choice of cell source still remains a question in approaches for cartilage tissue engineering with hyaluronic acid (HA) hydrogels. We showed that directly isolated and first passage auricular chondrocytes could produce cartilaginous tissue in 2wt% MeHA hydrogels with comparable properties to that of native auricular cartilage. However, for applications in articular cartilage repair, would articular chondrocytes perform more successfully and how does the hydrogel environment influence successful neocartilage production? Chondrocytes can be isolated from a variety of sources including articular (AR), auricular (AU), nasoseptal, and costal cartilage, and each type of cartilage tissue has discrete chemical, physical, and mechanical properties. As chondrocyte behavior is dependent on where it is isolated from, it is important to determine how chondrocytes from each source function and behave in an engineered environment (e.g. biomaterial, soluble factors, mechanical loading).

To date, researchers have shown differences among chondrocyte sources with respect to cell yields, proliferation rates, and phenotype retention[1-4]. In a study by van Osch *et al*, higher cell yields and faster proliferation rates were obtained for AU chondrocytes when compared to AR chondrocytes[1]. Furthermore, these AU chondrocytes were able to retain their chondrocytic phenotype when cultured in alginate beads. Likewise, nasal chondrocytes can proliferate four times faster than AR chondrocytes in monolayer[3], and can be seeded at very low densities with an 838-fold expansion in one passage without extensive dedifferentiation[2]. With the addition of

growth factors, AU, nasal, and costal chondrocytes all exhibit increased proliferation, GAG/DNA content, and up-regulation of type II collagen expression; however, redifferentiation was achieved only in AU and nasal chondrocyte cell pellets [4]. These studies provide motivation for exploring multiple chondrocyte sources towards tissue engineering approaches.

Source dependent differences can also be found in the resulting engineered cartilage tissues, including differences in construct size, gene expression, biochemical content, and mechanical properties. Panossian and coworkers showed that AU chondrocyte-seeded samples produced neocartilage with greater biochemical and histological similarity to that of native cartilage than AR counterparts when implanted *in vivo*[5]. Xu *et al* have also shown that AU chondrocytes encapsulated in fibrin exhibited the highest equilibrium modulus compared to those encapsulated with AR and costal chondrocytes[6]. In a comparison study of bovine nasal, AR, costal, and AU chondrocytes grown on poly(L-lactide- $\epsilon$ -caprolactone) scaffolds[7], construct size and gene expression varied with chondrocyte type. AU chondrocyte-seeded constructs had the largest diameter while costal chondrocyte-seeded constructs had the greatest thickness, and costal chondrocytes, followed by nasoseptal, AR, and AU chondrocytes had the highest expression of type II collagen and aggrecan. However, despite cell differences, Johnson *et al* demonstrated that AR, AU, and costal chondrocytes were all able to form new cartilaginous matrix when cultured in fibrin glue-cartilage composites *in vivo* [8]. This information is important towards isolating a specific cell source, yet the behavior of cells is dependent on the biomaterial used as a carrier. Specifically, variables in biomaterial design, such as mechanics, permeability, and incorporation of biological motifs can dictate cellular behavior. Thus, data on the source-dependent differential responses of chondrocytes can assist in biomaterial choice, scaffold type, and cartilage repair application, e.g. in plastic, reconstructive, or orthopaedic surgery. The objective of this study was to investigate and characterize the differences in cell behavior of AU and AR chondrocytes when encapsulated and cultured in MeHA hydrogels.

## **7.2 Materials & Methodology**

### *7.2.1 Macromer Synthesis and Polymerization*

Methacrylated hyaluronic acid (MeHA) was synthesized as described in Chapter 4. 64 kDa MeHA (Lifecore) was sterilized with exposure to the germicidal lamp in a laminar flow hood for 30 minutes and dissolved in a sterile solution of PBS containing 0.05 wt% I2959 (Ciba) for cell encapsulation. A switch to 64 kDa molecular weight was due to availability from Lifecore. However, as determined in Chapters 4 and 5, molecular weight can alter the viscosity of the macromer solution, but insignificantly affects hydrogel properties and neocartilage formation.

### *7.2.2 Chondrocyte Isolation and Photoencapsulation*

Cartilage tissue was harvested in a sterile fashion from the ears (AU) and the knees (AR) of 3 to 6 month old swine. The harvested cartilage was cut into  $\sim 1\text{mm}^3$  pieces, washed in PBS, and digested overnight at 37°C in DMEM containing 0.1% and 0.05% collagenase (Worthington) for AU and AR cartilage, respectively. Digested tissue was passed through a 100  $\mu\text{m}$  filter and centrifuged to obtain a chondrocyte pellet. Chondrocytes were washed with PBS, counted using a hemacytometer, and determined viable using the trypan blue exclusion dye test prior to encapsulation. Chondrocytes (40 million cells/ml) were photoencapsulated in hydrogels by suspension in a 2 wt% macromer (MeHA) solution, injection into sterile molds (50  $\mu\text{l}$  volume) and polymerization with ultraviolet light for 10 minutes using a long-wave ultraviolet lamp (Topbulb, F8T5BLB).

### *7.2.3 In Vivo and In Vitro Culture Methods*

For *in vivo* culture, constructs (n=5/group per time point) were implanted subcutaneously in nude mice within 2 hours of gelation. Nude mice were anesthetized with isoflurane and 5 subcutaneous pockets were made using an incision and blunt dissection. One

chondrocyte/hydrogel construct was placed in each of these pockets and the wound was closed with sterile stainless steel skin clips. After 6 and 12 weeks, mice were euthanized and constructs were harvested for analysis. NIH guidelines for the care and use of laboratory animals (NIH Publication #85-23 Rev. 1985) were observed.

For *in vitro* culture, AU and AR-seeded constructs, fabricated in the same manner as described above, were cultured for 14 days in DMEM supplemented with 10% fetal bovine serum, 1% penicillin/streptomycin, 1% sodium bicarbonate, 1% non-essential amino acids, and 50 $\mu$ g/mL ascorbic acid 2-phosphate (growth media). Media was changed every 2 days. Relative gene expression and histology were analyzed after 6 and 14 days of culture.

#### 7.2.4 Mechanical Stimulation

Loading parameters for *in vitro* mechanical stimulation in the bioreactor system were validated using an Instron 5848 Microtester equipped with a 50N load cell and the WaveMaker Software package. Acellular HA macromer solution was polymerized between glass plates (2.25mm thickness) and cylindrical hydrogels were produced with a 5mm diameter biopsy punch. Samples (n=3) were immersed in a PBS custom bath at room temperature and positioned between two impermeable platens. A 5% static compression was applied and after equilibrium was achieved, dynamic compression was applied with a sinusoidal waveform of 10% amplitude and a frequency of 1 Hz. Loading was carried out for a minimum of 10 minutes and each test was repeated three times. Additional tests with larger amplitudes (15%) and higher frequencies (3 Hz) were also tested. For mechanical stimulation of cell-seeded constructs within the bioreactor system, hydrogels (n=4/group per time point) were formed in the same fashion with a seeding density of 40 million cells/ml. After 5 days of subculture, the hydrogels were immersed in growth media and subjected to uniaxial unconfined cyclic compression (5% tare, 10% strain, 1 Hz) in a custom made bioreactor[9]. Dynamic loading was carried out for 3 hours per day for 1 or 5 consecutive days at 37°C and 5% CO<sub>2</sub> in a humidified environment. Samples were removed

from the bioreactor after each mechanical loading session. At the end of loading on day 1 or day 5, samples were removed from culture and analyzed for gene expression and compared to free-swelling controls. A general schematic of the experimental layout is illustrated in Figure 7.1.

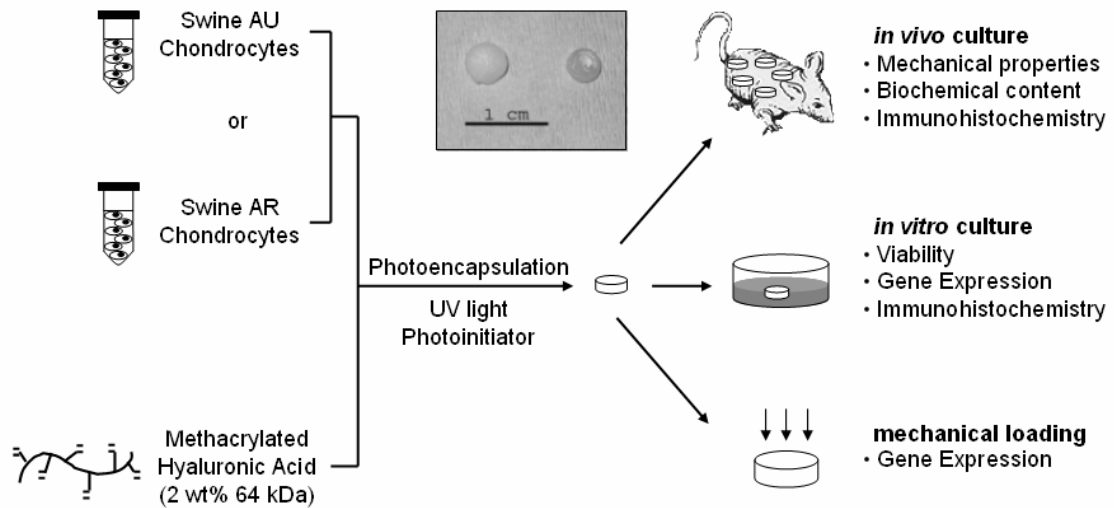


**Figure 7.1** General schematic of chondrocyte isolation, encapsulation, and analysis. Inset: Macroscopic image of explanted AU (left) and AR (right) chondrocyte-seeded constructs after 12 weeks of *in vivo* subcutaneous culture.

#### 7.2.5 Mechanical Testing

Explanted samples (n=5) were cored with a 3/16 inch diameter punch and weighed (wet weight). Cored samples were mechanically tested in confined compression in a PBS bath. To ensure complete confinement, samples were initially loaded in creep to a tare load of 5 grams until reaching equilibrium (defined as less than 10  $\mu\text{m}$  of change in 10 min) before undergoing stress relaxation. Stress relaxation was carried out by applying a ramped displacement (1  $\mu\text{m/s}$ ) to 10% strain, after which the sample was allowed to relax to equilibrium (defined as less than 0.5 g of change in 10 min). The equilibrium confined compression aggregate modulus ( $E_V$ ) for each sample was calculated by dividing the equilibrium load by the sample cross-sectional area and the applied strain. Native AU and AR cartilage samples were similarly tested (n=5).



#### 7.2.6 Biochemical Analysis

For biochemical analysis (n = 5), mechanically tested samples were lyophilized, weighed (dry weight), and digested in a proteinase K solution (200 µg/ml proteinase K (Roche), 100 mM ammonium acetate, pH 7.0) overnight at 60°C. Proteinase K was then inactivated at 100°C for 5 min. Total DNA, GAG, and collagen contents were determined using the PicoGreen dsDNA Assay[10], the dimethylmethylene blue dye method[11] with chondroitin sulfate as a standard, and the hydroxyproline assay[12] using a collagen to hydroxyproline ratio of 7.25[13,14], respectively as outlined in section 5.2. Values reported for DNA, GAG, and collagen content were normalized to the sample wet weight. The proteinase K digestion solution was used as a negative control.

#### 7.2.7 Viability

The viability of AU and AR chondrocytes in the HA hydrogel was determined using an MTT assay. Mitochondrial activity (n=3) was assessed on days 0 (2 hrs after encapsulation), 7, and 14 of *in vitro* culture. Briefly, 100µl of MTT reagent was added to 1ml of media and incubated for 4 hours. Samples were then removed from the media, homogenized in the detergent solution with a tissue grinder, and incubated for 4 hrs before reading in a spectrophotometer. Absorbance readings at 570 nm were normalized to day 0 values to account for differences in mitochondrial activity between cell sources.

#### 7.2.8 Gene Expression Analysis

Samples (n=4) were homogenized in Trizol Reagent (Invitrogen) with a tissue grinder and RNA was extracted according to the manufacturer's instructions. RNA concentration was determined using an ND-1000 spectrophotometer (Nanodrop Technologies). One microgram of RNA from each sample was reverse transcribed into cDNA using reverse transcriptase (Superscript II, Invitrogen) and oligoDT (Invitrogen). Polymerase chain reaction (PCR) was

performed on an Applied Biosystems 7300 Real-Time PCR system using a 25µl reaction volume for SybrGreen and Taqman (5'-nuclease) reactions. Primers and probes specific for glyceraldehydes 3-phosphate dehydrogenase (GAPDH), type I and type II collagen, aggrecan, and hyaluronidases (Hyal) 1, 2 and 3 are listed in Table 7.1. SybrGreen reaction was used for all genes except type II collagen and GAPDH was used as the housekeeping gene. The relative gene expression was calculated using the  $\Delta\Delta C_T$  method, where fold difference was calculated using the expression  $2^{-\Delta\Delta C_T}$ .

**Table 7.1** Porcine primer and probe sequences for real-time PCR.

Gene	Forward Primer	Reverse Primer	Probe
GAPDH	CGTCCCTGAGACACGATGGT	CCCGATGCGGCCAAAT	
Collagen I [15]	GGCTCCTGCTCCTCTTAGCG	CATGGTACCTGAGGCCGTTC	
Collagen II	CTCCTGGCACGGATGGT	CTGGAGGGCCCTGAGC	CCCAAAGGCGCATCTG
Aggrecan [16]	GCAGACCAGAAGCTGTGTGAGA	TGACGATGCTGCTCAGGTGT	
HYAL1 [17]	TGCCCTATGCCCAGATCTTC	CAGCTCCTCCCGAGACAGAA	
HYAL2 [17]	AGGGCTTAGCGAGATGGATCT	TGTCAGGTAATCCTTGAGGTATTGG	
HYAL3 [17]	TGAACCTGTGCAGACCATTGGT	GCCAACACTCCTCCTCAGAACT	

### 7.2.9 Histological Analysis

For histological analysis, constructs were fixed in 10% formalin for 24 hours, embedded in paraffin, and processed using standard histological procedures. The histological sections (7 µm thick) were stained for aggrecan and collagen distributions using the Vectastain ABC kit (Vector Labs) and the DAB Substrate kit for peroxidase (Vector Labs). Sections were predigested in 0.5 mg/ml hyaluronidase for 30 min at 37°C and incubated in 0.5 N acetic acid for 4 hours at 4°C to swell the samples prior to overnight incubation with primary antibodies at dilutions of 1:100, 1:200, and 1:3 for chondroitin sulfate (mouse monoclonal anti-chondroitin sulfate, Sigma), and type I (mouse monoclonal anti-collagen type 1, Sigma) and type II collagen antibodies (mouse monoclonal anti-collagen type II, Developmental Studies Hybridoma Bank),

respectively. Non-immune controls underwent the same procedure without primary antibody incubation.

#### 7.2.10 Statistical Analysis

All values are reported as the mean  $\pm$  the standard error of the mean (SEM). ANOVA was used to determine significant differences among groups, with  $p \leq 0.05$ . Sensitivity of the data was analyzed using a non-parametric Wilcoxon Rank-Sum test, given small sample sizes.

### 7.3. Results & Discussion

Chondrocytes can be isolated from a variety of sources and behave and respond differently to their local environment (e.g., exposure to mechanical forces, soluble factors, varying compositions of ECM molecules, or scaffold material) depending on the chondrocyte source[18]. Thus, it is important to investigate the response of specific chondrocyte sources to this microenvironment for assessment of tissue engineering approaches. This study focused specifically on differences in neocartilage production by AU and AR chondrocytes in HA hydrogels. AU cartilage is a non-load bearing and elastic tissue found primarily in the ear and epiglottis, whose primary role is to maintain shape and structure. Alternatively, AR cartilage is a hyaline cartilage that is capable of distributing mechanical loads and providing low friction articulation in diarthrodial joints. Therefore, chondrocytes isolated from these two types of cartilage differ in the ECM they produce in order to carry out their respective physiological roles[19].

#### 7.3.1 *In Vivo* Culture

Dramatic differences in neocartilage formation were observed *in vivo* depending on whether AU or AR chondrocytes were used as a cell source, suggesting differential cell interactions with the HA scaffold. These interactions could be affected by differences in cell

specific binding to the hydrogels, matrix degradation through enzyme production, and the reproduction of the environment seen natively by these cells, i.e. non-loaded, subcutaneous environment versus mechanically loaded joint. The macroscopic appearance (Figure 7.1 inset) of AU and AR chondrocyte-seeded samples after 12 weeks of culture show dramatic differences, where AU constructs increased in size in all dimensions and were shiny and white in appearance after subcutaneous culture, while AR samples more closely resembled implanted constructs and retained their size and translucency.

The neocartilage mechanical properties reflected these macroscopic observations, where the confined compression aggregate modulus of AU explants ( $28.2 \pm 2.2$  kPa,  $79.3 \pm 6.7$  kPa) was significantly greater than that of AR explants ( $7.0 \pm 0.3$  kPa,  $8.0 \pm 0.7$  kPa) after 6 and 12 weeks, respectively (Figure 7.2), and increased with culture.

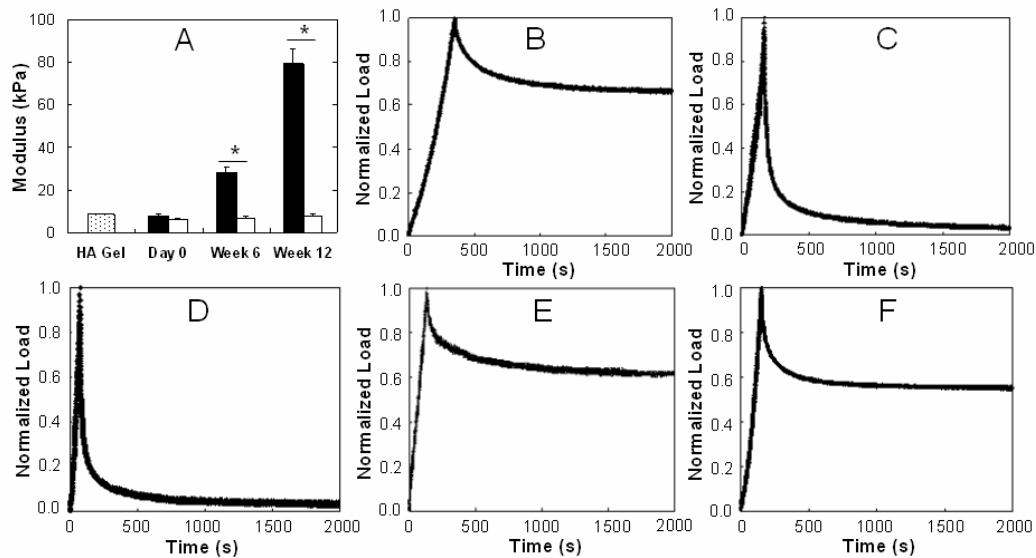


**Figure 7.2** Mechanical properties of explanted constructs. (A) Modulus of AU (black) and AR (white) chondrocyte-seeded constructs compared to HA hydrogel alone (shaded). Representative stress relaxation curves for AU chondrocyte-seeded (B) and AR chondrocyte-seeded explants (C) after 12 weeks of *in vivo* culture compared to HA hydrogel alone (D) and native AU (E) and AR (F) cartilage. Stress relaxation curves are normalized to peak stress. Significant differences ( $p \leq 0.05$ ) between AU and AR groups are denoted by \*.

Increases in modulus correlated with decreases in water content and increases in GAG content (Figure 7.3 and 7.4), in accordance with previously established data [20,21]. When normalized to their peak load, stress relaxation curves for AU explants more closely resembled those of native AU and AR cartilage, while those of AR explants more closely resembled profiles of HA hydrogel alone with a high peak load followed by rapid relaxation. This suggests a higher permeability of AR constructs compared to AU constructs and native cartilage. The aggregate modulus of AU constructs represented ~226% and ~31% of native AU and AR cartilage, respectively, while the modulus of AR constructs only represented ~23% and ~3% of the native tissue values, respectively.

The change in water content indirectly influences mechanical properties as a decrease in water content can represent an increase in ECM within the constructs. A decrease in water content was observed in both AU ( $87.8\% \pm 2.7\%$  water) and AR ( $95.0\% \pm 1.4\%$  water) constructs after 12 weeks when compared to HA hydrogel alone ( $97.0\% \pm 0.3\%$  water), with a greater decrease observed for AU constructs.

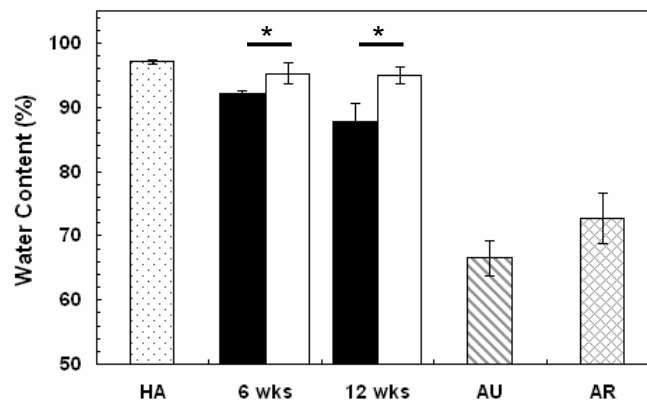


**Figure 7.3** Water content of explanted AU (black) and AR (white) constructs compared to acellular HA hydrogel (shaded) and native auricular (striped) and articular cartilage (hashed). Significant differences ( $p \leq 0.05$ ) between AU and AR groups are denoted by \*.

After 12-weeks of subcutaneous culture, the DNA content was significantly greater in AU constructs ( $1.35 \pm 0.17$  million chondrocytes) versus AR constructs ( $0.54 \pm 0.08$  million chondrocytes), although the DNA content was similar between these groups when normalized to the wet weight (Figure 7.4). Since the number of chondrocytes per sample remained relatively constant over time, the decrease in DNA content per wet weight from 6 to 12 weeks was observed and may be attributed to the accumulation of newly synthesized ECM (i.e., increased GAG and collagen content). It is also important to note that cell loss was observed during photoencapsulation; thus, the number of cells encapsulated may be less than the seeding density would suggest. However, comparisons between cell types are still valid.

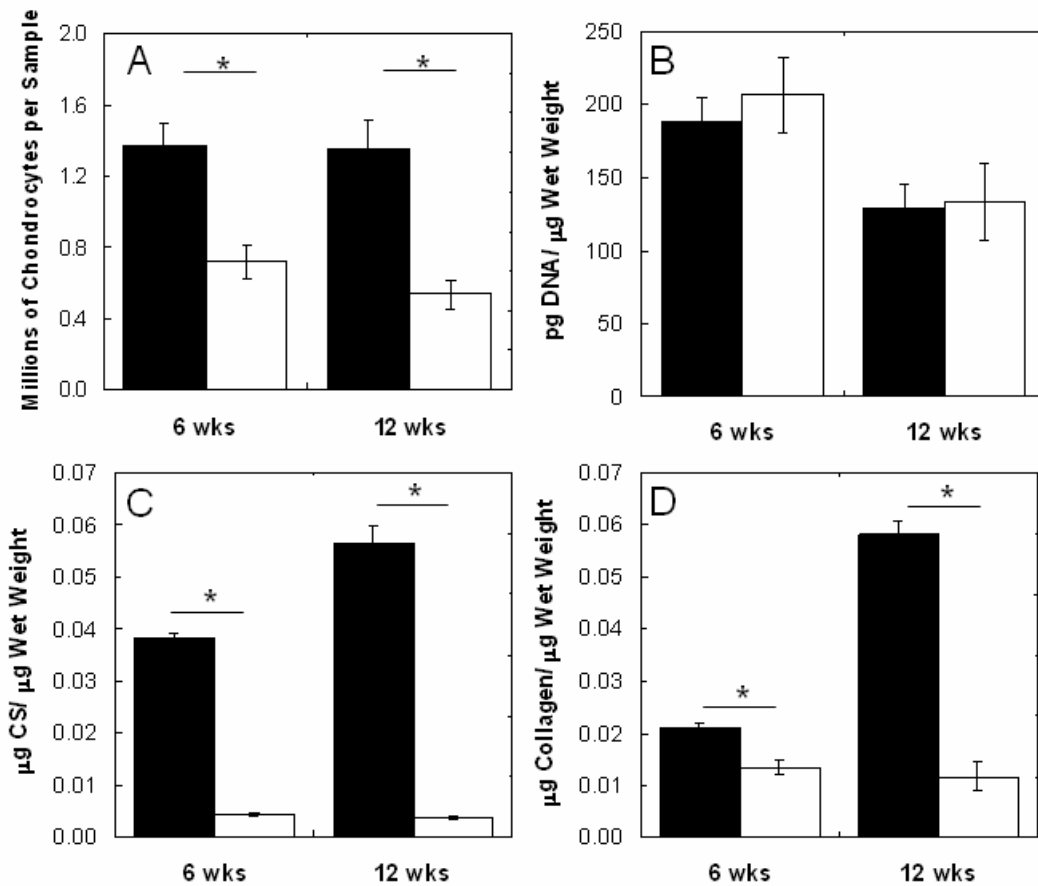


**Figure 7.4** Biochemical content of AU (black) and AR (white) explants reported as millions of chondrocytes per sample (A) and DNA (B), chondroitin sulfate (C) and collagen content (D) per wet weight. Significant differences ( $p \leq 0.05$ ) between AU and AR groups are denoted by \*.

Sulfated-GAG and collagen contents also reflect the macroscopic differences between the two cell sources. After 12-weeks of *in vivo* culture, AU constructs were comprised of  $0.056 \pm 0.003$   $\mu\text{g}$  chondroitin sulfate (CS)/  $\mu\text{g}$  wet weight and  $0.58 \pm 0.003$   $\mu\text{g}$  collagen/  $\mu\text{g}$  wet weight, while AR constructs contained  $0.004 \pm 0.0002$   $\mu\text{g}$  CS/  $\mu\text{g}$  wet weight and  $0.012 \pm 0.$   $\mu\text{g}$  collagen/  $\mu\text{g}$  wet weight (Figure 7.4). The biochemical content of AU constructs more closely resembled that of native cartilage tissues. Specifically, the GAG content was ~92% of AU and ~65% of AR cartilage and the collagen content was ~64% of AU and ~57% of AR cartilage after 12 weeks of *in vivo* culture. The orientation of these ECM components was not assessed in this work.

Immunohistochemistry of the constructs (Figure 7.5) was used to assess the distribution of cells and ECM components in the neocartilage. Greater type II collagen staining versus type I collagen staining was observed for both AU and AR constructs, suggesting phenotype retention. An even distribution of type II collagen and CS was observed in AU constructs, while more clustering of cells and ECM proteins was observed in AR constructs. Within the HA hydrogel, AR chondrocytes appeared to undergo interstitial growth, forming lacunae and isogenous groups surrounded by pericellular and territorial matrix. Since the orientation of the collagen and CS in the constructs was not assessed, no conclusions can be made regarding this potential difference with respect to mechanics.

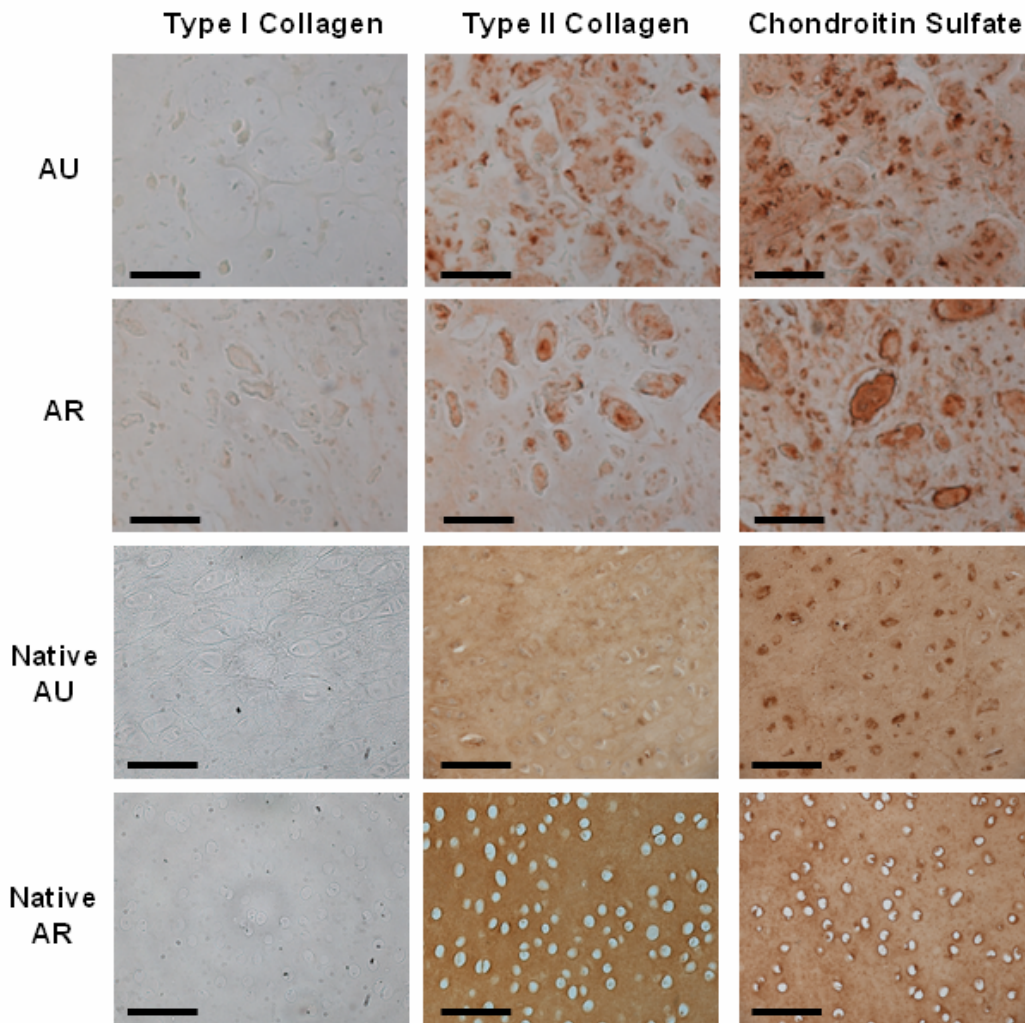


**Figure 7.5** Representative sections of AU and AR constructs stained for type I and II collagen and chondroitin sulfate after 12 weeks of subcutaneous *in vivo* culture compared to native cartilage tissue sections. Scale bar = 100 $\mu$ m.



### 7.3.2 In Vitro Culture

With dramatic differences observed in neocartilage formation *in vivo*, short-term *in vitro* cultures were used to investigate the potential causes of these differences, including comparisons of viability, gene expression, and ECM deposition. AU and AR constructs showed comparable viability in HA hydrogels, and both exhibited increases in mitochondrial activity from day 7 to day 14 (Figure 7.6).

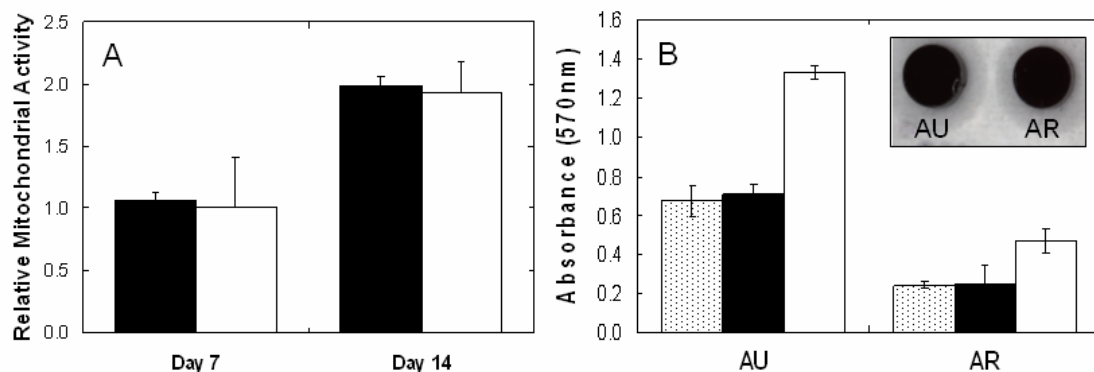


**Figure 7.6** (A) Relative mitochondrial activity of AU (black) and AR (white) hydrogels cultured *in vitro* for 7 and 14 days. Values were normalized to day 0 absorbance readings. (B) Absorbance readings at 570 nm for AU and AR constructs at day 0 (shaded), 7 (black) and 14 (white). Inset: Macroscopic image of constructs at day 0 after 4 hrs of MTT reagent incubation. The dark purple color is indicative of mitochondrial activity.

The hydrated hydrogel environment allowed cells to maintain a rounded morphology, which can assist in cell proliferation and phenotype retention. The lower mitochondrial activity level observed for AR chondrocytes in HA hydrogels on day 0 compared to AU chondrocytes may result from inherent differences between cell sources and may play a role in the differences in neocartilage formation. Free radical polymerization effects on cell death were deemed negligible, as the photoinitiating system implemented has been used extensively and others have shown it to be cytocompatible[22], and AR chondrocytes exposed to the photoinitiator and radical polymerization conditions have shown comparable cell survival to unexposed controls[23]. Thus,

free radicals present during polymerization should not significantly affect the survival or mitochondrial activity of AR chondrocytes over AU chondrocytes.

Gene expression data (Figure 7.7) was collected at 6 and 14 days of culture and normalized to the gene expression of the respective chondrocytes at the time of encapsulation. Although similar trends in gene expression were observed for AU and AR chondrocytes in HA hydrogels, the type I and type II collagen expression was significantly different between the two cell sources. Specifically, the normalized type I collagen expression was greater in AR samples and the normalized type II collagen expression was greater in AU samples. Natively, less type I collagen and more type II collagen is found in AR versus AU cartilage[19]. Thus, differences in gene expression may reflect differences in the primary cells rather than differential response *in vitro*. However, the data does suggest that AU chondrocytes behave more like primary cells than AR chondrocytes when cultured *in vitro* in HA hydrogels, since AR chondrocytes exhibited a greater increase in type I collagen and a greater decrease in type II collagen expression during culture compared to isolated cells. Both groups exhibited a trend of increased type I collagen expression with culture time and fairly constant type II collagen expression, though down-regulated when compared to respective cells at encapsulation.

Hyaluronidase expression within the hydrogels was also examined to gain insight on the potential catabolism of the HA scaffold by encapsulated cells. Hyaluronidases are enzymes that cleave the  $\beta$ -1,4-glycosidic bonds between glucuronic acid and N-acetylglucosamine[24] and are responsible for HA turnover, which can affect cell migration, differentiation, and matrix catabolism. Hyal 1 cleaves HA into small molecular masses of less than 20kDa[25], while Hyal 2, the most prominent hyaluronidase in cartilage, hydrolyzes high molecular mass HA into intermediate-sized fragments of approximately 20kDa[26]. Hyal 3 has also been detected in cartilage, but little is known about its enzymatic activity[27].

With *in vitro* culture, both AU and AR constructs exhibited decreased gene expression of Hyal 2 and 3, suggesting down-regulation of HA turnover and matrix catabolism. When

comparing between cell sources, AR constructs exhibited equal or higher expression levels of three isoforms of hyaluronidases.

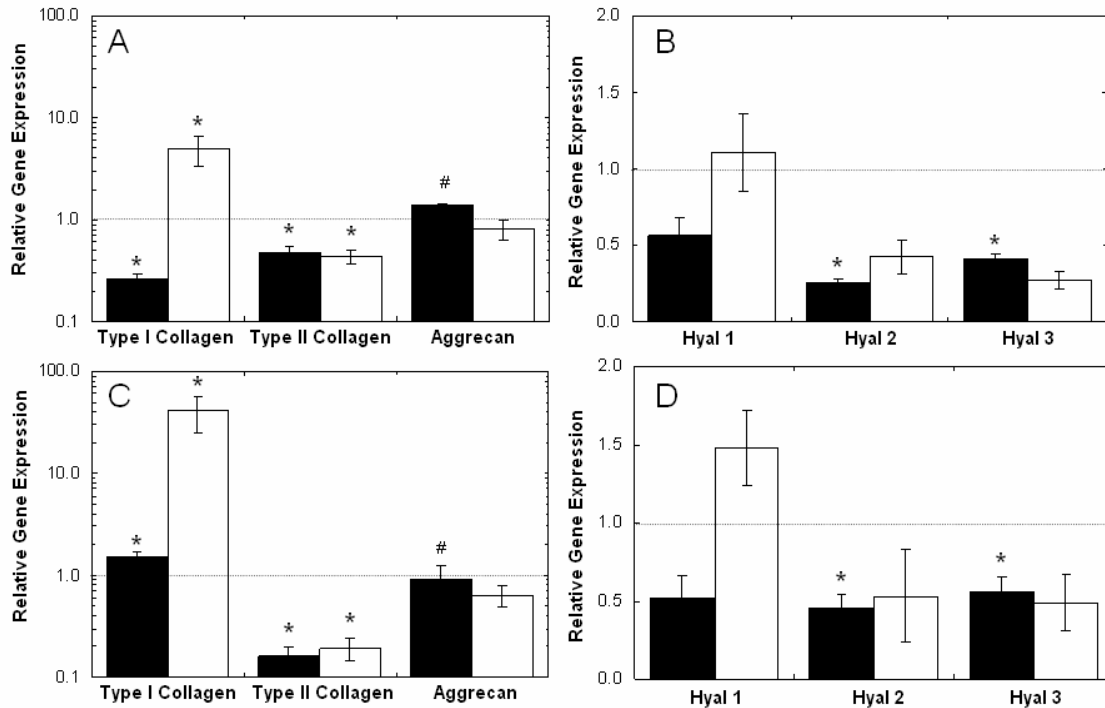


**Figure 7.7** Relative gene expression for AU (A, B) and AR (C, D) constructs after 6 (black) and 14 (white) days of *in vitro* culture. GAPDH was used as the housekeeping gene and expression was normalized to cells encapsulated at day 0. Significant differences ( $p \leq 0.05$ ) between AU and AR groups are denoted by \* using parametric and non-parametric statistics or # using parametric only.

Histological analysis indicated pericellular staining of type II collagen and evenly distributed staining for CS throughout the gel in both AU and AR samples after 14 days of *in vitro* culture (Figure 7.8). Although staining for both type I and II collagen was observed in the perimeter of the hydrogel, no type I collagen staining was observed within the core of the hydrogel. Positive staining for type II collagen and aggrecan was observed for both *in vivo* and *in*

*vitro* culture; however, type II collagen was more distributed within the constructs after 12 weeks of *in vivo* culture.

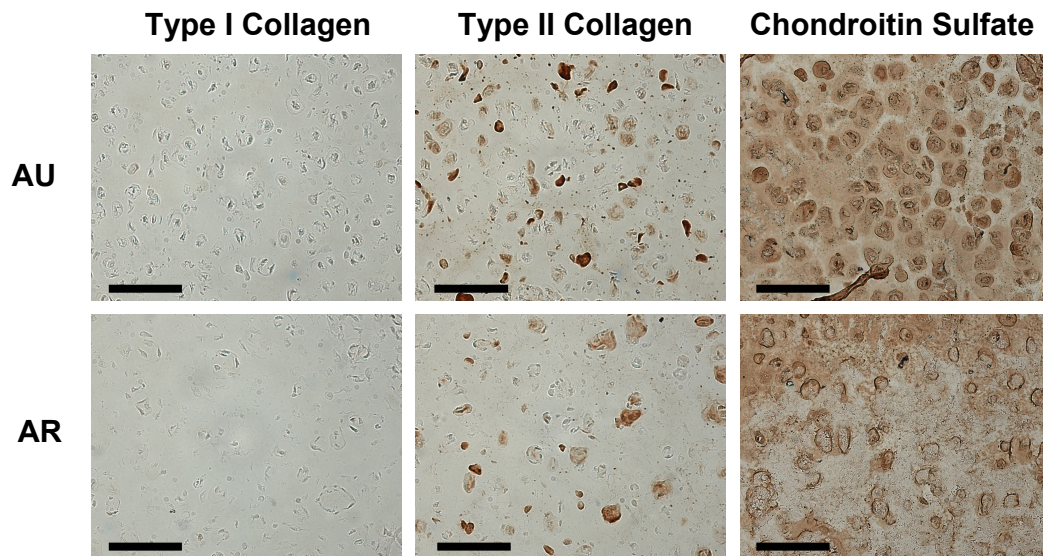


**Figure 7.8** Representative sections of AU and AR constructs stained for type I and II collagen and chondroitin sulfate after 2 weeks of *in vitro* culture. Scale bar = 100 $\mu$ m.

### 7.3.3 Mechanical Stimulation

With *in vivo* and *in vitro* culture, AU chondrocyte-seeded constructs exhibited greater neocartilage formation and better phenotype retention. However, in these cultures, the encapsulated chondrocytes are exposed to a non-load bearing environment that more closely resembles that of native AU cartilage. Thus, it was hypothesized that exposure to external mechanical stimulation would have a positive effect on AR chondrocytes, since they have responded to dynamic compression loading regimes in other scaffolds[28]. Hydrogels are capable of transducing mechanical loads, which may stimulate ECM production via cell signaling resulting from cell deformation or mechanotransduction by cell surface receptors. However, it is important to note that scaffold chemistry and properties, as well as loading regime can affect chondrocyte response[29].

Validation of mechanical loading parameters was performed on acellular HA hydrogels (Figure 7.9A). Hydrogels were subjected to a 5% tare strain with a superimposed dynamic axial strain of 10% at 1 Hz, where load and displacement during cyclic compression were acquired. Load response showed no capping or other deviation from the sinusoidal path under these conditions, indicating that the HA hydrogel remained in contact with the indenter without any evidence of lift-off occurring.

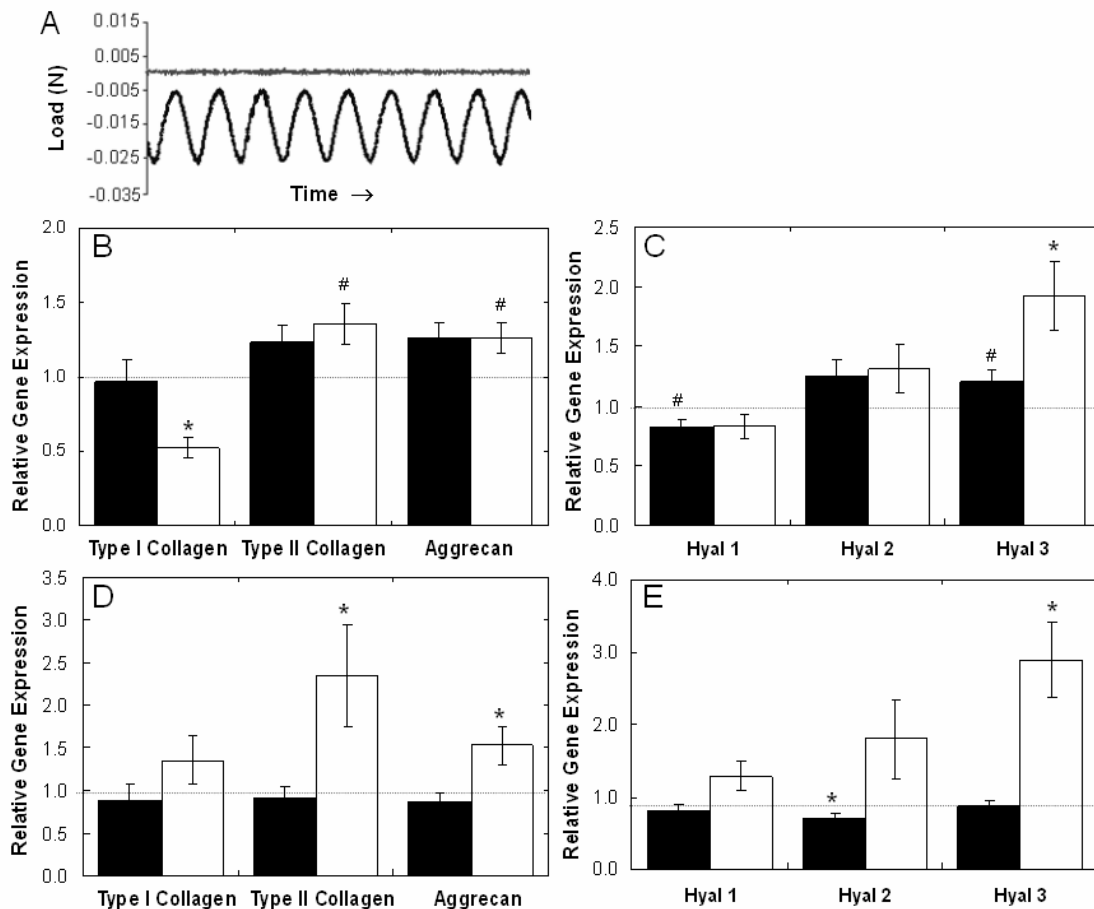


**Figure 7.9** Validation of mechanical loading of HA hydrogels at 5% tare, 10% strain, and frequency of 1 Hz (A). Relative gene expression of dynamically loaded AU (B, C) and AR (D, E) hydrogels for 1 (black) and 5 days (white) normalized to free-swelling controls. Significant differences ( $p \leq 0.05$ ) between free-swelling and mechanically loaded samples are denoted by \* using parametric and non-parametric statistics and # using parametric only.

Using these validated loading parameters, dynamic mechanical stimulation was applied to cell-seeded HA constructs and the effects of stimulation were monitored with relative gene expression (Figure 7.9). Up-regulation of type II collagen and aggrecan was evident for both AU and AR samples after 5 days of consecutive loading, where significant differences for loaded constructs over free-swelling constructs were noted for AU samples with only parametric statistics, while significant differences ( $p \leq 0.05$ ) for AR samples were determined with both parametric and non-parametric tests. For loaded AR constructs, 2.3- and 1.5-fold increases in type II collagen and aggrecan, respectively, over free-swelling controls was observed, while only 1.4- and 1.3-fold increases were observed for loaded AU samples. This data indicates that dynamic compression alone, without the addition of growth factors, is capable of stimulating type II collagen and aggrecan expression. Additionally, type I collagen gene expression was significantly down-regulated for AU constructs after 5 days of loading.

Furthermore, studies have shown catabolic and anabolic effects of compressive loading, hinting at a structural remodeling effect of the newly synthesized matrix through loading [30]. In our study, cyclic compressive loading also increased gene expression of Hyal 3 for both cell sources, with greater increases observed for AR samples (2.9-fold) over AU samples (1.9-fold), which suggests that mechanical loading may stimulate local HA turnover and matrix remodeling.

## 7.4 Conclusions

In conclusion, we have shown that AU and AR chondrocytes photoencapsulated in HA hydrogels exhibit differences in cell behavior in both *in vivo* and *in vitro* culture, and differ in their response to mechanical stimulation. AU chondrocytes excelled in producing neocartilage *in vivo*, in a subcutaneous environment that more closely resembled native AU cartilage, while AR chondrocytes exhibited enhanced gene expression in a mechanically loaded environment, more akin to that of a loaded joint environment.

**References:**

- [1] van Osch GJVM, Mandl EW, Jahr H, Koevoet W, Nolst-Trenite G, Verhaar JA. Considerations on the use of ear chondrocytes as donor chondrocytes for cartilage tissue engineering. *Biorheology* 2004;41(3-4):411-21.
- [2] Hicks DL, Sage AB, Schumacher BL, Sah RL, Watson D. Growth and phenotype of low-density nasal septal chondrocyte monolayers. *Otolaryng Head Neck* 2005;133(3):417-22.
- [3] Kafienah W, Jakob M, Demarteau O, Frazer A, Barker MD, Martin I, et al. Three-dimensional tissue engineering of hyaline cartilage: Comparison of adult nasal and articular chondrocytes. *Tissue Engineering* 2002;8(5):817-26.
- [4] Tay AG, Farhadi J, Suetterlin R, Pierer G, Heberer M, Martin I. Cell yield, proliferation, and postexpansion differentiation capacity of human ear, nasal, and rib chondrocytes. *Tissue Engineering* 2004;10(5-6):762-70.
- [5] Panossian A, Ashiku S, Kirchhoff CH, Randolph MA, Yaremchuk MJ. Effects of cell concentration and growth period on articular and ear chondrocyte transplants for tissue engineering. *Plastic and Reconstructive Surgery* 2001;108(2):392-402.
- [6] Xu JW, Zaporozan V, Peretti GM, Roses RE, Morse KB, Roy AK, et al. Injectable tissue-engineered cartilage with different chondrocyte sources. *Plast Reconstr Surg* 2004;113(5):1361-71.
- [7] Isogai N, Kusuhara H, Ikada Y, Ohtani H, Jacquet R, Hillyer J, et al. Comparison of different chondrocytes for use in tissue engineering of cartilage model structures. *Tissue Engineering* 2006;12(4):691-703.
- [8] Johnson TS, Xu JW, Zaporozan VV, Mesa JM, Weinand C, Randolph MA, et al. Integrative repair of cartilage with articular and nonarticular chondrocytes. *Tissue Eng* 2004;10(9-10):1308-15.
- [9] Mauck RL, Byers BA, Yuan X, Tuan RS. Regulation of cartilaginous ECM gene transcription by chondrocytes and MSCs in 3D culture in response to dynamic loading. *Biomech Model Mechanobiol* 2007;6(1-2):113-25.

- [10] Singer VL, Jones LJ, Yue ST, Haugland RP. Characterization of PicoGreen reagent and development of a fluorescence-based solution assay for double-stranded DNA quantitation. *Anal Biochem* 1997;249(2):228-38.
- [11] Farndale RW, Sayers CA, Barrett AJ. A direct spectrophotometric microassay for sulfated glycosaminoglycans in cartilage cultures. *Connect Tissue Res* 1982;9(4):247-8.
- [12] Stegemann H, Stalder K. Determination of hydroxyproline. *Clin Chim Acta* 1967;18(2):267-73.
- [13] Herbage D, Bouillet J, Bernengo JC. Biochemical and physiochemical characterization of pepsin-solubilized type-II collagen from bovine articular cartilage. *Biochem J* 1977;161(2):303-12.
- [14] Williamson AK, Chen AC, Sah RL. Compressive properties and function-composition relationships of developing bovine articular cartilage. *J Orthop Res* 2001;19(6):1113-21.
- [15] Upton ML, Chen J, Guilak F, Setton LA. Differential effects of static and dynamic compression on meniscal cell gene expression. *J Orthop Res* 2003;21(6):963-9.
- [16] Wenger KH, Woods JA, Holecek A, Eckstein EC, Robertson JT, Hasty KA. Matrix remodeling expression in annulus cells subjected to increased compressive load. *Spine* 2005;30(10):1122-6.
- [17] Gatphayak K, Knorr C, Beck J, Brenig B. Molecular characterization of porcine hyaluronidase genes 1, 2, and 3 clustered on SSC13q21. *Cytogenet Genome Res* 2004;106(1):98-106.
- [18] Chung C, Burdick, J.A. Engineered Cartilage Tissue. *Adv Drug Deliv Rev* in press.
- [19] Naumann A, Dennis JE, Awadallah A, Carrino DA, Mansour JM, Kastenbauer E, et al. Immunochemical and mechanical characterization of cartilage subtypes in rabbit. *J Histochem Cytochem* 2002;50(8):1049-58.
- [20] Armstrong CG, Mow VC. Variations in the intrinsic mechanical properties of human articular cartilage with age, degeneration, and water content. *J Bone Joint Surg Am* 1982;64(1):88-94.



- [21] Kempson GE, Muir H, Swanson SA, Freeman MA. Correlations between stiffness and the chemical constituents of cartilage on the human femoral head. *Biochim Biophys Acta* 1970;215(1):70-7.
- [22] Bryant SJ, Nuttelman CR, Anseth KS. Cytocompatibility of UV and visible light photoinitiating systems on cultured NIH/3T3 fibroblasts in vitro. *J Biomater Sci Polym Ed* 2000;11(5):439-57.
- [23] Williams CG, Malik AN, Kim TK, Manson PN, Elisseeff JH. Variable cytocompatibility of six cell lines with photoinitiators used for polymerizing hydrogels and cell encapsulation. *Biomaterials* 2005;26(11):1211-8.
- [24] Chow G, Knudson CB, Knudson W. Expression and cellular localization of human hyaluronidase-2 in articular chondrocytes and cultured cell lines. *Osteoarthritis Cartilage* 2006;14(9):849-58.
- [25] Frost GI, Csoka AB, Wong T, Stern R. Purification, cloning, and expression of human plasma hyaluronidase. *Biochem Biophys Res Commun* 1997;236(1):10-5.
- [26] Lepperdinger G, Strobl B, Kreil G. HYAL2, a human gene expressed in many cells, encodes a lysosomal hyaluronidase with a novel type of specificity. *J Biol Chem* 1998;273(35):22466-70.
- [27] Flannery CR, Little CB, Hughes CE, Caterson B. Expression and activity of articular cartilage hyaluronidases. *Biochem Biophys Res Commun* 1998;251(3):824-9.
- [28] Mauck RL, Soltz MA, Wang CCB, Wong DD, Chao PHG, Valhmu WB, et al. Functional tissue engineering of articular cartilage through dynamic loading of chondrocyte-seeded agarose gels. *J Biomech Eng-T Asme* 2000;122(3):252-60.
- [29] Bryant SJ, Chowdhury TT, Lee DA, Bader DL, Anseth KS. Crosslinking density influences chondrocyte metabolism in dynamically loaded photocrosslinked poly(ethylene glycol) hydrogels. *Ann Biomed Eng* 2004;32(3):407-17.
- [30] De Croos JNA, Dhaliwal SS, Grynpas MD, Pilliar RM, Kandel RA. Cyclic compressive mechanical stimulation induces sequential catabolic and anabolic gene changes in

chondrocytes resulting in increased extracellular matrix accumulation. *Matrix Biology* 2006;25(6):323-31.

## CHAPTER 8

### *Mesenchymal Stem Cell Chondrogenesis in Hyaluronic Acid Hydrogels*

(Adapted from: **C Chung** and JA Burdick, "Influence of Three-Dimensional Hyaluronic Acid Microenvironments on Mesenchymal Stem Cell Chondrogenesis," *Tissue Eng Part A*, 2009, 15(2): 243-54.)

#### **8.1 Introduction**

Mesenchymal stem cells (MSCs) are multipotent progenitor cells that have the ability to self-replicate and differentiate down multiple cell lineages when given the appropriate environmental cues[1]. Although they were first identified in bone marrow by Friedenstein and colleagues[2] in the 1970s, MSCs have since been isolated from various adult tissues and differentiated into several cell types, including osteoblasts, chondrocytes, and adipocytes[1,3-5]. With their plasticity and self-renewal capacity, these cells have generated significant interest for applications in cell replacement therapies and tissue regeneration.

Particularly, MSCs have garnered interest as an alternative cell source for cartilage tissue engineering, since they can be isolated from adults via a bone marrow biopsy. To induce chondrogenic differentiation, MSCs are typically grown in pellet culture in the presence of transforming growth factor- $\beta$ s (TGF- $\beta$ s) [6-10], and differentiation is monitored by the production of cartilaginous matrix proteins such as sulfated glycosaminoglycans (GAGs) and type II collagen. In recent years, both natural and synthetic biomaterials have been used to create niches or microenvironments to control stem cell behavior and differentiation [11,12]. These biomaterials serve as 3D scaffolds capable of enhancing and templating tissue formation through cell morphology and organization, intercellular interactions, mechanical forces, and/or the delivery of bioactive molecules [11,13].

For this study, the ability of MSCs to undergo chondrogenesis in photocrosslinked HA hydrogels was investigated. Previous chapters documented the optimization of a methacrylated HA (MeHA) hydrogel system for the encapsulation of chondrocytes. Cytocompatibility, phenotype retention, and neocartilage formation within these hydrogels was characterized using both auricular and articular chondrocytes. However, inherent limitations to the use of chondrocytes (e.g., low cell yields and a tendency to dedifferentiate when expanded *in vitro*, as emphasized in chapter 6) have motivated the use of MSCs as an alternative cell source. MSCs are easily expanded *in vitro* without loss of differentiation potential and can express CD44[14], one of the primary receptors for HA. Thus, we hypothesized that photocrosslinked MeHA hydrogels could provide a favorable niche for MSC chondrogenesis.

## **8.2 Materials & Methodology**

### ***8.2.1 CD44 Staining and Flow Cytometry***

To determine the presence of CD44 receptors, human MSCs (Lonza Walkersville, Inc.) were cultured in 2D on glass coverslips and fixed in accustain (Sigma) for immunofluorescent staining. Briefly, the cells were blocked with 5% fetal bovine serum (FBS), stained with primary antibody anti-CD44 clone A3D8 (4 $\mu$ g/ml, Sigma) for 2 hours, incubated with secondary antibody anti-mouse IgG (whole molecule) F(ab')<sub>2</sub> fragment-FITC (1:50 dilution) for 15 minutes, and counterstained with DAPI (2 $\mu$ g/ml) for nuclei visualization. In addition, MSCs were labeled with phycoerythrin (PE)-conjugated CD44 (0.25  $\mu$ g/ml, eBioscience) monoclonal antibody for 1 hr on ice and analyzed by flow cytometry (Guava EasyCyte 3.10).

### ***8.2.2 Macromer Syntheses***

Methacrylated HA (MeHA) was synthesized as previously described in chapter 4. Briefly, methacrylic anhydride (Sigma) was added to a solution of 1 wt% HA (Lifecore, MW = 64 kDa) in

deionized water, adjusted to a pH of 8 with 5 N NaOH, and reacted on ice for 24 hours. The macromer solution was purified via dialysis (MW cutoff 6-8k) against deionized water for a minimum of 48 hours with repeated changes of water. The final product was obtained by lyophilization and stored at -20°C in powder form prior to use. Poly(ethylene glycol)-diacrylate (PEGDA) was synthesized as previously reported[15]. Briefly, triethylamine (1.5 molar excess) was added to PEG-4600 (Sigma) dissolved in methylene chloride. Acryloyl chloride (1.5 molar excess) was added dropwise under nitrogen and reacted on ice for 6 hrs, followed by reaction at room temperature for 30 hours. The product was precipitated in ethyl ether, filtered, dried in a vacuum oven, redissolved in deionized water, dialyzed for 3 days, lyophilized, and stored at -20°C in powder form prior to use. The macromer structure was characterized by  $^1\text{H}$  NMR (Bruker Advance 360 MHz, Bruker). Macromers were sterilized using a germicidal lamp in a laminar flow hood for 30 minutes and dissolved in a sterile solution of phosphate buffered saline (PBS) containing 0.05 wt% I2959 for polymerization. Hydrogels were polymerized by injecting the macromer solution into a mold or between glass slides and exposing to ultraviolet light (Eiko,  $\sim 1.9 \text{ mW/cm}^2$ ) for 10 minutes.

### *8.2.3 Mechanical Characterization*

Acellular hydrogels (n=5) with  $\sim 7\text{mm}$  diameter and  $\sim 1\text{mm}$  thickness were tested in unconfined compression with a Dynamic Mechanical Analyzer Q800 (DMAQ800, TA Instruments) in a PBS bath. Hydrogels were compressed at a rate of 10%/min until failure or until 70% of the initial thickness. The modulus was determined as the slope of the stress versus strain curve at low strains ( $<20\%$ ). The elastic modulus of PEG hydrogels was matched to 2wt% MeHA hydrogels by varying the macromer concentration (5-10 wt%).

#### 8.2.4 MSC Photoencapsulation and Culture

Human MSCs were expanded to passage 4 in growth media consisting of  $\alpha$ -MEM with 16.7% FBS and 1% penicillin/streptomycin. MSCs ( $20 \times 10^6$  cells/ml) were photoencapsulated in hydrogels by suspension in 2 wt% MeHA or 5.5 wt% PEG solutions with or without 200ng/ml TGF- $\beta$ 3. The cell/macromer solutions were pipetted into sterile molds (50  $\mu$ l volume) and polymerized with ultraviolet light (Eiko,  $\sim 1.9$  mW/cm<sup>2</sup>) for 10 minutes.

To evaluate chondrogenesis, MSC-laden MeHA hydrogels were cultured *in vitro* in either growth media or DMEM supplemented with 1% penicillin/streptomycin, 1% ITS+, 1mM sodium pyruvate, 40mg/ml L-proline, 100nM dexamethasone, 50 $\mu$ g/ml ascorbic acid 2-phosphate, and 10ng/mL TGF- $\beta$ 3 (chondrogenic media). For *in vivo* culture, MSCs were encapsulated in MeHA hydrogels with (HA+T3) and without (HA-MSCs) TGF- $\beta$ 3 and implanted in nude mice, or cultured *in vitro* in chondrogenic media for 2 weeks prior to implantation (HA-C). Nude mice were anesthetized with isoflurane, a 2 cm midline incision was made on the dorsum of each mouse, and 5 subcutaneous pockets were made using blunt dissection. One construct was placed in each pocket and the wound was closed with sterile stainless steel skin clips. Constructs were cultured *in vivo* for 2 weeks. NIH guidelines for the care and use of laboratory animals (NIH Publication #85-23 Rev. 1985) were observed. For scaffold comparison, MSCs were encapsulated in PEG hydrogels and cultured *in vitro* and *in vivo* in the same manner as the MeHA hydrogels.

#### 8.2.5 Viability

The viability of MSCs in the MeHA and PEG hydrogels was assessed using a live/dead cytotoxicity kit (Molecular Probes) and an MTT assay (ATCC). Live/dead images were taken 1 and 24 hrs after encapsulation. Mitochondrial activity (n=3) was assessed after 7 and 14 days of *in vitro* culture. Briefly, 100 $\mu$ l of MTT reagent was added to 1ml of media and incubated for 4 hours. Samples were then removed from the media, homogenized in the detergent solution with

a tissue grinder, incubated for 4 hrs, and read at an absorbance of 570nm in a Synergy HT™ (Bio-Tek Instruments) spectrophotometer.

### 8.2.6 Gene Expression Analysis

Samples (n=4) were homogenized in Trizol Reagent (Invitrogen) with a tissue grinder and RNA was extracted according to the manufacturer's instructions. RNA concentration was determined using an ND-1000 spectrophotometer (Nanodrop Technologies). One microgram of RNA of each sample was reverse transcribed into cDNA using reverse transcriptase (Superscript II, Invitrogen) and oligoDT (Invitrogen). Polymerase chain reaction (PCR) was performed on an Applied Biosystems 7300 Real-Time PCR system using a 25µl reaction volume for Taqman (5'-nuclease) reactions. Primers and probes specific for glyceraldehydes 3-phosphate dehydrogenase (GAPDH), type I and type II collagen, aggrecan, sox 9 and hyaluronidases (Hyal) 1, 2 and 3 are listed in Table 8.1. GAPDH was used as the housekeeping gene. Relative gene expression was calculated using the  $\Delta\Delta C_T$  method, where fold difference was calculated using the expression  $2^{-\Delta\Delta C_T}$ .

**Table 8.1** Human quantitative PCR primers and probes.

Gene	Forward Primer	Reverse Primer	Probe
GAPDH	AGGGCTGCTTTTAACTCTGGTAAA	GAATTTGCCATGGGTGGAAT	CCTCAACTACATGGTTTAC
Col I	AGGACAAGAGGCATGTCTGGTT	GGACATCAGGCGCAGGAA	TTCCAGTTCGAGTATGGC
Col II	GGCAATAGCAGGTTACGTACA	CGATAACAGTCTTGCCCCACTT	CTGCACGAAACATAC
Acan	TCGAGGACAGCGAGGCC	TCGAGGGTGTAGCGTAGAGA	ATGGAACACGATGCCTTTCACACGA
Sox 9	AAGCTCTGGAGACTTCTGAACGA	GCCCGTTCTTCACCGACTT	
HYAL1	AAAATACAAGAACCAAGGAATCATGTC	CGGAGCACAGGGCTTGACT	
HYAL2	GGCGCAGCTGGTGTATC	CCGTGTCAGGTAATCTTTGAGGTA	
HYAL3	GCCTCACACACCGGAGATCT	GCTGCACTCACACCAATGGA	

### 8.2.7 Microarray Assay

Isolated total RNA (n=3 per group) from day 14 *in vitro* samples were processed by the Penn Microarray Facility. RNA was amplified and hybridized to GeneChip® Human Exon 1.0 ST array (Affymetrix). Microarray expression data was analyzed using Partek Genomics Software Package Suite 6.4 to determine fold change and Significant Analysis of Microarray (SAM) 3.02 to determine significant differences between MSC-laden MeHA and PEG hydrogels. Ingenuity pathway analysis was also used to explore potential differentially regulated pathways.

### 8.2.8 Histological Analysis

For histological analysis, constructs were fixed in 10% formalin for 24 hours, embedded in paraffin, and processed using standard histological procedures. The histological sections (7  $\mu$ m thick) were stained for aggrecan and collagen distributions using the Vectastain ABC kit (Vector Labs) and the DAB Substrate kit for peroxidase (Vector Labs). Sections were predigested in 0.5 mg/ml hyaluronidase for 30 min at 37°C and incubated in 0.5 N acetic acid for 4 hours at 4°C to swell the samples prior to overnight incubation with primary antibodies at dilutions of 1:100, 1:200, and 1:3 for chondroitin sulfate (mouse monoclonal anti-chondroitin sulfate, Sigma), and type I (mouse monoclonal anti-collagen type 1, Sigma) and type II collagen antibodies (mouse monoclonal anti-collagen type II, Developmental Studies Hybridoma Bank), respectively. Non-immune controls underwent the same procedure without primary antibody incubation.

### 8.2.9 Statistical Analysis

All values are reported as the mean  $\pm$  SEM. Student's t-test and Wilcoxon Sum-Rank test were used to determine significant differences among groups, with  $p < 0.05$ .



### 8.3 Results & Discussion

Recently, MSCs have been explored as an alternative cell source for cartilage regeneration and repair due to their chondrogenic potential and their ease of isolation from sources such as bone marrow without damage to native cartilage tissue. To this end, 3D scaffolds have been developed to create microenvironments for stem cells, where numerous factors including material chemistry, functionalization with biological cues, interactions with surrounding cells, and mechanical properties[11] play a role to direct stem cell differentiation. In this study, we investigated the use of a photocrosslinked HA hydrogel to provide a favorable niche for MSC chondrogenesis both *in vitro* and *in vivo* by providing cell interactive cues with a naturally found polysaccharide. Increases in the gene expression and production of cartilaginous matrix proteins were used as markers for chondrogenesis.

#### 8.3.1 MSC interactions with HA

One of the advantages of using an HA-based scaffold is the potential for cell/scaffold interactions via cell surface receptors, which could direct cell behaviors and assist in stem cell differentiation. CD44 is a cell surface receptor that binds to HA, providing a means to retain and anchor proteoglycan aggregates to the plasma membrane of a cell. In addition, intimate association with the underlying cytoskeleton permits CD44 to initiate intracellular signaling[16,17], allowing it to sense changes in the ECM environment and signal a cellular response. This receptor is also of particular interest because it is essential for the maintenance of cartilage homeostasis[17] and plays a role in the catabolism of HA via phagocytosis[18]. To demonstrate the potential of MSCs to interact with our HA scaffold, CD44 expression was verified with immunofluorescent staining and flow cytometry (Figure 8.1 A and B). This HA receptor was present on 99.6% of the cell population and stained uniformly on MSCs cultured in 2D. In addition, nearly all of the MSCs remained viable (>98%) as indicated by live/dead staining 6 hours after encapsulation (Figure 8.1C), indicating that these MeHA hydrogels could be

successfully used as MSC delivery vehicles. The even distribution of cells throughout the hydrogel demonstrates the advantage of using photopolymerization as a facile means to encapsulate cells in a 3D hydrogel matrix.

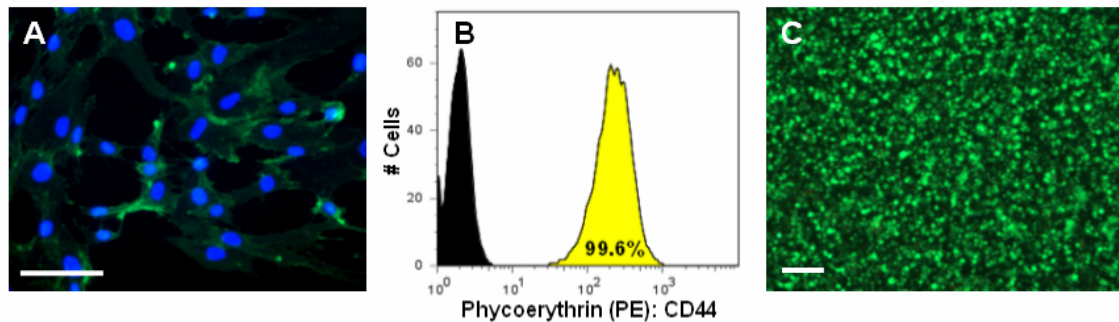


**Figure 8.1** (A) Immunofluorescence staining of CD44 (green) with nuclear counterstain (blue) of MSCs cultured in 2D on glass coverslips (scale bar = 100µm) (A), (B) flow cytometry staining for CD44 (yellow) compared to an unstained (black) population of MSCs prior to encapsulation, and (C) live (green)/ dead (red) image of MSCs encapsulated in MeHA hydrogel 6 hours after photopolymerization (scale bar = 200µm).

### 8.3.2 MSC Chondrogenesis

MSC chondrogenesis in MeHA hydrogels was induced *in vitro* by culture in chondrogenic media containing TGF-β3, which has been shown to induce chondrogenesis in a variety of other scaffolds[19,20]. Comparisons between MSC-laden HA hydrogels cultured in growth and chondrogenic media (+TGF-β3) showed significant differences in gene expression between culture media at 3, 7, and 14 days of culture (Figure 8.2).

Specifically, up-regulation of sox 9 (a transcription factor required for successive steps in chondrogenesis), type II collagen, and aggrecan was observed for constructs cultured in chondrogenic media over cultures in growth media at all time points. In addition, with the exception for aggrecan at day 3, an up-regulation of the chondrogenic genes (type II collagen,

aggrecan, sox 9) and down-regulation of the fibroblastic marker (type I collagen) was observed compared to initially encapsulated cells for all hydrogels cultured in chondrogenic media. Interestingly, type II collagen was also initially up-regulated in hydrogels cultured in growth media with decreases in expression after day 3. This suggests potential chondrogenic effects of the hydrogel alone on MSC differentiation.

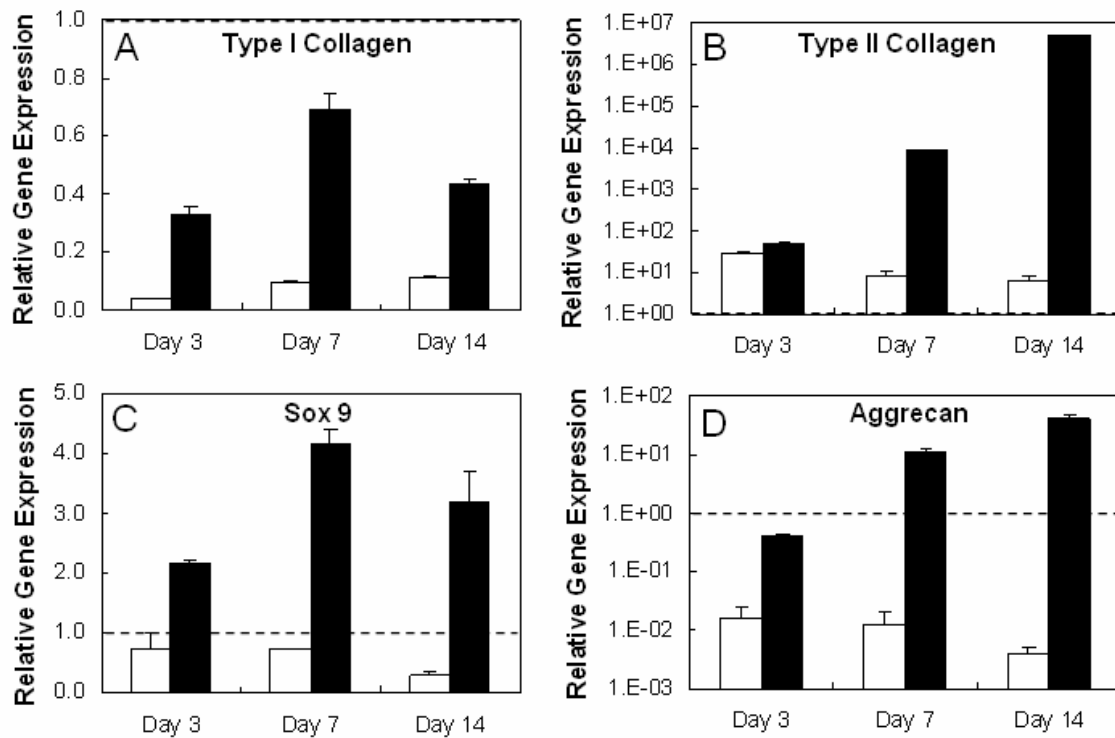


**Figure 8.2** Relative gene expression of type I and type II collagen, sox 9 and aggrecan for MSCs encapsulated in hydrogels cultured *in vitro* in growth (white) and chondrogenic (black) media. GAPDH is used as the housekeeping gene and expression is normalized to cells at the time of encapsulation (indicated by the dashed line). Gene expression of MSCs cultured in chondrogenic media is significantly different than MSCs cultured in growth media ( $p < 0.05$ ) for all genes at all time points.

In addition, the expression of hyaluronidases observed in MSCs indicates the potential for HA hydrogel remodeling. Hyaluronidases are enzymes that cleave the  $\beta$ -1,4-glycosidic bonds between glucuronic acid and N-acetyl-glucosamine[21], which can affect cell differentiation and matrix catabolism. Each enzyme isoform plays a specific role in cleaving HA into discrete fragment sizes that regulate different cellular processes[22-24]. Significant differences in hyaluronidase expression were observed between culture media for hyal 2 and 3 (Figure 8.3) at several time points.

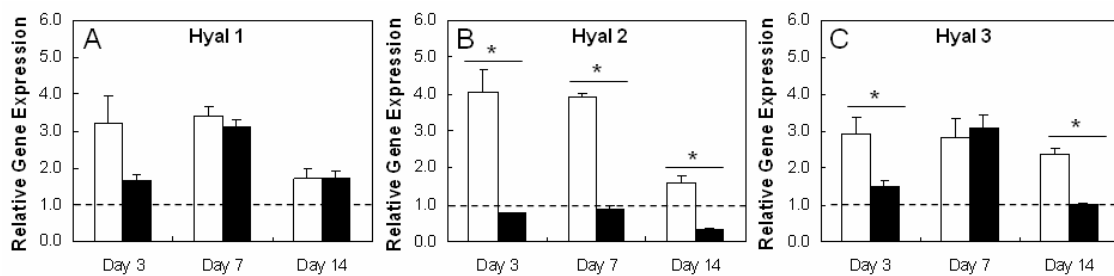


**Figure 8.3** Relative gene expression of hyaluronidases (Hyal) for MSCs encapsulated in hydrogels cultured in growth (white) and chondrogenic (black) media. GAPDH is used as the housekeeping gene and expression is normalized to cells at the time of encapsulation (indicated by the dashed line). Significant differences ( $p < 0.05$ ) between hydrogels cultured in growth and chondrogenic media are denoted by \*.

Histologically, increased deposition of type II collagen and chondroitin sulfate (CS) was observed for MSC-laden HA hydrogels cultured in chondrogenic media (Figure 8.4), where intense pericellular staining was observed after only 14 days of culture. In addition, in agreement with gene expression data, light staining for type II collagen and CS in hydrogels cultured in growth media, suggesting that the scaffold alone could promote chondrogenesis. Light staining for type I collagen was also observed in hydrogels cultured in chondrogenic media. MSCs are known to produce type I collagen, and it remains unclear whether complete inhibition of type I collagen is possible during chondrogenic differentiation.

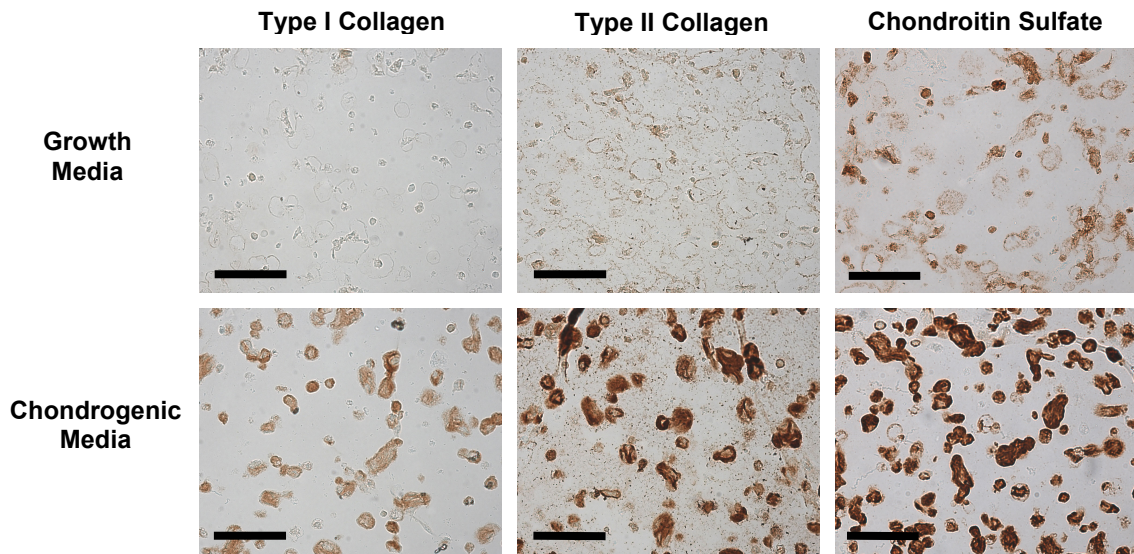


**Figure 8.4** Representative stains for type I and II collagen and chondroitin sulfate for MSC-laden hydrogels cultured in growth and chondrogenic media for 14 days *in vitro*. Scale bar = 100 $\mu$ m.

*In vivo*, MSC chondrogenesis was explored with and without TGF- $\beta$ 3, which was delivered without a carrier via direct encapsulation within the hydrogel. MSCs in all groups (HA-MSC, HA+T3, HA-C) exhibited increases in gene expression for all genes of interest (Figure 8.5) compared to cells at the time of encapsulation after 14 days of implantation. Without growth factors present, there were ~3000-, ~18-, and ~13-fold increases in type II collagen, aggrecan, and sox 9 gene expression, respectively. With the addition of TGF- $\beta$ 3 (HA+T3 group) and with 2 weeks of pre-culture in chondrogenic media (HA-C group), type II collagen increased ~17.5- and ~2370-fold and aggrecan increased ~3.7 and ~4.6-fold, respectively, compared to the HA-MSC group. These results indicate that the MeHA hydrogel as a cell delivery vehicle alone supports MSC chondrogenesis, which is then further enhanced with the addition of TGF- $\beta$ 3. It is important to note that the single dose of encapsulated TGF- $\beta$ 3 was capable of altering gene expression during short-term *in vivo* culture. In addition, data showed that the pre-programming of MSCs toward chondrogenesis with 2 weeks of pre-culture *in vitro* was also sufficient to maintain

chondrogenesis in short-term *in vivo* culture. Furthermore, increases in hyaluronidase expression *in vivo* may reflect potential cell-dictated remodeling of the MeHA hydrogel.

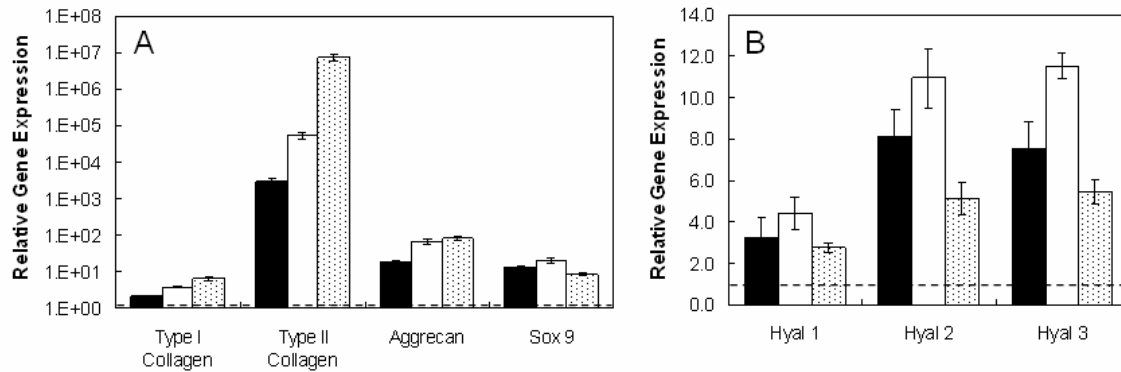


**Figure 8.5** Relative gene expression for type I and type II collagen, aggrecan, sox 9 (A) and hyaluronidases (B) for MSCs encapsulated in hydrogels cultured 2 weeks *in vivo*. GAPDH is used as the housekeeping gene and expression is normalized to cells at the time of encapsulation (indicated by the dashed line). The groups included the hydrogel alone (HA-MSC, black), hydrogels with TGF- $\beta$ 3 co-encapsulated with cells (HA+T3, white), and hydrogels pre-cultured in chondrogenic media for 2 weeks (HA-C, shaded). All groups are significantly different ( $p < 0.05$ ) for type I and II collagen, while HA-MSC is significantly different from both HA+T3 and HA-C for aggrecan. In addition, HA+T3 is significantly different from HA-C for Hyal 2 and 3 and sox 9.

Histological analysis of the *in vivo* samples showed pericellular staining for HA-MSC and HA+T3 groups for type II collagen and CS, with more elaborate staining for the HA-C group (Figure 8.6). Again, some staining was also noted for type I collagen in these samples, similar to *in vitro* results. Though the bolus delivery of TGF- $\beta$ 3 initiated the expression and deposition of type II collagen and aggrecan, optimization of TGF- $\beta$ 3 quantity and delivery method, as well as hydrogel degradation properties could improve ECM synthesis, deposition, and distribution within the constructs *in vivo*, and will be addressed in later chapters.

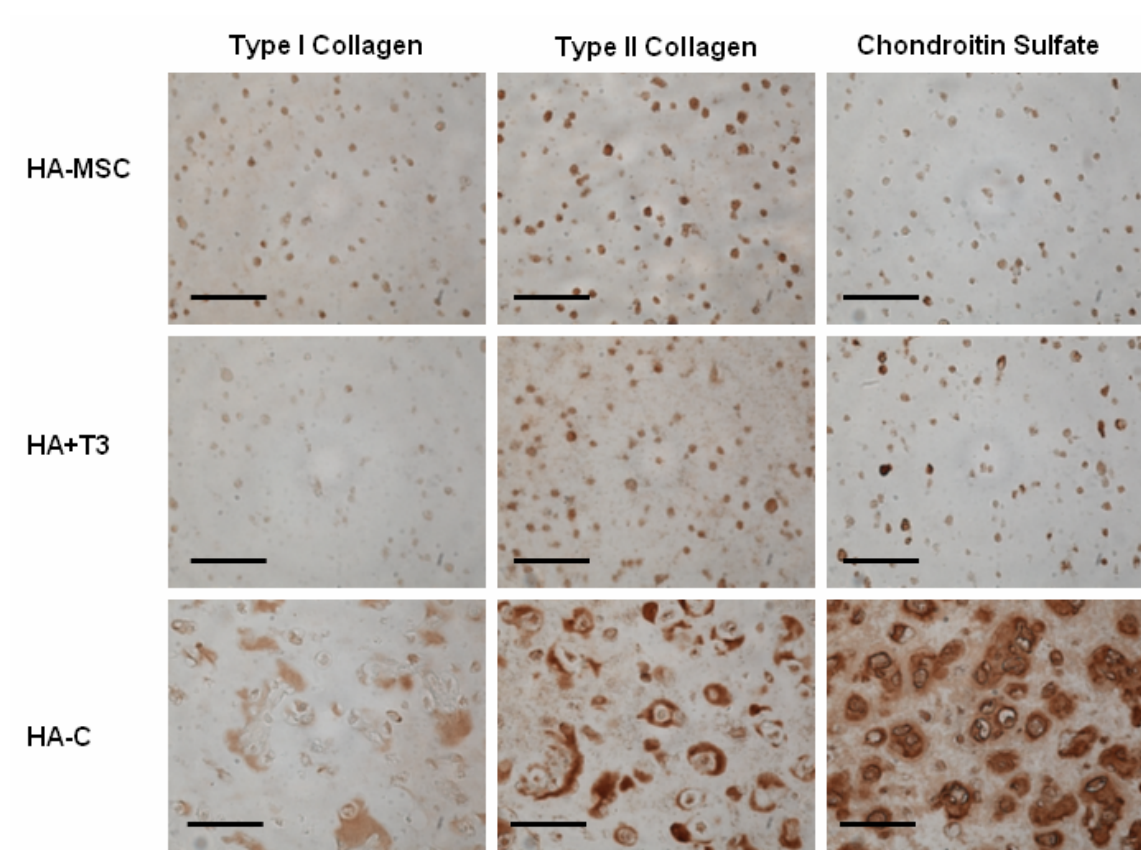


**Figure 8.6** Representative stains for type I and II collagen and chondroitin sulfate for HA-MSC, HA+T3, and HA-C groups after 3 week culture *in vivo*. Scale bar = 100 $\mu$ m.

### 8.3.3 Comparison between HA and PEG hydrogels

To better evaluate the effect of scaffold material on MSC chondrogenesis, MeHA hydrogels were compared to a relatively inert PEG hydrogel system. PEG hydrogels were used as comparative controls due to their resistance to protein adsorption and relatively inert interaction with cells. First, the elastic modulus of PEG hydrogels was matched to 2 wt% MeHA hydrogels by altering macromer concentration. A 5.5 wt% PEG formulation with a modulus of  $13.3 \pm 1.0$  kPa was found to be comparable (i.e., no statistical differences between moduli) to the 2 wt% MeHA hydrogels ( $13.0 \pm 1.4$  kPa) and was used for all comparison studies to minimize mechanical influences on cellular differentiation (Figure 8.7A). In addition, live/dead staining and an MTT assay (Figure 8.7B, C) demonstrated that viable MSCs were successfully encapsulated in both hydrogel systems and exhibited no statistical difference in cell viability.

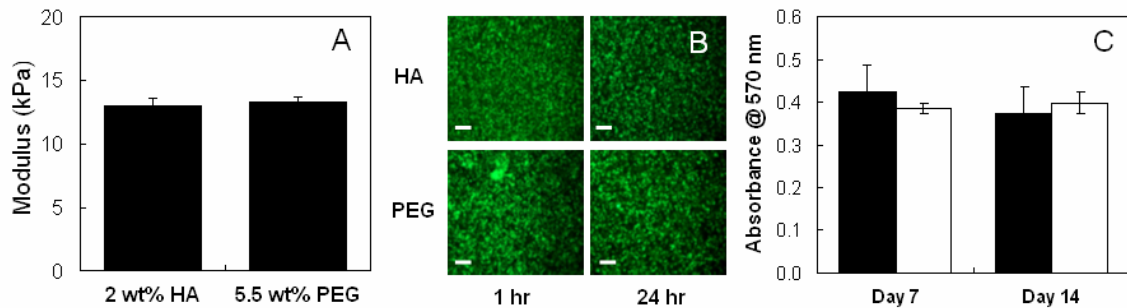


**Figure 8.7** MeHA compared to PEG. Modulus of acellular HA and PEG hydrogels (A), live (green)/dead (dead) images of MSC-laden hydrogels at 1 and 24 hrs after polymerization; scale bar = 200 mm (B), relative mitochondrial activity for HA (black) and PEG (white) hydrogels after 7 and 14 days of *in vitro* culture (C). There were no statistical differences in hydrogel moduli and viability between HA and PEG groups.

With both *in vitro* and *in vivo* cultures, the gene expression of encapsulated MSCs differed depending on the hydrogel chemistry. With *in vitro* culture, type II collagen expression by MSCs in MeHA hydrogels was up-regulated ~7.3- and ~6.6-fold over PEG counterparts after 7 and 14 days, respectively (Figure 8.8). Aggrecan was also up-regulated in MeHA hydrogels (~1.5- and ~1.2-fold after 7 and 14 days, respectively), but to a lesser extent. These differences



were also observed in immunohistochemical staining, where more intense type II collagen and CS staining is observed in MeHA over PEG hydrogels (Figure 8.9).

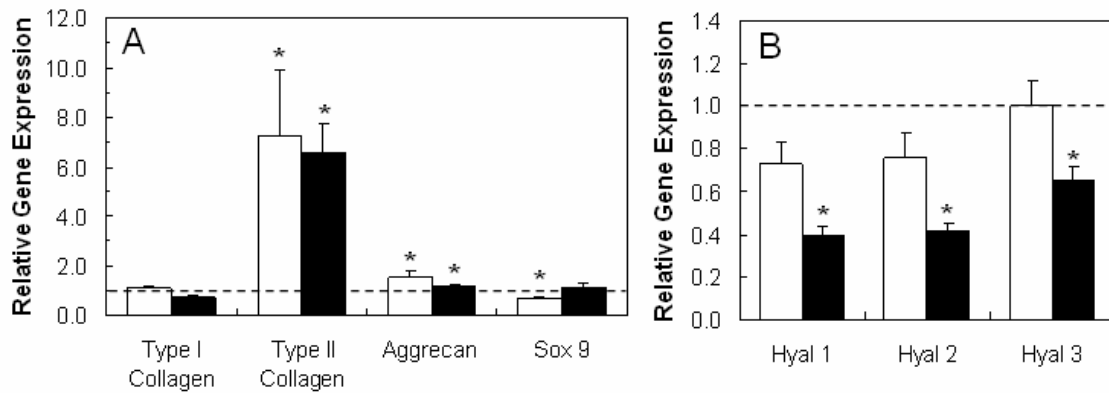


**Figure 8.8** Relative gene expression of type I and type II collagen, sox 9, and aggrecan (A) and hyaluronidases (B) for MSCs encapsulated in HA hydrogels cultured *in vitro* in chondrogenic media for 7 (white) and 14 days (black). GAPDH is used as the housekeeping gene and expression is normalized to PEG counterparts (indicated by the dashed line). Significant differences ( $p < 0.05$ ) between HA and PEG hydrogels are denoted by \*.

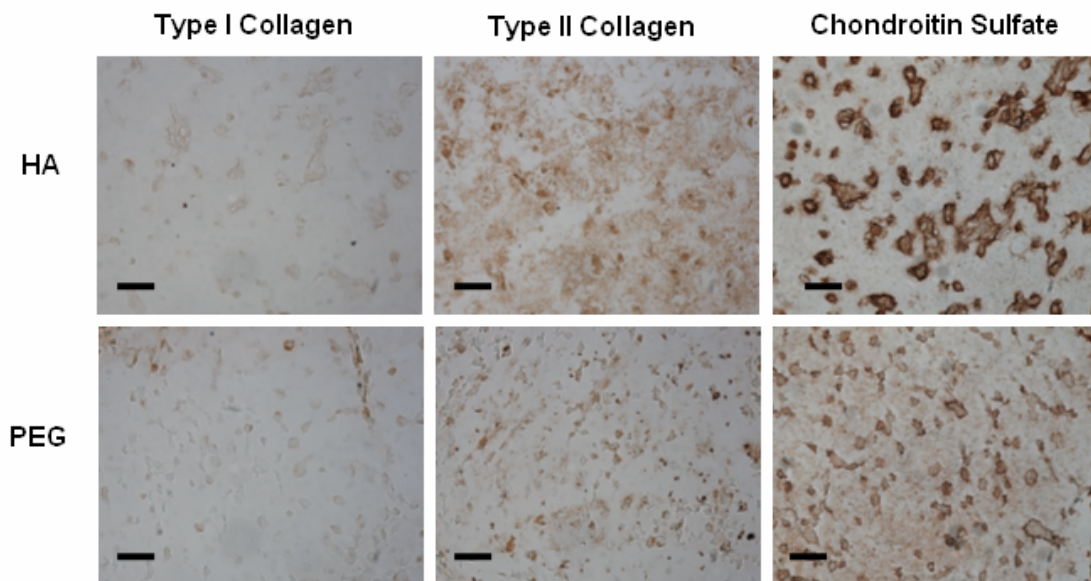


**Figure 8.9** Representative stains for type I and II collagen and chondroitin sulfate for MSC-laden HA and PEG hydrogels cultured in chondrogenic media for 14 days *in vitro*. Scale bar = 200 $\mu$ m.

For *in vivo* culture, differences between MeHA and PEG hydrogels are most noticeable for MSCs plus scaffold alone, where type II collagen and aggrecan were up-regulated by ~43- and ~6-fold, respectively, for MSCs in MeHA hydrogels compared to PEG hydrogels (Figure 8.10), indicating that hydrogel chemistry alone can greatly influence the commitment of MSCs to undergo chondrogenesis. These differences between MeHA and PEG decreased to ~11.5- and ~4.1-fold with the addition of TGF- $\beta$ 3, suggesting more prominent induction by chondrogenic growth factor addition, and become negligible (~0.7- and ~1.5-fold) when chondro-induced MSCs are encapsulated in both hydrogel systems. With pericellular deposition after 2 weeks of *in vitro* culture, MSCs may interact with newly deposited matrix rather than the surrounding scaffold material; thus, differences as a result of polymer choice are minimized when compared after *in vivo* culture. Hyaluronidase expression also differed, where the expression of enzymes was down-regulated *in vitro* but up-regulated *in vivo* for HA+T3 and HA-C groups when compared to their PEG counterparts.

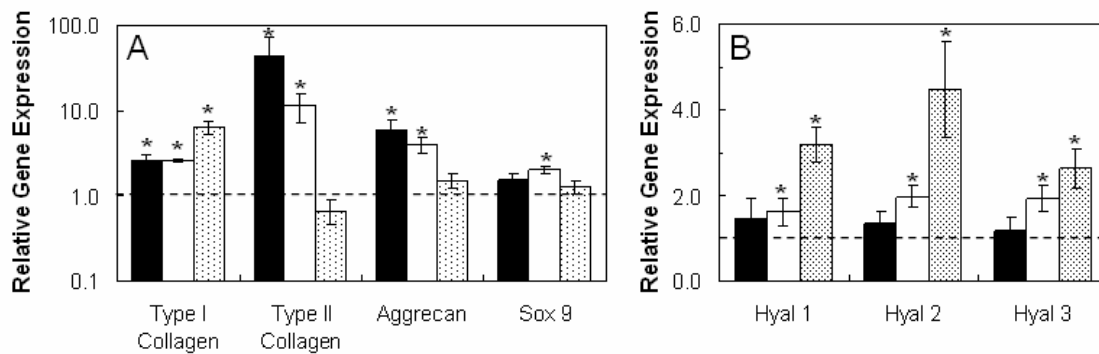


**Figure 8.10** Relative gene expression for type I and II collagen, aggrecan, sox 9 (A) and hyaluronidases (B) of MSCs in HA-MSC (black), HA+T3 (white), and HA-C (shaded) groups cultured *in vivo* for 2 weeks. GAPDH is used as the housekeeping gene and expression is normalized to PEG counterparts (indicated by the dashed line). Significant differences ( $p < 0.05$ ) between HA and PEG hydrogels are denoted by \*.

To further investigate the effects of hydrogel chemistry on MSC chondrogenesis, genome expression profiling of MSC-laden HA and PEG hydrogels cultured *in vitro* was assayed by microarray. The principle component analysis (PCA) plot demonstrates distinct differences between HA and PEG groups (Figure 8.11).

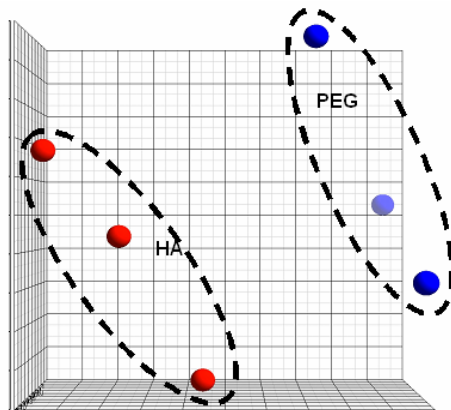


**Figure 8.11** PCA plot of MSC-laden HA (red) and PEG (blue) hydrogels after 14 days of *in vitro* culture.

Significant differences between the two groups, as illustrated by the heat map (Figure 8.12), can shed light on possible mechanisms of HA enhanced chondrogenesis. Chondrogenesis is controlled by a complex interplay of regulatory factors. Sox9, a Sry-related HMG box transcription factor expressed throughout chondrogenesis, is required for the activation of early cartilage markers[25]. It also acts as an activator of Sox5 and -6, which are co-expressed with Sox9 in cartilage[26]. These Sox genes regulate the activation of Col2a1, Col9a1, and Col11a1. While Sox5 is active during embryogenesis, Sox6 is active postnatally [27]. From the microarray analysis, it is observed that both Sox9 and Sox6 are significantly up-regulated in HA hydrogels over PEG counterparts, which may have resulted in the subsequent up-regulation of type 2, 9, and 11 collagens. Type 2 collagen makes up 85-90% of collagen in hyaline cartilage and is responsible for providing cartilage with its tensile strength. Type 11 collagen is a regulatory collagen whose role is to initiate assembly of thin fibrils and limit the radial growth of collagen fibrils, providing cartilage with structural integrity [28]. Type 9 collagen is a fibril associated collagen with interrupted triple helices (FACIT) that associates with both type 2 and 11 collagens.

In addition, there are a range of other genes that are up-regulated in HA hydrogels (over PEG) and are related to ECM synthesis and stabilization. These include chondroitin sulfate N-acetylgalactosaminyltransferase 1 (CSGALNACT1) which is responsible for the initiation and elongation of chondroitin sulfate synthesis [29], and leucine proline-enriched proteoglycan 1 (LEPRE1) that encodes for a collagen prolyl hydroxylase enzyme that is required for the proper synthesis and assembly of collagen. Matrix stabilizers upregulated in HA gels include hyaluronan and proteoglycan link protein 1 (HAPLN1) and matrilin 3 (MATN3). HAPLN1, also regulated by Sox9, stabilizes HA-aggrecan interaction and can form ternary complexes with versican and HA [30,31]. Matrilins are non-collagenous ECM adapter proteins that form filamentous networks connecting type 2 and type 9 collagen, aggrecan, small proteoglycans, and cartilage oligomeric matrix protein (COMP). MATN1 and 3 are cartilage specific and microarray studies have shown that these are among the most up-regulated ECM proteins during MSC chondrogenesis [9]. Pei *et al.* showed that MATN1 and 3 work in conjunction with TGF- $\beta$ 1 to maintain and enhance chondrogenesis with increased GAG accumulation [32]. The most differentially up-regulated gene (48-fold) was C-type lectin domain family 3, member A (CLEC3A). This sugar-binding protein, found only in cartilage, likely plays a role in matrix organization or the formation of fibrillar structures, and is most abundant in the epiphysis region, where considerable remodeling of the ECM is performed [33]. CLEC3A is cleaved by MMP-7, which was also differentially up-regulated in the HA group. While some matrix metalloproteinases (MMPs) are up-regulated, others like MMP-13, which preferentially cleaves type 2 collagen, are down-regulated.

Genes associated with signaling pathways that regulate chondrocyte maturation were also differentially regulated. These include signaling molecules like Indian hedgehog (IHH), parathyroid hormone-like hormone (PTHrP), Wnts, and Smads which play important roles in skeletal development and function. IHH promotes chondrocyte proliferation and maturation while PTHrP is its antagonist inhibiting chondrocyte maturation [34]. Wnt5a has been shown to promote early chondrogenesis and inhibit terminal hypertrophic differentiation, while Wnt-1 and -7a increase cell adhesion and arrest of chondrogenic differentiation [35]. In this microarray

experiment, IHH was up-regulated in HA hydrogels, indicating the potential for eventual hypertrophic differentiation. However, type 10 collagen, a common hypertrophic marker, was not differentially up-regulated.

Using Ingenuity pathway analysis, growth differentiation factor 2 (GDF2), bone morphogenetic protein-2 (BMP-2), and PTHLH were recognized as potential key players in differential gene regulation, as several downstream genes were differentially up-regulated in HA over PEG hydrogels. GDF2 regulates cell growth and differentiation, while BMP-2 and PTHLH regulate cartilage and bone formation. Microarray results are also in agreement with real time PCR data.

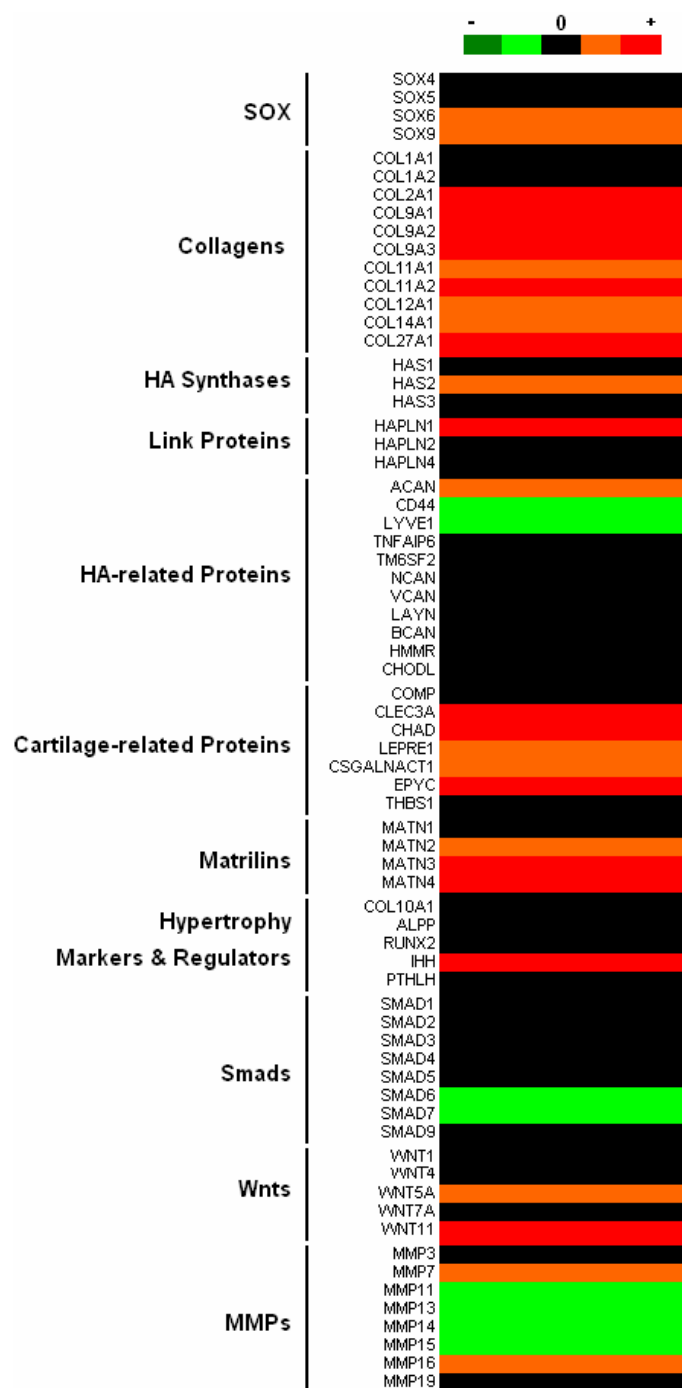


**Figure 8.12** Heat map comparison of MSC-laden HA and PEG hydrogels after 14 days of *in vitro* culture. Significantly up-regulated (red) and down-regulated (green) genes in HA hydrogels compared to PEG hydrogels, with a false discovery rate < 5%. Black denotes no significant difference.

## 8.4 Conclusions

This chapter demonstrated that MSCs are capable of undergoing chondrogenesis in photocrosslinked HA hydrogels *in vitro* and *in vivo* in short-term culture. Gene expression showed that scaffold choice affects the expression of cartilaginous matrix proteins, where favorable cell/scaffold interactions can assist in chondrogenic differentiation. Though the mechanisms behind this interaction are not well understood, the microarray data has provided some insight on genes of interest to be further investigated. Additionally, we have shown that TGF- $\beta$ 3 can be delivered within HA hydrogels and alter gene expression of encapsulated MSCs *in vivo*. The following chapter will address methods to optimize the MSC-laden HA hydrogel system for enhanced ECM distribution and tissue maturation.

**References:**

- [1] Pittenger MF, Mackay AM, Beck SC, Jaiswal RK, Douglas R, Mosca JD, et al. Multilineage potential of adult human mesenchymal stem cells. *Science* 1999;284(5411):143-7.
- [2] Friedenstein AJ, Gorskaja JF, Kulagina NN. Fibroblast precursors in normal and irradiated mouse hematopoietic organs. *Exp Hematol* 1976;4(5):267-74.
- [3] Alhadlaq A, Mao JJ. Mesenchymal stem cells: isolation and therapeutics. *Stem Cells Dev* 2004;13(4):436-48.
- [4] Zuk PA, Zhu M, Ashjian P, De Ugarte DA, Huang JI, Mizuno H, et al. Human adipose tissue is a source of multipotent stem cells. *Mol Biol Cell* 2002;13(12):4279-95.
- [5] Ashton BA, Allen TD, Howlett CR, Eaglesom CC, Hattori A, Owen M. Formation of bone and cartilage by marrow stromal cells in diffusion chambers in vivo. *Clin Orthop Relat Res* 1980;(151):294-307.
- [6] Barry FP. Biology and clinical applications of mesenchymal stem cells. *Birth Defects Res C Embryo Today* 2003;69(3):250-6.
- [7] Johnstone B, Hering TM, Caplan AI, Goldberg VM, Yoo JU. In vitro chondrogenesis of bone marrow-derived mesenchymal progenitor cells. *Exp Cell Res* 1998;238(1):265-72.
- [8] Mackay AM, Beck SC, Murphy JM, Barry FP, Chichester CO, Pittenger MF. Chondrogenic differentiation of cultured human mesenchymal stem cells from marrow. *Tissue Eng* 1998;4(4):415-28.
- [9] Sekiya I, Vuoristo JT, Larson BL, Prockop DJ. In vitro cartilage formation by human adult stem cells from bone marrow stroma defines the sequence of cellular and molecular events during chondrogenesis. *Proc Natl Acad Sci U S A* 2002;99(7):4397-402.
- [10] Yoo JU, Barthel TS, Nishimura K, Solchaga L, Caplan AI, Goldberg VM, et al. The chondrogenic potential of human bone-marrow-derived mesenchymal progenitor cells. *J Bone Joint Surg Am* 1998;80(12):1745-57.



- [11] Dawson E, Mapili G, Erickson K, Taqvi S, Roy K. Biomaterials for stem cell differentiation. *Adv Drug Deliv Rev* 2008;60(2):215-28.
- [12] Varghese S, Hwang NS, Canver AC, Theprungsirikul P, Lin DW, Elisseeff J. Chondroitin sulfate based niches for chondrogenic differentiation of mesenchymal stem cells. *Matrix Biol* 2007.
- [13] Chung C, Burdick JA. Engineering cartilage tissue. *Adv Drug Deliv Rev* 2008;60(2):243-62.
- [14] Zhu H, Mitsuhashi N, Klein A, Barsky LW, Weinberg K, Barr ML, et al. The role of the hyaluronan receptor CD44 in mesenchymal stem cell migration in the extracellular matrix. *Stem Cells* 2006;24(4):928-35.
- [15] Burdick JA, Anseth KS. Photoencapsulation of osteoblasts in injectable RGD-modified PEG hydrogels for bone tissue engineering. *Biomaterials* 2002;23(22):4315-23.
- [16] Jiang H, Peterson RS, Wang W, Bartnik E, Knudson CB, Knudson W. A requirement for the CD44 cytoplasmic domain for hyaluronan binding, pericellular matrix assembly, and receptor-mediated endocytosis in COS-7 cells. *J Biol Chem* 2002;277(12):10531-8.
- [17] Knudson W, Loeser RF. CD44 and integrin matrix receptors participate in cartilage homeostasis. *Cell Mol Life Sci* 2002;59(1):36-44.
- [18] Vachon E, Martin R, Plumb J, Kwok V, Vandivier RW, Glogauer M, et al. CD44 is a phagocytic receptor. *Blood* 2006;107(10):4149-58.
- [19] Haider M, Cappello J, Ghandehari H, Leong KW. In Vitro Chondrogenesis of Mesenchymal Stem Cells in Recombinant Silk-elastinlike Hydrogels. *Pharm Res* 2007.
- [20] Mehlhorn AT, Schmal H, Kaiser S, Lepski G, Finkenzeller G, Stark GB, et al. Mesenchymal stem cells maintain TGF-beta-mediated chondrogenic phenotype in alginate bead culture. *Tissue Eng* 2006;12(6):1393-403.
- [21] Chow G, Knudson CB, Knudson W. Expression and cellular localization of human hyaluronidase-2 in articular chondrocytes and cultured cell lines. *Osteoarthritis Cartilage* 2006;14(9):849-58.

- [22] Frost GI, Csoka AB, Wong T, Stern R. Purification, cloning, and expression of human plasma hyaluronidase. *Biochem Biophys Res Commun* 1997;236(1):10-5.
- [23] Lepperdinger G, Strobl B, Kreil G. HYAL2, a human gene expressed in many cells, encodes a lysosomal hyaluronidase with a novel type of specificity. *J Biol Chem* 1998;273(35):22466-70.
- [24] Flannery CR, Little CB, Hughes CE, Caterson B. Expression and activity of articular cartilage hyaluronidases. *Biochem Biophys Res Commun* 1998;251(3):824-9.
- [25] Bi W, Deng JM, Zhang Z, Behringer RR, de Crombrughe B. Sox9 is required for cartilage formation. *Nat Genet* 1999;22(1):85-9.
- [26] Lefebvre V, Li P, de Crombrughe B. A new long form of Sox5 (L-Sox5), Sox6 and Sox9 are coexpressed in chondrogenesis and cooperatively activate the type II collagen gene. *Embo J* 1998;17(19):5718-33.
- [27] Smits P, Li P, Mandel J, Zhang Z, Deng JM, Behringer RR, et al. The transcription factors L-Sox5 and Sox6 are essential for cartilage formation. *Dev Cell* 2001;1(2):277-90.
- [28] Yingst S, Bloxham K, Warner LR, Brown RJ, Cole J, Kenoyer L, et al. Characterization of collagenous matrix assembly in a chondrocyte model system. *J Biomed Mater Res A* 2008.
- [29] Sato T, Gotoh M, Kiyohara K, Akashima T, Iwasaki H, Kameyama A, et al. Differential roles of two N-acetylgalactosaminyltransferases, CSGalNAcT-1, and a novel enzyme, CSGalNAcT-2. Initiation and elongation in synthesis of chondroitin sulfate. *J Biol Chem* 2003;278(5):3063-71.
- [30] Kou I, Ikegawa S. SOX9-dependent and -independent transcriptional regulation of human cartilage link protein. *J Biol Chem* 2004;279(49):50942-8.
- [31] Shi S, Grothe S, Zhang Y, O'Connor-McCourt MD, Poole AR, Roughley PJ, et al. Link protein has greater affinity for versican than aggrecan. *J Biol Chem* 2004;279(13):12060-6.
- [32] Pei M, Luo J, Chen Q. Enhancing and maintaining chondrogenesis of synovial fibroblasts by cartilage extracellular matrix protein matrilins. *Osteoarthritis Cartilage* 2008;16(9):1110-7.

- [33] Neame PJ, Tapp H, Grimm DR. The cartilage-derived, C-type lectin (CLECSF1): structure of the gene and chromosomal location. *Biochim Biophys Acta* 1999;1446(3):193-202.
- [34] Kim YJ, Kim HJ, Im GI. PTHrP promotes chondrogenesis and suppresses hypertrophy from both bone marrow-derived and adipose tissue-derived MSCs. *Biochem Biophys Res Commun* 2008;373(1):104-8.
- [35] Church V, Nohno T, Linker C, Marcelle C, Francis-West P. Wnt regulation of chondrocyte differentiation. *J Cell Sci* 2002;115(Pt 24):4809-18.

## CHAPTER 9

### *Synthesis of Hydrolytically Degradable Hyaluronic Acid Hydrogels*

(Adapted from: S Sahoo, **C Chung**, S Khetan, JA Burdick, "Hydrolytically degradable hyaluronic acid hydrogels with controlled temporal structures," *Biomacromolecules*, 2008, 9(4):1088-92. **C Chung**, M Beecham, RL Mauck, JA Burdick, "The Influence of Degradable Characteristics of Hyaluronic Acid Hydrogels on In Vitro Neocartilage Formation by Mesenchymal Stem Cells." *Biomaterials*, 2009, Epub.

#### 9.1 Introduction

HA is a linear polysaccharide of alternating D-glucuronic acid and N-acetyl-D-glucosamine, found natively in many tissues (e.g., cartilage)[1-3], and degrades primarily by hyaluronidases found throughout the body or through oxidative mechanisms to yield oligosaccharides and glucuronic acid[4]. HA plays a role in cellular processes like cell proliferation, morphogenesis, inflammation, and wound repair, and interacts with cells through surface receptors (CD44, CD54, and CD168)[1,2,5,6]. These biological interactions make HA a candidate for the development of biomaterials that can directly interact with cells.

Importantly, HA can be readily modified through its carboxyl and hydroxyl groups to form hydrogels in the presence of water[7-13]. These hydrogels have found numerous applications in tissue regeneration [8,13-15], drug delivery[12], and microdevices[16]. However, the design of these current hydrogels is limiting in that (i) enzymes are needed to degrade the hydrogel, which can hinder the diffusion of growth factors, migration of cells, and distribution of extracellular matrix proteins if enzymes are not abundant and (ii) degradation products are typically modified forms of HA (e.g., due to methacrylate addition) rather than potentially biologically active unmodified HA[17-20]. Although an ester group may exist between the HA backbone and the reactive group,

this bond is typically very stable, potentially due to steric hindrance or the hydrophobicity of the surrounding chemical groups.

These limitations motivated our work in designing the next generation of HA hydrogels with superior properties. Specifically, we sought to design a new macromer that forms hydrogels that are hydrolytically degradable to allow further control over their structures towards a range of biological applications. These macromers can be polymerized into hydrogels alone or copolymerized with other macromers to produce hydrogels with diverse properties, specifically related to temporal structures with degradation. Here, we report the synthesis of the novel HA macromer and illustrate potential diversity in applications through the release of drugs and interactions with cells.

## **9.2 Materials & Methodology**

### *9.2.1 Methacrylated HA (MeHA) Macromer Synthesis*

MeHA was synthesized as previously stated (chapter 4, section 4.2) by the addition of methacrylic anhydride (~20-fold excess, Sigma) to a solution of 1 wt% HA (Lifecore, 64 kDa) in deionized water adjusted to a pH of 8 with 5 N NaOH and reacted on ice for 24 hours[7,21]. For purification, the macromer solution was dialyzed (MW cutoff 5-8kDa) against deionized water for at least 48 hours and the final product was obtained by lyophilization. <sup>1</sup>H NMR was used to determine the final functionality and purity of the MeHA. The reaction schematic for the synthesis of MeHA can be found in chapter 4.

### *9.2.2 Methacrylated Lactic Acid HA (MeLAHA) Macromer Synthesis*

The reaction schematic for MeLAHA is illustrated in Figure 9.1. 2-hydroxyethyl methacrylate (HEMA) (Across organics) is reacted with dl-lactide (Polysciences) in a 1:1.5 molar ratio via a ring opening polymerization (110°C, 1 hour, under nitrogen) in the presence of a catalytic amount of stannous octoate (tin 2-ethylhexanoate) (Sigma) to obtain MeLA-OH.

Hydroquinone (Sigma) was added in trace amounts to the reaction mixture to inhibit free-radical polymerization of the methacrylate groups. The number of lactic acid units was determined by  $^1\text{H}$  NMR from the ratio of the integral area of the methacrylate peak and the methylene peak of the lactic acid unit.

The hydroxyl end group was converted into a carboxylic acid via a 1:1 reaction of MeLA-OH with succinic anhydride (Sigma) in the presence of pyridine (Sigma) and dimethylaminopyridine (DMAP) (Sigma) in anhydrous tetrahydrofuran (THF) at 50°C for 24 hours under nitrogen to obtain MeLA-COOH. After cooling to room temperature, the solvent was evaporated under vacuum and the residue was dissolved in dichloromethane followed by three washes with a 0.1M HCL solution. The organic phase was dried over magnesium sulfate and concentrated in a rotary evaporator, and kept at 4°C until used further.

The end group of the MeLA-COOH was functionalized by reacting with N-hydroxysuccinimide (NHS) (Sigma) and dicyclohexylcarbodiimide (DCC) (Acros organics) in a 1:1:1 molar ratio in anhydrous dichloromethane at 0°C for 4 hours, followed by room temperature for 24 hours under nitrogen to obtain MeLA-NHS. Insoluble N,N'-dicyclohexyl urea (DCU) was removed by filtration and the filtrate was concentrated by rotary evaporation. In order to solubilize HA in dimethyl sulfoxide (DMSO), the sodium salt of HA (Lifecore, 64 kDa) was converted to a tetrabutylammonium (TBA) (Sigma) salt by acidic ion exchange at room temperature for 8 hours with Dowex 50 W x 8-200 resin (Acros), filtered, and neutralized in aqueous TBA hydroxide. The TBA-HA was then lyophilized and stored at -20°C until further use.

TBA-HA was coupled with MeLA-NHS in anhydrous DMSO in the presence of triethylamine at 40°C for 24 hours. The reaction was cooled to room temperature and a 2.5 wt% sodium chloride solution (20% (v/v)) was added to exchange the TBA salt with a sodium salt. The resultant solution was purified through precipitation in acetone to obtain MeLAHA, which was stored in acetone at -20°C until use.

Each product was confirmed by  $^1\text{H}$  NMR (Bruker DMX 360 and 300 MHz spectrometer). Diffusion-ordered NMR spectroscopy (DOSY) spectrum were recorded using stimulated echo

pulse sequence using bipolar gradients with a longitudinal eddy current delay in Bruker DMX 600 MHz NMR spectrometer having z-gradient (maximum strength of 70 G/cm). The sine shaped gradient pulse with 3.0 ms duration was logarithmically incremented in 32 steps, from 2% up to 95% of maximum gradient strength. Diffusion time was set to 300 ms and a longitudinal eddy current delay of 5 ms was used. After Fourier transformation and base line correction, DOSY spectrum was processed using Bruker Topspin software's DOSY package.

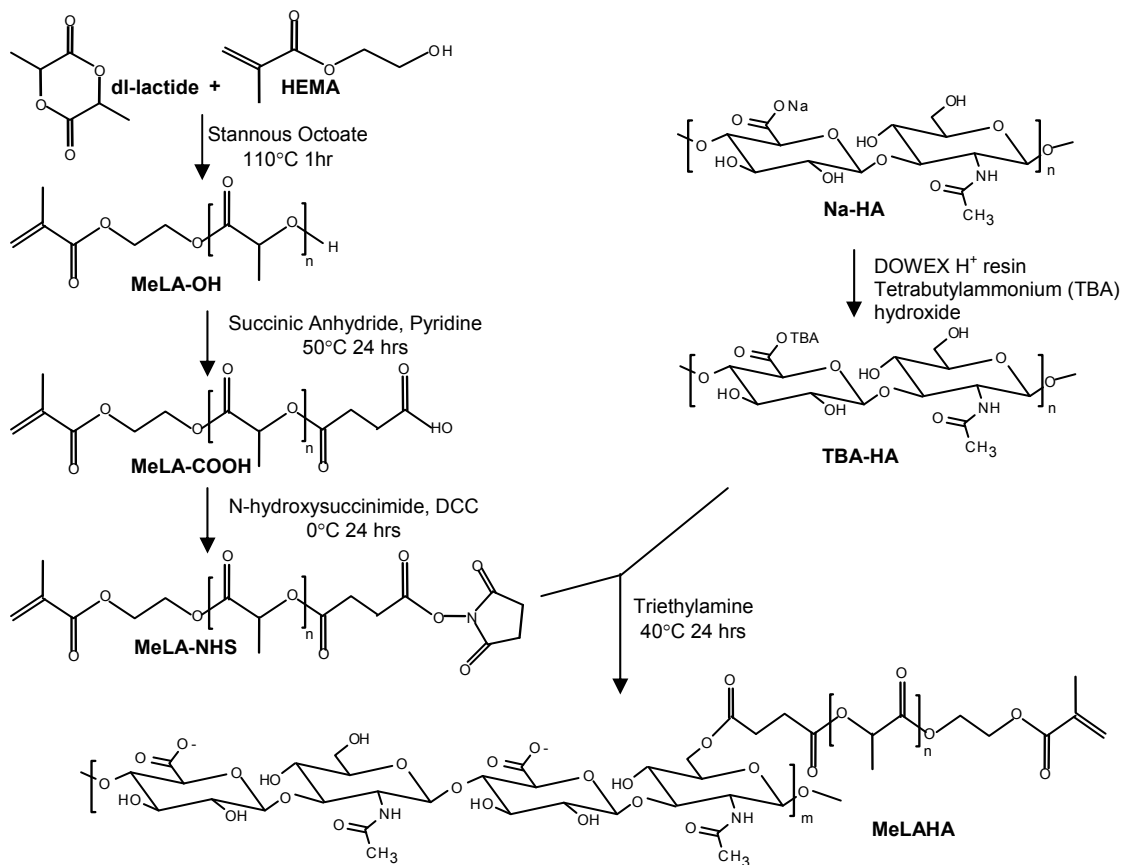


**Figure 9.1** Reaction schematic for the synthesis of MeLAHA.

### 9.2.3 Methacrylated Caprolactone HA (MeCLHA) Macromer Synthesis

The synthesis of methacrylated caprolactone HA (MeCLHA) was based on that of MeLAHA with slight modifications to simplify the reaction scheme (Figure 9.2). 2-hydroxyethyl methacrylate (HEMA) (Acros organics) was reacted with  $\epsilon$ -caprolactone (Sigma) via a ring opening polymerization in the presence of stannous octoate (Sigma) at 130°C for 1hr to obtain

MeCL-OH. The end group was then functionalized into a carboxylic acid (MeCL-COOH) via reaction with succinic anhydride (Sigma) in the presence of N-methylimidazole at 65°C in dichloroethane for 13 hrs. MeCL-COOH was washed three times in 0.1M HCL solution. The organic phase was dried over magnesium sulfate, filtered, concentrated in the rotary evaporator, and kept at 4°C until use.

Again, the sodium salt form of HA was converted to a TBA salt by acidic ion exchange with Dowex 50 W x 8-200 resin for solubilization in DMSO. MeCL-COOH was coupled to TBA-HA via an esterification reaction with di-t-butyl dicarbonate (BOC<sub>2</sub>O) as an activating agent with DMAP[22] for 20 hrs at 45°C in anhydrous DMSO. A 2.5 wt% sodium chloride solution (20% (v/v)) was added to exchange the TBA salt with a sodium salt. The final product (MeCLHA) was precipitated and washed in acetone, dissolved in DI water, dialyzed (MW cutoff 6-8k) for 24 hours at 4°C, lyophilized, and stored at -20°C in powder form prior to use. The intermediate and final macromer products were confirmed by <sup>1</sup>H NMR.

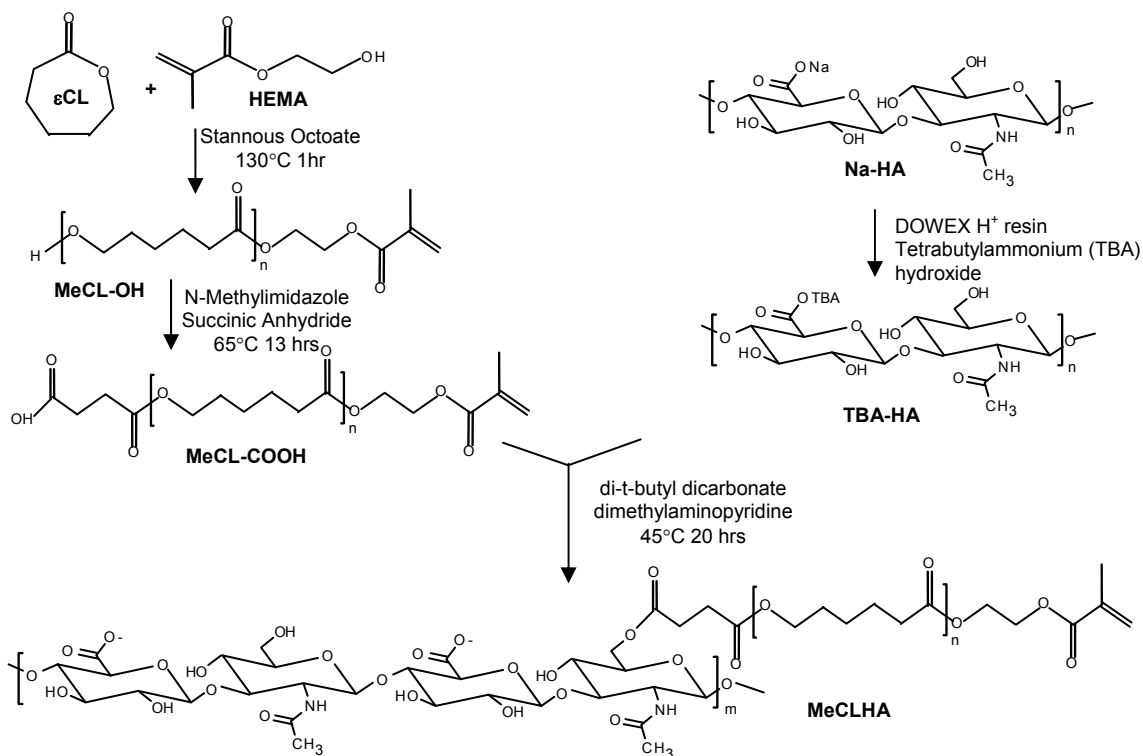


**Figure 9.2** Reaction schematic for the synthesis of MeCLHA macromer.



#### 9.2.4 Hydroxyethyl Methacrylated HA (Hema-HA) Macromer Synthesis

Hydroxyethyl methacrylated HA was synthesized in the same manner as MeCLHA minus the initial ring opening polymerization. 2-hydroxyethyl methacrylate was functionalized to HEMA-COOH via reaction with succinic anhydride in a 1:1 molar ratio in the presence of N-methylimidazole at 65°C in dichloroethane for 13 hrs, and then coupled to TBA-HA via an esterification reaction with BOC<sub>2</sub>O with DMAP for 20 hrs at 45°C in anhydrous DMSO. The final product (HEMA-HA) was precipitated and washed in acetone, dissolved in DI water, dialyzed (MW cutoff 6-8k) for 4-6 hour, frozen, lyophilized, and stored in powder form at -20°C until use.

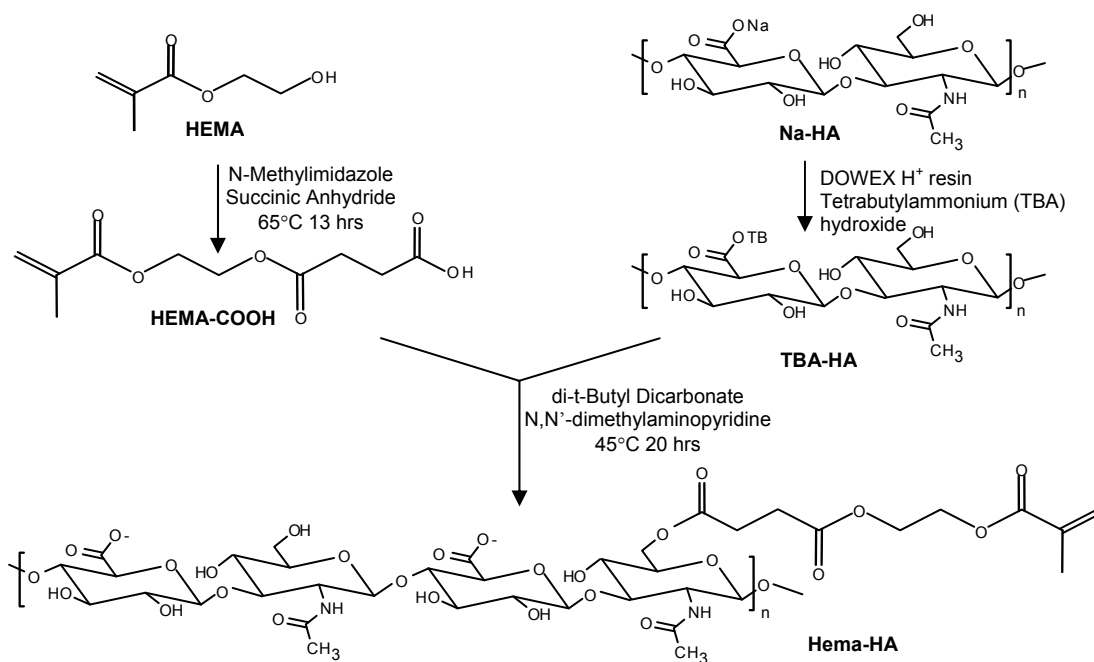


**Figure 9.3** Reaction schematic for the synthesis of Hema-HA macromer.

#### 9.2.5 Hydrogel Formation and Acellular Characterization

Hydrogels were synthesized by dissolving the HA macromers at various concentrations and compositions in phosphate buffered saline (PBS), with 0.05 wt% photoinitiator, 2-methyl-1-[4-

hydroxyethoxy)phenyl]-2-methyl-1-propanone (Irgacure 2959). The macromer solution was then placed into a mold (5 mm diameter, 2 mm thick) and polymerized with  $\sim 2\text{mW/cm}^2$  ultraviolet light ( $\sim 365\text{ nm}$ , EIKO bulb) for 10 minutes. For degradation studies, hydrogels ( $n = 3$  per composition) were placed in separate wells of a 24-well plate containing 1 ml of PBS and placed on an orbital shaker at  $37^\circ\text{C}$ . PBS solution was changed at every time point, and the amount of uronic acid (a degradation component of HA) released during degradation was measured using a previously established carbazole reaction technique[23,24] (Chapter 4, section 4.2).

#### 9.2.6 Short-Term Cell Viability and Matrix Elaboration *In Vitro*

Mesenchymal stem cells (MSCs) (Lonza) were expanded to passage 4 in growth media consisting of  $\alpha$ -MEM with 16.7% FBS and 1% penicillin/streptomycin, and then photoencapsulated (20 million cells/ml) in various MeHA: MeLAHA copolymer hydrogels (2:0, 1.5:0.5, 1:1, and 0.5:1.5 MeHA wt%: MeLAHA wt%). Cell-laden hydrogels were cultured in DMEM supplemented with 1% penicillin/streptomycin, 1% ITS+, 1mM sodium pyruvate, 40mg/ml L-proline, 100nM dexamethasone, 50 $\mu\text{g/ml}$  ascorbic acid 2-phosphate, and 10 ng/ml of TGF- $\beta$ 3 (chondrogenic media, CM+) for up to 2 weeks *in vitro*. Cell viability was quantified using MTT viability assay (ATCC) as measured by mitochondrial activity. Matrix distribution was visualized by immunohistochemical staining for chondroitin sulfate (CS) after 2 weeks of culture. Samples were fixed in 10% formalin for 24 hours, embedded in paraffin, and processed using standard histological procedures. The histological sections (7  $\mu\text{m}$  thick) were stained for CS using the Vectastain ABC kit (Vector Labs) and the DAB Substrate kit for peroxidase (Vector Labs). Sections were predigested in 0.5 mg/ml hyaluronidase for 30 min at  $37^\circ\text{C}$  and incubated in 0.5N acetic acid for 4 hours at  $4^\circ\text{C}$  to swell the samples prior to overnight incubation with primary antibody at 1:100 (mouse monoclonal anti-chondroitin sulfate, Sigma). Non-immune controls underwent the same procedure without primary antibody incubation. Hematoxylin and eosin (H&E) staining was also performed.

### 9.3 Results & Discussion

The inclusion of hydrolytically degradable repeat units between the HA backbone and the polymerizing moiety (e.g., methacrylate) yielded hydrolytically degradable HA macromers that formed hydrolytically degradable hydrogels. Since  $\alpha$ -hydroxy esters (e.g., lactic acid, caprolactone) are highly versatile in design, hydrolyzable, and approved by the FDA for several biomedical applications[25,26], they were ideal groups to incorporate into the hydrogel. By changing the number and type of degradable repeat units, hydrogels could be tunable with respect to degradation, structure, and mechanical properties.

#### 9.3.1 Synthesis of MeLAHA Macromer

Lactic acid was polymerized off the hydroxy terminal group of HEMA using a ring opening polymerization of lactide monomer in the bulk phase with stannous octoate as a catalyst to form a hydroxyl terminated methacrylated poly(lactic acid) (MeLA-OH). The polymerization proceeds through a coordination-insertion mechanism and the number of lactic acid repeat units is readily controlled through the stoichiometric amount of lactide monomer to HEMA used in the reaction. The  $^1\text{H}$  NMR spectrum of this polymer (Figure 9.4A) displayed characteristic resonances for the methacrylate protons at  $\delta$  6.12 and 5.60 ppm and  $-\text{CH}$  and  $-\text{CH}_3$  protons of lactic acid at  $\delta$  5.19 and 1.52 ppm, respectively. From the integration ratio of the  $-\text{CH}$  proton corresponding to the lactic acid units to the methylene protons of the methacrylate group, the number of lactic acid repeat units was estimated ( $\sim 3$  for reported experiments). Importantly, the number of degradable units can be used to control the hydrolysis rate of hydrogels incorporating lactic acid[27], with more repeat units leading to more rapid degradation based on the probability of ester cleavage.

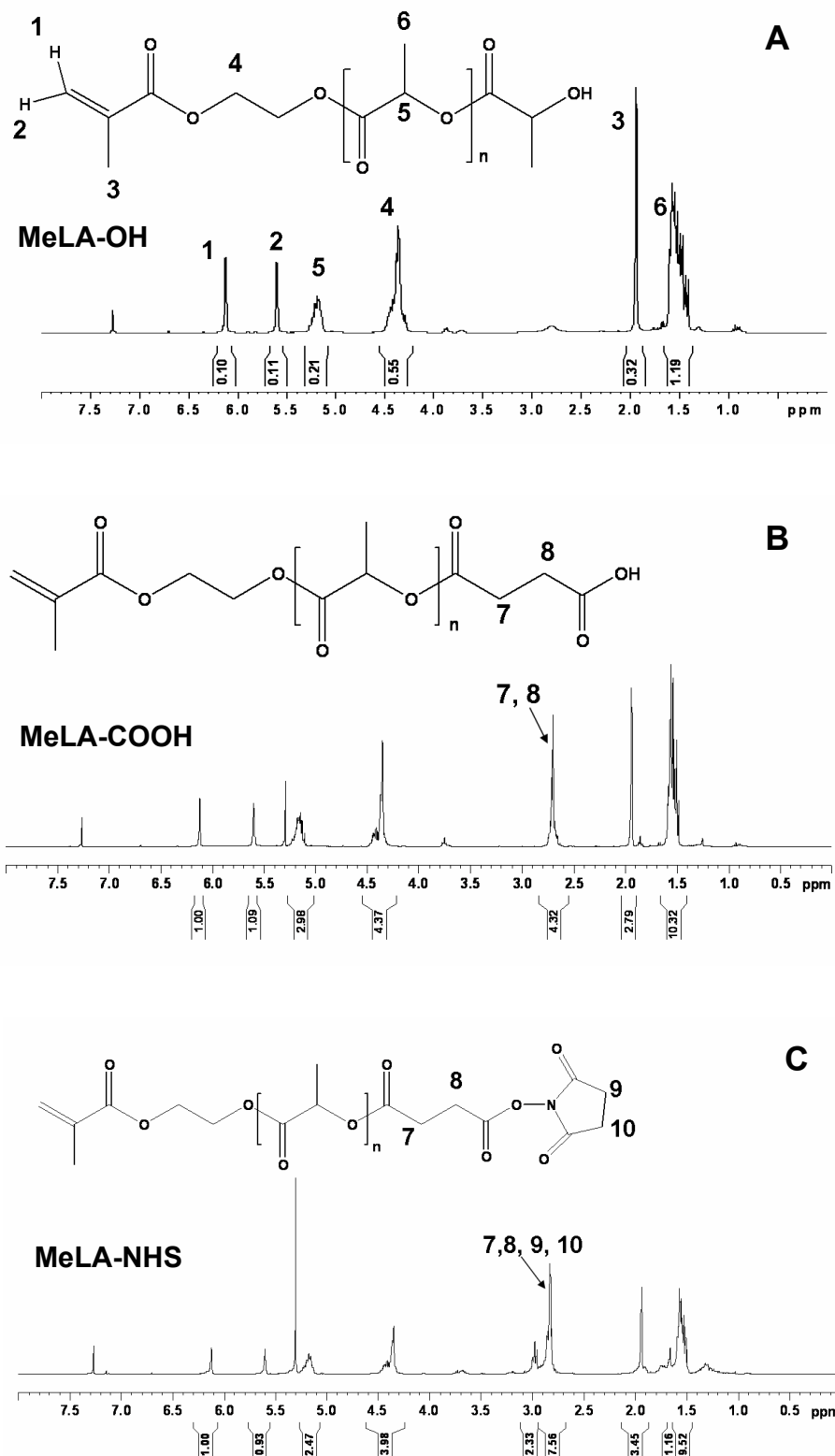


**Figure 9.4**  $^1\text{H}$  NMR spectrum ( $\text{CDCl}_3$ ) of (A) MeLA-OH, (B) MeLA-COOH, and (C) MeLA-NHS.

For coupling to HA, it was not possible to directly react the free hydroxyl group of MeLA-OH with HA since HA possesses both carboxylic acid and hydroxyl groups that would interfere with the reaction. Thus, the hydroxyl group of lactic acid was converted to a carboxylic acid through an esterification reaction with succinic anhydride in the presence of pyridine and DMAP as an esterification catalyst (Figure 9.1) to form a carboxyl terminated methacrylated poly(lactic acid) (MeLA-COOH). The reaction was carried out in anhydrous THF since the acid anhydride is subjected to hydrolysis in aqueous medium. The conversion of –OH to –COOH was confirmed by  $^1\text{H}$  NMR (Figure 9.4B) with the  $\delta$  2.72 ppm resonance corresponding to the –  $(\text{CH}_2)_2$  group of succinic anhydride observed in the spectrum. The NHS ester derivative was formed for coupling to HA through reaction of MeLA-COOH with NHS in the presence of DCC, where DCC promotes esterification by reacting with the end carboxyl group through nucleophilic substitution. The final product (MeLA-NHS) was obtained after filtering DCU as the byproduct and  $^1\text{H}$  NMR confirmed successful modification (Figure 9.4C).

Since the solubility of the sodium salt of HA (Figure 9.5A) is limited to aqueous solutions and the MeLA-NHS is not water-soluble, HA was converted to its TBA salt (Figure 9.5B) to make it soluble in highly polar organic solvents. After freeze-drying, HA-TBA was dissolved in anhydrous DMSO and reacted with TEA and MeLA-NHS for coupling. The product was converted back to the sodium salt and precipitated in acetone to form MeLAHA. The derivatization reaction was confirmed by  $^1\text{H}$  NMR analysis (Figure 9.6) and exhibited distinct resonances from the – $\text{CH}_3$  protons of lactic acid at  $\delta$  1.58 ppm and the two protons of the methacrylate at  $\delta$  6.18 and 5.80 ppm. The degree of modification (~10.5%) was determined by the peak areas of the HA backbone and those of methacrylate groups.

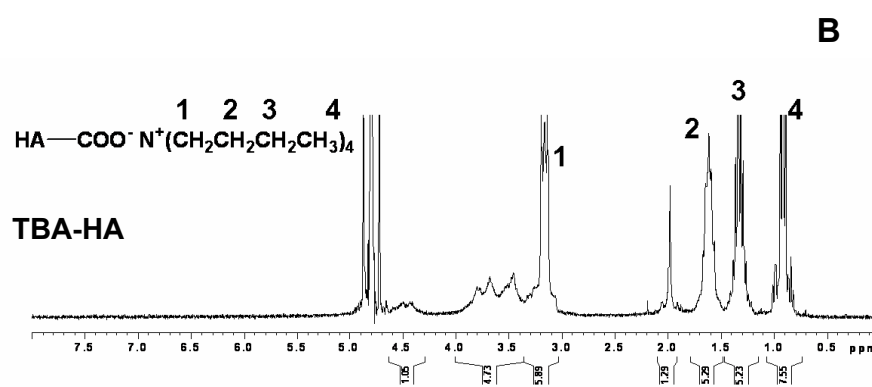
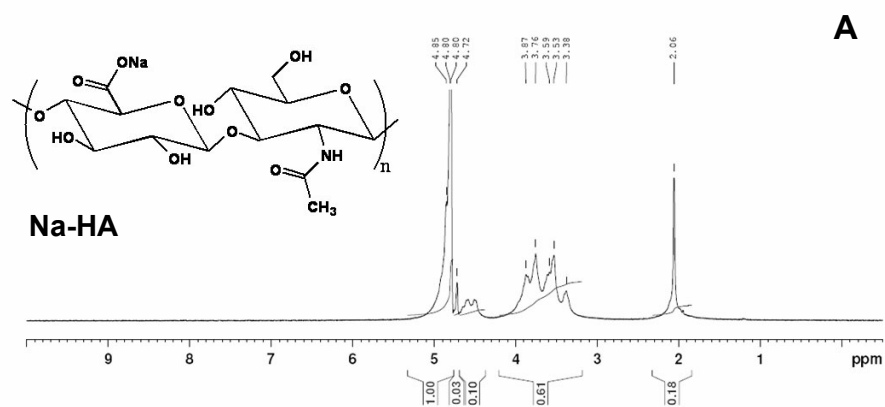


**Figure 9.5** <sup>1</sup>H NMR spectrum (D<sub>2</sub>O) of (A) sodium and (B) TBA salt of hyaluronic acid.

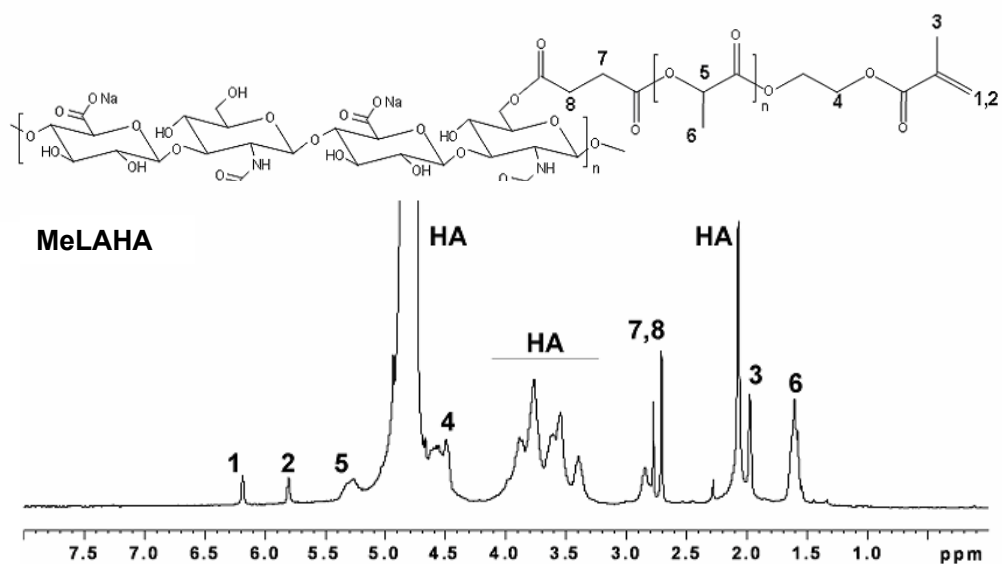


**Figure 9.6** <sup>1</sup>H NMR spectrum (D<sub>2</sub>O) of MeLAHA macromer (n≈3, 10.5% modification).

DOSY was used to analyze the purified MeLAHA product (Figure 9.7 B, D) to discriminate between different components of the sample by their chemical shift and diffusion behavior simultaneously. The separation in the diffusion dimension among various peaks is based on the self-diffusion coefficient of different species present in the solution. In DOSY spectrum, molecules with lower molecular weights exhibit higher diffusion coefficients compared to polymers. However, if the same small molecule is attached to the polymer chain, the self-diffusion coefficient will be similar to the polymer.

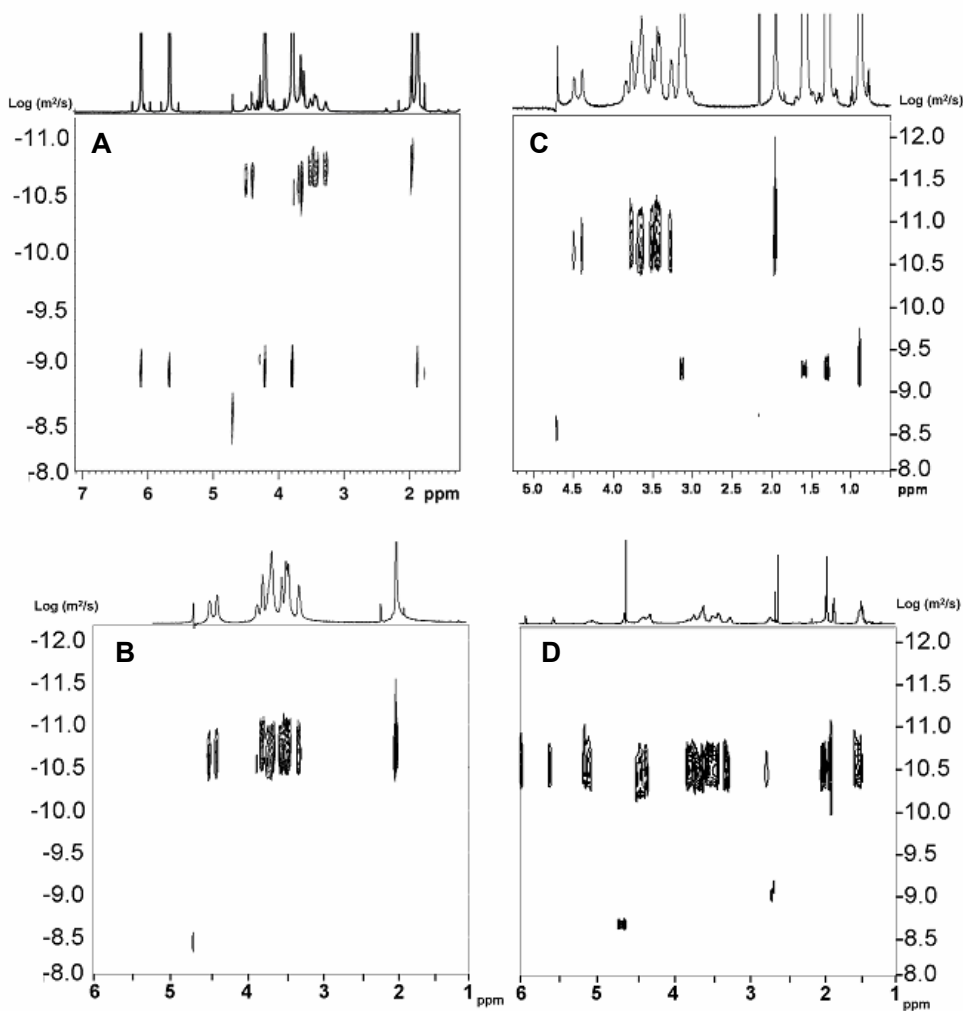


**Figure 9.7** DOSY spectrum of (A) a two component mixture of unmodified HA and MeLA-OH, (B) unmodified HA, (C) HA-TBA, (D) and MeLAHA, which demonstrates successful coupling.

Comparing DOSY spectra (Figure 9.7B and D), it is clear that peaks due to MeLA (1.0-3.0 ppm and > 5.0 ppm) shows similar diffusion coefficient as the HA peaks and confirms the coupling of MeLA to HA. In contrast, physical mixing of MeLA and HA shows significantly higher diffusion coefficient values for MeLA compared to HA (Figure 9.7 A and B). In addition, a slight reduction in the overall diffusion coefficient of MeLAHA was observed after coupling, indicating a higher molecular weight compared to unmodified HA.

### 9.3.2 Synthesis of MeCLHA and Hema-HA Macromers

With successful synthesis of the MeLAHA macromer, MeCLHA and Hema-HA macromers were synthesized to further tailor hydrogel properties. Successful syntheses of these macromers were verified by  $^1\text{H}$  NMR (Figure 9.8), displaying characteristic resonances for the methacrylate protons at  $\delta$  6.12 and 5.60 ppm,  $-\text{CH}_2$  protons (labeled as 11, Figure 9.8A) of caprolactone at  $\delta$  2.28 ppm, and  $-\text{CH}_2$  protons (labeled as 7 and 8, Figure 9.8B) of Hema-COO-group at  $\delta$  2.65 ppm. The number of caprolactone repeats was estimated by integrating the ratio of methacrylate protons and the  $-\text{CH}_2$  protons corresponding to caprolactone, and determined to be  $\sim 3.8$  repeat units for all experiments. From the integration ratio of methacrylate protons and the 10 protons on the HA backbone between  $\delta$  3.2-4.1 ppm, the degree of modification was determined to be 7.5% and 6.2% for MeCLHA and Hema-Ha, respectively.



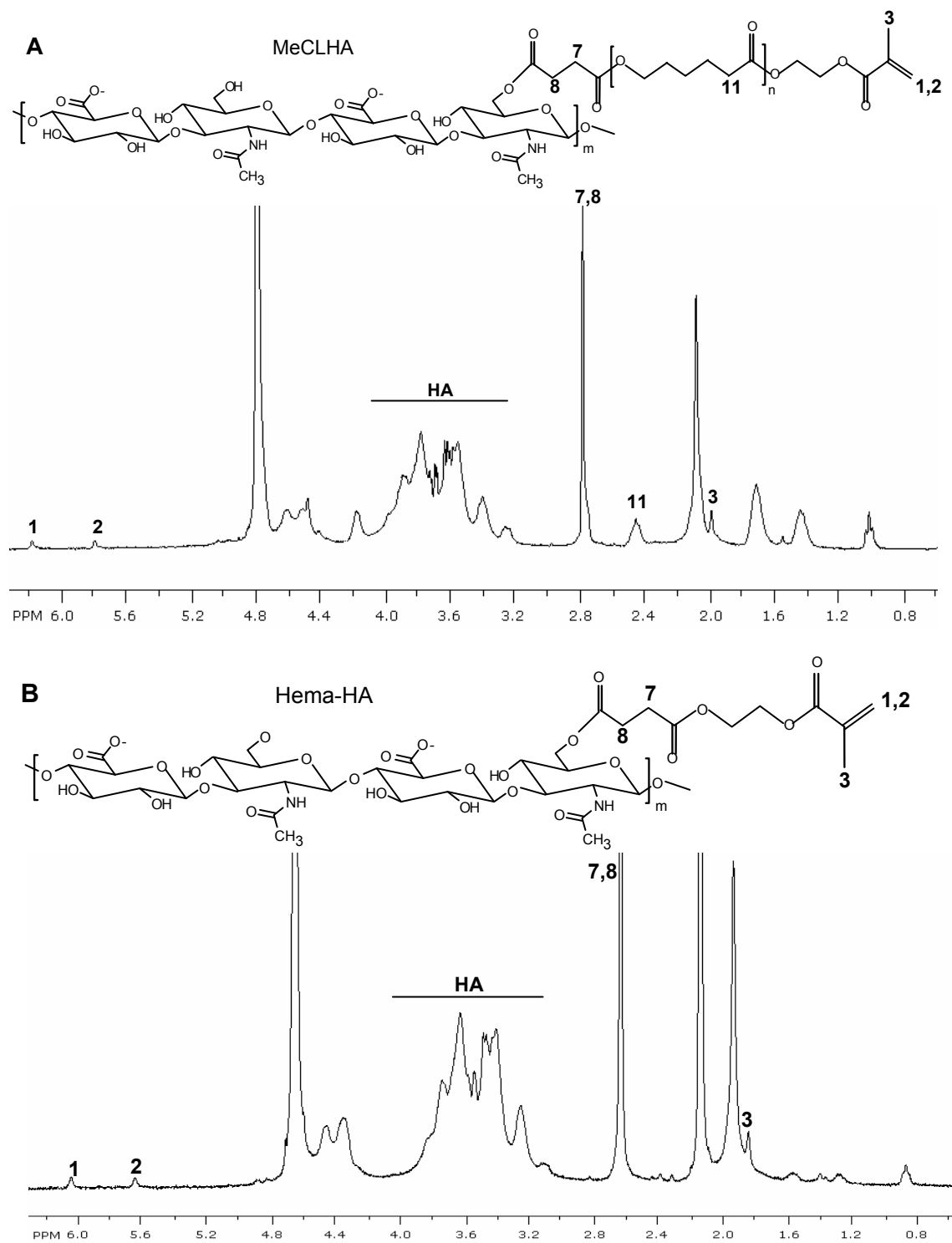


**Figure 9.8**  $^1\text{H}$  NMR of (A) MeCLHA ( $n = \sim 3.8$ ,  $\sim 7.5\%$  modification) and (B) Hema-HA (6.2% modification).

### 9.3.3 Characterization of Hydrolytically Degradable HA Hydrogels

In this system, a variety of parameters can be readily controlled. These include: the molecular weight of the HA, the type (e.g., lactic acid, caprolactone), the number of hydrolytically degradable repeat units, the extent of coupling (percent of HA repeat units modified), and the concentration of macromer used for hydrogel formation.

For degradation studies, homopolymer hydrogels of varying type (MeLAHA, MeCLHA, Hema-HA) and macromer concentrations (1 to 5 wt%) were incubated in PBS at 37°C and monitored for HA release with time. All hydrogels degraded in PBS without the addition of exogenous hyaluronidase enzyme, whereas enzymatically degradable MeHA hydrogels required exogenous enzyme for complete degradation (Chapter 4). In addition, these hydrolytically degradable hydrogels swell over time, suggesting a bulk degradation mechanism. Increases in macromer concentration, i.e., increases in crosslinking density, result in increased degradation time for all polymer types (Figure 9.9). However, notable differences among macromer types were observed, with the fastest degradation seen in MeLAHA hydrogels and the slowest degradation seen in MeCLHA hydrogels (2wt% hydrogels degraded in 2.5 days and 7 days, respectively), where slight differences in local hydrophobicity surrounding the ester linkages can result in the differences in degradation profiles of these hydrogels. Though the number of hydrolytically degradable units was not altered in this study, increases in the number of repeat units would increase degradation rate as the probability of hydrolysis is increased in the hydrogel.

In addition, MeHA and hydrolytically degradable HA macromers can be copolymerized to further fine tune hydrogel degradation profiles (Figure 9.10). These differential degradation profiles can be utilized, as others have done with purely synthetic hydrogels [28,29], to enhance matrix distribution within the hydrogel, which will be discussed in further detail in the following chapter.

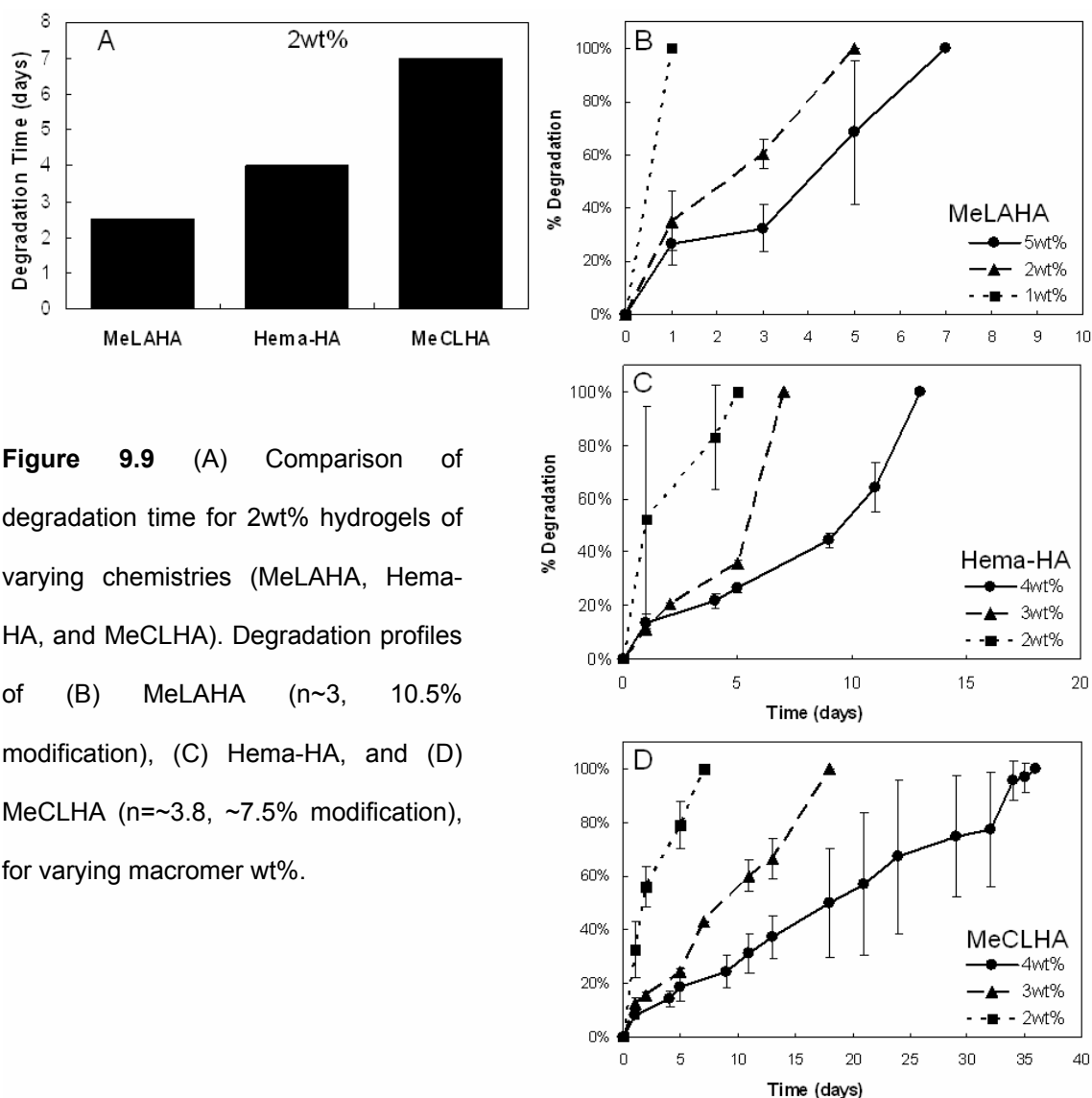
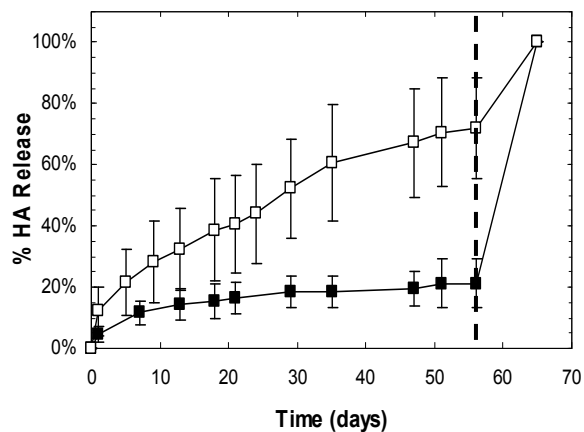


**Figure 9.9** (A) Comparison of degradation time for 2wt% hydrogels of varying chemistries (MeLAHA, Hema-HA, and MeCLHA). Degradation profiles of (B) MeLAHA ( $n \sim 3$ , 10.5% modification), (C) Hema-HA, and (D) MeCLHA ( $n \sim 3.8$ ,  $\sim 7.5\%$  modification), for varying macromer wt%.

**Figure 9.10** Degradation of 2 wt% MeHA: 3 wt% MeCLHA copolymer hydrogels (white) and 5 wt% MeHA (black) hydrogels in PBS at  $37^\circ\text{C}$  for 8 weeks, followed by the addition of exogenous hyaluronidase enzyme denoted by the dashed line.



#### 9.3.4 Cell Viability and Matrix Elaboration

To assess the utility of hydrolysis in copolymer hydrogels for matrix elaboration, MSCs were encapsulated in hydrogels and cultured in chondrogenic media. Viability (Figure 9.11A) as measured by mitochondrial activity after 7 days showed no statistical difference between all groups, indicating that the addition of MeLAHA did not compromise the viability of the encapsulated cells. The insignificant decrease in mitochondrial activity in the 0.5:1.5 hydrogels may have resulted from a loss of cells to culture media, as this composition contained the greatest portion of MeLAHA which is mostly degraded by 2 weeks. Overall, by increasing the MeLAHA content within the copolymer hydrogels, an increase in chondroitin sulfate deposition and distribution was observed (Figure 9.11B), where the 2:0 hydrogels exhibited pericellular staining compared to more homogeneous distribution of ECM in the 0.5:1.5 hydrogels.

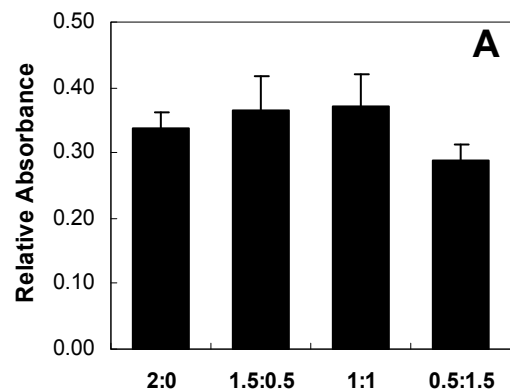
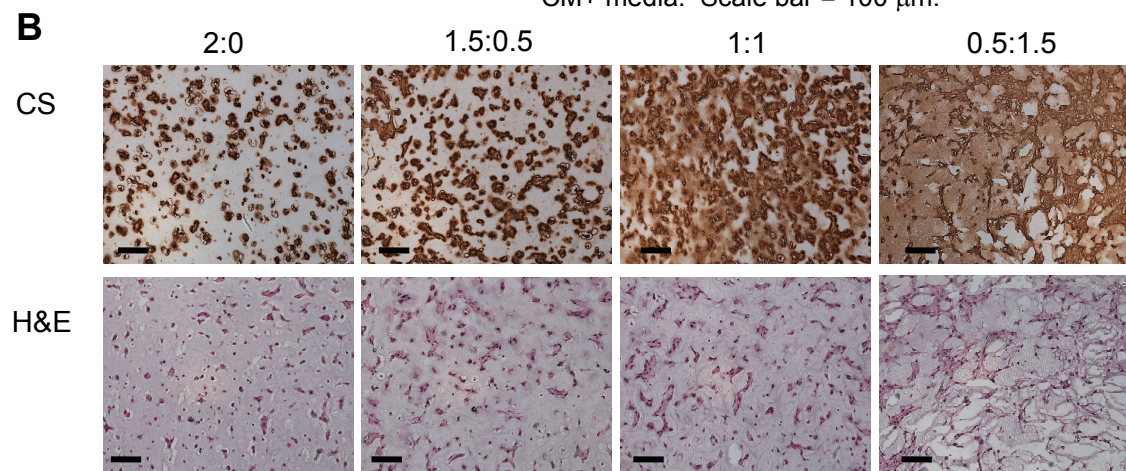


**Figure 9.11** (A) Mitochondrial activity (MTT Assay) of MeHA:MeLAHA copolymer hydrogels after 7 days of culture in CM+ media. No significant differences between groups. (B) Chondroitin sulfate (CS) and hematoxylin and eosin (H&E) staining after 14 days of culture in CM+ media. Scale bar = 100  $\mu$ m.



## **9.4 Conclusions**

In summary, the synthesis of hydrolytically degradable HA macromers and formation of HA hydrogels capable of both hydrolytic and enzymatic degradation was achieved. The tunable degradative component of this system provides enhanced control over hydrogel properties. Others have shown that hydrogel chemistry and hydrogel properties (e.g., mechanics and degradation) may play a role in the differentiation of stem cells and matrix distribution[30-32]. Therefore, this HA system can be optimized to tailor the stem cell microenvironment, control stem cell differentiation, and enhance the deposition and distribution of cartilaginous matrix proteins. The next chapter (chapter 10) will explore the long-term effects of temporal degradation in HA-based hydrogels on neocartilage formation.

**References:**

- [1] Toole BP. Hyaluronan in morphogenesis. *Semin Cell Dev Biol* 2001;12(2):79-87.
- [2] Jiang D, Liang J, Noble PW. Hyaluronan in tissue injury and repair. *Annu Rev Cell Dev Biol* 2007;23:435-61.
- [3] Allison DD, Grande-Allen KJ. Review. Hyaluronan: a powerful tissue engineering tool. *Tissue Eng* 2006;12(8):2131-40.
- [4] Stern R, Kogan G, Jedrzejewski MJ, Soltes L. The many ways to cleave hyaluronan. *Biotechnology Advances* 2007;25(6):537-57.
- [5] Chen WYJ, Abatangelo G. Functions of hyaluronan in wound repair. *Wound Repair and Regeneration* 1999;7(2):79-89.
- [6] Toole BP. Hyaluronan: from extracellular glue to pericellular cue. *Nat Rev Cancer* 2004;4(7):528-39.
- [7] Smeds KA, Pfister-Serres A, Miki D, Dastgheib K, Inoue M, Hatchell DL, et al. Photocrosslinkable polysaccharides for in situ hydrogel formation. *J Biomed Mater Res* 2001;54(1):115-21.
- [8] Chung C, Mesa J, Randolph MA, Yaremchuk M, Burdick JA. Influence of gel properties on neocartilage formation by auricular chondrocytes photoencapsulated in hyaluronic acid networks. *J Biomed Mater Res A* 2006;77A(3):518-25.
- [9] Jia XQ, Burdick JA, Kobler J, Clifton RJ, Rosowski JJ, Zeitel SM, et al. Synthesis and characterization of in situ cross-linkable hyaluronic acid-based hydrogels with potential application for vocal fold regeneration. *Macromolecules* 2004;37(9):3239-48.
- [10] Leach JB, Bivens KA, Patrick CW, Schmidt CE. Photocrosslinked hyaluronic acid hydrogels: Natural, biodegradable tissue engineering scaffolds. *Biotechnol Bioeng* 2003;82(5):578-89.

- [11] Chung C, Mesa J, Miller GJ, Randolph MA, Gill TJ, Burdick JA. Effects of auricular chondrocyte expansion on neocartilage formation in photocrosslinked hyaluronic acid networks. *Tissue Engineering* 2006;12(9):2665-73.
- [12] Cai S, Liu Y, Zheng Shu X, Prestwich GD. Injectable glycosaminoglycan hydrogels for controlled release of human basic fibroblast growth factor. *Biomaterials* 2005;26(30):6054-67.
- [13] Zheng Shu X, Liu Y, Palumbo FS, Luo Y, Prestwich GD. In situ crosslinkable hyaluronan hydrogels for tissue engineering. *Biomaterials* 2004;25(7-8):1339-48.
- [14] Shu XZ, Ahmad S, Liu Y, Prestwich GD. Synthesis and evaluation of injectable, in situ crosslinkable synthetic extracellular matrices for tissue engineering. *J Biomed Mater Res A* 2006;79(4):902-12.
- [15] Velema J, Kaplan D. Biopolymer-based biomaterials as scaffolds for tissue engineering. *Adv Biochem Eng Biotechnol* 2006;102:187-238.
- [16] Khademhosseini A, Eng G, Yeh J, Fukuda J, Blumling J, Langer R, et al. Micromolding of photocrosslinkable hyaluronic acid for cell encapsulation and entrapment. *J Biomed Mater Res A* 2006;79A(3):522-32.
- [17] Slevin M, Krupinski J, Gaffney J, Matou S, West D, Delisser H, et al. Hyaluronan-mediated angiogenesis in vascular disease: Uncovering RHAMM and CD44 receptor signaling pathways. *Matrix Biology* 2007;26(1):58-68.
- [18] Joddar B, Ibrahim S, Ramamurthi A. Impact of delivery mode of hyaluronan oligomers on elastogenic responses of adult vascular smooth muscle cells. *Biomaterials* 2007;28(27):3918-27.
- [19] Joddar B, Ramamurthi A. Fragment size- and dose-specific effects of hyaluronan on matrix synthesis by vascular smooth muscle cells. *Biomaterials* 2006;27(15):2994-3004.
- [20] Wilkinson TS, Bressler SL, Evanko SP, Braun KR, Wight TN. Overexpression of hyaluronan synthases alters vascular smooth muscle cell phenotype and promotes monocyte adhesion. *J Cell Physiol* 2006;206(2):378-85.

- [21] Burdick JA, Chung C, Jia X, Randolph MA, Langer R. Controlled degradation and mechanical behavior of photopolymerized hyaluronic acid networks. *Biomacromolecules* 2005;6(1):386-91.
- [22] Goossen LJ, Dohring A. A convenient protocol for the esterification of carboxylic acids with alcohols in the presence of di-t-butyl dicarbonate. *Synlett* 2004;(2):263-6.
- [23] Bitter T, Muir HM. A modified uronic acid carbazole reaction. *Anal Biochem* 1962;4(4):330-4.
- [24] Burdick JA, Chung C, Jia XQ, Randolph MA, Langer R. Controlled degradation and mechanical behavior of photopolymerized hyaluronic acid networks. *Biomacromolecules* 2005;6(1):386-91.
- [25] Lu L, Peter SJ, Lyman MD, Lai HL, Leite SM, Tamada JA, et al. In vitro degradation of porous poly(L-lactic acid) foams. *Biomaterials* 2000;21(15):1595-605.
- [26] Li WJ, Cooper JA, Mauck RL, Tuan RS. Fabrication and characterization of six electrospun poly(alpha-hydroxy ester)-based fibrous scaffolds for tissue engineering applications. *Acta Biomater* 2006;2(4):377-85.
- [27] Metters AT, Anseth KS, Bowman CN. Fundamental studies of a novel, biodegradable PEG-b-PLA hydrogel. *Polymer* 2000;41(11):3993-4004.
- [28] Bryant SJ, Anseth KS. Controlling the spatial distribution of ECM components in degradable PEG hydrogels for tissue engineering cartilage. *J Biomed Mater Res A* 2003;64A(1):70-9.
- [29] Bryant SJ, Durand KL, Anseth KS. Manipulations in hydrogel chemistry control photoencapsulated chondrocyte behavior and their extracellular matrix production. *J Biomed Mater Res A* 2003;67A(4):1430-6.
- [30] Hwang NS, Varghese S, Elisseeff J. Controlled differentiation of stem cells. *Adv Drug Deliv Rev* 2008;60(2):199-214.
- [31] Lee HJ, Yu C, Chansakul T, Hwang NS, Varghese S, Yu SM, et al. Enhanced chondrogenesis of mesenchymal stem cells in collagen mimetic peptide-mediated microenvironment. *Tissue Eng Part A* 2008;14(11):1843-51.



- [32] Salinas CN, Anseth KS. The enhancement of chondrogenic differentiation of human mesenchymal stem cells by enzymatically regulated RGD functionalities. *Biomaterials* 2008;29(15):2370-7.

## CHAPTER 10

### *Influence of Temporal Degradation on Matrix Deposition in Hyaluronic Acid Hydrogels*

(Adapted from: **C Chung**, M Beecham, RL Mauck, JA Burdick, "Tailored Hydrogel Crosslinking and Degradation to Enhance Neocartilage Formation by Mesenchymal Stem Cells," *Biomaterials*, 2009, in press)

#### **10.1 Introduction**

In efforts to develop clinically translatable approaches for cartilage repair, mesenchymal stem cells (MSCs) have been shown to undergo chondrogenesis and deposit neocartilage in a variety of tissue engineering scaffolds[1]. However, we are still limited in recapitulating the properties of native tissues. For example, Mauck *et al*[2] showed that the biochemical and mechanical properties of matured MSC-laden agarose scaffolds are lower than those containing donor matched chondrocytes. The diminished ability of MSCs to produce functional cartilage tissue is troubling, as the quality of tissue they produce determines their success as a viable cell source for cartilage repair and regeneration. Beyond the amount and type of matrix produced, the distribution of this matrix is essential for the optimization of tissue properties (e.g., mechanics). Thus, the design of biomaterials that support the distribution of formed tissue is crucial for the optimization of neocartilage formation by MSCs.

Hyaluronic acid (HA) hydrogels are formed by the simple addition of a reactive group to the HA backbone and subsequent crosslinking[3]. These hydrogels are tunable, where hydrogel parameters can be varied by degree of methacrylation, macromer molecular weight, and macromer concentration, providing a wide range of hydrogel properties (e.g., volumetric swelling ratios, mechanical properties)[4], and undergo enzymatic degradation via hyaluronidases. For applications in cartilage repair, we have shown that these HA hydrogels not only support and maintain chondrocyte viability and phenotype when cultured *in vitro* and *in vivo* [5,6], but also that HA hydrogel chemistry supports and promotes the chondrogenic differentiation of MSCs[7,8].

However, ECM distribution is limited without adequate space for diffusion in these slow enzymatically degrading hydrogels and techniques to better control network evolution with culture are needed.

Ideally, scaffold degradation should coincide with ECM deposition and accumulation. In engineered hydrogel scaffolds, degradation can alter the diffusion of nutrients and waste, cell-scaffold interactions, and the distribution and retention of ECM proteins. Therefore, to tailor temporal degradation of a scaffold, others have introduced hydrolytically degradable components[9], matrix metalloproteinase (MMP)-sensitive peptides[10,11], and/or exogenous enzymes[12,13] into scaffold designs. In the previous chapter, we engineered hydrolytically degradable HA macromers with the inclusion of poly(caprolactone) between the HA backbone and the polymerizing moiety (e.g., methacrylate). In this study, the long-term effects of temporal network structure on neocartilage formation by MSCs *in vitro* were investigated. We present a system that exploits both the advantages of HA in cartilage regeneration, as well as tunable degradation for the optimization of engineered tissue properties.

## **10.2 Materials & Methodology**

### *10.2.1 Macromer Syntheses*

Methacrylated HA (MeHA) was synthesized as reported in previous chapters [3]. Briefly, methacrylic anhydride (Sigma) was added to a solution of 1 wt% HA (Lifecore, MW = 74 kDa) in deionized water, adjusted to a pH of 8 with 5 N NaOH, and reacted on ice for 24 hours. The macromer solution was purified via dialysis (MW cutoff 6-8k) against deionized water for a minimum of 48 hours with repeated changes of water. The final product was obtained by lyophilization and stored at -20°C in powder form prior to use.

Methacrylated caprolactone HA (MeCLHA) was synthesized as reported in Chapter 9. Briefly, 2-hydroxyethyl methacrylate (HEMA) (Acros organics) was reacted with  $\epsilon$ -caprolactone (Sigma) via a ring opening polymerization in the presence of stannous octoate (Sigma) at 130°C

for 1 hr. The end group was then functionalized into a carboxylic acid (MeCL-COOH) via reaction with succinic anhydride (Sigma) in the presence of N-methylimidazole at 65°C in dichloroethane for 13 hrs. The sodium salt form of HA was converted to a tetrabutylammonium (TBA) salt by acidic ion exchange with Dowex 50 W x 8-200 resin, followed by resin filtration and neutralization with aqueous TBA hydroxide for solubilization in dimethyl sulfoxide (DMSO). MeCL-COOH was coupled to TBA-HA via an esterification reaction with di-t-butyl dicarbonate (BOC<sub>2</sub>O) as an activating agent with dimethylaminopyridine (DMAP)[14] for 20 hrs at 45°C. The final product (MeCLHA) was precipitated and washed in acetone, dissolved in DI water, dialyzed (MW cutoff 6-8k) for 24 hours at 4°C, lyophilized, and stored at -20°C in powder form prior to use. The intermediate and final macromer products were confirmed by <sup>1</sup>H NMR. Lyophilized macromers were dissolved in phosphate buffered saline (PBS) containing 0.05 wt% 2-methyl-1-[4-(hydroxyethoxy)phenyl]-2-methyl-1-propanone (I2959, Ciba) for photopolymerization.

#### *10.2.2 Acellular Characterization*

To monitor swelling and mechanical properties over time, acellular copolymer hydrogels of MeHA and MeCLHA were formed at various wt% ratios (5:0, 4:1, 3:2, 2:3, 2:0, 1.5:0.5, 1:1, 1:0) and incubated in PBS at 37°C. Wet and dry (after lyophilization) weights were recorded at each time point to determine volumetric swelling ratio, as described in chapter 4. The mechanical properties of the hydrogels were analyzed at various time points for up to 8 weeks in unconfined compression (Dynamic Mechanical Analyzer Q800, TA Instruments) in a PBS bath. Hydrogels were compressed at a rate of 10%/min until 60% of the initial thickness was reached. The modulus was determined as the slope of the stress versus strain profile at low strains (<20%).

#### *10.2.3 MSC Photoencapsulation and Culture*

For cell encapsulation, macromers were sterilized using a germicidal lamp in a laminar flow hood for 30 minutes prior to dissolving in a sterile solution of PBS containing 0.05 wt% I2959

for polymerization. Human MSCs (Lonza) were expanded to passage 4 in growth media consisting of  $\alpha$ -MEM with 16.7% FBS and 1% penicillin/streptomycin. MSCs were photoencapsulated (20 million cells/mL) in hydrogels (50  $\mu$ l) of varying macromer concentration (e.g., 5, 2, and 1 wt%) and type (e.g., MeHA, MeCLHA). Hydrogels consisting of 5:0, 4:1, 3:2, 2:3, 2:0, 1.5:0.5, 1:1, and 1:0 MeHA wt%: MeCLHA wt% (Table 10.1) were cultured in DMEM supplemented with 1% penicillin/streptomycin, 1% ITS+, 1mM sodium pyruvate, 40mg/ml L-proline, 100nM dexamethasone, 50 $\mu$ g/ml ascorbic acid 2-phosphate, and 10 ng/ml of TGF- $\beta$ 3 (chondrogenic media) for up to 8 weeks *in vitro*.

**Table 10.1** MeHA:MeCLHA hydrogel compositions

Total Macromer wt%	MeHA wt%	MeCLHA wt%
5	5	0
	4	1
	3	2
	2	3
2	2	0
	1.5	0.5
	1	1
1	1	0

#### 10.2.4 Cellular Characterization

The viability of MSCs in HA hydrogels was assessed using a live/dead cytotoxicity kit (Molecular Probes) at 1, 7 and 14 days and an Alamar Blue assay (Invitrogen) (n=3) at 7 and 14 days of *in vitro* culture according to manufacturer's instructions.

For short term gene expression analysis (3 and 14 days of culture), samples were homogenized in Trizol Reagent (Invitrogen) with a tissue grinder, RNA was extracted according to the manufacturer's instructions, and RNA concentration was determined using an ND-1000 spectrophotometer (Nanodrop Technologies). One microgram of RNA from each sample was reverse transcribed into cDNA using reverse transcriptase (Superscript II, Invitrogen) and oligoDT (Invitrogen). Polymerase chain reaction (PCR) was performed on an Applied Biosystems 7300 Real-Time PCR system using a 25 $\mu$ l reaction volume for Taqman (5'-nuclease) reactions.

Primers and probes specific for glyceraldehydes 3-phosphate dehydrogenase (GAPDH, housekeeping gene), type I and type II collagen, and aggrecan are listed in Chapter 8, Table 8.1. Relative gene expression was calculated using the  $\Delta\Delta C_T$  method, where fold difference was calculated using the expression  $2^{-\Delta\Delta C_T}$ . Results (n=4-8) from two replicate experiments were combined and samples with poor RNA quality were excluded.

Additional samples (n=5) were measured (diameter and height), weighed (wet weight) and tested in unconfined compression on a custom mechanical tester[15,16] after 1, 14, 35, and 56 days of culture. The mechanical tester consists of a computer-controlled stepper motor, a linear variable differential transformer to measure displacement, and a 250g load cell to measure load. Labview software (National Instruments) was used for stepper motor control and data acquisition. Samples were loaded between impermeable glass plates in creep with a 2g tare load until equilibrium (~300s), followed by stress relaxation with a single ramp displacement of 10% strain at a rate of 10%/minute. The samples were allowed to relax to equilibrium (~1200s), and the equilibrium confined compression moduli were calculated by dividing the equilibrium load by the area loaded and the % strain for each sample.

Mechanically tested samples were then lyophilized, weighed (dry weight), and digested in a proteinase K solution (200  $\mu$ g/ml proteinase K (Roche), 100mM ammonium acetate, pH 7.0) overnight at 60°C. Proteinase K was then inactivated at 100°C for 5 min. Total DNA, GAG, and collagen contents (n=5) were determined using the PicoGreen dsDNA Assay[17], the dimethylmethylene blue dye method[18] with chondroitin sulfate as a standard, and the hydroxyproline assay[19] using a collagen to hydroxyproline ratio of 7.25[20,21], respectively. The proteinase K digestion solution was used as a negative control.

Samples for histological analysis were fixed in 10% formalin for 24 hours, embedded in paraffin, and processed using standard histological procedures. The histological sections (7  $\mu$ m thick) were stained for chondroitin sulfate and collagen distributions using the Vectastain ABC kit (Vector Labs) and the DAB Substrate kit for peroxidase (Vector Labs). Sections were predigested in 0.5 mg/ml hyaluronidase for 30 min at 37°C and incubated in 0.5 N acetic acid for

4 hours at 4°C to swell the samples prior to overnight incubation with primary antibodies at dilutions of 1:100, 1:200, and 1:3 for chondroitin sulfate (mouse monoclonal anti-chondroitin sulfate, Sigma), and type I (mouse monoclonal anti-collagen type 1, Sigma) and type II collagen antibodies (mouse monoclonal anti-collagen type II, Developmental Studies Hybridoma Bank), respectively. Non-immune controls underwent the same procedure without primary antibody incubation.

#### *10.2.5 Statistical Analysis*

ANOVA with Tukey's post-hoc test was used to determine significant differences ( $p < 0.05$ ). All values are represented as the mean  $\pm$  standard deviation.

### **10.3 Results & Discussion**

The use of MSCs as a cell source for cartilage repair depends on the ability to form adequate neocartilage with the use of engineered materials. Due to the avascular nature of cartilage, native cartilage tissue and engineered constructs rely mainly on diffusion for nutrient supply and metabolic waste removal. With hydrogels, both the initial and temporal crosslinking densities control the diffusion of nutrients, wastes, and newly synthesized ECM proteins[4,22]. Thus, by developing techniques to better control network evolution with time, we may be able to improve overall tissue formation by encapsulated MSCs. In the previous chapter, we demonstrated the tunable degradation of the HA hydrogel system by the inclusion of hydrolytically degradable moieties. In this study, we investigated the effects of network evolution on *in vitro* neocartilage formation by encapsulated human MSCs in HA hydrogels.

#### *10.3.1 Acellular Characterization*

Coupled to changes in hydrogel degradation, the swelling and mechanical properties of the hydrogel change with time in these copolymer hydrogels. The use of copolymer hydrogels

were chosen to provide network stability while incorporating temporal degradation. Macromer concentrations (1, 2, and 5 wt%) were chosen based on cell viability, which was compromised at high crosslinking densities (Chapter 4), and the formation of a stable scaffold after photopolymerization, where concentrations lower than 1 wt% did not form a hydrogel. The solubility of MeCLHA dictated an upper limit to the various ratios of MeHA to MeCLHA. As both 2wt% MeLAHA and Hema-HA degraded rapidly, MeCLHA was chosen for further studies.

The elastic moduli of acellular hydrogels are dictated by total macromer concentration, macromer composition, and hydrogel degradation. Initial moduli (1 day after polymerization) significantly decreased with decreasing macromer wt% and decreases in moduli were observed over time coinciding with increased hydrogel degradation (Figure 10.1). The differences in elastic moduli within wt% groups (5, 2, and 1 wt%) between homopolymer and copolymer hydrogels can be attributed to different degrees of HA macromer modification, where MeHA modification was ~3 times greater than that of MeCLHA, or from degradation differences within the first 24 hours, which would both result in decreased crosslinking densities. In addition, slight temporal decreases in the elastic moduli of MeHA only (5:0, 2:0, 1:0) hydrogels were also observed.

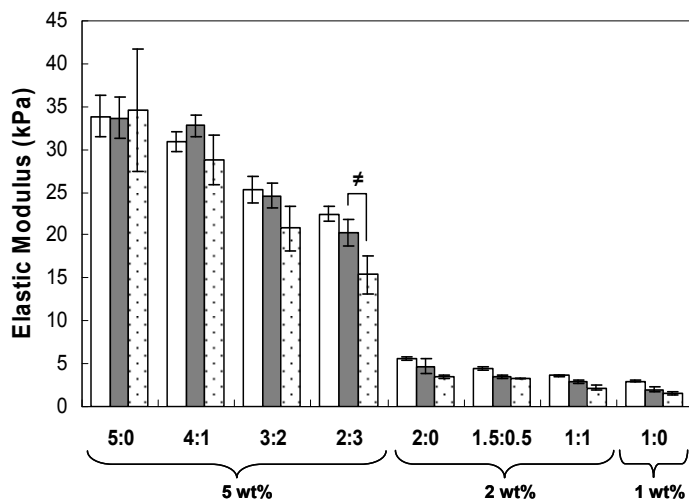


**Figure 10.1** Elastic moduli of MeHA:MeCLHA copolymer hydrogels at various wt% ratios for 1 (white), 7 (gray), and 14 (shaded) days. Significant difference ( $p < 0.05$ ) in moduli over time within each group is denoted by #.

The volumetric swelling ratios ( $Q_v$ ) were calculated from wet and dry weights of the hydrogel at specific time points and were found to be inversely related to total macromer



concentration and increased with incubation time ranging from  $32.5 \pm 2.5$  to  $68.5 \pm 3.6$  at day 1 and increasing to  $40.8 \pm 3.3$  to  $70.1 \pm 8.2$  by day 56 (Table 10.2). Initial volumetric swelling ratios within each wt% groups were insignificantly different, suggesting that macromer wt% plays a more prominent role in swelling than crosslinking density, where higher concentrations of the negatively charged HA macromer result in the greater retention of water within the hydrogel. However, as HA is released from the hydrogel via hydrolytic degradation, swelling ratios increase with the increased mesh size.

**Table 10.2** Volumetric swelling ratios (n=3). Values are reported as mean  $\pm$  standard deviation.

[Macromer]	wt% MeHA: wt% MeCLHA	$Q_v$ , t = 1 day	$Q_v$ , t = 56 day
5 wt%	5:0	$36 \pm 2$	$41 \pm 3$
	4:1	$37 \pm 4$	$42 \pm 5$
	3:2	$33 \pm 3$	$47 \pm 4$
	2:3	$36 \pm 2$	$52 \pm 2$
2 wt%	2:0	$51 \pm 14$	$63 \pm 6$
	1.5:0.5	$47 \pm 5$	$68 \pm 9$
	1:1	$67 \pm 3$	$67 \pm 2$
1 wt%	1:0	$68 \pm 4$	$70 \pm 8$

### 10.3.2 Cellular Characterization

The photoencapsulated MSCs retained rounded cell morphologies in all hydrogels. Viability assessed by live/dead staining indicated greater than 90% viability in hydrogels for cultures up to 14 days *in vitro* with only a slight increase in the fraction of dead cells for 5:0 hydrogels at day 14 (Figure 10.2). This slight decrease in viability in the 5:0 hydrogels (the most densely crosslinked of the hydrogels investigated) may have resulted from nutrient and waste diffusion limitations or increased radical concentrations during crosslinking, while the inclusion of a hydrolytically degradable component in copolymer counterparts allowed for the maintenance of cell viability. All groups showed comparable metabolic activity as measured by the Alamar blue assay up to 14 days of *in vitro* culture with the exception of a decrease in metabolic activity in 1:0

hydrogels from day 7 to day 14 (Figure 10.3). There were no significant increases or decreases in metabolic activity between day 7 and day 14 in all hydrogels, suggesting limited proliferation in these environments.

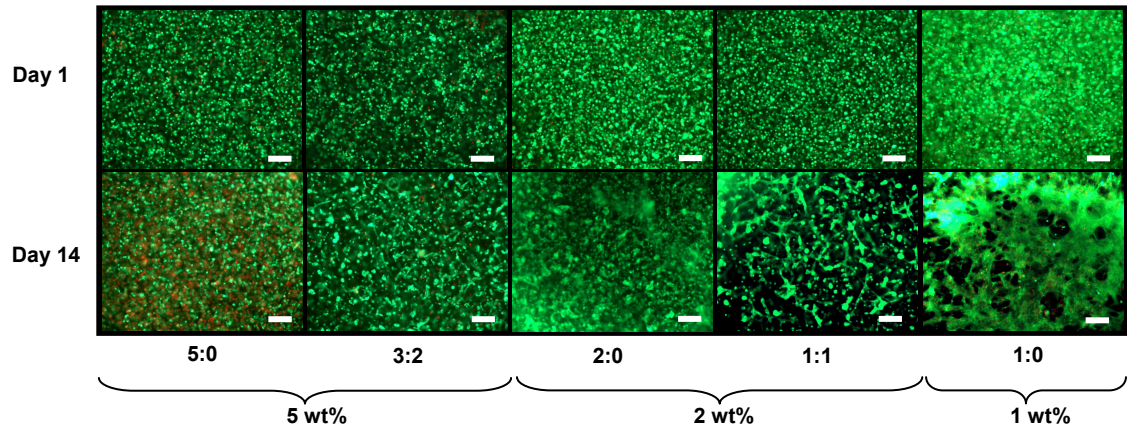


**Figure 10.2** Representative Live (green)/ Dead (red) stains of MeHA:MeCLHA copolymer hydrogels after 1 and 14 days of culture. Scale bar = 200 $\mu$ m.

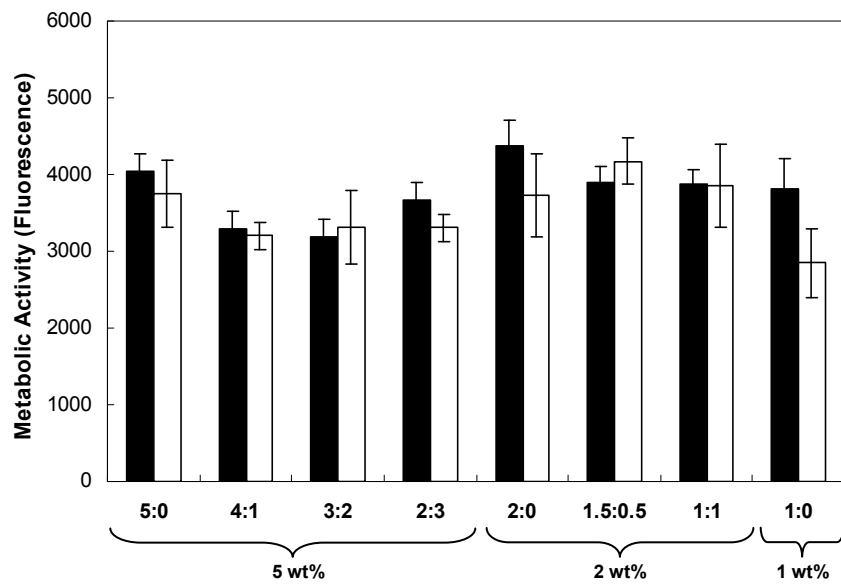


**Figure 10.3** Metabolic activity (n=3), as measured by Alamar blue assay, of MSC-laden HA constructs at 7 (black) and 14 (white) days of *in vitro* culture.

### 10.3.3 Gene Expression Analysis

Short-term gene expression for type I and type II collagen and aggrecan was assessed after 3 and 14 days of *in vitro* culture. Type II collagen and aggrecan are positive markers for chondrogenic differentiation, while type I collagen indicates transformation to a more fibrochondrocytic phenotype. Each sample was internally normalized to GAPDH, and each group was normalized to expression of MSCs isolated at the time of encapsulation (i.e., after expansion and before differentiation); thus, relative expression greater than 1 represents up-regulation with culture, while relative expression less than 1 represents down-regulation of that gene compared to that of initially encapsulated MSCs. No significant differences between groups were observed for type I collagen at either of the two time points, and overall expression of type I collagen was not significantly different compared to initially encapsulated MSCs (Figure 10.4A). Up-regulation of type II collagen (note that the plot is on a log-scale) and aggrecan expression was indicative of chondrogenic differentiation in all hydrogels and was found to be statistically higher at day 3 for the 1:1 and 1:0 hydrogels compared to all other groups (Figure 10.4). At day 14, an increasing trend of aggrecan expression in 2 wt% hydrogels was observed with increased MeCLHA content. Furthermore, the 1:1 hydrogels exhibited significantly higher type II collagen and aggrecan expression over both 2:0 and 1:0 hydrogels. Relative gene expression of type II collagen for 5, 2, and 1 wt% MeHA only hydrogels were also all significantly different from each other at day 14.

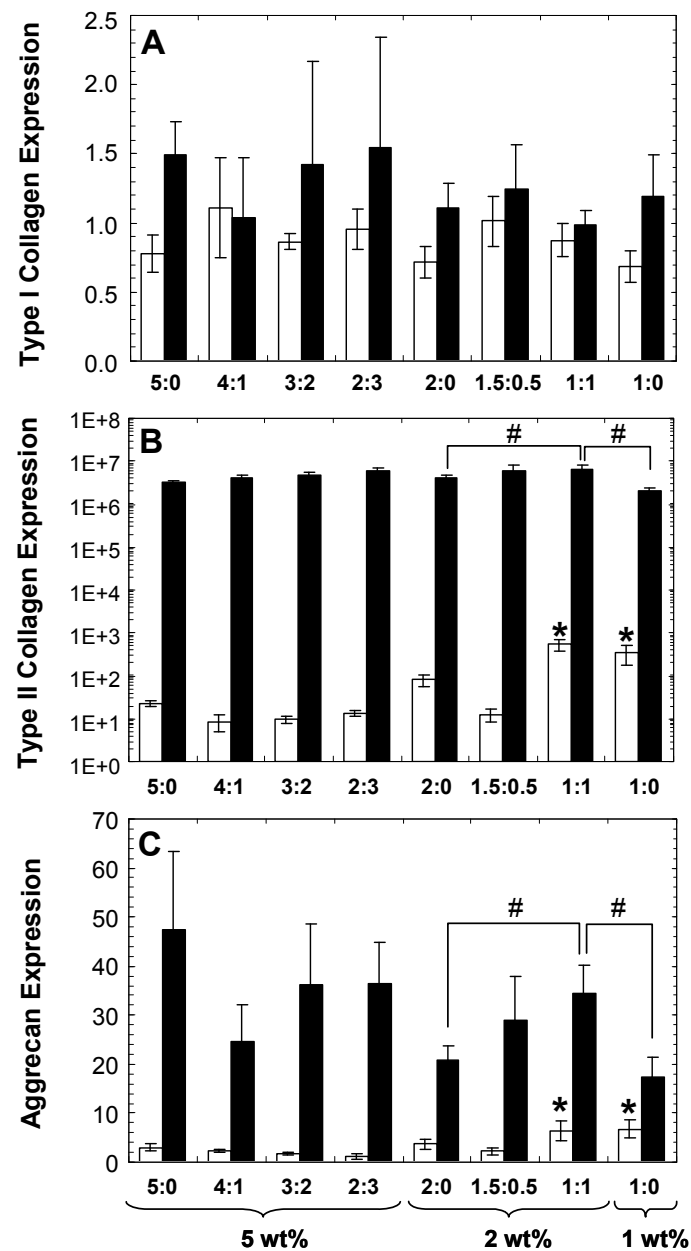


**Figure 10.4** Relative gene expression of (A) type I collagen, (B) type II collagen, and (C) aggrecan for all HA hydrogel formulations after 3 (white) and 14 (black) days of culture. Statistical analysis of relevant comparisons: \* denotes significant difference between starred groups and all other groups for the specified time point and # denotes significant difference between bracketed groups.

#### 10.3.4 Long-Term In Vitro Culture

With longer culture, samples demonstrated varying degrees of neocartilage formation; macroscopically, 2 and 1 wt% hydrogels were more opaque in appearance after 8 weeks of *in vitro* culture compared to higher wt% hydrogels (Figure 10.5 top). Significant differences in hydrogel diameters were observed among groups at various time points and within individual formulations with culture time. The initial hydrogel diameters were dependent on total macromer concentration, with significant decreases in diameter with decreased macromer wt%. As mentioned in the previous chapter, macromer wt% may play a more prominent role in initial hydrogel swelling and size than crosslinking density, where the higher concentrations of the negatively charged HA macromer result in the greater retention of water within the hydrogel. Though no significant differences in diameter were found within each 5, 2 and 1 wt% groups initially, regardless of the formulation; at later time points, a general trend of increased diameter was noticed in 5 wt% hydrogels with increased MeCLHA content (Figure 10.5A). Increased hydrogel diameters in 5 and 2 wt% groups over time reflect hydrogel degradation, as temporal decreases in crosslinking density allow for increased volumetric swelling, as well as ECM elaboration and neocartilage formation. Changes in height were less noticeable as height dimensions were smaller than corresponding diameter measurements and may have been limited by the measuring technique. With culture, all 5 and 2 wt% hydrogel diameters increased with culture time, while slight but insignificant increases in height for some compositions were also observed (Figure 10.5B). Overall, the most notable difference in hydrogels dimensions was seen with 1:0 hydrogels, as these hydrogels were significantly smaller in diameter and height compared to all other groups at every time point (Figure 10.5A and B). These differences in hydrogel dimensions may result from cell-scaffold interactions, where MSCs are able to undergo cellular condensation in the less crosslinked and weaker 1 wt% MeHA hydrogels.

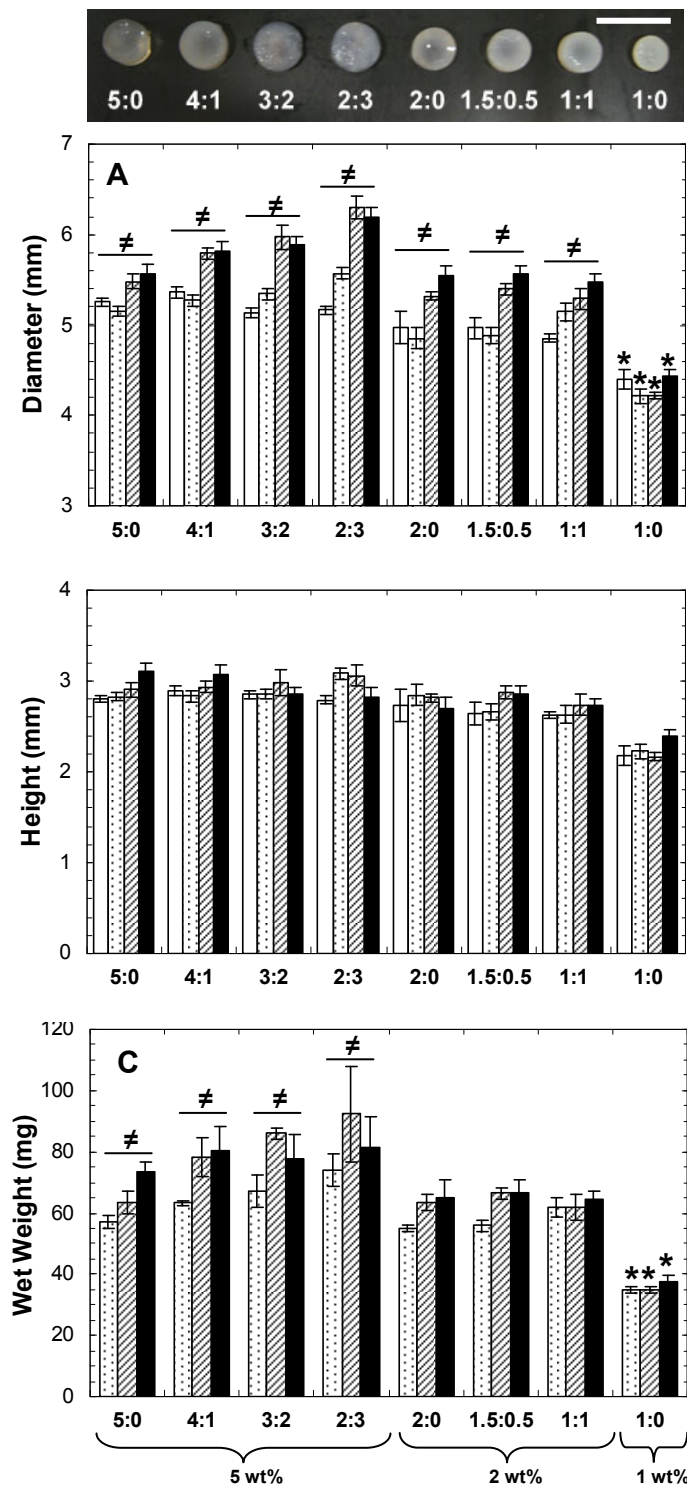


**Figure 10.5** Macroscopic appearance of constructs after 8 weeks of *in vitro* culture (scale bar = 1cm) (top). Diameter (A), height (B), and wet weight (C) of constructs after 1 (white), 14 (dotted), 35 (striped), and 56 (black) days of *in vitro* culture. Statistical analysis of relevant comparisons: \* denotes significant difference between starred groups and all other groups for the specified time point and # denotes significant difference over time within each group.

Trends in hydrogel dimensions were also correlated to hydrogel wet weight (Figure 10.5C). Again, wet weights of 1:0 hydrogels were significantly lower than all other groups at all time points. Also, a general trend in 5 wt% hydrogels of increased wet weight with increased MeCLHA content was observed, where at day 35 the wet weight of 5:0 hydrogels were significantly lower than that of all other 5 wt% hydrogels.

### *10.3.5 Mechanical Properties*

When mechanically tested in uniaxial, unconfined compression, changes in the compressive equilibrium modulus (Figure 10.6A) and the peak stress (Figure 10.6B) were observed among groups at each time point and within specific formulations over time. While initial moduli (day 1) was dictated by macromer concentration (similar to acellular hydrogels), moduli at day 35 and 56 was dictated by ECM production. 2 and 1 wt% samples exhibited an increase in moduli over time with significant increases at days 35 and 56. At day 35, 2 wt% hydrogels containing MeCLHA content (i.e., 1.5:0.5 and 1:1) exhibited moduli ( $30.4 \pm 2.3$  kPa and  $32.3 \pm 7.4$  kPa, respectively) that were both significantly higher than that of the MeHA only (i.e., 2:0 had moduli of  $14.4 \pm 2.3$  kPa) samples. By day 56, moduli of 1:1 ( $49 \pm 7$  kPa) and 1:0 ( $57 \pm 10$  kPa) samples were significantly greater than all other groups. However, there was little change in the mechanics among the 5 wt% formulations and the 4:1 hydrogels had the highest moduli of  $27 \pm 8$  kPa after 56 days. Furthermore, decreases in moduli for the 3:2 and 2:3 hydrogels were observed from day 35 to day 56. Peak stresses obtained during mechanical testing indicated similar trends as the compressive equilibrium moduli. Peak stress reflects water retention within the sample, and is usually an earlier indicator of functional matrix development. Again, peak stress increased with increased MeCLHA content in 2 wt% hydrogels. Peak stress obtained in 1:1 and 1:0 hydrogels were significantly greater than all other groups at days 35 and 56.

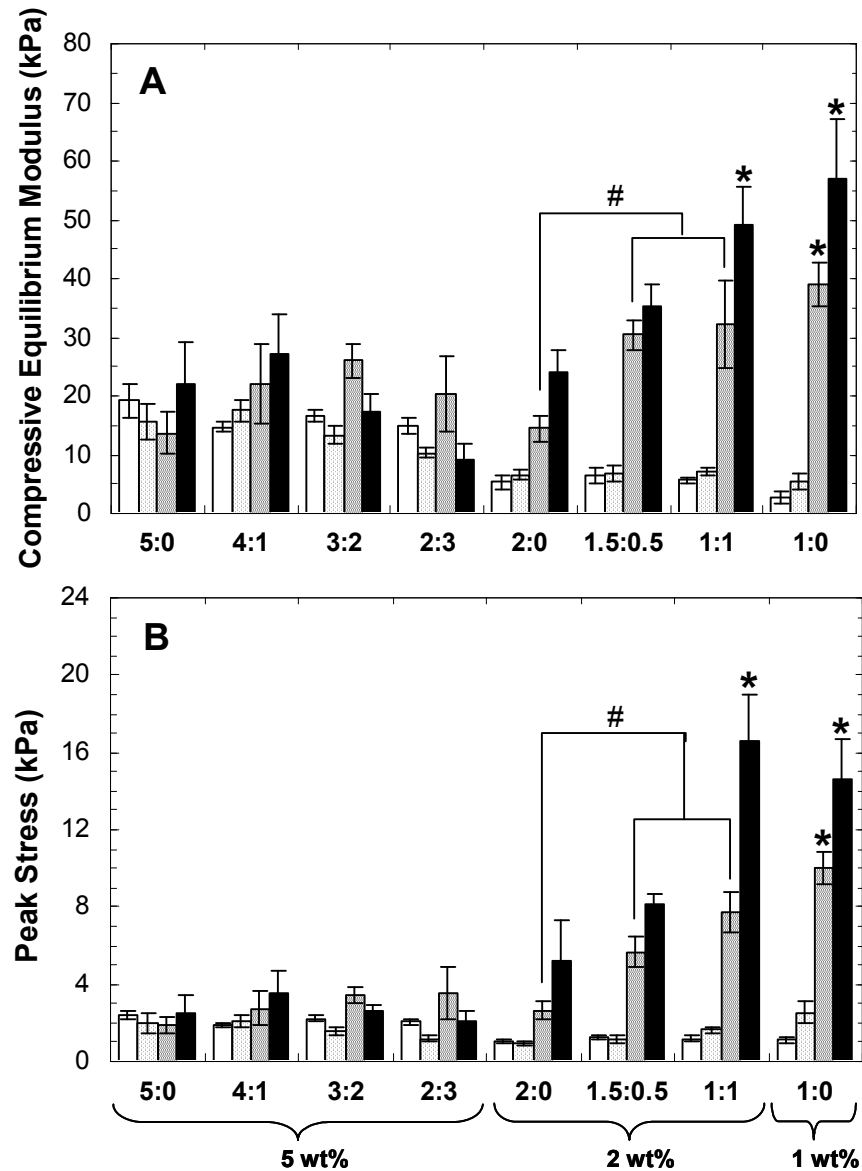


**Figure 10.6** Compressive equilibrium moduli (A) and peak stresses (B) of constructs at 1 (white), 14 (dotted), 35 (striped), and 56 (black) days of *in vitro* culture. Statistical analysis or relevant comparisons: \* denotes significant difference between starred groups and all other groups for the specified time point and # denotes significant differences between bracketed groups. Significant increases in both moduli and peak stresses over time within each formulation were also observed for all 2 and 1 wt% groups (not denoted). Significant decrease in moduli for 2:3 constructs from day 35 to day 56 was also observed (not denoted).



### 10.3.6 DNA and Biochemical Content

Mechanically tested samples were digested to determine DNA, sGAG, and collagen contents. DNA content remained relatively constant among all groups at each time point and within groups over time (Figure 10.7A). The only significant changes in DNA content were observed at day 56 with a decrease in DNA content for 3:2 and 2:3 groups. When normalized to DNA content, the GAG content in the samples showed significant changes between groups at each time point and within formulations over time (Figure 10.7B). Generally, GAG content increased within wt% formulations with increased MeCLHA content, with trends seen as early as 14 days. By day 35, MeHA only (5:0 and 2:0) hydrogels had significantly lower GAG content compared to their copolymer counterparts. By the end of the 8 week culture, the 1:1 hydrogels had the greatest GAG content and was significantly higher in GAG/DNA content ( $201 \pm 4.3$  mg/mg) than both 2:0 ( $169 \pm 22$  mg/mg) and 1:0 hydrogels ( $137 \pm 4.3$  mg/mg). No significant differences in collagen content were observed between groups at each time point. However, collagen content increased with culture time in all formulations, with 1.5:0.5 hydrogels attaining the highest collagen content ( $654 \pm 189$   $\mu$ g/sample) after 56 days.

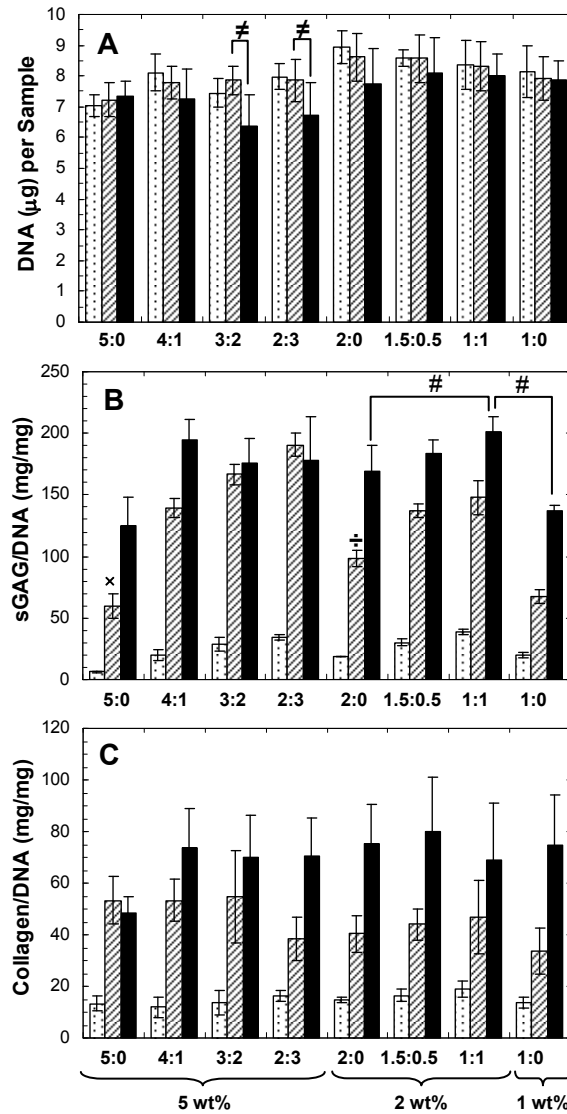


**Figure 10.7** DNA (A), sulfated GAG/DNA (B), and collagen/DNA (C) contents of constructs at 14 (dotted), 35 (striped), and 56 (black) days of *in vitro* culture. Statistical analysis of relevant comparisons: \* denotes significant difference between starred groups and all other groups for the specified time point, # denotes significant difference between bracketed groups, ≠ denotes significant difference over time between bracketed groups, ÷ denotes significant difference between marked group and all other 2wt% groups, and × denotes significant difference between marked group and all other 5 wt% groups. Significant increases in collagen/DNA content over time were observed for all groups (not denoted).

### 10.3.7 Immunohistochemical Analysis

Immunohistochemical staining of type I and type II collagen and chondroitin sulfate was performed on all groups at 14 and 56 days of culture. At day 14, pericellular staining of chondroitin sulfate was observed for MeHA only (5:0 and 2:0) hydrogels while greater distribution of staining was observed for their copolymer counterparts with increased distribution in hydrogels with increased MeCLHA content (Figure 10.8). By 56 days of culture, chondroitin sulfate was evenly distributed throughout the hydrogels for all groups. Hydrogels also stained positive for type II collagen in varying degrees for all groups with 5:0 hydrogels showing the least amount of staining compared to copolymer hydrogels showing the most staining (Figure 10.8). In general, type II collagen staining increased from 14 days to 56 days in all constructs. Clustering of type II collagen in copolymers was also observed. Little to no staining of type I collagen was present in all hydrogels and non-immune controls also stained negative.

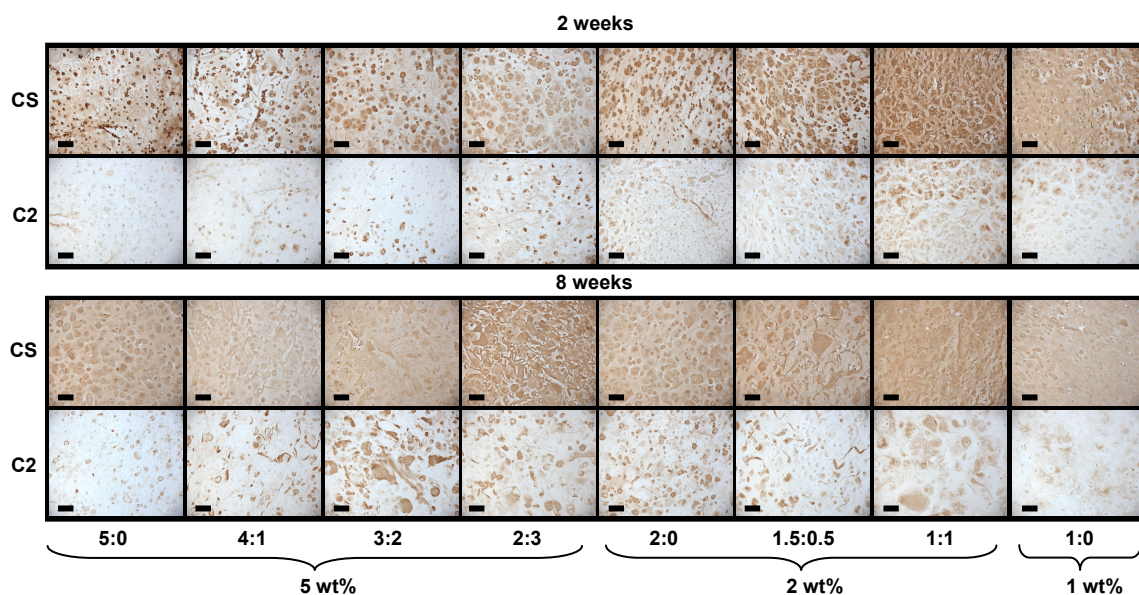


**Figure 10.8** Immunohistochemical staining of chondroitin sulfate (CS) and type II collagen (C2) of constructs after 2 and 8 weeks of culture. Scale bar = 100 $\mu$ m.

### *10.3.8 Importance of Degradation Rate*

In this study, it is important to note that the timing and rate of degradation is crucial for functional tissue development. If the degradation rate is faster than ECM deposition, large void spaces created by degradation can result in the loss of cells and ECM proteins into the culture medium. Specifically, the loss of GAGs from the hydrogel can result in compromised mechanical properties, as GAG content is highly correlated to the compressive modulus of native and engineered cartilage tissues[23]. In the case of the 5 wt% hydrogels, the compressive equilibrium moduli decreased in hydrogels with increased MeCLHA content (3:2 and 2:3 hydrogels) and there is no increased GAG accumulation within the hydrogels from day 35 to day 56 that is seen for all other groups. However, when degradation rate compliments the rate of ECM deposition and allows for the distribution of cartilaginous proteins within the hydrogel, compressive moduli increase, as observed in the 2 wt% hydrogels that show an increasing trend in moduli with increased MeCLHA content. Increased distribution of ECM proteins is visualized with immunohistochemical staining. Specifically, at 14 days of culture, staining clearly depicts increased distribution and quantity of chondroitin sulfate in hydrogels with increased MeCLHA content, and at 56 days of culture, increased type II collagen distribution reflects diffusion of larger ECM proteins. Faster and increased distribution of chondroitin sulfate over type II collagen reflect differences in protein size, where the smaller chondroitin sulfate diffuses with greater ease compared to the larger type II collagen fibers[24]. The decrease in acellular elastic moduli and the increase in biochemical content, equilibrium compressive moduli, and ECM distribution in the 2wt% copolymer hydrogels reflect a cooperative match in hydrogel degradation rate and ECM deposition.

### *10.3.9 Importance of a Dynamic Hydrogel*

Furthermore, this study emphasizes the importance of network evolution, where a hydrogel that starts at a higher wt% and decreases to a lower wt% is not equivalent to static

hydrogels that start at the higher or lower wt%. Specifically, the 1:1 hydrogels were shown to express up-regulation of type II collagen and aggrecan over the 2:0 and 1:0 hydrogels. Also of importance is hydrogel size and shape throughout culture time. Unlike the dramatic decreases in height and diameter of 1:0 hydrogels, which can pose problems in translation to clinical applications, the 1:1 hydrogels more closely retain their size and shape. With increased GAG/DNA content and size retention, the 1:1 hydrogels show greater promise as an MSC-laden scaffold for cartilage repair compared to 2:0 and 1:0 hydrogels. In addition, although matrix distribution is fairly consistent across groups by 8 weeks, early changes in gel structure are obviously important with respect to final construct properties.

To increase ECM deposition and distribution, others have tailored the degradation of engineered scaffolds. Poly(ethylene glycol) dimethacrylate (PEGDM) has been copolymerized with poly(lactic acid)-b-poly(ethylene glycol)-b-poly(lactic acid) end capped with acrylate groups (PEG-LA-DA) to form degradable PEG hydrogels. These chondrocyte-laden constructs showed increased collagen content and distribution in hydrogels with greater degradable content[9]. In addition, cell-dictated degradation via MMP-based matrix remodeling has been shown to up-regulate expression of type II collagen and aggrecan in MMP-sensitive PEG hydrogels with encapsulated bovine chondrocytes[11]. More recently, degradation triggered by exogenous addition of enzyme has also been explored. In a study by Ng *et al*, enzyme (agarase) treatment applied to agarose hydrogels resulted in elevated collagen content and dynamic compressive modulus after an initial loss of scaffold properties immediately after enzyme treatment[12]. Furthermore, Rice *et al*[13] showed that the timing and duration of enzyme (lipase) addition to PEG hydrogels with caprolactone blocks greatly affected cartilaginous matrix properties.

Like others, we showed that the inclusion of hydrolytically degradable linkages in crosslinked hydrogels results in increased ECM deposition and distribution by encapsulated cells. However, this study focuses specifically on the use of MSCs, rather than isolated chondrocytes. We showed clear increasing trends in sGAG/DNA content with degradable content for the 2 wt% groups compared to trends in collagen/DNA content. While sGAG and collagen content still pale

in comparison to native cartilage tissue (composed of 2-10% sGAG/wet weight and 5-30% collagen/wet weight[25]), we showed improvements in sGAG content/wet weight and increasing equilibrium moduli in the 2wt% hydrogels with increasing MeCLHA content. In addition, the properties of the 2wt% hydrogels continued to improve (increased biochemical content and moduli) during the course of this study rather than reaching a plateau that had been seen in MSC-laden agarose hydrogels[2]. This could suggest that the dynamic HA hydrogel environment may enhance the potential of neocartilage maturation.

By developing dynamic hydrogels based on HA, a linear polysaccharide found natively in cartilage, we also capitalize on the biological advantages of this molecule. During development, HA regulates a variety of cellular functions (e.g., gene expression, signaling, proliferation, motility, adhesion, and morphogenesis)[26], where HA interactions are MW dependent and mediated through cell surface receptors (e.g., CD44, ICAM-1, and RHAMM)[27,28]. Thus, HA-based hydrogels have the potential to interact with encapsulated cells via cell surface receptors, and HA macromers released from the hydrogel can serve as biological cues that have the potential to initiate cell signaling pathways or sequester proteoglycan aggregates. The ability to tailor HA macromer release through controlled hydrogel degradation during cartilage repair may play an important role in mimicking the natural time course of cartilage formation and maturation. In native cartilage, HA turns over rapidly with a half-life of 1-3 weeks[29,30]. Primarily degraded by hyaluronidases (HYAL1, HYAL2, and HYAL3), HA macromers are broken down into HA fragments, which can also induce the expression of MMP-3[31] and nitric oxide synthase[32], synergizing the breakdown and remodeling process. With HA-based hydrogels, these enzymes and other cell-generated reactive oxygen species can assist in the complete breakdown and remodeling of the scaffold over time. Though the degradation products of these hydrogels yield HA fragments with kinetic chain fragments, we believe that some HA biological cues are imparted on encapsulated MSCs, as Chapter 8 has previously shown that HA chemistry can enhance chondrogenesis[7]. The soluble delivery of HA from these hydrogels would be an added benefit, but was not explored within the scope of this study. However, in this study, we do show that

temporal network structure can influence neocartilage formation within HA hydrogels *in vitro*. Thus, a photocrosslinkable scaffold with a dynamic network structure, biological relevance, and the ability to support MSC chondrogenesis, as a potential candidate for cartilage repair, was developed.

#### **10.4 Conclusions**

This study indicates that the tuning of temporal scaffold properties can be used to control neocartilage production by MSCs in HA hydrogels. The faster degrading MeCLHA component of the hydrogel increases the mesh size and creates void spaces, allowing for the deposition and enhanced distribution of newly synthesized ECM proteins, while the MeHA component provides structural support, maintaining the size and shape of the scaffold, until it is eventually degraded and remodeled by the encapsulated cells. The timing of hydrogel degradation is important since rapid degradation may result in the reduced retention of ECM proteins, whereas hydrogels that degrade too slowly can inhibit tissue formation and distribution. Thus, a careful balance of slow and fast degrading components is needed for optimal growth. Here, the 1:1 hydrogels, with increased mechanical properties and biochemical content over time, while retaining construct size, show great potential as a scaffold to support the production of functional cartilage tissue by MSCs.

**References:**

- [1] Chung C, Burdick JA. Engineering cartilage tissue. *Adv Drug Deliver Rev* 2008;60(2):243-62.
- [2] Mauck RL, Yuan X, Tuan RS. Chondrogenic differentiation and functional maturation of bovine mesenchymal stem cells in long-term agarose culture. *Osteoarthritis and Cartilage* 2006;14(2):179-89.
- [3] Smeds KA, Pfister-Serres A, Miki D, Dastgheib K, Inoue M, Hatchell DL, et al. Photocrosslinkable polysaccharides for in situ hydrogel formation. *J Biomed Mater Res* 2001;54(1):115-21.
- [4] Burdick JA, Chung C, Jia XQ, Randolph MA, Langer R. Controlled degradation and mechanical behavior of photopolymerized hyaluronic acid networks. *Biomacromolecules* 2005;6(1):386-91.
- [5] Chung C, Erickson IE, Mauck RL, Burdick JA. Differential behavior of auricular and articular chondrocytes in hyaluronic acid hydrogels. *Tissue Eng Pt A* 2008;14(7):1121-31.
- [6] Chung C, Mesa J, Randolph MA, Yaremchuk M, Burdick JA. Influence of gel properties on neocartilage formation by auricular chondrocytes photoencapsulated in hyaluronic acid networks. *J Biomed Mater Res A* 2006;77A(3):518-25.
- [7] Chung C, Burdick JA. Influence of three-dimensional hyaluronic Acid microenvironments on mesenchymal stem cell chondrogenesis. *Tissue Eng Pt A* 2009;15(2):243-54.
- [8] Erickson IE, Huang AH, Chung C, Li RT, Burdick JA, Mauck RL. Differential maturation and structure-function relationships in mesenchymal stem cell- and chondrocyte-seeded hydrogels. *Tissue Eng Pt A* 2009;15(5):1041-52.
- [9] Bryant SJ, Anseth KS. Controlling the spatial distribution of ECM components in degradable PEG hydrogels for tissue engineering cartilage. *J Biomed Mater Res A* 2003;64A(1):70-9.
- [10] Lutolf MP, Lauer-Fields JL, Schmoekel HG, Metters AT, Weber FE, Fields GB, et al. Synthetic matrix metalloproteinase-sensitive hydrogels for the conduction of tissue



regeneration: Engineering cell-invasion characteristics. P Natl Acad Sci USA 2003;100(9):5413-8.

- [11] Park Y, Lutolf MP, Hubbell JA, Hunziker EB, Wong M. Bovine primary chondrocyte culture in synthetic matrix metalloproteinase-sensitive poly(ethylene glycol)-based hydrogels as a scaffold for cartilage repair. Tissue Eng 2004;10(3-4):515-22.
- [12] Ng KW, Kugler LE, Doty SB, Ateshian GA, Hung CT. Scaffold degradation elevates the collagen content and dynamic compressive modulus in engineered articular cartilage. Osteoarthritis Cartilage 2009;17(2):220-7.
- [13] Rice MA, Anseth KS. Controlling cartilaginous matrix evolution in hydrogels with degradation triggered by exogenous addition of an enzyme. Tissue Eng 2007;13(4):683-91.
- [14] Goossen LJ, Dohring A. A convenient protocol for the esterification of carboxylic acids with alcohols in the presence of di-t-butyl dicarbonate. Synlett 2004;(2):263-6.
- [15] Mauck RL, Wang CCB, Oswald ES, Ateshian GA, Hung CT. The role of cell seeding density and nutrient supply for articular cartilage tissue engineering with deformational loading. Osteoarthritis and Cartilage 2003;11(12):879-90.
- [16] Soltz MA, Ateshian GA. Experimental verification and theoretical prediction of cartilage interstitial fluid pressurization at an impermeable contact interface in confined compression. J Biomech 1998;31(10):927-34.
- [17] Singer VL, Jones LJ, Yue ST, Haugland RP. Characterization of PicoGreen reagent and development of a fluorescence-based solution assay for double-stranded DNA quantitation. Anal Biochem 1997;249(2):228-38.
- [18] Farndale RW, Sayers CA, Barrett AJ. A direct spectrophotometric microassay for sulfated glycosaminoglycans in cartilage cultures. Connect Tissue Res 1982;9(4):247-8.
- [19] Stegemann H, Stalder K. Determination of hydroxyproline. Clin Chim Acta 1967;18(2):267-73.

- [20] Herbage D, Bouillet J, Bernengo JC. Biochemical and physiochemical characterization of pepsin-solubilized type-II collagen from bovine articular cartilage. *Biochem J* 1977;161(2):303-12.
- [21] Williamson AK, Chen AC, Sah RL. Compressive properties and function-composition relationships of developing bovine articular cartilage. *J Orthop Res* 2001;19(6):1113-21.
- [22] Bryant SJ, Nuttelman CR, Anseth KS. The effects of crosslinking density on cartilage formation in photocrosslinkable hydrogels. *Biomed Sci Instrum* 1999;35:309-14.
- [23] Pfeiffer E, Vickers SM, Frank E, Grodzinsky AJ, Spector M. The effects of glycosaminoglycan content on the compressive modulus of cartilage engineered in type II collagen scaffolds. *Osteoarthritis and Cartilage* 2008;16(10):1237-44.
- [24] Buxton AN, Zhu J, Marchant R, West JL, Yoo JU, Johnstone B. Design and characterization of poly(ethylene glycol) photopolymerizable semi-interpenetrating networks for chondrogenesis of human mesenchymal stem cells. *Tissue Eng* 2007;13(10):2549-60.
- [25] Muir H. The chemistry of the ground substance of a joint cartilage. In: Sokoloff L, editor. *The Joints and Synovial Fluid*. New York: Academic Press, 1980. p. 27-94.
- [26] Kogan G, Soltes L, Stern R, Gemeiner P. Hyaluronic acid: a natural biopolymer with a broad range of biomedical and industrial applications. *Biotechnol Lett* 2007;29(1):17-25.
- [27] Knudson CB, Knudson W. Hyaluronan-Binding Proteins in Development, Tissue Homeostasis, and Disease. *Faseb J* 1993;7(13):1233-41.
- [28] Menzel EJ, Farr C. Hyaluronidase and its substrate hyaluronan: biochemistry, biological activities and therapeutic uses. *Cancer Lett* 1998;131(1):3-11.
- [29] Morales TI, Hascall VC. Correlated Metabolism of Proteoglycans and Hyaluronic-Acid in Bovine Cartilage Organ-Cultures. *J Biol Chem* 1988;263(8):3632-8.
- [30] Ng CK, Handley CJ, Preston BN, Robinson HC. The Extracellular Processing and Catabolism of Hyaluronan in Cultured Adult Articular-Cartilage Explants. *Arch Biochem Biophys* 1992;298(1):70-9.

- [31] Ohno S, Ohno-Nakahara M, Knudson CB, Knudson W. Induction of MMP-3 by hyaluronan oligosaccharides in temporomandibular joint chondrocytes. *J Dent Res* 2005;84(11):1005-9.
- [32] Iacob S, Knudson CB. Hyaluronan fragments activate nitric oxide synthase and the production of nitric oxide by articular chondrocytes. *Int J Biochem Cell B* 2006;38(1):123-33.

## CHAPTER 11

### *Conclusions, Limitations, and Future Directions*

#### **11.1 Conclusions**

*Aim 1: Synthesize and characterize photocrosslinked methacrylated hyaluronic acid hydrogels.*

A cartilage tissue engineering (TE) scaffold was developed based on a natural polysaccharide found natively in cartilage tissue, called hyaluronic acid (HA). To form a covalently crosslinked network, hydroxyl groups on the HA backbone were methacrylated, yielding double bonds that could participate in photoinitiated polymerization, creating stable, yet enzymatically degradable HA (MeHA) hydrogels. Properties of the hydrogel could then be tuned by varying molecular weight, macromer concentration, and degree of modification. Increases in molecular weight decreased the efficiency of the methacrylation reaction and increased the viscosity of the prepolymer solution, while effects of molecular weight on swelling, mechanics, and degradation were insignificant. Increases in macromer concentration, however, had more profound effects on hydrogel properties, resulting in increased elastic moduli and degradation times (in the presence of hyaluronidase), and decreased volumetric swelling ratios, which can be correlated to crosslinking density and hydrogel mesh size. Therefore, with tunable properties, MeHA hydrogels could be tailored and applied to a variety of applications.

In particular, for application in cartilage TE, these hydrogel properties affected chondrocyte viability and neocartilage formation. Hydrogels with increased HA molecular weight yielded inhomogeneities in cell and extracellular matrix (ECM) distribution within the hydrogel due to the viscosity of the prepolymer solution, while increased macromer concentration resulted in cell death due to limitations in nutrient and waste diffusion and greater radical concentrations during photopolymerization. The greatest cell viability and ECM deposition was observed in the 2 wt% MeHA hydrogels; and in particular, the 50 kDa group had the most homogenous distribution of both chondrocytes and ECM. Within these hydrogels, chondrocytes maintained a rounded

morphology and continued to deposit cartilage specific matrix proteins when cultured subcutaneously *in vivo*.

*Aim 2: Investigate cellular response and neocartilage formation of encapsulated chondrocyte and mesenchymal stem cells in photocrosslinked HA hydrogels.*

What a cell senses from its surrounding can dictate its behavior and response. Once removed from their native environment, harvested cells are exposed to stimulation from a variety of environments. This may include: growth on tissue culture polystyrene (TCPS) in 2D during cell expansion, culture in a cell pellet at high densities with high cell-cell contact, and encapsulation in 3D scaffolds where cell-scaffold interactions can also impart different cellular cues. This change from their native environment can negatively or positively influence cell phenotype, growth, and biosynthesis.

Due to the limited availability of cartilage tissue for cell isolation and the small percentage of the tissue comprised by chondrocytes, the need to expand chondrocytes *in vitro* is indisputable if chondrocytes are to be considered as a viable cell source in strategies for cartilage repair. However, for harvested chondrocytes, expansion in 2D on TCPS can result in dedifferentiation, characterized by a loss in cell morphology and the increased expression and production of type I collagen [1,2]. The encapsulation of *in vitro*-expanded chondrocytes in MeHA hydrogels led to compromised neocartilage formation (i.e., biochemical content and biomechanical properties) *in vivo* (in subcutaneous culture) as early as the second passage, i.e. chondrocytes that had been expanded twice in 2D on TCPS after the initial harvest.

In addition, chondrocyte behavior in MeHA hydrogels was highly dependent on the tissue source of the chondrocyte. Various types of cartilage (elastic, hyaline, and fibrocartilage) are found in different parts of the body, and chondrocytes isolated from each region serve specific functions and differ in their response to stimuli. This was demonstrated as auricular (from the ear) and articular (from the knee) chondrocyte behavior differed when cultured in MeHA hydrogels exposed to different culture conditions (static *in vitro* culture, subcutaneous *in vivo*

culture, and exposure to cyclic compression *in vitro*). Though both auricular and articular chondrocytes demonstrated good viability in MeHA hydrogels, they exhibited differences in metabolic activity and phenotype retention as illustrated by the temporal changes in the expression of cartilage specific genes *in vitro*. In subcutaneous culture, encapsulated auricular chondrocyte succeeded in producing more functional matrix, with mechanical properties of the constructs increasing over time, compared to the articular chondrocyte group. However, when mechanically stimulated in MeHA gels *in vitro*, to more closely simulate the loaded environment of the knee joint, articular chondrocytes exhibited greater up-regulation of type II collagen and aggrecan compared to auricular chondrocytes. Thus, similar to what others have observed [3-9], differences in cartilage tissue source yield diverse chondrocytes that respond differently to specific environments. While this aim only investigated the differential response of chondrocyte type in MeHA hydrogels, it is important to remember that the TE scaffold itself can play a large role in the success of each chondrocyte type[10].

As the use of chondrocytes in cartilage TE is limited clinically, many investigators have turned to exploring the potential of mesenchymal stem cells (MSCs). During embryogenesis, MSCs are surrounded by a dynamic matrix in which HA of varying molecular weights play specific roles in limb development[11,14]. *In vitro*, substrate bonded HA has been shown to stimulate MSC chondrogenic differentiation. HA can interact directly with cells via surface receptors or indirectly through the binding of other matrix proteins or structuring water for cell exclusion to encourage cell aggregation. Given the presence of HA in MSC chondrogenic differentiation, the developed HA-based hydrogel was hypothesized to provide an advantageous environment for MSC chondrogenic differentiation. *In vitro* culture of MSC-laden MeHA hydrogels demonstrated that these hydrogels supported MSC chondrogenesis with the addition of soluble TGF- $\beta$ 3. Comparisons with an inert, photocrosslinked PEG hydrogel implied that HA hydrogel chemistry can enhance chondrogenesis, and microarray data suggests that the HA chemistry can lead to up-regulation of matrix stabilizers (e.g. collagens, HA link protein, matrilins) to improve and sustain chondrogenic differentiation.

*Aim 3: Develop hydrolytically degradable HA macromers to enhance ECM deposition and distribution.*

Despite the ability of MeHA hydrogels to permit and promote MSC chondrogenesis, ECM accumulation was predominantly limited to pericellular regions. This pericellular localization of ECM can result from diffusional limitations of the large proteins in the hydrogel and delay construct maturation. By incorporating faster, hydrolytically degradable moieties into the hydrogel, pores created during hydrogel degradation can improve the distribution of deposited ECM, resulting in improved construct properties[12,13].

To this end, hydrolytically cleavable ester linkages were added between the HA backbone and the reactive methacrylate group to form methacrylated lactic acid (MeLA), methacrylated caprolactone (MeCL) and hydroxyethyl methacrylate (HEMA) HA. By altering the chemistry and the number of repeat units of the hydrolytically degradable group, the degradation rate of the hydrogel could be controlled. The inclusion of more ester linkages resulted in faster degradation (but lower solubility), while the addition of a more hydrophobic group (e.g., CL versus LA) resulted in slower degradation. Hydrogels made entirely of these hydrolytically degradable HA macromers completely degraded in phosphate buffered saline (PBS) without the addition of hyaluronidase enzyme over a period of days to weeks. Similar to the MeHA hydrogels, increases in macromer concentration increased the time for complete degradation, as more crosslinks created during the polymerization need to be broken. With time, ester linkages within the hydrogel are cleaved, resulting in larger mesh sizes, swelling of the hydrogel, and a loss of mechanical properties.

When seeded with MSCs, the inclusion of hydrolytically degradable units improved the ECM distribution within the hydrogels, but the stability of the hydrogel was compromised when the ratio of hydrolytically degradable HA (MeLAHA, MeCLHA, HEMA-HA) to enzymatically degradable HA (MeHA) was too high. In addition, rapid hydrolytic degradation can result in the loss of cells and sulfated glycosaminoglycans (GAGs), which leads to compromised mechanical properties, as in the case of MeHA:MeCLHA copolymer hydrogels of 3:2 and 2:3 compositions.

However, when temporal degradation is appropriately timed, increases in the mechanical properties of the constructs reflect the increased deposition of GAGs and the increased distribution of ECM within the hydrogel; and indicate the development of functional tissue.

Importantly, the development of a “dynamic” hydrogel, or a hydrogel whose mesh size changes over time as a result of degradation, can be superior to a “static” hydrogel, or pure MeHA hydrogels that are stable and slow degrading. This is demonstrated by the up-regulation of cartilage specific genes and subsequent increased deposition of cartilage specific ECM proteins in the 1:1 MeHA:MeCLHA hydrogels over the 2:0 and 1:0 MeHA only hydrogels. These 1:1 hydrogels allowed for the diffusion of ECM proteins within the construct over time and provided structural stability to prevent the contraction of the hydrogel by MSCs. After 8 weeks of *in vitro* culture, mechanical properties of the 1:1 hydrogel continued to improve without signs of plateau. Thus, the material design of the hydrogel was vital in the transformation of MSCs to chondrocytes and in the production of functional matrix.

## **11.2 Limitations**

While this dissertation explores the development and characterization of HA hydrogels for cartilage regeneration, several limitations to these studies must also be considered. Though lightly touched upon, the biological significance of HA was not explored in detail, as only the tip of the surface was grazed on its interaction with cells and its potential role in MSC chondrogenesis. Additionally, the release of HA (alone or with kinetic chain fragments) from the hydrogels may initiate cell signaling pathways, as molecular weight-dependent HA fragments dictate varied cellular processes in embryogenesis and natural wound healing [14,15]. However, the effects of the attached kinetic fragments (be it stimulatory, inhibitory, or insignificant) in the MeHA components on the HA-cell interaction remains unexplored. Also, the complete degradation and remodeling of HA-based hydrogels was not fully characterized *in vivo*. As HA degradation can occur by free radicals generated in a number of chemical and enzymatic reactions [16] and is



also managed by hyaluronidases that reside within the cell [15], the degradation of these hydrogels can be dictated by both encapsulated cells and the local environment surrounding the hydrogel. Thus, the *in vitro* degradation of the hydrogels in PBS with and without exogenous hyaluronidase at 37°C served primarily as a material characterization parameter rather than a discrete timeline for hydrogel degradation.

Secondly, the delivery of transforming growth factor- $\beta$  (TGF- $\beta$ 3) needs attention as we look towards the desired *in situ* polymerization of these HA-based hydrogels or implantation of immature constructs for clinical application, particularly with MSCs. With a shift from *in vitro* culture (the primary culture method used in this dissertation for MSCs) to an *in vivo* environment (for clinical application), controlled delivery of soluble TGF- $\beta$ 3 to the encapsulated MSCs provides a challenge that needs to be solved, and was not addressed in this research. While the water swollen network provides a good medium for the passive diffusion of nutrients and growth factors during *in vitro* culture, the facile diffusion of directly encapsulated molecules out of the hydrogel diminishes the availability and influence of these molecules on encapsulated cells *in vivo*. Various methods and ideas for growth factor delivery are addressed and discussed in future directions (Section 11.3). Here, concentration, availability, and activity of the growth factor must be sufficient to induce chondrogenic differentiation of MSCs, promote their continued maturation into chondrocytes, and induce matrix formation into a functional tissue.

A final limitation to this work is the lack of assessment of the cell-laden HA hydrogels in a clinically relevant defect model. Subcutaneous culture in nude mice was used to gauge the ability of chondrocytes and MSCs to produce neocartilage tissue in an *in vivo* environment, but this fails to mimic the mechanical loads and inflammatory molecules (e.g. cytokines) that are present in an injured or diseased cartilage defect site of the knee or hip. Local stimuli (mechanical or soluble) can alter cell response and tissue formation. In addition, without a defect model, integration of the scaffold with the surrounding native cartilage during repair *in vivo* was not examined. Without adequate integration of the scaffold with the surrounding native cartilage, complete repair can be compromised as the hydrogel may not be secure in the defect site. However, it would have been

premature to initiate this analysis until questions regarding growth factor delivery were addressed for this system.

### 11.3 Future Directions

#### 11.3.1 TGF- $\beta$ 3 Delivery

As mentioned in the previous section (11.2), the delivery of TGF- $\beta$  *in vivo* remains a challenge. Members of the TGF- $\beta$  superfamily of growth factors play a major role in bone and cartilage development. In a study by Heine *et al.*, immunohistochemical staining for TGF- $\beta$  in developing mouse embryos demonstrated localization of TGF- $\beta$  in tissues derived from the mesenchyme. Intense staining was observed during the remodeling of these tissues, as during the formation of digits from limb buds [17]. This demonstrated TGF- $\beta$ 's importance in mesenchyme cell differentiation and its regulation of ECM synthesis. Accordingly, since then, TGF- $\beta$ s have been shown to induce a chondrogenic response in a variety of cells (chondrocytes [18-20], MSCs [21-23], fibroblasts [24]), resulting in the up-regulation of chondrocytic markers and subsequent deposition of sulfated glycosaminoglycan (sGAG) and collagen.

Three different isoforms of TGF- $\beta$  (TGF- $\beta$ 1, TGF- $\beta$ 2, and TGF- $\beta$ 3) have been discovered in mammalian species, and these isoforms can differ in their effects on chondroprogenitor cells [25-28]. TGF- $\beta$ 1 is responsible for initial cell-cell interaction between condensing progenitor cells, and stimulates new matrix synthesis by chondrocytes [28]. TGF- $\beta$ 2 regulates hypertrophic differentiation of chondrocytes via Indian hedgehog (Ihh) and parathyroid growth hormone peptide (PTHrP) expression[25]. While all isoforms of TGF- $\beta$  can induce chondrogenesis in human bone marrow derived MSCs, a study by Barry *et al.* showed that TGF- $\beta$ 2 and - $\beta$ 3 are able to produce more rapid accumulations of proteoglycan and type II collagen compared to TGF- $\beta$ 1 [29].

In chapter 8, human MSCs were shown to undergo chondrogenesis in HA hydrogels *in vitro* with the addition of soluble TGF- $\beta$ 3 delivered via the culture media. For *in vivo* studies, TGF- $\beta$ 3 was encapsulated directly in the hydrogels during photopolymerization, where the high water content of the hydrogel can mimic the environment of native soft tissue, providing a suitable means to deliver bioactive molecules. While short-term gene expression showed up-regulation of cartilage specific markers, immunohistochemical staining demonstrated lesser degrees of matrix accumulation compared to *in vitro* cultured hydrogels. With direct encapsulation, growth factor release is controlled by diffusion; and the highly permissible nature of the hydrogel can lead to its rapid initial release, which decreases the concentration of growth factor seen by the encapsulated cells. Additionally, *in vivo* culture with direct growth factor encapsulation lacks the luxury of growth factor delivery at a constant concentration over an extended period of time, which can compromise chondrogenesis.

As a result, a variety of growth factor delivery methods have been investigated. These include the use of microspheres[30-33], covalent tethers [34], affinity ligands[35], biomimetic peptides[36] and adenoviruses[37]. Growth factor-loaded microspheres can provide additional control over TGF- $\beta$  release and have been delivered in both hydrogels[19] and pellet cultures[32]. Previous work by Mann *et al.* has shown the ability to tether TGF- $\beta$ 1 to stimulate ECM production in poly(ethylene glycol) (PEG) hydrogels[34]. Furthermore, the incorporation of degradable linkers between the tether and the bioactive molecule allow for pre-determined liberation and controlled release rates[38,39]. Although covalent tethering provides an effective means to control the availability of the growth factor, covalent conjugation may also reduce growth factor bioactivity, as presentation of the protein to the cell can be altered. Recently, ligands that reversibly bind TGF- $\beta$  have been targeted as a means to sequester growth factors. One such ligand is heparin [35], which binds to a broad variety of growth factors via non-specific electrostatic interactions. However, its potential immunogenicity and binding of numerous proteins may complicate release *in vivo*; thus, the incorporation of biomimetic peptides have been explored as another alternative method of growth factor delivery. In a study by Hao *et al*, rat bone marrow derived MSCs

transfected with a recombinant adenovirus encoding TGF- $\beta$ 3 were encapsulated in agarose hydrogels, and were shown to express type II collagen on days 2 and 3 post infection[37].

A pilot study was completed to address growth factoring sequestering in HA hydrogels. In Chapter 10, the inclusion of degradable HA was shown to increase functional matrix deposition and distribution *in vitro*. However, *in vivo*, temporal degradation can accelerate the diffusion of encapsulated TGF- $\beta$ 3 *in vivo* and compromise the benefits of the dynamic hydrogel. When hydrogels of 2:0, 1:1 and 1:0 MeHA wt%: MeCLHA wt% were used to encapsulate MSCs and TGF- $\beta$ 3 (10ng/gel), the 2:0 hydrogels, with the highest crosslinking density of the three groups, exhibited the greatest up-regulation of type II collagen, suggesting that higher crosslinking density may yield better retention of TGF- $\beta$ 3 within the hydrogel.

Additionally, various concentrations of TGF- $\beta$ 3 (0, 200 and 2000ng/ml) were encapsulated in 1:1 hydrogels to investigate the effects of TGF- $\beta$ 3 concentration delivered via direct encapsulation. Others have shown that the differentiation pathway can dictate the amount of TGF- $\beta$  that is required, where 10ng/ml is optimal for chondrogenesis while 2ng/ml is adequate for neurogenesis *in vitro* [40-42]. However, for *in vivo* culture, the optimized TGF- $\beta$  dosage and delivery protocol have not been established. In the pilot study, a 2-fold increase in aggrecan expression was observed for the 2000ng/ml group. However, no differences in gene expression for types I and II collagen were seen between TGF- $\beta$ 3 groups. The rate of TGF- $\beta$ 3 diffusion from the hydrogel may be rapid, resulting in low effective growth factor concentrations as seen by the encapsulated cells for both TGF- $\beta$ 3 concentrations. In subsequent studies, conjugation of a Cy5.5 fluorophore to TGF- $\beta$ 3 [35] can be used to visualize the diffusion of the growth factor *in vivo* via transdermal fluorescent imaging of implants cultured subcutaneously in the dorsum of nude mice.

Additionally, the bolus dosage delivery method for TGF- $\beta$ 3 can be compromised by the short half life and consumption of the growth factor. When 1:1 hydrogels with 200ng/ml of encapsulated TGF- $\beta$ 3 were cultured in chondrogenic minus (CM-) media (without the continuous

addition of soluble TGF- $\beta$ 3), constructs were less opaque than those cultured with continuous growth factor supplementation. Macroscopically, those lacking TGF- $\beta$ 3 supplementation were opaque in the center and translucent on the periphery of the construct after 2 weeks, suggesting that growth factor quickly diffused from the exposed surfaces of the hydrogel, and was unable to induce chondrogenesis and matrix deposition in those regions.

Lastly, the pilot study explored the use of a thrombospondin-1 (TSP-1) based peptide as an affinity ligand for the retention of TGF- $\beta$ 3 within the hydrogel [43]. In native tissue, the ECM serves as a reservoir for growth factors, where these signaling molecules can be bound in latent or active form by ECM proteins. By synthesizing an acrylated TGF- $\beta$  binding peptide (Acry-GGKGGWSHW), the affinity ligand could be covalently bound within the hydrogel network. To investigate the effects of peptide addition, 10 $\mu$ M of TGF- $\beta$  binding or missense peptides were incorporated into 1:1 hydrogels with directly encapsulated TGF- $\beta$ 3 (200ng/ml). Hydrogels cultured in CM- media *in vitro* and subcutaneously *in vivo* in nude mice, showed no significant differences in gene expression with or without binding or missense peptides.

The lack of improved chondrogenesis may have resulted from a number of reasons. In a study by Lin *et al* [44], linear spacers of glycine (G<sub>2</sub>, G<sub>7</sub>, and G<sub>12</sub>) were shown to improve the availability of the growth factor binding site to the cells within poly(ethylene glycol) diacrylate hydrogels with increased spacer length. Thus, the availability of the TGF- $\beta$  binding site may have been sterically hindered by the HA network. In future affinity binding peptide designs, a longer spacer for the pendant binding peptide should be taken into consideration as it may be more effective in growth factor retention. Additionally, the use of fluorescence resonance energy transfer can be used to visualize and quantify the binding of the growth factor to the peptide.

In addition, the binding affinity of the peptide to the growth factor may not be optimal. Protein binding is typically weak and low binding affinities may not be sufficient for growth factor retention within the hydrogel. However, if binding is too strong, the growth factor can be sequestered and unavailable to the encapsulated cells. Furthermore, the specificity of the binding can also affect the success of the affinity peptide. Non-specific binding of the peptide

may result in competitive binding, decreasing the percentage of bound growth factor. Thus, a careful balance of binding and specificity must be satisfied for successful use of a biomimetic affinity peptide for growth factor retention. With this in mind, additional TGF- $\beta$ 3 specific binding proteins should be investigated and binding assays should be performed to screen differences in binding affinity in subsequent studies.

Another approach that can be taken for sustained TGF- $\beta$ 3 delivery to encapsulated cells is the incorporation of biomimetic peptides that are able to activate latent TGF- $\beta$ 3. MSCs, along with several other cell types, produce and secrete latent TGF- $\beta$ 3 [45-48]. The secretion of latent growth factor during MSC chondrogenesis should first be examined to determine the feasibility of this approach. If they are found to secrete adequate quantities of TGF- $\beta$ 3, this approach could provide a cell-driven positive feed back loop. The peptide sequence that is responsible for TGF- $\beta$  activation on TSP-1 has already been determined. Again, spacers, multivalency design, and conformational presentation of the peptide must be examined and considered in the development of a bioactive peptide for growth factor delivery.

### 11.3.2 *In Vivo Defect Model*

Once an effective growth factor delivery method has been optimized in subcutaneous *in vivo* culture, the next step is to investigate repair in an *in vivo* defect model. While *in vitro* and non-weight bearing subcutaneous models provided a means to characterize, develop, and optimize HA tissue engineered constructs, they fail to mimic the native joint environment where cartilage repair is most needed for clinical application, as mentioned in Section 11.2. Unfortunately, due to the physiological and anatomical differences between the human joint and those of experimental animals, no animal defect model is directly applicable to humans.

However, small animal models such as rabbits may be used for initial evaluation of developed constructs since they provide a practical approach to investigate scaffold integration and the quality/functionality of the repaired tissue in a dynamically loaded environment, before

performing more costly studies in larger animals (e.g., swine, goat, sheep). Additionally, procedural complications in the injection and photopolymerization of the scaffold within the defect site can also be examined. Importantly, careful choice of the animal and the defect site, size, and type must be taken into consideration. Initial pilot studies in full-thickness swine articular defects demonstrated that partial polymerization would be needed to localize the injection of the cell-laden scaffold due to low viscosity of the cell/macromer solution. Developing a facile injection protocol would illustrate the feasibility of performing *in situ* photopolymerization for HA hydrogel based cartilage repair in a minimally invasive manner, as desired clinically.

**References:**

- [1] Takigawa M, Shirai E, Fukuo K, Tajima K, Mori Y, Suzuki F. Chondrocytes dedifferentiated by serial monolayer culture form cartilage nodules in nude mice. *Bone Miner* 1987;2(6):449-62.
- [2] von der Mark K, Gauss V, von der Mark H, Muller P. Relationship between cell shape and type of collagen synthesised as chondrocytes lose their cartilage phenotype in culture. *Nature* 1977;267(5611):531-2.
- [3] Isogai N, Kusuhashi H, Ikada Y, Ohtani H, Jacquet R, Hillyer J, et al. Comparison of different chondrocytes for use in tissue engineering of cartilage model structures. *Tissue Eng* 2006;12(4):691-703.
- [4] Johnson TS, Xu JW, Zaporozhan VV, Mesa JM, Weinand C, Randolph MA, et al. Integrative repair of cartilage with articular and nonarticular chondrocytes. *Tissue Eng* 2004;10(9-10):1308-15.
- [5] Kafienah W, Jakob M, Demarteau O, Frazer A, Barker MD, Martin I, et al. Three-dimensional tissue engineering of hyaline cartilage: comparison of adult nasal and articular chondrocytes. *Tissue Eng* 2002;8(5):817-26.
- [6] Panossian A, Ashiku S, Kirchhoff CH, Randolph MA, Yaremchuk MJ. Effects of cell concentration and growth period on articular and ear chondrocyte transplants for tissue engineering. *Plast Reconstr Surg* 2001;108(2):392-402.
- [7] Tay AG, Farhadi J, Suetterlin R, Pierer G, Heberer M, Martin I. Cell yield, proliferation, and postexpansion differentiation capacity of human ear, nasal, and rib chondrocytes. *Tissue Eng* 2004;10(5-6):762-70.
- [8] Van Osch GJ, Mandl EW, Jahr H, Koevoet W, Nolst-Trenite G, Verhaar JA. Considerations on the use of ear chondrocytes as donor chondrocytes for cartilage tissue engineering. *Biorheology* 2004;41(3-4):411-21.



- [9] Xu JW, Zaporozhan V, Peretti GM, Roses RE, Morse KB, Roy AK, et al. Injectable tissue-engineered cartilage with different chondrocyte sources. *Plast Reconstr Surg* 2004;113(5):1361-71.
- [10] Erickson IE, Huang AH, Chung C, Li RT, Burdick JA, Mauck RL. Differential maturation and structure-function relationships in mesenchymal stem cell- and chondrocyte-seeded hydrogels. *Tissue Eng Part A* 2009;15(5):1041-52.
- [11] Royal PD, Sparks KJ, Goetinck PF. Physical and immunochemical characterization of proteoglycans synthesized during chondrogenesis in the chick embryo. *J Biol Chem* 1980;255(20):9870-8.
- [12] Bryant SJ, Anseth KS. Controlling the spatial distribution of ECM components in degradable PEG hydrogels for tissue engineering cartilage. *J Biomed Mater Res A* 2003;64(1):70-9.
- [13] Martens PJ, Bryant SJ, Anseth KS. Tailoring the degradation of hydrogels formed from multivinyl poly(ethylene glycol) and poly(vinyl alcohol) macromers for cartilage tissue engineering. *Biomacromolecules* 2003;4(2):283-92.
- [14] Kujawa MJ, Carrino DA, Caplan AI. Substrate-bonded hyaluronic acid exhibits a size-dependent stimulation of chondrogenic differentiation of stage 24 limb mesenchymal cells in culture. *Dev Biol* 1986;114(2):519-28.
- [15] Stern R. Hyaluronan catabolism: a new metabolic pathway. *Eur J Cell Biol* 2004;83(7):317-25.
- [16] Holmes MW, Bayliss MT, Muir H. Hyaluronic acid in human articular cartilage. Age-related changes in content and size. *Biochem J* 1988;250(2):435-41.
- [17] Heine U, Munoz EF, Flanders KC, Ellingsworth LR, Lam HY, Thompson NL, et al. Role of transforming growth factor-beta in the development of the mouse embryo. *J Cell Biol* 1987;105(6 Pt 2):2861-76.
- [18] Fortier LA, Nixon AJ, Mohammed HO, Lust G. Altered biological activity of equine chondrocytes cultured in a three-dimensional fibrin matrix and supplemented with transforming growth factor beta-1. *Am J Vet Res* 1997;58(1):66-70.

- [19] Park H, Temenoff JS, Holland TA, Tabata Y, Mikos AG. Delivery of TGF-beta1 and chondrocytes via injectable, biodegradable hydrogels for cartilage tissue engineering applications. *Biomaterials* 2005;26(34):7095-103.
- [20] van Susante JL, Buma P, van Beuningen HM, van den Berg WB, Veth RP. Responsiveness of bovine chondrocytes to growth factors in medium with different serum concentrations. *J Orthop Res* 2000;18(1):68-77.
- [21] Huang CY, Reuben PM, D'Ippolito G, Schiller PC, Cheung HS. Chondrogenesis of human bone marrow-derived mesenchymal stem cells in agarose culture. *Anat Rec A Discov Mol Cell Evol Biol* 2004;278(1):428-36.
- [22] Johnstone B, Hering TM, Caplan AI, Goldberg VM, Yoo JU. In vitro chondrogenesis of bone marrow-derived mesenchymal progenitor cells. *Exp Cell Res* 1998;238(1):265-72.
- [23] Mackay AM, Beck SC, Murphy JM, Barry FP, Chichester CO, Pittenger MF. Chondrogenic differentiation of cultured human mesenchymal stem cells from marrow. *Tissue Eng* 1998;4(4):415-28.
- [24] Pei M, Luo J, Chen Q. Enhancing and maintaining chondrogenesis of synovial fibroblasts by cartilage extracellular matrix protein matrilins. *Osteoarthritis Cartilage* 2008;16(9):1110-7.
- [25] Alvarez J, Sohn P, Zeng X, Doetschman T, Robbins DJ, Serra R. TGFbeta2 mediates the effects of hedgehog on hypertrophic differentiation and PTHrP expression. *Development* 2002;129(8):1913-24.
- [26] Chimal-Monroy J, Diaz de Leon L. Differential effects of transforming growth factors beta 1, beta 2, beta 3 and beta 5 on chondrogenesis in mouse limb bud mesenchymal cells. *Int J Dev Biol* 1997;41(1):91-102.
- [27] Goessler UR, Bugert P, Bieback K, Deml M, Sadick H, Hormann K, et al. In-vitro analysis of the expression of TGFbeta -superfamily-members during chondrogenic differentiation of mesenchymal stem cells and chondrocytes during dedifferentiation in cell culture. *Cell Mol Biol Lett* 2005;10(2):345-62.

- [28] Shuler FD, Georgescu HI, Niyibizi C, Studer RK, Mi Z, Johnstone B, et al. Increased matrix synthesis following adenoviral transfer of a transforming growth factor beta1 gene into articular chondrocytes. *J Orthop Res* 2000;18(4):585-92.
- [29] Barry F, Boynton RE, Liu B, Murphy JM. Chondrogenic differentiation of mesenchymal stem cells from bone marrow: differentiation-dependent gene expression of matrix components. *Exp Cell Res* 2001;268(2):189-200.
- [30] DeFail AJ, Chu CR, Izzo N, Marra KG. Controlled release of bioactive TGF-beta 1 from microspheres embedded within biodegradable hydrogels. *Biomaterials* 2006;27(8):1579-85.
- [31] Elisseeff J, McIntosh W, Fu K, Blunk BT, Langer R. Controlled-release of IGF-I and TGF-beta1 in a photopolymerizing hydrogel for cartilage tissue engineering. *J Orthop Res* 2001;19(6):1098-104.
- [32] Fan H, Zhang C, Li J, Bi L, Qin L, Wu H, et al. Gelatin microspheres containing TGF-beta3 enhance the chondrogenesis of mesenchymal stem cells in modified pellet culture. *Biomacromolecules* 2008;9(3):927-34.
- [33] Jaklenec A, Hinckfuss A, Bilgen B, Ciombor DM, Aaron R, Mathiowitz E. Sequential release of bioactive IGF-I and TGF-beta 1 from PLGA microsphere-based scaffolds. *Biomaterials* 2008;29(10):1518-25.
- [34] Mann BK, Schmedlen RH, West JL. Tethered-TGF-beta increases extracellular matrix production of vascular smooth muscle cells. *Biomaterials* 2001;22(5):439-44.
- [35] Park JS, Woo DG, Yang HN, Lim HJ, Chung HM, Park KH. Heparin-bound transforming growth factor-beta3 enhances neocartilage formation by rabbit mesenchymal stem cells. *Transplantation* 2008;85(4):589-96.
- [36] Maynard HD, Hubbell JA. Discovery of a sulfated tetrapeptide that binds to vascular endothelial growth factor. *Acta Biomater* 2005;1(4):451-9.

- [37] Hao J, Yao Y, Varshney RR, Wang L, Prakash C, Li H, et al. Gene transfer and living release of transforming growth factor-beta3 for cartilage tissue engineering applications. *Tissue Eng Part C Methods* 2008;14(4):273-80.
- [38] DuBose JW, Cutshall C, Metters AT. Controlled release of tethered molecules via engineered hydrogel degradation: model development and validation. *J Biomed Mater Res A* 2005;74(1):104-16.
- [39] Schoenmakers RG, van de Wetering P, Elbert DL, Hubbell JA. The effect of the linker on the hydrolysis rate of drug-linked ester bonds. *J Control Release* 2004;95(2):291-300.
- [40] Mehlhorn AT, Schmal H, Kaiser S, Lepski G, Finkenzeller G, Stark GB, et al. Mesenchymal stem cells maintain TGF-beta-mediated chondrogenic phenotype in alginate bead culture. *Tissue Eng* 2006;12(6):1393-403.
- [41] Moioli EK, Mao JJ. Chondrogenesis of mesenchymal stem cells by controlled delivery of transforming growth factor-beta3. *Conf Proc IEEE Eng Med Biol Soc* 2006;1:2647-50.
- [42] Peterziel H, Unsicker K, Kriegelstein K. TGFbeta induces GDNF responsiveness in neurons by recruitment of GFRalpha1 to the plasma membrane. *J Cell Biol* 2002;159(1):157-67.
- [43] Schultz-Cherry S, Chen H, Mosher DF, Misenheimer TM, Kruttsch HC, Roberts DD, et al. Regulation of transforming growth factor-beta activation by discrete sequences of thrombospondin 1. *J Biol Chem* 1995;270(13):7304-10.
- [44] Lin C-C, Anseth KS. Controlling Affinity Binding with Peptide-Functionalized Poly(ethylene glycol) Hydrogels. *Adv Funct Mater* 2009;19:1-7.
- [45] Montes R, Ligeró G, Sanchez L, Catalina P, de la Cueva T, Nieto A, et al. Feeder-free maintenance of hESCs in mesenchymal stem cell-conditioned media: distinct requirements for TGF-beta and IGF-II. *Cell Res* 2009;19(6):698-709.
- [46] Roberts AB, Sporn MB. Transforming growth factor beta. *Adv Cancer Res* 1988;51:107-45.
- [47] Sporn MB, Roberts AB, Wakefield LM, Assoian RK. Transforming growth factor-beta: biological function and chemical structure. *Science* 1986;233(4763):532-4.

- [48] Zheng ZH, Li XY, Ding J, Jia JF, Zhu P. Allogeneic mesenchymal stem cell and mesenchymal stem cell-differentiated chondrocyte suppress the responses of type II collagen-reactive T cells in rheumatoid arthritis. *Rheumatology (Oxford)* 2008;47(1):22-30.